AN ABSTRACT OF THE DISSERTATION OF

Caroline Kate Glidden for the degree of Doctor of Philosophy in Integrative Biology presented on June 1, 2020.

Title: INDIVIDUAL HOST TO POPULATION SCALE DYNAMICS OF PARASITE ASSEMBLAGES IN AFRICAN BUFFALO OF KRUGER NATIONAL PARK, SOUTH AFRICA

Abstract approved:

_____

Anna E. Jolles

The last century has experienced a marked increase in emerging infectious disease (EID, hereafter) – jeopardizing human, domestic animal, and wildlife health. EIDs are commonly associated with spillover from one host species into a novel host species, with many destructive diseases, for both livestock and wildlife, emerging at the wildlife-livestock interface. As global change continues to erode the boundaries between human and wildlife systems, it will become increasingly more important to understand the key components influencing host susceptibility as well as pathogen/parasite spread and persistence.

However, understanding disease systems, especially within wildlife, is complex, as processes at multiple scales of biological organization are relevant to pathogen/parasite dynamics. At the within-host scale, pathogens interact with host cells and co-infecting pathogens, and these within-host dynamics affect host susceptibility, infectious period, and pathogen transmission potential. At the host population-level scale, heterogeneity across hosts as well as pathogen dispersal between hosts interacts with within-host processes to ultimately influence the distribution of infectious agents within-hosts, across hosts, and over time. Studying disease in natural systems enables researchers to observe the outcome of interactions of numerous multi-scale sources of variation and predict

realistic parasite/pathogen dynamics. Ultimately, this work should enable the development of adaptive disease management.

For my PhD dissertation, I explored how within-host patterns and processes inform population-level patterns in African buffalo (*Syncerus caffer*) of Kruger National Park (KNP), South Africa. Specifically, I studied infectious agents associated with two diseases that infect cattle and buffalo at the South African wildlife-livestock interface: the bovine respiratory disease complex and theileriosis. In Chapter 2, I found that evolutionarily conserved immune responses (i.e., non-specific inflammatory response) can be used to detect disease exposure without *a priori* knowledge of pathogen identity – a tool than can be further developed for EID surveillance. In Chapter 3, I weighed the effect of host traits, pathogen co-occurrence and environmental variability on probability of infection by viral and bacterial pathogens within the bovine respiratory disease complex as well as characterized temporal trends in pathogen incidence. I found that the importance of each factor was inconsistent across pathogens – co-occurrence was the best indicator of virus occurrence whereas host ID was the best indicator of bacterial infection. Importantly, I found that within-host dynamics only partially elucidated seasonal cycling in population-level disease dynamics. In Chapter 4, I developed molecular methods to quantify cryptic spatio-temporal variation in vector-borne, hemoparasite (*Theileria:* the etiological agent of theileriosis) assemblages of African buffalo. In Chapter 5, I used the high resolution data from Chapter 4 to describe the structure of *Theileria* assemblages within and across hosts, in both space and time. Chapter 5 uses novel analytical approaches to distill complex *Theileria* assemblages into functional groups based upon their life-history patterns. This characterization enabled me to estimate the relative importance of dispersal and host heterogeneity on distribution of these parasites thereby enabling me to predict efficacy and side-effects of vector-borne disease management tools.

INDIVIDUAL HOST TO POPULATION SCALE DYNAMICS OF PARASITE ASSEMBLAGES IN AFRICAN BUFFALO OF KRUGER NATIONAL PARK, SOUTH AFRICA

by

Caroline Kate Glidden

A DISSERTATION

submitted to

Oregon State University

in partial fulfillment of
the requirements for the
degree of

Doctor of Philosophy

Presented June 1, 2020
Commencement June 2021

Doctor of Philosophy dissertation of Caroline Kate Glidden presented on June 1, 2020

APPROVED:

Major Professor, representing Integrative Biology

Head of the Department of Integrative Biology

Dean of the Graduate School

I understand that my dissertation will become part of the permanent collection of Oregon State University libraries. My signature below authorizes release of my dissertation to any reader upon request.

Caroline Kate Glidden, Author

ACKNOWLEDGEMENTS

Anna, thank-you for your dedicated mentorship and guidance throughout my PhD. Thank-you for providing me with the opportunity to be involved in so many different research projects as well as always supporting my many intellectual pursuits. Thank-you for providing me the opportunity to live and do fieldwork in Kruger National Park, South Africa as well as the encouragement to collaborate with the University of Melbourne (and live in Melbourne, Australia for a year). I can't imagine a better (or more fun) graduate school experience.

Thank-you to the National Science Foundation, Achievement Rewards for College Scientists, and University of Melbourne for funding this work. I also thank my graduate committee: Dave Lytle, Jan Medlock, Virginia Lesser, and Taal Levi. Thank-you for your input on this work at its multiple stages of development. Your constructive comments were helpful and much appreciated.

Thank-you members of the Jolles Lab, past and present, for support and feedback on my work throughout graduate school. Special thanks to Dr. Brianna Beechler for leading the FMDV field project as well as providing me many more research projects and opportunities to travel back to South Africa. Thank-you Dr. Hannah Tavalire for being an amazingly supportive mentor and friend, and for always going above and beyond to provide me feedback on analyses, grants and manuscripts. Thank-you Dr. Michelle Steinauer for providing thoughtful guidance, even though our schistosome manuscript didn't make it into my dissertation. Thank-you members of the Jabbar Lab and Gasser Lab for being such wonderful hosts while I was at the University of Melbourne – and for kindly teaching me so many different laboratory techniques and protocols.

Thank-you South Africa National Parks, especially the Veterinary Wildlife Services and Game Capture Team. This work would not have been possible without you.

Thank-you Drs. Lindsay Biga, Lori Kayes, Carmen Harjoe, and Devon Quick for providing unparalleled teaching support and guidance.

I cannot imagine graduate school without the unwavering support of so many compassionate, smart, and fun friends: Vanessa Constant, Hannah Tavalire, Carmen Harjoe, Tim Schrautemeier, Trang Weitemier, Miram Gleiber, Alissa Rickborn, Ashely Friedland, Kaylyn Bopp, Megan Page, Claire Taylor, and Shannon Mason. Special thanks

to Vanessa Constant for always lending an ear, keeping me laughing, and keeping me optimistic. Thank-you Kris and Margaret T. Bauer for your unconditional support.

Finally and foremost, thank-you to my family: Sarah-Kate, Peter, Diana, Sean, Rachael, Nicolette, Luke, Sage, and Cole. Grandad and Grandma, thank-you for instilling in me a love of wildlife and travel. Rachael, Nicolette, Luke thank-you for always being forgiving and always being there for me. Mom, thank-you for always being proud of my accomplishments, encouraging my dreams, and being such an amazing role model.

CONTRIBUTION OF AUTHORS

Chapter 2: Caroline K. Glidden led analyses and writing and was involved in field work and laboratory work; Anna Jolles was project PI, PhD advisor to CG, involved in study conceptualization, field work, lab work and manuscript writing; Bree Beechler was involved in study conceptualization, field work, lab work, analyses; Peter Buss was scientific liaison for South African National Parks Veterinary Wildlife Services; Bryan Charleston was project PI for the Pirbright Institute, involved in project design and lab work; Lin-Mari de Klerk-Lorist was a state veterinarian involved in project design and leading the experimental study; Francois Maree was involved in diagnostic lab work, experimental study design and implementation; Timothy Muller was involved in analysis of data from the FMDV experiment; Eva Pérez-Martin was involved in field work, lab work; Katherine Scott was involved in field work, lab work; Ockert Louis van Schalkwyk was a state veterinarian involved in project design and leading the experimental study.

Chapter 3: Caroline K. Glidden led analyses and writing and was involved in study conceptualization and laboratory work; Anna Jolles was project co-PI, PhD advisor to CG, involved in study conceptualization, field work, lab work and manuscript writing; Courtney Coon was involved in study conceptualization, analyses, and manuscript writing; Bree Beechler was involved in field work and lab work; Chase McNulty was involved in laboratory work; Vanessa Ezenwa was project co-PI, involved in field work, lab work and manuscript writing.

Chapter 4: Caroline K. Glidden was involved in study design, field work, laboratory work and led bioinformatics, phylogenetic, and community analyses as well as manuscript preparation. Anna E. Jolles led the field study design, contributed towards manuscript preparation and acted as mentor to CKG. Anson V. Koehler contributed toward study design of analytical (NGSA and qPCR) tool development, helped with bioinformatics and phylogenetic analyses. Ross S. Hall helped with bioinformatics analyses. Muhammad A. Saeed and Mauricio Coppo contributed toward the development and analyses of the quantitative PCR. Brianna R. Beechler helped manage and design the field study. Bryan Charleston contributed to study design. Robin B. Gasser supported the

study through the provision of computing infrastructure, informatic support, and associated salaries (AVK and RSH). Abdul Jabbar contributed toward design of analytical (NGSA and qPCR) tool development, manuscript preparation as well as acted as mentor to CKG during her Graduate Opportunities Worldwide Fellowship.

Chapter 5: Caroline K. Glidden led study conceptualization, lab work, analyses, manuscript writing and was involved in field work. Anna E. Jolles was project PI, led the field study design, contributed towards manuscript preparation and acted as mentor to CKG. Chenyang Duan and Yuan Jiang led development of the weighted basis-spline regression approach for analyzing non-linear compositional data. Jan Medlock contributed towards study conceptualization and design of the analytical workflow. Hannah Tavalire contributed towards field work and the genome wide association analysis. Robert Spaan calculated NDVI values. Danielle Sisson counted tick abundances and identified ticks to genera.

TABLE OF CONTENTS

TABLE OF CONTENTS (continued)

LIST OF FIGURES

LIST OF FIGURES (Continued)

LIST OF TABLES

LIST OF APPENDIX FIGURES

LIST OF APPENDIX TABLES

Appendix Page

LIST OF APPENDIX TABLES (continued)

Appendix Page

CHAPTER 1: GENERAL INTRODUCTION

Infectious agents that cause disease (parasites and/or pathogens) are key drivers behind ecological and evolutionary trajectories, and individual health outcomes, in animal and plant communities (Hudson, Dobson & Newborn 1998; Stearns 2016). However, anthropogenic alterations are quickly changing the impact parasites and pathogens have on an ecosystem. For instance, human encroachment on wildlife habitat (Hassell et al., 2017) and translocation of domestic animals (Wiethoelter et al., 2015) increases opportunities for infectious agents to spread to new host species and throughout new geographic locations. The human facilitated transfer of disease from livestock to wildlife, and vice versa, has repeatedly caused mass mortality and economic loss (e.g., Roeder, Mariner & Kock 2013; Loots et al., 2017). Thus, understanding how parasites and pathogens spread across, and persist within, natural systems, is critical in better predicting, and possibly managing, the impact of disease on wildlife populations as well as at the wildlife-livestock- human interface.

However, understanding disease systems, especially within wildlife, is complex, as processes at multiple scales of biological organization are relevant to pathogen/parasite dynamics. At the within-host scale, pathogens interact with host cells and co-infecting pathogens (i.e., other strains and species simultaneously infecting the host (Johnson, de Roode & Fenton 2015), and these within-host dynamics affect host susceptibility (Gorsich et al., 2018), infectious period (Arafat et al., 2018), and pathogen transmission potential (Ezenwa & Jolles 2015), connecting within-host processes to population level disease dynamics. At the host population-level scale, behavioral, physiological and ecological heterogeneity across hosts, typically manifesting as proportion of hosts infected (prevalence) (White, Forester & Craft 2018), as well as pathogen dispersal between hosts (Craft 2015) interacts with within-host processes to ultimately influence the distribution of infectious agents within-hosts, across hosts, and over time.

For my PhD dissertation, I explored how within-host patterns and processes inform population-level patterns in African buffalo (*Syncerus caffer*) of Kruger National Park (KNP), South Africa. I primarily examined how host physiology and within-host parasite/pathogen assemblage dynamics elucidate temporal variation in prevalence. My

PhD research was based upon two large field studies: Study (1) (used in Chapter 3) sampled a herd of 200 free ranging African buffalo every six months for four years; Study (2) (used in Chapters 2, 4, 5) sampled a herd of 65 semi-free ranging African buffalo every two-three months for two years. Study (2) awarded me the opportunity to live in KNP and participate in field sampling for ~ 1.5 years of my PhD. The unique, longitudinal nature of these studies was ideal for exploring multi-scale disease systems, as they enabled me to map individual and population level infection histories, revealing temporal patterns not discoverable with typical cross-sectional study designs.

The advantage of using African buffalo of KNP for my dissertation research was two-fold: (i) African buffalo are a tractable model system to study foundational disease ecology and eco-immunology (Jolles, Beechler & Dolan 2014; Ezenwa & Jolles 2015; Ezenwa et al., 2019); (ii) African buffalo share a multitude of parasites/pathogens with cattle, thus, studying multi-scale disease dynamics in African buffalo unlocks avenues of research for adaptive disease management at the human-wildlife interface.

The African buffalo is a model system for studying disease ecology and eco-immunology as they can be tracked in naturally variable systems, allowing researchers to observe disease outcomes that would not occur in a laboratory or clinical setting (Jolles, Beechler & Dolan 2015). Furthermore, African buffalo are close relatives of domestic cattle, thus, disease diagnostics and immunological assays developed for cattle can be implemented in buffalo (e.g., Ezenwa & Jolles 2015; Gorsich et al., 2015; Henrichs et al., 2016). Livestock are globally important for food and economic security, thus, there is a multitude of cattle disease diagnostics and immunological assays that can be used for African buffalo research (Jolles, Beechler & Dolan 2015).

Kruger National Park (KNP), located in the top north-eastern corner of the country, is South Africa's largest game reserve at 19,485 km^2, and supports ~37,000 buffalo (SANPARKS 2010-2011). African buffalo play important ecological roles as they are bulk grazers, opening up habitat for short-grass grazers (Prins 1996), and are prey species, particularly for lions (Owen-Smith & Mills 2008). The African buffalo is highly prized by the tourism industry throughout southern Africa (Michel & Bengis 2012). However, central to this dissertation, the African buffalo is a reservoir host (i.e, a primary host that harbors a parasite/pathogen but shows little or no ill effects of infection)

for destructive livestock diseases (Michel & Bengis 2012). KNP borders many small-scale farms where cattle are the primary source of household wealth / economic security (Sikhweni & Hassan 2013). Thus, understanding disease dynamics in buffalo is important for promoting the livelihoods of people surrounding KNP as well as easing tension, and thereby promoting wildlife conservation, at this human-wildlife interface.

In chapter 2, I demonstrate how evolutionarily conserved immune responses (i.e., non-specific inflammatory response) can be utilized to detect emerging infectious disease. In chapter 3, I examine the relative effect of host traits, environment, and co-infection on the within-host occurrence of upper respiratory infections (viruses and bacteria) associated with the bovine respiratory disease complex, a complex that is common and economically destructive in cattle (Taylor et al., 2010). I also characterize monthly and yearly trends in population-level disease dynamics (number of new cases per month: incidence) to evaluate if within-host patterns inform population-level patterns. In chapter 4, I develop diagnostic methods to describe community structure, both within- and among hosts, of blood-borne protists (*Theileria*) infecting African buffalo. African buffalo and cattle share the same *Theileria* species (3 species-clades) and subtypes (Mans et al., 2016), with African buffalo the purported reservoir host for *Theileria*s that cause significant economic loss at the wildlife-livestock interface (Norval, Perry & Young 1992). African buffalo are typically co-infected with all three species-clades, with prevalence (proportion of animals infected) of each clade ranging from 65-100% in adult animals. In chapter 5, I identify potential processes structuring *Theileria* assemblages within and across hosts and identify how the meta-community ecology of *Theileria* in buffalo can be used to better understand *Theileria* co-existence in African buffalo as well as evaluate the efficacy of management practices in cattle surrounding KNP.

References

Arafat, N., Eladl, A. H., Marghani, B. H., Saif, M. A., & El-Shafei, R. A. (2018). Enhanced infection of avian influenza virus H9N2 with infectious laryngeotracheitis vaccination in chickens. *Veterinary Microbiology*, *219*, 8–16. https://doi.org/10.1016/j.vetmic.2018.04.009

Craft, M. E. (2015). Infectious disease transmission and contact networks in wildlife and livestock. *Philosophical Transactions of the Royal Society of London. Series B, Biological Sciences*, *370*(1669). https://doi.org/10.1098/rstb.2014.0107

Ezenwa, V. O., Jolles, A. E., Beechler, B. R., Budischak, S. A., & Gorsich, E. E. (2019). The causes and consequences of parasite interactions: Afrivan buffalo as a case study. In C. U. Press (Ed.), *Wildlife Disease Ecology*. New York.

Ezenwa, V. O., & Jolles, A. E. (2015). Opposite effects of anthelmintic treatment on microbial infection at individual versus population scales. *Science*, *347*(6218), 175–177. https://doi.org/10.1126/science.1261714

Gorsich, E. E., Bengis, R. G., Ezenwa, V. O., & Jolles, A. E. (2014). Evalution of the sensitivity and specificity of an enzyme-linked immunosorbent assay for diagnosing brucellosis in African buffalo (Syncerus caffer). *Journal of Wildlife Diseases*, *51*(1), 9–18. https://doi.org/10.7589/2013-12-334

Gorsich, E. E., Etienne, R. S., Medlock, J., Beechler, B. R., Spaan, J. M., Spaan, R. S., … Jolles, A. E. (2018). Opposite outcomes of coinfection at individual and population scales. *Proceedings of the National Academy of Sciences*, *115*(29), 7545 LP – 7550. https://doi.org/10.1073/pnas.1801095115

Hassell, J. M., Begon, M., Ward, M. J., & Fevre, E. M. (2017). Urbanization and Disease Emergence: Dynamics at the Wildlife-Livestock-Human Interface. *Trends in Ecology & Evolution*, *32*(1), 55–67. https://doi.org/10.1016/j.tree.2016.09.012

Henrichs, B., Oosthuizen, M. C., Troskie, M., Gorsich, E., Gondhalekar, C., Beechler, B. R., … Jolles, A. E. (2016). Within guild co-infections influence parasite community membership: a longitudinal study in African Buffalo. *The Journal of Animal Ecology*, *85*(4), 1025–1034. https://doi.org/10.1111/1365-2656.12535

Hudson, P. J., Dobson, A. P., & Newborn, D. (1998). Prevention of Population Cycles by Parasite Removal. *Science*, *282*(5397), 2256 LP – 2258. https://doi.org/10.1126/science.282.5397.2256

Johnson, P. T. J., de Roode, J. C., & Fenton, A. (2015). Why infectious disease research needs community ecology. *Science (New York, N.Y.)*, *349*(6252), 1259504. https://doi.org/10.1126/science.1259504

Jolles, A. E., Beechler, B. R., & Dolan, B. P. (2015). Beyond mice and men: environmental change, immunity and infections in wild ungulates. *Parasite Immunology*, *37*(5), 255–266. https://doi.org/10.1111/pim.12153

Mans, B. J., Pienaar, R., Ratabane, J., Pule, B., & Latif, A. A. (2016). Investigating the diversity of the 18S SSU rRNA hyper-variable region of Theileria in cattle and Cape buffalo (Syncerus caffer) from southern Africa using a next generation sequencing approach. *Ticks and Tick-Borne Diseases*, *7*(5), 869–879. https://doi.org/10.1016/j.ttbdis.2016.04.005

Michel, A. L., & Bengis, R. G. (2012). The African buffalo: a villain for inter-species spread of infectious diseases in southern Africa. *The Onderstepoort Journal of Veterinary Research*, *79*(2), 453. https://doi.org/10.4102/ojvr.v79i2.453

Norval, R., Perry, B. D., & Young, A. S. (1992). *The Epidemiology of Theileriosis in Africa.* San Diego, CA: Academic Press Inc.

Owen-Smith N & Mills, M.G.L. (2008) Shifting prey selection generates constrasting herbivore dynamics within a large-mammal predatory-prey web. *Ecology*, *89*, 1120-1133.

Prins, H. H. (1996). *Ecology and behavior of the African buffalo: Social inequality and decision making*. London, UK: Chapman & Hall.

Roeder, P., Mariner, J., & Kock, R. (2013). Rinderpest: the veterinary perspective on eradication. *Philosophical Transactions of the Royal Society of London. Series B, Biological Sciences*, *368*(1623), 20120139. https://doi.org/10.1098/rstb.2012.0139

SANPARKS (2010-2011) Kruger National Park Biodiversity Statistics. https://www.sanparks.org/parks/kruger/conservation/scientific/ff/biodiversity_statistics.php

Sikhweni, N.P. & Hassan, R. (2013). Opportunities and challenges facing small-scale cattle farmers living adjacent to Kruger National Park , Limpopo Province NP Sikhweni and R Hassan Corresponding Author : NP Sikhweni. *Journal of Emerging Trends in Economics and Management Sciences*, *5*(1), 38–43.]

Taylor, J. D., Fulton, R. W., Lehenbauer, T. W., Step, D. L., & Confer, A. W. (2010). The epidemiology of bovine respiratory disease: What is the evidence for predisposing factors? *The Canadian veterinary journal = La revue veterinaire canadienne*, *51*(10), 1095–1102.

White, L. A., Forester, J. D., & Craft, M. E. (2018). Covariation between the physiological and behavioral components of pathogen transmission: host heterogeneity determines epidemic outcomes. *Oikos*, *127*(4), 538–552. https://doi.org/10.1111/oik.04527

Wiethoelter, A. K., Beltrán-Alcrudo, D., Kock, R., & Mor, S. M. (2015). Global trends in infectious diseases at the wildlife–livestock interface. *Proceedings of the National Academy of Sciences*, *112*(31), 9662 LP – 9667. https://doi.org/10.1073/pnas.1422741112

DETECTION OF PATHOGEN EXPOSURE IN AFRICAN BUFFALO USING NON-SPECIFIC MARKERS OF INFLAMMATION

Caroline K. Glidden, Brianna Beechler, Peter Erik Buss, Bryan Charleston, Lin-Mari de Klerk-Lorist, Francois Frederick Maree, Timothy Muller, Eva Pérez-Martin, Katherine Anne Scott, Ockert Louis van Schalkwyk, and Anna E. Jolles

Frontiers in Immunology

SA Avenue du Tribunal Fédéral 34, Lausanne, Switzerland 1005

Available online: https://doi.org/10.3389/fimmu.2017.01944

CHAPTER 2: DETECTION OF PATHOGEN EXPOSURE IN AFRICAN BUFFALO USING NON-SPECIFIC MARKERS OF INFLAMMATION

Abstract

Detecting exposure to new or emerging pathogens is a critical challenge to protecting human, domestic animal, and wildlife health. Yet current techniques to detect infections typically target known pathogens of humans or economically important animals. In the face of the current surge in infectious disease emergence, non-specific disease surveillance tools are urgently needed. Tracking common host immune responses indicative of recent infection may have potential as a non-specific diagnostic approach for disease surveillance. The challenge to immunologists is to identify the most promising markers, which ideally should be highly conserved across pathogens and host species, become upregulated rapidly and consistently in response to pathogen invasion, and remain elevated beyond clearance of infection. This study combined an infection experiment and a longitudinal observational study to evaluate the utility of non-specific markers of inflammation [NSMI; two acute phase proteins (haptoglobin and serum amyloid A), two pro-inflammatory cytokines (IFNγ and TNF-α)] as indicators of pathogen exposure in a wild mammalian species, African buffalo (*Syncerus caffer*). Specifically, in the experimental study, we asked (1) How quickly do buffalo mount NSMI responses upon challenge with an endemic pathogen, foot-and-mouth disease virus; (2) For how long do NSMI remain elevated after viral clearance and; (3) How pronounced is the difference between peak NSMI concentration and baseline NSMI concentration? In the longitudinal study, we asked (4) Are elevated NSMI associated with recent exposure to a suite of bacterial and viral respiratory pathogens in a wild population? Among the four NSMI that we tested, haptoglobin showed the strongest potential as a surveillance marker in African buffalo: concentrations quickly and consistently reached high levels in response to experimental infection, remaining elevated for almost a month. Moreover, elevated haptoglobin was indicative of recent exposure to two respiratory pathogens assessed in the longitudinal study. We hope this work motivates studies investigating suites of NSMI as indicators for pathogen exposure in a broader range of both pathogen and host species, potentially transforming how we track disease burden in natural populations.

2.1 Introduction

Emerging infectious diseases cause human suffering (Shears & Dempset 2015, Kelser 2016), threaten food security (Vurro, Bonciani & Vannacci 2010), and contribute to the decline of vulnerable populations and species (Genton et al, 2012). As such, in the face of elevated rates of infectious disease emergence in humans (Brierley et al., 2016, Meyer et al., 2016), domestic animals (Openshaw et al., 2016) and wildlife (Adlard et al., 2015, Ingersoll et al., 2016, Price eta al., 2016), effective surveillance for pathogen exposure is increasingly important.

Surveillance for emerging infections is challenging because it requires detection of previously unreported infectious agents, and/or diagnosis of exposure or infection in understudied animal species. Indeed, animals are hosts to hundreds of pathogens and parasites (Pérez et al., 2006) with previously unidentified species regularly documented (Blackwell 2011, Woolhouse et al., 2012, Rodicio et al., 2004). Yet, available disease diagnostics typically target known infections that cause detectable pathology in humans or economically important domestic animals resulting in a relatively narrow range of tests that are highly pathogen specific. Common molecular techniques to detect pathogens include tests that detect genetic material of the pathogen itself and antibody-based diagnostics that detect the host's antibodies to a given pathogen. Advancing sequencing methods show promise for simultaneously detecting a wider range of pathogens (Metzker 2010, Petti 2007) but, while genetically based techniques often have high sensitivity and specificity, they are limited to detection of active infections. Many infections last only a few days and thus may escape detection unless sampling can occur on a tight time frame. Most importantly, diagnostic techniques based on amplifying pathogen genetic material still require pathogen specific primers and/or previous publication of genetic sequences and are, thus, unsuitable in situations where the identity of the pathogens are uncertain. Antibody-based techniques, such as enzyme-linked immunosorbent assays or immunofluorescence assays, offer a way to detect infection after pathogen exposure has occurred because antibody titers to many infections can remain elevated for months to years after primary infection (Guerrant, Walker & Weller 2011). However, antibody-based techniques typically used in disease diagnostics are highly pathogen specific, which limits their utility in detecting novel infections.

An ideal diagnostic approach for monitoring (often unknown) infections in natural populations would complement existing genetic and antibody techniques by detecting the presence of pathogens non-specifically, using immunological markers that indicate recent presence of infection. Ideal markers should increase rapidly and reliably in response to a broad range of pathogens and remain elevated for a consistent period after active infection has subsided. A test that detects exposure both early in infection, as well as past pathogen clearance, could aid in monitoring population health and improve surveillance for emerging infections.

Here, we suggest that non-specific markers of inflammation (NSMI hereafter) have potential for use in detecting pathogen exposure in natural populations. NSMI include APP [this study: haptoglobin, serum amyloid A (SAA)] and cytokines (here: TNF-α, IFNγ). APP are an integral part of the acute inflammatory response to pathogen exposure and engage in opsonization of pathogens and scavenging of toxic substances (Ceciliani et al., 2012). SAA is produced by the liver after acute phase induction by pro-inflammatory cytokines; its main functions include binding cholesterol from inflammation sites, modulating the function of innate immune cells, and opsonizing pathogens for destruction by immune cells (Ceciliani et al., 2012). Haptoglobin binds hemoglobin, which prevents oxidative damage and deprives bacteria of iron needed to grow (Ceciliani et al., 2012). Cytokines are small "messenger" proteins secreted by immune cells to mediate the immune response. TNF-α is a primary signaling molecule in systemic inflammatory reactions and is a vital component of the acute phase response; IFNγ is a key signaling molecule in clearance of intracellular pathogen infections (Murphy 2011).

We combined an infection experiment and a longitudinal observational study to evaluate the utility of these four NSMI as indicators of pathogen exposure in a wild mammalian species, African buffalo (*Syncerus caffer*) (Figure 1). Specifically, in the experimental study we asked (1) How quickly do buffalo mount NSMI responses upon challenge with an endemic pathogen, foot- and-mouth disease virus (FMDV); (2) For how long do NSMI remain elevated after viral clearance; and (3) How pronounced is the difference between peak NSMI concentration and baseline NSMI concentration? In the longitudinal study, we asked (4) Are elevated NSMI associated with recent exposure to

seven bacterial and viral respiratory pathogens, in a natural host population?

2.2 Methods

African buffalo (*Syncerus caffer*) included for this study were located within Kruger National Park (KNP), a 19,000 km^2 reserve located in northeastern South Africa. Two populations were used for the study: (1) 12 1- to 2-year-old bovine tuberculosis (BTB) and FMDV free wild-caught buffalo obtained from Hluhluwe iMfolozi Park and transferred to the Skukuza State Veterinary enclosure (FMDV experiment buffalo, hereafter); (2) a herd of 60–75 wild buffaloes, of mixed age and sex, contained within a 900-ha enclosure near Satara camp in the central area of KNP (cohort buffalo, hereafter) (Figure 2.1). The first population was used in a FMDV challenge experiment identifying triggers of FMDV transmission and tracing viral evolution; the second population is part of an ongoing observational study identifying drivers of FMDV dynamics. The study was conducted under South Africa Department of Agriculture, Forestry and Fisheries Section 20 permits Ref 12/11/1 and Ref 12/11/1/8/3, ACUP project number 4478 and 4861, Onderstepoort Veterinary Research Animal Ethics Committee project number 100261-Y5, and the Kruger National Park Animal Care and Use Committee project number JOLAE1157-12 and JOLAE1157-13.

2.2.1 Field sampling

2.2.1.1 FMDV experiment buffalo

Foot-and-mouth disease virus is an endemic viral infection of cloven-hoofed ungulates, with African buffalo acting as the maintenance host (Vosloo et al., 2017). Briefly, 12 buffalo were exposed to FMDV (day 2) by allowing them to mix with recently infected [via injection, using protocols optimized previously for buffalo: Maree et al. (2016)] animals. All 12 recipient animals were sedated on days 2, 4, 6, 8, 11, 14, and 30 days post FMDV exposure to allow for collection of blood samples for quantification of NSMI and FMD viremia. Immobilizations were conducted by South African State Veterinarians using standard protocols for buffalo (McKenzie 1993). Blood was collected

via jugular venipuncture directly into vacutainer tubes with (plasma, whole blood) or without (serum) heparin, and stored on ice for transport back to the laboratory. Immediately upon arrival at the laboratory, blood was centrifuged at 5000 × g for 10 min; plasma and serum pipetted off the cellular layer into sterile microcentrifuge tubes and stored at −80°C until analysis. In addition, 1.5 ml of whole blood, collected in tubes with heparin, was aliquoted into separate, sterile microcentrifuge tubes and incubated at 37°C for 72 h. After 72 h, plasma was pipetted off the cellular layer and stored at 4°C until cytokine analysis 24–72 h later (Ezenwa & Jolles 2015). Samples collected within 3 days of each other were all processed on the same cytokine assay; therefore, samples collected 3 days prior to running the assays were stored at 4°C for 72 h, samples collected 2 days prior to running the assays were stored at 4°C for 48 h and samples collected 1 day prior to running the assays were stored at 4°C for 24 h.

2.2.1.2 Cohort buffalo

Cohort buffalo were originally captured in 2001 from the North of KNP and have been maintained since then in the enclosure as a BTB free breeding herd. During our study period (2014–2016), the herd included 65–70 animals. Natural births and deaths occurred during the study, leading to a total of 77 individuals included in analyses.

The enclosure is entirely within KNP and has numerous other wild animals typical of the ecosystem (e.g., giraffes, zebra, warthogs, small mammals, and small predators). However, the enclosure excludes megaherbivores (rhino, hippo, elephant) and large predators (lion, leopard). Cohort buffalo graze and breed naturally and find water in seasonal pans and manmade (permanent) water points. In extreme dry seasons, supplemental grass and alfalfa hay are supplied.

Cohort buffalo were caught every 2–3 months from February 2014 to February 2016, totaling 10 capture periods. To sample, buffalo were herded into a capture corral, separated into groups of 4–10 animals, and sedated. Buffalo that evaded corral capture were darted individually from a helicopter. Sedation procedures are outlined in Couch et al. (2017). Animals were released from the capture corral within 1–5 days after captures.

The animals' sex was determined visually. Age was determined by a combination of incisor wear and tooth emergence for animals older than 2.5 years, and via body size

and horn growth in younger calves, as described in Jolles, Cooper & Levin (2005). Body condition was determined by assigning a score from 1 to 5 based on manually palpating four sites (ribs, hips, spine, and tail base); average score was used in all analyses (Ezenwa, Jolles & O'Brien 2009). At each capture period, blood was collected and processed identically to FMDV experiment procedures, with the addition of serum being stored for analysis of exposure by respiratory pathogens.

2.2.2 Laboratory methods

Foot-and-mouth disease virus qRT-PCR and respiratory pathogen ELISAs were run using serum samples. NSMI markers were quantified using plasma samples; cytokine assays were run using incubated plasma samples (outlined in field methods section) whereas haptoglobin and SAA assay were run using non-incubated plasma samples.

2.2.2.1 FMDV experiment buffalo

The number of FMDV RNA genome copies per ml of serum, expressed as $\log_{10}$, was measured using quantitative qRT-PCR methods outlined in Ref. (Maree et al., 2016). Buffalo were considered to have an active viral infection if genome copies per ml of serum were >3.2 $\log_{10}$. Thus, one individual was removed from the study as serum qRT-PCR results never exceeded >3.2 $\log_{10}$ genome copies/ml of serum.

Non-specific markers of inflammation were measured via sandwich ELISA per manufacturers' instructions (Haptoglobin: Life Diagnostics 2410; Serum amyloid A: Life Diagnostics SAA-11; TNF-α: Ray-Bio ELB-TNFa; IFNγ: Bio-Rad MCA5638KZZ). All NSMI ELISAs were run within 1 month of collection. Importantly, FMDV experimental buffalo were monitored for exposure to seven common respiratory pathogens, however, no animals seroconverted during the experiment. Pathogens tested for, and methods used to estimate seroconversion are identical to methods outlined below (Methods, laboratory methods, cohort buffalo).

2.2.2.2 Cohort buffalo

Identical to the FMDV experiment, APP were measured via sandwich ELISA per manufacturers' instructions (Haptoglobin: Life Diagnostics 2410; Serum amyloid A: Life

Diagnostics SAA-11; TNF-α: Ray-Bio ELB-TNFa; IFNγ: Bio-Rad MCA5638KZZ).

Seroconversion, a proxy for incidence, of seven common viral and bacterial respiratory pathogens (Figure 1) was measured for each capture period via sandwich ELISAs per manufacturers' instructions [Adenovirus (AD-3), parainfluenza virus (Pi-3), bovine herpes virus, *Mannheimia haemolytica* (MH), *Mycoplasma bovis* (MB): Bio-X IPAMM; bovine diarrhea virus (BVDV): Bio-X BVDV; bovine respiratory syncytial virus: Bio-X BRSV]. Samples were considered positive for pathogen antibodies if antibody titers exceeded threshold absorbance values calculated using the quality control procedures outlined in each Bio-X kit. Incidence was calculated as a binomial variable. Incidence was assigned a 1 if an animal seroconverted from t0 to t1 (i.e., absorbance values were below threshold concentrations at t0 but above threshold absorbance at t1) and 0 if the animal had not seroconverted.

With the exception of SAA, all NSMI and respiratory pathogen ELISAs were run within 2 weeks of capture periods. All SAA ELISAs were run in September 2016.

2.2.3 Mathematical & statistical analyses

2.2.3.1 FMDV experiment buffalo

Mathematical modeling was carried out using R [R Core Team (R version 3.2.3)]. To evaluate the response of each NSMI to FMDV infection, we calculated (i) the time to NSMI peak from initial FMDV exposure (i.e., from the first day FMDV serum genome copies/1 ml of serum >3.2 $\log_{10}$), and (ii) the period for which NSMI remained elevated after the host cleared the virus. In addition, mean peak concentration and baseline concentration were calculated for each NSMI.

The period for which NSMI remained elevated past viral clearance was calculated as follows: first, an exponential decay curve Eq. 1 was fit starting from peak NSMI concentration (Figure 1):

$$y = ae_{kt}. \qquad \text{Eq. 1}$$

Next, decay rate (k) and intercept (a) were extracted from individual exponential decay equations, and baseline NSMI (y_{BL}) levels were estimated from averaging day-2 and day-14 NSMI concentrations. The time when NSMI returned to baseline levels after their peak, (t_{BL}), was calculated using Eq. 2:

$$t_{BL} = \frac{\log(y_{BL}) - \log(a)}{k}. \quad \text{Eq. 2}$$

Time at viral clearance (t_{VC}) was assigned based on the first-day FMDV genome copies dropped below 3.2 $\log_{10}$/ml of serum after initial incidence. Days' NSMI was elevated past viral clearance which was calculated by Eq. 3:

$$t_{NSMI\ elevated\ from\ VC} = t_{BL} - t_{VC}. \quad \text{Eq. 3}$$

Animals in which the NSMI concentration did not exceed twofold baseline levels were determined not to have mounted that particular NSMI response and removed from future analysis (for that NSMI). If NSMI concentrations did not peak until 30 days post FMDV challenge these animals were removed from the analysis as their exponential decay curve would have been fit to only one data point. Final sample sizes included in each NSMI analysis are included in Table 2.1.

NSMI concentration by day is presented in Figure A1.

2.2.3.2 Cohort buffalo

Statistical analyses for cohort buffalo were performed in R using *lme4* (Bates et al., 2015) and *lmerTest* (Kuznetsova, Brockhoff & Christensen 2016).

Mixed effects logistic regressions were used to evaluate the effect of NSMI on respiratory disease incidence. Multiple samples per individual were used for all analyses, thus Animal ID was included as a random intercept to avoid pseudo-replication. Host traits (body condition, age, sex) and season may influence respiratory disease incidence (McNulty 2015); therefore, they were included as fixed effects within each model. A model was run for each combination of respiratory pathogen × NSMI (mixed effects

logistic regression model example Eq. 4):

$$logit\,\{P(incidence_{ij} = 1 | NSMI_{1j}, body\ condition_{2j}, sex_{3j}, age_{4j}, season_{5j}, \varepsilon_j)\} = \beta_0 + \beta_1 NSMI + \beta_2 body\ condition + \beta_3 sex + \beta_4 age + \beta_5 season + \varepsilon_j.$$

Eq.4

where $\varepsilon_j \sim N(0, \psi)$ represents Animal ID as a random intercept. The association of NSMI with respiratory disease incidence was evaluated post seroconversion. Our models asked whether prior disease incidence between [t_0 and t_1] was associated with elevated NSMI at t_1. Thus, each model was run with explanatory variables corresponding to the t_1 time step, and disease incidence measured for the preceding capture interval.

Haptoglobin and SAA spanned several orders of magnitude and were severely right skewed, thus were $\log_2$ transformed to increase model stability and avoid issues with influential data points.

To prevent errors that can arise from multiple testing, statistical significance of each dependent variable was defined using significance levels corrected via the Benjamini and Hochberg's false discovery rate controlling procedure (Benjamini & Yekutieli 2001). Benjamini and Hochberg's false discovery rate controlling procedure assigns a significance level based upon rank of p-value within the family of tests; therefore, the particular significance level for each model is specified within Table 2.2. The test statistic and resulting p-value were calculated using Satterthwaite's approximation of degrees of freedom (Kuznetsova, Brockhoff & Christensen 2016).

For significant associations between pathogen incidence and NSMI, average marginal predicted probabilities for given levels of NSMI concentration and area under the curve (AUC) were calculated using R packages *lme4* (Bates et al., 2015) and *pROC* (Xavier et al., 2011). Marginal predicted probabilities were calculated using models described in Eq. 4. 1,000 marginal predicted probabilities of pathogen incidence were calculated for 100 fixed values of NSMI and randomly selected (from the data) values of age, sex, body condition, season, and animal id. Average marginal predicted probability and 95% confidence intervals for pathogen incidence were then constructed from the

1,000 values calculated for each fixed NSMI concentration. AUC, or the area under the receiving operating characteristic curve, is a standard diagnostic analysis used to measure how well a parameter can distinguish between two diagnostic groups based upon the specificity (true negative rate) and sensitivity (true positive rate) of the test.

2.3. Results

2.3.1 FMDV experiment buffalo

Buffalo mounted robust NSMI responses to FMDV infection, as evidenced by differences between mean peak and baseline NSMI concentrations (Table 2.1; Figure 2.2).

The mean time from FMDV incidence to peak NSMI concentration was 3–7 days for all NSMI (Table 2.1; Figure 2.3). On average, viral clearance occurred at 4.72 (±0.20) days after initial FMDV infection (i.e., the first-day FMDV RNA copies >3.2 log10/ml of serum). Haptoglobin remained elevated for the greatest number of days past viral clearance (21 days on average), with the lowest interindividual variation in time elevated, followed by IFNγ, SAA, and TNF-α (Figures 2.1 & 2.3; Table 2.1).

All individuals showed increases in haptoglobin, SAA, and IFNγ, however, only 3/11 contact buffalo mounted detectable TNF-α responses. Haptoglobin displayed the greatest difference in mean peak and baseline concentration, followed by SAA, IFNγ, and TNF-α.

2.3.2 Cohort buffalo

For each NSMI, we tested whether elevated levels of the marker were indicative of infection by a range of respiratory pathogens during the preceding 2–3 months. Haptoglobin was a significant indicator of two respiratory pathogens: MB and Pi-3 (Table 2.2; Figure 2.4). After controlling for animal traits and season, for every twofold increase in haptoglobin there was a 21% increase in the odds of prior MB incidence and a 13% increase in the odds of prior Pi-3 incidence. As expected for NSMI, the sensitivity and specificity of haptoglobin as a marker of each particular pathogen was significant (Lower CI of AUC > 0.5) but moderate. The AUC for haptoglobin as a classifier of MB was 0.67 (95% CI 0.52–0.77) and Pi-3 was 0.586 (95% CI 0.53–0.64) (Figure 2.5).

Although not significant by standards of the Benjamini and Hochberg's false discovery rate controlling procedure, there was suggestive evidence (p-value <0.05) that IFNγ was an indicator of MB incidence (Table 2.2). For every unit increase in IFNγ, there was an 11% decrease in the odds of prior MB incidence

2.4. Discussion

Mitigating disease outbreaks and identifying pathogen presence is crucial in evaluating ecosystem health (Preston et al., 2016, Polley 2005), creating effective wildlife conservation plans (Hear et al., 2013, Thompson, Lymbery & Smith 2010, Smith, Sax & Lafferty 2006) and improving global health (Macpherson 2013, Colwell, Dantas-Torres & Otranto 2013). Current techniques to detect pathogen exposure are primarily limited to (1) tests that are highly specific to both pathogen and host, and (2) pathogens that cause detectable pathology in humans and economically important animals; yet, the diversity of pathogen communities in natural populations is only beginning to be uncovered (Anthony et al., 2013, Bailey et al., 2016) with specific diagnostic tools for novel infections generally unavailable.

Given the current surge in infectious disease emergence (Jones et al., 2008), new diagnostic approaches, which can detect diverse pathogens, over an extended time frame within a broad range of hosts, are urgently needed. Our study demonstrates a possible approach to detecting infections non-specifically, using inflammatory markers.

Despite the overwhelming diversity of pathogen species that can infect a given host, early stages of immunological response are considered evolutionarily conserved, and primary defenses are similar for a diversity of pathogens (Mogensen 2009) within many hosts (Rowley 1996). Consequently, tracking first-line immune response has potential as a non-specific diagnostic approach for monitoring the burden of disease in a population of interest. Invertebrate and vertebrate hosts initially respond to pathogen challenge by mounting an inflammatory response (Rowley 1996). Due to the ubiquity of the inflammatory response, proteins upregulated during this initial stage of infection may hold promise as non-specific markers of pathogen exposure.

In this study, we used experimental and observational approaches to explore the utility of four NSMI in detecting pathogen exposure. We included two APP (haptoglobin

and SAA) and two cytokines involved in inflammatory responses (IFNγ and TNF-α).

Buffalo mounted quick and robust acute phase responses to experimental challenge with FMDV, with the magnitude of NSMI responses similar to those reported in cattle (Cray, Zaias & Altman 2009). We found that, in response to FMDV infection, haptoglobin remained elevated the greatest number of days past viral clearance with the smallest degree of interindividual variation. Haptoglobin reached peak concentrations within a week of FMDV incidence and remained elevated for more than 3 weeks past FMDV clearance. Elevated haptoglobin levels were, thus, detectable both during and for several weeks after FMDV infection. Complementary to this, we found in our cohort study that haptoglobin was a significant indicator of recent natural incidence by two out of seven viral and bacterial respiratory pathogens.

Within the last 20 years, haptoglobin has been used to study inflammation in domestic animals (Cray, Zaias & Altman 2009) but has been more strongly associated with bacterial infections (Goodson et al., 1996). We found haptoglobin to be significantly associated with both a viral (Pi-3) and a bacterial (MB) pathogen. Abnormal haptoglobin concentrations have been found in cattle infected with FMDV (Höfner, Fosbery & Eckersall 1994, Stenfeldt et al., 2011) and Pi-3 (Rodrigues et al., 2015). All buffalo included in the experimental study mounted SAA and IFNγ responses to experimental FMDV infection within a week, however, on average, SAA remained elevated for just under 2 weeks and IFNγ remained elevated for just over 1 week. IFNγ was also a suggestive indicator of MB in our cohort study. TNF-α responses were detectable in one-fourth of our experimentally FMDV-infected buffalo, were short-lived for animals that mounted a response, and showed no associations with respiratory pathogens we monitored in our cohort study. Our results for SAA and IFNγ, especially IFNγ, suggest potential of NSMI for disease monitoring. Perhaps, inflammatory cytokines, particularly TNF- α, responses are mounted quickly, either very localized or low in magnitude, and short lived because of the collateral damage they elicit (Graham, Allen & Read 2005, Sears et al., 2011). Haptoglobin contributes to “cleaning up” products of inflammation (Murphy 2011) and, thus, should cause significantly less immunopathology. The function of haptoglobin may, thus, explain the comparatively long lived, high magnitude responses we observed.

We found haptoglobin to be a significant classifier of MB and Pi-3, however, specificity would be considered low by veterinary and human medical diagnostic standards. Low specificity is expected, given that haptoglobin responds to multiple inflammatory processes including exposure to unknown pathogens, stress, trauma, and autoimmune disorders (Cray, Zaias & Altman 2009); and indeed, the goal here was to find non-specific markers indicative of pathogen exposure. Although sensitivity and specificity was low, and haptoglobin only detected two out of seven respiratory pathogens, our results are particularly encouraging because we are likely to be underestimating the true sensitivity of haptoglobin and other NSMI in the cohort study, due to the "mismatch" between capture interval (2–3 months) and NSMI response (e.g., haptoglobin: 3 weeks). This is likely caused by an increased number of false negatives—animals that were exposed to a given pathogen, but had no detectable elevation in NSMI at time of capture. More frequent captures should thus improve the performance of NSMI in detecting pathogen exposures. In addition, using a combination of NSMI may help to tease apart sources of inflammation, allowing researchers to filter out non-infectious processes and improve test specificity.

Our work points to the possibility of defining markers for non-specific disease surveillance but raises many new questions about discovering which combinations of markers can potentially work in different host species, and for detection of different suites of pathogens. For example, future research could investigate a broader range of cytokines, such as inflammatory cytokines, Il-6 and Il-1beta, and additional APP, such as fibrinogen or C-reactive protein, and negative APP such as albumin or transferrin. Dugovich et al. (2017) recently described the utility of natural antibodies (nAbs), antibodies that associate with the innate immune response and bind to multiple microbial agents, in assessing immunological status of desert bighorn sheep. In addition, in mammals, toll-like receptors (TLRs), proteins integral in recognition of infection, are highly conserved to recognize broad groups of pathogens (Takeda, Kaisho & Akira 2003). As such, the utility of nABs and TLR expression as disease surveillance tools warrants future research.

A systematic approach could follow host responses to pathogenic challenge, from pathogen recognition to inflammation, and define effectors that typify responses to

different groups of pathogens. Immunologists could potentially tailor NSMI panels for detecting different groups of parasites, such as hemoparasites or gastro-intestinal infections—and explore whether taxonomic relatedness of parasites, or similarity of infection sites are most important in selecting appropriate NSMI.

Assays for APP and pro-inflammatory cytokines have been developed for domestic animals and laboratory model species, including cows, sheep, goats, horses, dogs, cats, mice, and rats. A handful of studies have used serum and urine based assays to monitor health and disease incidence in wildlife species including Grant's zebra (Cray, Hammond & Haefele 2013), European mouflon (Smitka et al., 2015), Przewalkski's horses (Sander et al., 2016), rhesus macaques (Krogh et al., 2014). As such, the tools for beginning to define panels of NSMI for disease monitoring, already exist for a broad range of mammalian host species. Due to the devastation that emerging infectious diseases have elicited in amphibian (Daszak et al., 1999) and marine invertebrate (Menge et al., 2016, Maynard et al., 2016) systems, identifying inflammatory markers that detect pathogen exposure in non-mammalian vertebrates and invertebrates could prove invaluable to conservation biologists.

For NSMI that are stable in stored samples, such as frozen sera, the utility of NSMI could extend beyond current surveil- lance to include retrospective studies—biobanks are a commonly available but underused resource for human, animal, and wild-life studies. Beechler et al. (2017) demonstrated that haptoglobin concentrations in stored serum remain stable for at least 4 years, and Hegemann et al. (2017) documented stability of haptoglobin, nAbs, and total immunoglobulins during extended storage, suggesting that undertaking retrospective evaluations of populations is a feasible and viable option for future studies.

Developing non-specific diagnostic tools is essential to detect emerging infections in animal and human populations and effectively tracking the burden of infection in natural populations. In the face of the vast diversity of pathogens and host species, an approach that tracks conserved inflammatory responses to a range of infections may provide a tractable pathway toward recognizing changes in disease burden that can then be followed up with specific diagnostic testing. Our study on infections in African buffalo provides a proof of concept, showing that APP and/or pro-inflammatory

cytokines can provide useful information about pathogen exposures. It is our hope that this work will open opportunities for investigating suites of NSMI as indicators for pathogen exposure, potentially transforming how we measure disease in natural populations.

2.5 Acknowledgements

We thank Kruger National Park Veterinary Wildlife Services and State Veterinarians for their help with animal capture. Lab work and field work was completed by members of the Jolles Lab group: Hannah Tavalire, Brian Dugovich, Courtney Coon, Claire Couch, Henri Combrink, Juliana Masseloux, Danielle Sisson, Daniel Trovillion, Abby Sage, Emma Devereux, and Kath Forssman. We would also like to thank two anonymous reviewers for helpful feedback that improved the manuscript. Both experimental and longitudinal studies were supported by the USDA-NIFA AFRI grant # 2013-67015-21291and by the UK Biotechnology and Biological Sciences Research Council grant # BB/L011085/1 as part of the joint USDA-NSF- NIH-BBSRC Ecology and Evolution of Infectious Diseases program. C. Glidden was supported by ARCS and NSF GRFP fellowships.

2.6 References

Adlard RD, Miller TL, Smit NJ. The butterfly effect: parasite diversity, environment, and emerging disease in aquatic wildlife. Trends Parasitol (2015) 31(4):160–6. doi:10.1016/j.pt.2014.11.001

Anthony SJ, Epstein JH, Murray KA, Navarrete-Macias I, Zambrana-Torrelio CM, Solovyov A, et al. A strategy to estimate unknown viral diversity in mammals. mBio (2013) 4(5):e000598. doi:10.1128/mBio.00598-13

Bailey AL, Lauck M, Ghai RR, Nelson CW, Heimbruch K, Hughes AL, et al. Arteriviruses, pegiviruses, and lentiviruses are common among wild African monkeys. J Virol (2016) 90(15):6724–37. doi:10.1128/JVI.00573-16

Bates D, Maechler M, Bolker B, Walker S. Fitting linear mixed-effects models using lme4. J Stat Softw (2015) 67(1):1–48. doi:10.18637/jss.v067.i01

Beechler BR, Jolles AE, Budischak SA, Corstjens PLAM, Ezenwa VO, Smith M, et al. Host
immunity, nutrition and coinfection alter longitudinal infection patterns of schistosomes in a free ranging African buffalo population. PLoS Negl Trop Dis (2017) 11(12):e0006122. doi:10.1371/journal.pntd.0006122

Benjamini Y, Yekutieli D. The control of the false discovery rate in multiple testing under
dependency. Ann Statist (2001) 29(4):665–1188.

Blackwell M. The fungi: 1,2,3…5.1 million species? Am J Bot (2011) 98(3):426–38. doi:10.3732/ajb.1000298

Brierley L, Vonhof MJ, Olival KJ, Daszak P, Jones KE. Quantifying global drivers of zoonotic bat viruses: a process-based perspective. Am Nat (2016) 187(2):E53–64. doi:10.1086/684391

Ceciliani F, Ceron JJ, Eckersall PD, Sauerwein H. Acute phase proteins in ruminants. J Proteomics (2012) 75(14):4207–31. doi:10.1016/j.jprot.2012.04.004

Colwell DD, Dantas-Torres F, Otranto D. Vector-borne parasitic zoonoses: emerging scenarios and new perspectives. Vet Parasitol (2013) 182(1):14–21. doi:10.1016/j.vetpar.2011.07.012

Couch CE, Movius MA, Jolles AE, Gorman ME, Rigas JD, Beechler BR. Serum biochemistry panels in African buffalo: defining reference intervals and assessing variability across season, age, sex. PLoS One (2017) 12(5):e0176830. doi:10.1371/journal.pone.0176830

Cray C, Zaias J, Altman NH. Acute phase response in animals: a review. Comp Med (2009) 59(6):517–26.

Cray C, Hammond E, Haefele H. Acute phase protein and protein electrophoresis values for captive Grant's zebra (*Equus burchelli*). J Zoo Wildl Med (2013) 44(4):1107–10. doi:10.1638/2013-0033R.1

Daszak P, Berger L, Cunningham AA, Hyatt AD, Green DE, Speare R. Emerging infectious diseases and amphibian population declines. Emerg Infect Dis (1999) 5(6):735–48. doi:10.3201/eid0506.990601

Dugovich BS, Peel MJ, Palmer AL, Zielke RA, Sikora AE, Beechler BR, et al. Detection of bacterial-reactive natural IgM antibodies in desert bighorn sheep populations. PLoS One (2017) 12(6):e0180415. doi:10.1371/journal. pone.0180415

Ezenwa VO, Jolles AE, O'Brien MP. A reliable body condition scoring technique for estimating condition in African buffalo. Afr J Ecol (2009) 47(4):476–81. doi:10.1111/j.1365-2028.2008.00960.x

Ezenwa VO, Jolles AE. Opposite effects of anthelmintic treatment on microbial infection at individual versus population scale. Science (2015) 347: 175–7. doi:10.1126/science.1261714

Genton C, Cristescu R, Gatti S, Levréro F, Bigot E, Caillaud D, et al. Recovery potential of a western lowland gorilla population following a major Ebola out- break: results from a ten year study. PLoS One (2012) 7(5):e37106. doi:10.1371/journal.pone.0037106

Godson DL, Campos M, Attah-Poku SK, Redmond MJ, Corediro DM, Manjeet SS, et al. Serum haptoglobin as an indicator of the acute phase response in bovine respiratory disease. Vet Immunol Immunopathol (1996) 51(3–4):277–92. doi:10.1016/0165-2427(95)05520-7

Graham AL, Allen JE, Read AF. Evolutionary causes and consequences of immunopathology. Annu Rev Ecol Evol Syst (2005) 36(1):373–97. doi:10.1146/annurev.ecolsys.36.102003.152622

Guerrant RL, Walker DH, Weller PF. Tropical Infectious Diseases. Edinburgh: Elsevier (2011).

Heard MJ, Smith KF, Ripp KJ, Berger M, Chen J, Dittmeier J, et al. The threat of disease increases as species move toward extinction. Conserv Biol (2013) 27(6):1378–88. doi:10.1111/cobi.12143

Hegemann A, Pardal S, Matson KD. Indices of immune function used by ecologists are mostly unaffected by repeated freeze-thaw cycles and methodological deviations. Front Zool (2017) 14:43. doi:10.1186/s12983-017-0226-9

Höfner MC, Fosbery MW, Eckersall PD. Haptoglobin response of cattle infected with foot-and-mouth disease virus. Res Vet Sci (1994) 57(1):125–8. doi:10.1016/0034-5288(94)90093-0

Ingersoll TE, Sewall BJ, Amelon SK. Effects of white-nose syndrome on regional population patterns of 3 hibernating bat species. Conserv Biol (2016) 30(5):1048–59. doi:10.1111/cobi.12690

Jones KE, Patel NG, Levy MA, Storeygard A, Balk D, Gittleman JL, et al. Global trends in emerging infectious disease. Nature (2008) 451:990–3. doi:10.1038/nature06536

Jolles AE, Cooper DV, Levin SA. Hidden effects of chronic tuberculosis in African buffalo. Ecology (2005) 86(9):2358–64. doi:10.1890/05-0038

Kelser EA. Meet dengue's cousin, Zika. Microbes Infect (2016) 18(3):163–6. doi:10.1016/jmicinf.2015.12.003

Krogh AK, Lundsgaard JF, Bakker J, Langermans JA, Verreck FA, Kjelgaard-Hansen M, et al. Acute-phase responses in healthy and diseased rhesus macaques (*Macaca mulatta*). J Zoo Wildl Med (2014) 45(2):306–14. doi:10.1638/2013-0153R.1

Kuznetsova A, Brockhoff P, Christensen RHB. lmerTest: Tests in Linear Mixed Effects Models. R Package Version 2.0-33 (2016). Available from: https://CRAN.R project.org/package=lmerTest.

Macpherson CN. The epidemiology and public health importance of toxocariasis: a zoonosis of global importance. Int J Parasitol (2013) 43(12–13): 999–1008.

doi:10.1016/j.ijpara.2013.07.004
Marree F, de Klerk-Lorist LM, Gubbins S, Zhang F, Seago J, Pérez-Martin E, et al. Differential persistence of foot-and-mouth disease virus in African buffalo is related to virus virulence. J Virol (2016) 90(10):5132–40. doi:10.1128/ JVI.00166-16
Maynard J, van Hooidonk R, Harvell CD, Eakin CM, Liu G, Willis BL, et al. Improving marine disease surveillance through sea temperature monitoring, outlooks and projections. Phil Trans R Soc (2016) 371:20150208. doi:10.1098/rstb.2015.0208
McKenzie A. The Capture and Care Manual: Capture, Care, and Accommodation, and Transportation of Wild African Animals. Lynwood Ridge, South Africa: South African Veterinary Foundation (1993).
McNulty C. African Buffalo as Reservoir Hosts for Infectious Respiratory Pathogens in Kruger National Park. MS Thesis, University of Wisconsin- Madison College of Veterinary Medicine, South Africa (2015).
Menge BA, Cerny-Chipman EB, Johnson A, Sullivan J, Gravem A, Chen F. Insights into differential population impacts, recovery, predation rate and temperature effects from long-term research. PLoS One (2016) 11(5): e0153994. doi:10.1371/journal.pone.0153994
Meyer Steiger DB, Ritchie SA, Laurance SGW. Mosquito communities and disease risk influenced by land use change and seasonality in the Australian tropics. Parasit Vectors (2016) 9:387. doi:10.1186/s13071-016-1675-2
Metzker M. Sequencing technologies – the next generation. Nat Rev Genet (2010) 11(1):31–46. doi:10.1038/nrg2626
Mogensen TH. Pathogen recognition and inflammatory signaling in innate immune defenses. Clin Microbiol Rev (2009) 22(2):240–73. doi:10.1128/ CMR.00046-08
Murphy K. Janeway's Immunobiology. New York, USA: Taylor & Francis Inc. (2011).
Openshaw JJ, Hegde S, Sazzad HM, Khan SU, Hossain MJ, Epstein JH, et al. Increased morbidity and mortality in domestic animals eating dropped and bitten fruit in Bangladeshi villages: implications for zoonotic disease transmission. Ecohealth (2016) 13(1):39–48. doi:10.1007/s10393-015-1080-x
Pérez JM, Meneguz PG, Dematteis A, Rossi L, Serrano E. Parasites and conservation biology: the 'ibex-ecosystem'. Biodivers Conserv (2006) 15:2033–47. doi:10.1007/s10531-005-0773-9
Petti CA. Detection and identification of microorganisms by gene amplification and sequencing. Clin Infect Dis (2007) 44(8):1108–14. doi:10.1086/512818
Polley L. Navigating parasite webs and parasite flow: emerging and re- emerging parasitic zoonoses of wildlife origin. Int J Parasitol (2005) 35 (11–12):1279–94. doi:10.1016/j.ijpara.2005.07.003
Preston DL, Mishler JA, Townsend AR, Johnson PTJ. Disease ecology meets ecosystem science. Ecosystems (2016) 19:737–48. doi:10.1007/ s10021-016-9965-2
Price SJ, Garner TWJ, Cunningham AA, Langton TES, Nichol RA. Reconstructing the emergence of a lethal infectious disease of wildlife sup- ports a key role for spread through translocations by humans. Proc Biol Sci (2016) 283:20160952. doi:10.1098/rspb.2016.0952
R Core Team. R: A Language and Environment for Statistical Computing. Vienna, Australia: R Foundation for Statistical Computing (2015).

Rodicio MR, Mendoza MC. Identification of bacteria through 16S rRNA sequencing: principles, methods, and applications in clinical microbiology. Enferm Infecc Microbiol Clin (2004) 22(4):238–45. doi:10.1157/13059055

Rodrigues MC, Cooke RF, Marques RS, Cappellozza BI, Arispe SA, Keisler DH, et al. Effects of vaccination against respiratory pathogens on feed intake, metabolic, and inflammatory responses in beef heifers. J Anim Sci (2015) 93(9):4443–52. doi:10.2527/jas.2015-9277

Rowley AF. The evolution of inflammatory mediators. Mediators Inflamm (1996) 5(1):3–13. doi:10.1155/S0962935196000014

Sander SJ, Joyner PH, Cray C, Rostein DS, Aitken-Palmer C. Acute phase proteins as a marker of respiratory inflammation in Prezewalski's horse (*Equus ferus prezwalski*). J Zoo Wildl Med (2016) 47(2):654–8. doi:10.1638/2015- 0059.1

Sears BF, Rohr JR, Allen JE, Martin LB. The economy of inflammation: when is less more? Trends Parasitol (2011) 27(9):382–7. doi:10.1016/j.pt.2011. 05.004

Shears P, O'Dempsey TJD. Ebola virus disease in Africa: epidemiology and nosocomial transmission. J Hosp Infect (2015) 90(1):1–9. doi:10.1016/j. jhin.2015.01.002

Smith KF, Sax DF, Lafferty KD. Evidence for the role of infectious disease in species extinction and endangerment. Conserv Biol (2006) 20(5):1349–57. doi:10.1111/j.1523-1739.2006.00524.x

Smitka P, Tóthová C, Curlík J, Lazar P, Bíres J, Posiváková T. Serum concen- tration of haptoglobin in European mouflon (Ovis musimon L.) from a game reserve. Acta Vet Brno (2015) 84:25–8. doi:10.2754/avb201584010025

Stenfeldt C, Heegaard PMH, Stockman A, Tjomehoj K, Belsham GJ. Analysis of the acute phase responses of serum amyloid A, haptoglobin and type 1 interferon in cattle experimentally infected with foot-and-mouth disease virus serotype O. Vet Res (2011) 42:66. doi:10.1186/1297-9716-42-66

Takeda K, Kaisho T, Akira S. Toll-like receptors. Annu Rev Immunol (2003) 21:335–76. doi:10.1146/annurev.immunol.21.120601.141126

Thompson RCA, Lymbery AJ, Smith A. Parasites, emerging disease and wildlife conservation. Int J Parasitol (2010) 40(10):1163–70. doi:10.1016/j.ijpara.2010.04.009

Vandegrift KJ, Wale N, Epstein JH. An ecological and conservation perspective on advances in the applied virology of zoonoses. Viruses (2011) 3(4):379–97. doi:10.3390/v3040379

Vosloo W, Thomson GR. Natural habitats in which foot-and-mouth disease viruses are maintained. In: Sobrino F, Domingo E, editors. Foot-and-Mouth Disease Virus: Current Research and Emerging Trends. Madrid, Spain: CSIC- UAM (2017). p. 179–210.

Vurro M, Bonciani B, Vannacci G. Emerging infectious diseases of crop plants in developing countries: impact on agriculture and socio-economic consequences. Food Sec (2010) 2:113. doi:10.1007/s12571-01-00627

Woolhouse M, Scott F, Hudson Z, Howey R, Chase-Topping M. Disease invasion impacts on biodiversity and human health. Philos T R Soc B (2012) 367(1604):2804–6. doi:10.1098/rstb.2012.0331

Xavier R, Turck N, Hainard A, Tiberti N, Lisacek F, Sanchez J, et al. pROC: an open-source package for R and S+ to analyze and compare ROC curves. BMC

Bioinformatics (2011) 12:77. doi:10.1186/1471-2105-12-77

Table 2.1 Foot-and-mouth disease virus (FMDV) experiment: mean (±SE) baseline non-specific marker of inflammation (NSMI) concentration, peak NSMI concentration, days from FMDV incidence to peak concentration and days elevated from viral clearance for the FMDV virus.

NSMI	# buffalo that responded	Baseline concentration (ng/mL)		Peak concentration (ng/mL)		Days to peak		Days elevated post viral clearance	
		Mean	S.E.	Mean	S.E.	Mean	S.E.	Mean	S.E.
Haptoglobin	11	401.26	22.38	491890.80	22722.45	5.40	0.29	21.23	0.39
Serum amyloid A	11	273.46	20.02	13806.46	135.45	3.33	1.17	11.18	2.66
TNF-α	3	0.88	0.45	3.18	1.61	6.67	0.19	7.75	2.56
IFNγ	11	0.52	0.08	7.30	0.49	4.40	0.30	16.51	1.74

Animals were considered to have mounted a NSMI response if NSMI concentration exceeded 2× baseline concentration after FMDV infection; with a total of 11 animals participating in the study. Days to peak was calculated by counting the number of days between the first day FMDV RNA copies exceeded 3.2 copies/5 µl of serum and the day NSMI reached peak concentration. Days elevated from viral clearance was calculated by estimating the time it took for NSMI to return to baseline concentrations after viral clearance (when FMDV RNA copies were less than 3.2 copies/5 µl serum post FMDV incidence). If peak concentrations were only reached on day 30, animals were excluded from mean calculations of days to peak and days elevated from viral

clearance. Notably, mean peak concentration for haptoglobin was approximately 1,226 times higher than mean baseline levels, 50 times higher for SAA, 14 times higher for IFNγ, and four times higher for TNF-α.

Table 2.2. Cohort study: results of logistic regression models examining the non-specific markers of inflammation (NSMI) as indicators of recent (2–3 months) parasite exposure after accounting for body condition, sex, age, season, and animal id.

Table 2.2

NSMI	Pathogen	β	SE	Test statistic	FDR sig level	*p*-value
$\log_2$ (Haptoglobin)						
	BHV	−0.06	0.04	−1.66	0.02	0.097
	PI-3	0.12	0.04	3.21	0.01	0.001
	BRSV	−0.06	0.06	−1.03	0.04	0.656
	BVDV	−0.03	0.04	−0.79	0.03	0.431
	AD-3	0.01	0.04	0.38	0.05	0.707
	MB	0.19	0.06	3.18	0.01	0.001
	MH	−0.02	0.04	−0.59	0.04	0.554
$\log_2$ (Serum amyloid A)						
	BHV	−0.04	0.02	−1.95	0.01	0.05
	PI-3	0.003	0.02	0.18	0.05	0.86
	BRSV	−0.03	0.03	−1.02	0.04	0.31
	BVDV	−0.1	0.08	−1.47	0.03	0.14
	AD-3	0.01	0.02	0.61	0.04	0.54
	MB	0.36	0.19	1.88	0.01	0.06
	MH	−0.05	0.03	−1.74	0.02	0.08
TNF-**α**						
	BHV	−0.19	0.31	−0.62	0.04	0.54
	PI-3	−0.32	0.26	−1.23	0.01	0.22
	BRSV	−0.63	0.71	−0.88	0.02	0.38
	BVDV	−0.24	0.36	−0.68	0.03	0.50
	AD-3	−0.10	0.21	−0.47	0.04	0.64
	MB	0.28	0.23	1.19	0.01	0.23
	MH	−0.06	0.24	−0.27	0.05	0.78
IFN**γ**						
	BHV	−0.77	0.59	−1.32	0.03	0.19
	PI-3	0.20	0.18	1.12	0.04	0.26
	BRSV	−3.63	2.19	−1.66	0.02	0.10
	BVDV	0.17	0.15	1.19	0.04	0.23
	AD-3	0.35	0.18	1.91	0.01	0.06
	MB	−2.23	1.03	−2.16	0.01	0.03
	MH	0.27	0.29	0.13	0.05	0.90

FDR significance levels are false discovery rate significance levels, which avoid issues for false positives that can occur when using multiple testing procedures. Bold values indicate statistically significant relationships.

Figure 2.1. A schematic illustrating the study design and analysis for the foot-and-mouth disease virus (FMDV) experiment and cohort buffalo longitudinal study. The bar graph (cohort study, middle panel) depicts the number of new cases throughout the study period of seven respiratory parasites. The number of new cases of viral parasites are displayed in dark gray (ad3 = Adenovirus; bhv = bovine herpes virus II; brsv = bovine respiratory syncytial virus; bvdv = bovine viral diarrheal virus; pi3 = Parainfluenza virus), the number of new cases of bacterial parasites are displayed in light gray (mb = *Mycoplasma bovis*, mh = *Mannheimia haemolytica*). The line graphs (FMDV experiment, bottom panel) illustrate the exponential decay curve fit from day of peak NSMI concentration to day NSMI returned to baseline for each animal. All animals mounted haptoglobin, SAA, and IFNγ responses, however, only three animals mounted a TNF-α response

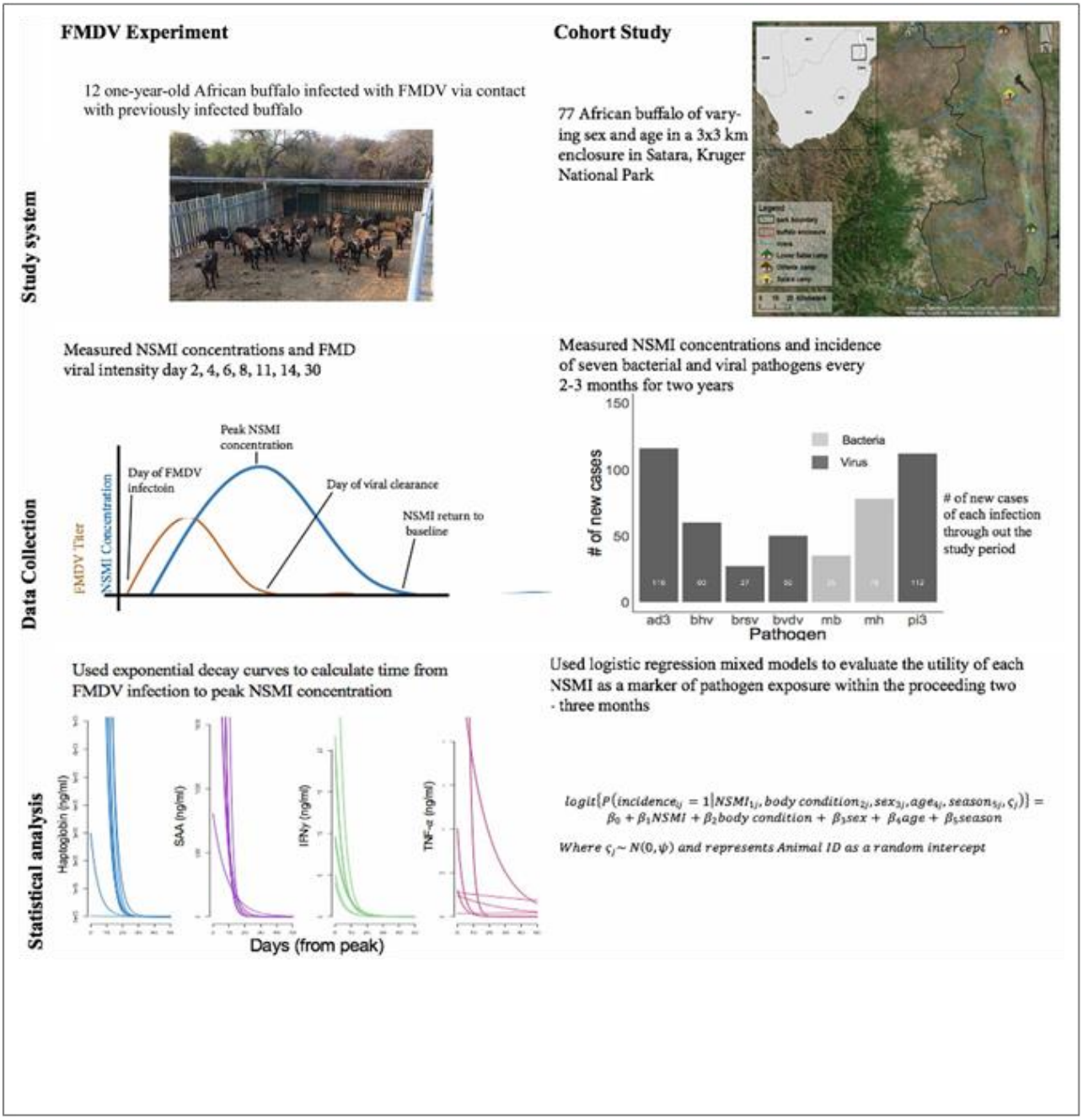
Study system
FMDV Experiment
12 one-year-old African buffalo infected with FMDV via contact with previously infected buffalo
Cohort Study
77 African buffalo of varying sex and age in a 3x3 km enclosure in Satara, Kruger National Park
Data Collection
Measured NSMI concentrations and FMD viral intensity day 2, 4, 6, 8, 11, 14, 30
Peak NSMI concentration
Day of FMDV infectoin
Day of viral clearance
NSMI return to baseline
FMDV Titer
NSMI Concentration
Measured NSMI concentrations and incidence of seven bacterial and viral pathogens every 2-3 months for two years
# of new cases
Bacteria
Virus
# of new cases of each infection through out the study period
ad3
bhv
brsv
bvdv
mb
mh
pi3
Pathogen
Statistical analysis
Used exponential decay curves to calculate time from FMDV infection to peak NSMI concentration
Haptoglobin (ng/ml)
SAA (ng/ml)
IFNγ (ng/ml)
TNF-α (ng/ml)
Days (from peak)
Used logistic regression mixed models to evaluate the utility of each NSMI as a marker of pathogen exposure within the proceeding two - three months
$logit\{P(incidence_{ij} = 1 | NSMI_{1j}, body\ condition_{2j}, sex_{3j}, age_{4j}, season_{5j}, \zeta_j)\} = \beta_0 + \beta_1 NSMI + \beta_2 body\ condition + \beta_3 sex + \beta_4 age + \beta_5 season$
Where $\zeta_j \sim N(0, \psi)$ and represents Animal ID as a random intercept

Figure 2.1

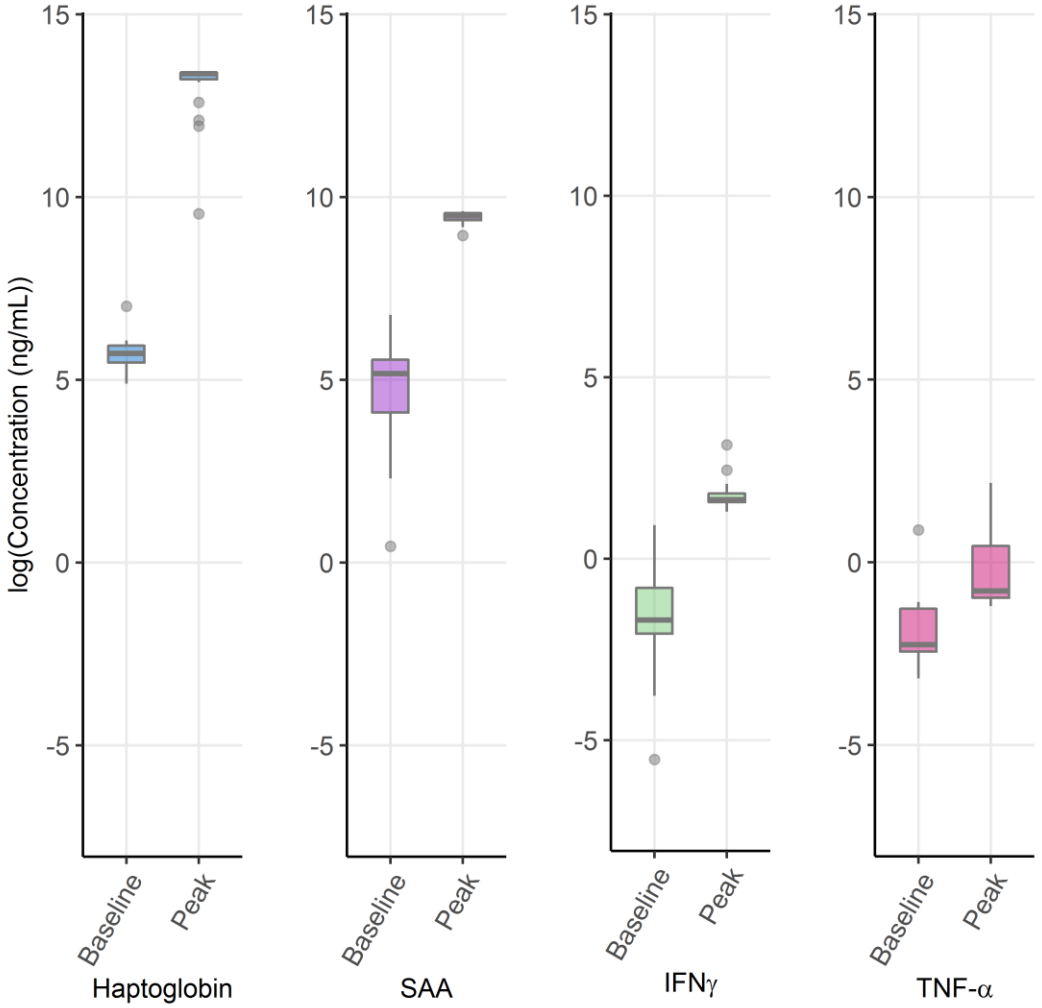

Figure 2.2. Foot-and-mouth disease virus experiment: mean baseline and peak NSMI. Y axes are log transformed for ease of visual comparison between non-specific markers of inflammation peak and baseline concentrations. Haptoglobin peak and baseline concentrations displayed the greatest difference and least variability followed by serum amyloid A (SAA), IFNγ, and TNF-α. The horizontal bands represent the 25, 50, and 75% quartiles whereas the vertical lines represent 1.5 times the interquartile range above the upper quartile and below the lower quartile, and dots represent outliers.

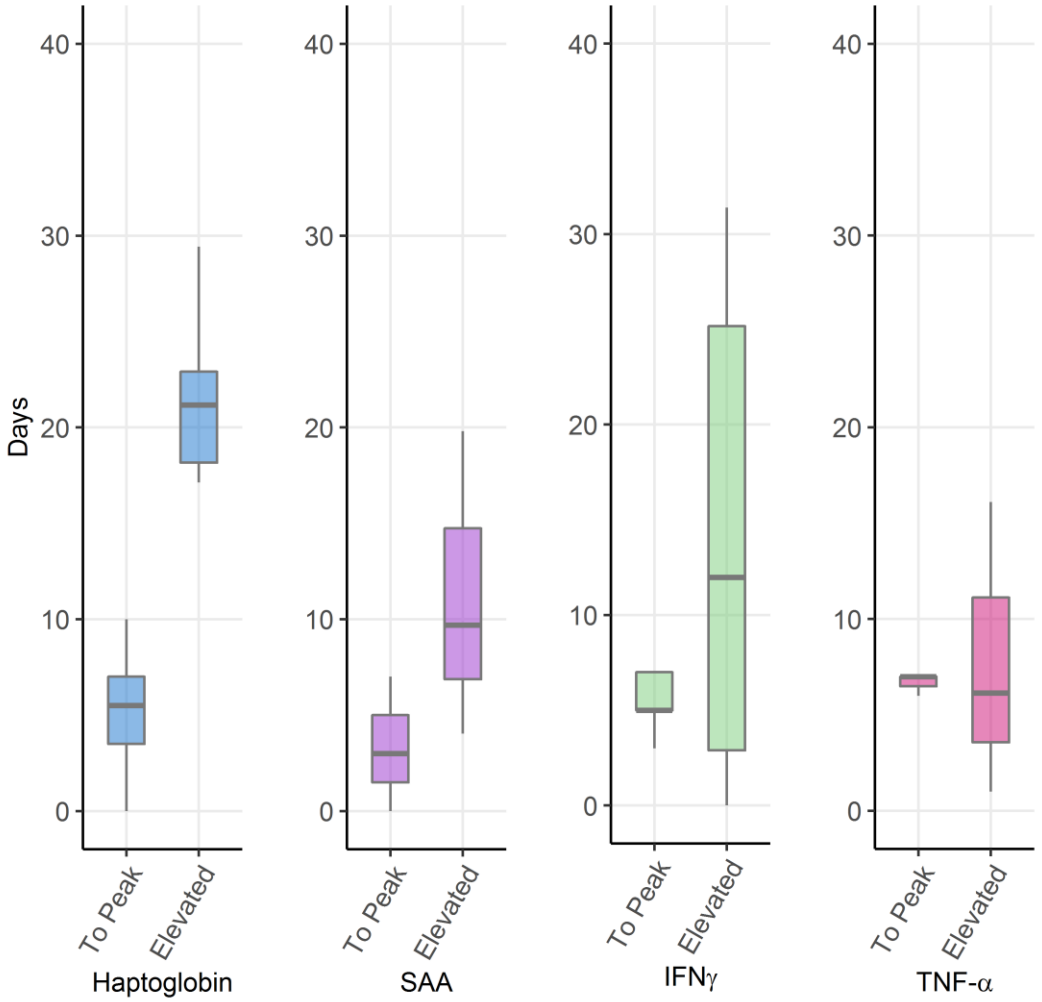

Figure 2.3 Foot-and-mouth disease virus experiment: time from first day of FMDV infection to peak non-specific markers of inflammation concentration and time NSMI remained elevated after viral clearance. On average, all NSMI concentrations reached peak in 3–7 days. Haptoglobin concentrations remained elevated the longest past viral clearance, with the least variability, followed by serum amyloid A (SAA), IFNγ, and TNF-α. Individuals where NSMI concentrations peaked on day 30 were excluded from calculations as this was thought to be due to a secondary infection. The horizontal bands represent the 25, 50, and 75% quartiles, whereas the vertical lines represent 1.5 times the interquartile range above the upper quartile and below the lower quartile, and dots represent outliers.

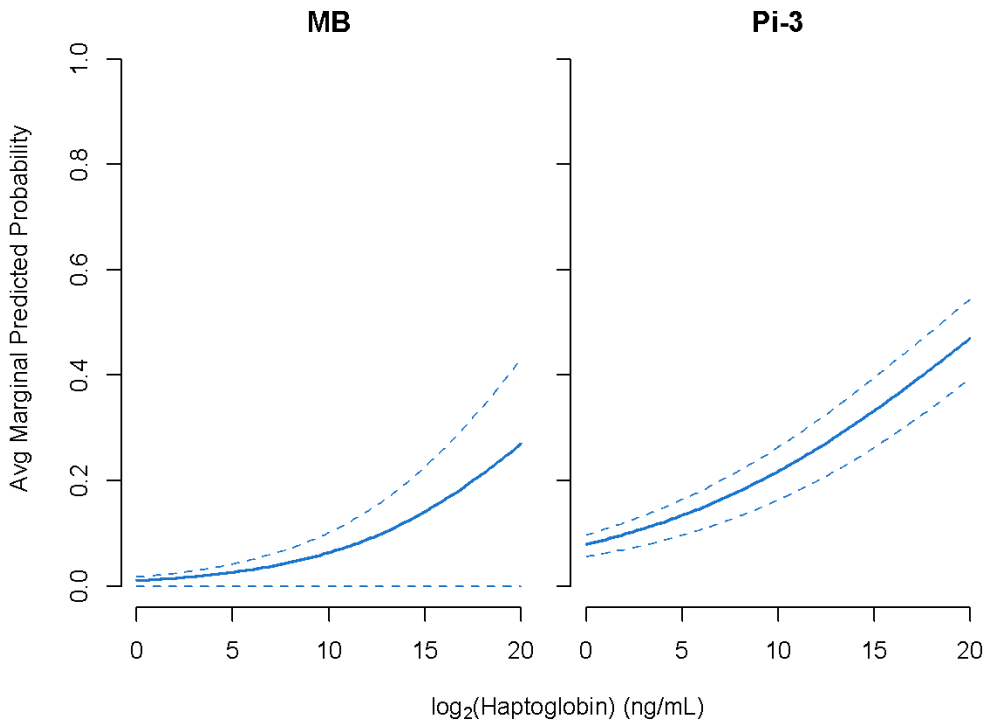

Figure 2.4 Cohort study: elevated haptoglobin was associated with *Mycoplasma bovis* (MB) and parainfluenza virus (Pi-3) exposure during the preceding 2–3 months. Y axes show average marginal predicted probabilities of pathogen incidence. Marginal predicted probabilities were calculated using models described in Eq. 4. 1,000 marginal predicted probabilities of pathogen incidence were calculated for 100 fixed values of NSMI and randomly selected (from the data) values of age, sex, body condition, season, and animal id. Average marginal predicted probability and 95% CI intervals for parasite incidence were then constructed from the 1,000 values calculated for each fixed NSMI concentration. Due to large seasonal variation, the lower confidence interval of MB is slightly higher than 0.

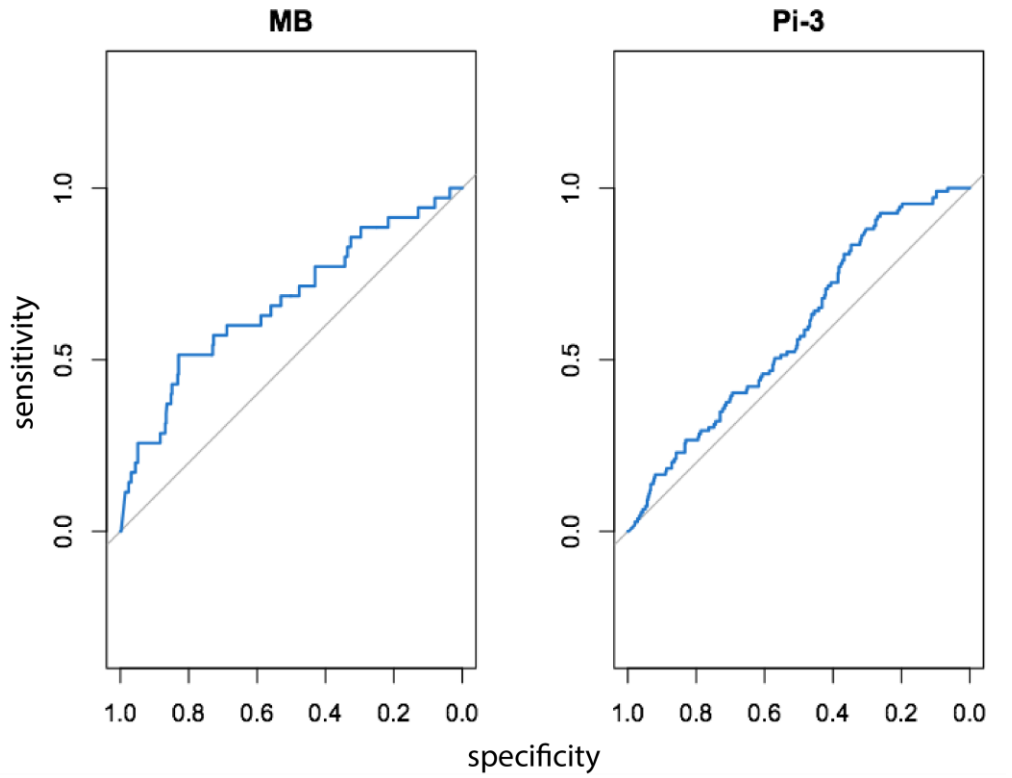

Figure 2.5 Cohort study: area under the curve (AUC) for detection of Mycoplasma bovis (MB) and Parainfluenza Virus (Pi-3) based on elevated haptoglobin. AUC, or the area under the receiving operating characteristic (ROC) curve, is a standard diagnostic analysis used to measure how well a parameter can distinguish between two diagnostic groups based on the specificity (true negative rate) and sensitivity (true positive rate) of the test. The gray line represents the trend the diagnostic parameter would follow if the AUC was equal to 0.5. The blue line represents the observed trend; the closer the curve follows the left and top border of the graph, the more accurate the test. If the blue line falls below the gray line (AUC < 0.5), it indicates that the test is not significantly better than random.

CHAPTER 3: FACTORS EXPLAINING VARIATION IN UPPER RESPIRATORY INFECTION IN A WILDLIFE HOST ARE DISTINCT DESPITE FUNCTIONAL SIMILARITIES AMONG PATHOGENS

Abstract

The dynamics of directly transmitted pathogens in natural populations are likely to result from the combined effects of seasonal variation in host physiological status, pathogen biology and interactions among pathogens within a host. Discovering how these factors work in concert to shape temporal variation in pathogen dynamics in natural host – multi-pathogen systems is fundamental to understanding population health. Here, we elucidate the effect of host trait and pathogen co-occurrence on within-host pathogen occurrence and relate findings to temporal trends in population-level disease dynamics (incidence) using one of the most comprehensive studies of co-infection in a wild population: a suite of seven directly-transmitted respiratory infections, all associated with the economically impactful bovine respiratory disease complex (BRDC), from a four-year study of 200 free-ranging African buffalo (*Syncerus caffer*). Occurrence of upper respiratory infections was common among buffalo throughout the study. The strongest indicator of single-pathogen occurrence for respiratory viruses within our system was, in fact, pathogen co-occurrence. The strongest predictor for respiratory bacterial was host ID. We observed distinct seasonal peaks in incidence of four out seven pathogens and bovine-syncytial virus exhibited clear outbreak dynamics in our final study year. Co-occurrence dynamics as well as a handful of host traits may explain these trends. However, we observed a large portion of unexplained variation in within-host occurrence suggesting that there are a number of other physiological, behavioral, environmental and, perhaps, higher-level processes influence temporal patterns in population level disease dynamics. Our study indicates new avenues of research for monitoring and managing BRDC, especially at this wildlife-livestock interface.

3.1 Introduction

A central goal of epidemiology and disease ecology is to understand and predict the dynamics of infectious diseases in host populations. Work in these fields have emphasized the fundamental role of fluxes in the proportion of susceptible, infected, and recovered hosts in determining disease dynamics by reproducing the range of temporal patterns seen in nature – from cyclic to endemic – with elegantly simple models. However, beyond modelling general disease dynamic patterns, understanding temporal variation in disease incidence has remained challenging (Germann et al., 2006, Hall et al., 2006).

Even in the simplest case of direct pathogen transmission between hosts, temporal patterns in disease dynamics are likely to result from the interplay between variation in host behavior and physiology, and factors affecting pathogen viability outside the host. Contact patterns among hosts can change dramatically in response to seasonal fluctuations in aggregation (e.g., during breeding seasons) or changes in the distribution of resources (e.g., convening near water during dry periods), and this can drive variability in pathogen transmission. For example, rotavirus, measles and *Streptococcus pneumoniae* outbreaks have all been linked to aggregation of children during the fall school term (Fine & Clarkson 1982; Cook et al., 1990; Dowell et al., 2003). Likewise, raccoons (*Procyon lotor)* with clumped food resources had higher prevalence of directly transmitted parasites than those populations with dispersed resources (Wright & Gompper 2005). The availability of susceptible hosts may also change with seasonal or annual shifts in immune and reproductive status of hosts (Nelson & Demas 1996; Jolles, Beechler & Dolan 2015). For instance, outbreaks of ovine pneumonia in bighorn sheep (*Ovis canadensis*) tend to co-occur with the peak of the mating season in the fall (Cassirer et al., 2013). Finally, pathogen viability outside the host can change with humidity, temperature and exposure to UV radiation which allows risk forecasting based on meteorological information for some pathogens, such as cholera (Colwell 1996) and influenza (Lowen et al., 2007).

Though less well understood, interactions among pathogens infecting the same hosts can add yet another layer of complexity to temporal patterns of disease transmission. For example, in human childhood diseases, temporary (i.e. quarantine) or

permanent (i.e. death) removal of hosts from the susceptible pool due to one pathogen, can slow transmission of a secondary pathogen, resulting in biennial disease cycles, instead of annual cycles that would be expected if the two pathogens were circulating independently (Rohani et al., 1998; Huang & Rohani 2006). Within a host, co-occurring pathogens can also interact either directly through competition for shared resources or indirectly through immune-mediated interactions (Graham 2008; Griffiths et al., 2011). Effects of these interactions on the transmission dynamics of one or both co-infecting pathogens have been demonstrated (Telfer et al., 2010; Beechler et al., 2015; Susi et al., 2015; Gorsich et al., 2019); and in some cases co-infecting pathogens appear to equal or outweigh environmental and host factors in importance as predictors of infection (Telfer et al., 2010; Henrichs et al., 2016).

Discovering how host, pathogen, and environmental factors interact to shape variation in infection risk in typical but complex multi-pathogen systems within hosts (Cox 2001; Pedersen & Fenton 2007) is fundamental to understanding population health in the context of rapidly changing environments and ultimately, to the development of adaptive disease management strategies. Yet, the breadth and depth of data needed to dissect the causes of multi-pathogen disease dynamics in natural populations are rarely attainable: longitudinal studies assessing multiple, potentially co-infecting pathogens, and detailed data on host physiological status across different seasons.

Here we present such data from a four-year study of 200 free-ranging, female African buffalo (*Syncerus caffer*) in Kruger National Park, South Africa. Every six months, buffalo were captured, screened for seven directly transmitted respiratory pathogens (Table 3.1), and their physical and reproductive status evaluated (Table 3.2). Specifically, we monitored host factors that have been shown to correlate with disease susceptibility and contact frequency (body condition, reproductive status, age, herd association, co-infection (Rodwell, Whyte & Boyce 2001; Keeling & Rohani 2008; Gorsich et al., 2015)) in a population where half of the individuals were treated with an anthelmintic drug (Ezenwa & Jolles 2015).

We ask: (1) What is the relative significance of host traits and pathogen co-occurrence on within-host pathogen occurrence of seven respiratory pathogens and (2) do

host-traits and co-occurrence patterns elucidate monthly and annual population-level disease incidence?

For our first question, we used a joint-species distribution model (JSMD) to partition the variance in disease occurrence associated with host traits (Table 3.2), variation and co-variation (pathogen co-occurrence) associated with sample, host ID, year. The pathogens we investigate are associated with the common, but economically destructive (Griffin 1997), bovine respiratory disease complex (BRDC) in cattle (Lillie 1974). Within BRDC, viruses (Pi-3, AD-3, BVDV, BHV, BRSV) typically occur simultaneously within a host, or nearly so, and are then followed by bacterial infections (MH and/or MB) (Smith et al., 2019). Thus, we hypothesized that concomitant viral infection would explain the largest portion of variation in virus occurrence. We further expected that host traits associated with contact rates and networks (i.e., pregnancy and calf status (Swain et al., 2105), food availability via body condition (Spaan et al., 2019), herd association (Krause et al., 2015)) would explain a moderate but secondary portion of variance in virus occurrence.

In BRDC, bacterial infections occur subsequent to viral infections, so we expected bacterial infections to be weak indicators of viral infections and vice versa. Though, we did expect some co-variacen between MH and pathogens known to significantly damage the respiratory tract, namely Pi-3, BHV, BRSV and BVDV ((Lopez, Thomson & Savan 1976; Rice et al., 2007; Srikumaran, Kelling & Ambagala 2007). Instead, we expected that host traits associated with immunocompetence (e.g., lactation (Mallard et al., 1998; Trillmich et al., 2020), poor body condition, and age-horn residuals (Ezenwa & Jolles 2008)) would explain the most variation in bacterial infection because the bacterial infections we studied here are typically commensal microbes that become virulent under stressful conditions.

To answer our second question, we characterized monthly and yearly trends in pathogen occurrence to determine whether the results of our JSDM align with temporal variation in population-level disease dynamics, thereby corroborating the effects of seasonal variation on host traits. We hypothesized that if within-host pathogen occurrence was mostly predicted by variables that describe seasonally fluctuating behaviors or changes in immune status, such as body condition or reproductive status, then we would

observe similarly timed seasonal trends in population-incidence rates. For example, if we found a correlation between pathogen occurrence and body condition, which might indicate the importance of contact rates due to seasonal resource aggregation (Spaan et al., 2019), then we would expect peak occurrence during the wet season (November-April). Likewise, if the JDSMs suggest a correlation between pathogen occurrence and pregnancy status or calf status (i.e. whether a female was caring for calf), then we would expect to see seasonal peaks in pathogen occurrence either before December or after January, respectively, because the main calving season is December – January.

In absence of any clear markers of temporal variation in our JSDM, the temporal trend analyses may indicate the effects of variables that were not included in the initial JDSM. For example, our study design enrolled similarly-aged animals, so the range in age was small and the herds collectively aged. So, if we observed a sustained decline in pathogen occurrence it may indicate that as animals gain acquired immunity over time (Simon et al., 2015). Static host traits including herd (representing similar contacts and shared resources) and age-horn residuals (representing static host quality and immuno-competence) may obscure any temporal trends in occurrence.

3.2 Methods

3.2.1. Study area

Kruger National Park (KNP) is located in the north-eastern corner of South Africa between 22.5 and 25.5°S, and 31.0 and 31.6°E (Supp fig 1). The area of the KNP is 19,485 km^2, but since 2002, the area available to wildlife has effectively doubled due to the removal of fences between private game reserves in the west and Mozambique in the east. The population of African buffalo in the park is about 37,000 animals (SANPARKS 2010-2011). Our four-year project was restricted to buffalo in the southern KNP and took place between June 2008 and June 2012.

On average, 84% of KNP's total rainfall is concentrated between November to April (Zambatis 2003) with approximately 600 mm of rainfall per year in the southern KNP (Venter & Gertenbach 1986). The dry season typically occurs May – October. Rather than using calendar year in our analyses, we used rainfall year, hereafter referred to as "year," with year commencing in November.

3.2.2. Sampling regime

Young (2-5 years old), female African buffalo were captured as part of a study on parasite interactions in free-ranging buffalo (Ezenwa & Jolles 2015). The first 100 buffalo were captured from the Lower Sabie herd between 23 June and 5 July, 2008 (Figure B1). The second 100 buffalo were captured from the Crocodile Bridge herd between 1 and 8 October, 2008 (Figure B1). Buffalo were re-captured approximately every 6 months after this initial capture, through June 2012. Any buffalo that died or emigrated from the study area during the study period was replaced with an animal of similar age so that a near-constant sample size of 200 was maintained at each capture (sampling design is explained in detail in Spaan et al., 2019).

3.2.3. Sample and data collection

Buffalo were located and identified via radio-collars (7 GPS collars to locate herds, 193 VHF collars to identify individuals). At capture, buffalo were chemically immobilized with etorphine hydrochloride (M99) and ketamine by darting from a truck or helicopter. Following sample and data collection, immobilization was reversed using diprenorphine (M5050).

While buffalo were immobilized, blood and host-trait data were collected from each animal. Blood samples for serological assays were collected via jugular venipuncture in sterile tubes containing no anticoagulant. Blood was placed on ice and stored in a cooler box within 5 minutes for transportation back to the laboratory. At the laboratory, serum was collected after centrifugation for 20 minutes at 2,000 *g* and stored at -20°C until analysis. Host-trait measures included age, body condition, horn width, pregnancy status, lactation status and calf-at-heel status using previously published methods (Table 2).

Half of the studied buffalo in each herd were administered an oral anthelmintic treatment in the form of a Panacur® slow-release bolus at every capture. The bolus contains the active ingredient fenbendazole. Nematode egg shedding is effectively eliminated in buffalo for ~160 days after a single administration (Ezenwa et al., 2010)

and alters African buffalo response to infection by microparasites (Ezenwa & Jolles 2015). The other half of each herd did not receive Panacur® at any capture.

All animal procedures were approved by SANParks internal research permit process, Oregon State University (ACUP 4478, ACUP 3267) and the University of Georgia (A2010 10-190-Y3-A5) Institutional Animal Care and Use Committees (IACUC), which follow the 8th Edition of the Guide for the Care and Use of Laboratory Animals (Guide), NRC 2011; the Guide for the Care and Use of Agricultural Animals in Research and Teaching (Ag Guide), FASS 2010; and the European Convention for the Protection of Vertebrate Animals Used for Experimental and Other Scientific Purposes, Council of Europe (ETS 123).

3.2.4. Serology

Buffalo sero-status for each of the respiratory pathogens were determined using commercially available assays after each capture, as previously described (Glidden et al., 2018). Briefly, monoclonal antibodies specific to the F protein of BRSV and the NS3 protein of BVDV were detected in serum using separate competitive ELISA kits (Bio-X Diagnostics, Belgium) while BHV, Pi-3, AD-3, MB and MH serostatuses were assessed using direct ELISA test kits (Bio-X Diagnostics, Belgium). Buffalo were tested for bTB using the BOVIGAM ELISA kit (Prionics, Switzerland) which is a standard whole blood interferon-gamma (IFNγ) assay (Wood & Jones 2001; Schiller et al., 2009). This kit in particular has been optimized for use in African buffalo (Michel et al., 2011).

3.2.5. Statistical analyses

3.2.5.1 Classifying occurrence

All animals were recruited as adults so it was impossible to determine whether the first detected increases in antibody titers were due to a primary exposure, re-exposure or recrudescence (Table 3.1). For this reason, we define pathogen “occurrence” to include all three possibilities. We expect the within-host and population-dynamics to be similar for each type of occurrence as they represent initiation of active, transmissible infections. Identical to Glidden et al., (2018), BRSV and BVDV were tested using a competitive

ELISA which give scores of 0-100% positive). Samples were deemed positive if ELISA scores were > 50%, per manufacturer instructions. If the animal was tested 6 or more times with only one, weakly positive (<65%) result, we assumed the test result was a false positive. Occurrence of BRSV or BVDV was counted if test results went from negative (<50%) to positive (>50%) or if positive animals had a 15+% increase in their competitive ELISA score from one capture to the next (Glidden et al., 2018). We observed low occurrence of BVDV and thus excluded it from further analyses (Figure 3.1). For BHV, Pi-3, AD-3, MH and MB, ELISAs were scored on a 0-5 scale and occurrence was counted if the ELISA score increased by 2 or more points between two captures, per manufacturer instructions. ELISA results were previously shown to correlate with other markers of inflammation and infection (Glidden et al., 2018).

bTB is an active, chronic infection that displays disparate behavior from the other pathogens of interest which are self-limiting or chronic but with latent periods (Table 3.1). For this reasons, we did not include it as one of our respiratory pathogens of interest. However, bTB correlates with a change in immune system signaling (Ezenwa & Jolles 2015, Tavalire et al., 2019) thus, we controlled for the effect of bTB by including if and when the animal converted to bTB positive as a host trait. To determine bTB conversion we considered an animal's full IFNγ bTB data set (all sampling points): an animal was considered to have become bTB positive only if we observed at least two consecutive negative tests followed by at least two consecutive positive tests (Ezenwa & Jolles 2015). Out of the animals included in our final data set (section 3.2.5.2), 72 converted to bTB+ throughout the study.

3.2.5.2 Estimating the relative significance of host traits, environment and pathogen co-occurrence on pathogen occurrence

Joint Species Distribution Models (JSDM) (Ovaskainen et al., 2017) allow for detection of abiotic (e.g., climate) and biotic (e.g., species interactions) on community assembly. As JSMD are hierarchical multivariate models, they allow us estimate the effect of specified covariates on pathogen occurrence as well as use the between-pathogen residual association to quantify pathogen co-variance (co-occurrence) after accounting for covariates that might underlie co-variance patterns (Ovaskainen et al.,

2017). Accounting for covariates that may underlie pathogen co-occurrence allows us hone in on true interactions versus species correlations. We fit our JSDM using Bayesian inference in the R package *Hmsc* (*Hierarchical Modelling of Species Communities*) (Ovaskainen et al., 2017). As a response matrix (Y matrix (Okaskainen et al., 2017)), we used the presence-absence of the six respiratory pathogens (probit models): Pi-3, AD-3, BHV, MH, MB, BRSV. As fixed effects (X matrix (Ovaskainen et al., 2017)), we included host traits hypothesized to influence within-host occurrence: age, capture herd, body condition, age-horn residual, pregnancy status, lactation status, calf at heel status (Table 3.2). As stated previously, bTB status and anthelmintic bolus status influence immune response (Ezenwa & Jolles 2015); thus, we controlled for the effect of each by including them as covariates in the X matrix. We also included season to account for seasonally-fluctuating host traits or pathogen biology (i.e., viability in the environment) not defined in our model. Continuous variables were rescaled by centering and dividing by two standard deviations in the R package *arm* (Gelman et al., 2008; Gelman 2018) so that effect sizes were comparable among continuous covariates.

We included three random effects in our model, at the sample-level, animal-level and year level thereby modeling variation in pathogen occurrence and co-occurrence within a single sample, within an individual over time and year (structure of random effects matrices described in detail in Ovaskainen et al., 2016). More specifically, the sample-level random effect describes co-variation among pathogens over time (i.e. pathogens are more likely or less likely to co-occur within a sample), after accounting for all other fixed and random effects (i.e., residual association) (Ovaskainen et al., 2016; Ovaskainen et al., 2017). The animal-level random effect (animal ID) describes residual variation derived from a pathogen occurring within the same host over many sampling points as well as the co-variation among pathogens within those hosts, after accounting for other fixed and random effects (residual association). Animals collectively aged throughout the study which means that any effect of age on occurrence could be confounded by study year. For this reason, we included year to control for the effect of year on pathogen occurrence. Similarly to sample and animal ID, the year-level random effect indicates whether a pathogen was more likely to occur in the same year and if pathogens are more or less likely to occur within the same year.

We evaluated model explanatory power using area under the receiving operator characteristic (AUC), root-mean-squared-error (RMSE) and Tjur's R^2. AUC measures the ratio between true and false positives. RMSE measures the squared difference between estimated occurrence and true species occurrence. Tjur's R^2 is a pseudo-R^2 used to evaluate model fit for logistic regressions (Tjur 2009). More specifically, Tjur's R^2 is the difference between the average predicted probability for every entered value of the dependent variable and the average predicted probability for each category (0 or 1) of the dependent variable (Okaskainen et al., 2017; Dallas et al., 2019). To compare the variation explained by each factor, we partitioned variance explained into specified host traits (Table 3.2) and season as well as sample, animal ID and year. We defined a variable as having strong statistical support if 95% of the posterior probability distribution did not overlap 0 and moderate statistical support if 90% of the posterior probability distribution did not overlap 0. We utilized flat priors (*Hmsc* default priors) as we did not have enough information about the system to estimate informative priors (described in full detail in Ovaskainen et al., 2017). We recorded 10,000 MCMC samples, which consist of a record from of a state from the MCMC chain, from four MCMC chains (the first 1000 of which were burn-in), while skipping 10 MCMC steps between samples. Visual inspection of MCMC traces, effective sample and the Gelman-Rubin diagnostic (a partial scale reduction factor) were used to assess model convergence. We included 705 samples from 191 individuals in our analyses.

3.2.5.3 Characterizing monthly and yearly variation in population-level disease dynamics

We examined population-level temporal trends in the number of new cases of each pathogen (incidence) using general additive models in the R package *mgcv* (Wood 2011). For the purposes of the model a new case was defined identically to "occurrence" in section 3.2.5.1. For each month of the study and for each pathogen, we summed the number of new cases and used this as the dependent variable (Poisson errors) in each model (six models total, one per pathogen). We included calendar month and rainfall year as independent, smooth terms. For month, the penalized smoothing basis was a cyclic cubic regression spline. We used a cyclic cubic regression spline because it allows us to account for months occurring in a loop since environmental conditions in the last month

of the year (December) are similar to the first month of the year (January) (Kiguchi & Minami 2012). For year, the penalized smoothing basis was a P-spline (Eliers & Marx 1996). Number of animals sampled per month-year was included as a fixed effect to account for sampling effort. For each pathogen, we selected the best fit model by selecting the model with the lowest second-order Akaike information criteria (AICc: Hurvich & Tsai 1989). We further evaluated model fit using deviance explained (Wood 2017). Model diagnostics were evaluated using the 'gam.check' function in the *mcgv* package which plots quantile-quantile plots of residuals, the linear predictor versus residuals, the histogram of residuals and the plot of fitted values versus response. We also used 'gam.check' to check whether the basis dimension for the smooth term was adequate. We omitted the first study year from the analyses because there was only two months of data for that year, which left a total of 43 sampling time points for these analyses.

3.3 Results

3.3.1. Summary of prevalence and co-infection rate

With the exception of BVDV, occurrence of respiratory infections in buffalo were common (Table 3.1): in a given six-month capture interval, nearly 50% of our study animals acquired at least one respiratory infection. Co-infection was also common: buffalo had between 0 and 4 pathogen occurrences at each sampling event, with an average of 1.34 occurrences of respiratory infections per animal per year (Figure 3.1.).

3.3.2. Estimating the relative significance of host traits, environment and pathogen co-occurrence on pathogen occurrence

Which factors explained the largest portion of variance in pathogen occurrence were inconsistent across pathogens. We found that a collection of specified host traits had a significant effect on pathogen occurrence of AD-3, Pi-3, BHV, BRSV and a moderate effect on MH and MH occurrence but there was not one consistent host trait indicating occurrence of all pathogens or even within taxonomic groups (Figure 3.2, Figure 3.3, Figure B3, Table B1). Importantly, host traits generally explained on a very small portion of variance in occurrence of each pathogen (Figure 3.2, Figure 3.3, Figure B3, Table B1).

Pi-3, AD-3 and BHV models had the highest explanatory power, followed by BRSV, MH and MB (Tjur R2: AD-3 = 0.219, Pi-3 = 0.216, BHV=0.166, BRSV=0.152, MH=0.134, MB=0.035; Figure 3.2, Table B5).

The sample-level random effect comprised the highest portion of variance explained in occurrence of three viral infections – AD-3, Pi-3 and BHV – which all displayed strong, positive co-variance patterns with each other (Figure 3.2, Figure 3.3, Table B2, Table B6). These results indicate that the best indicator of occurrence of one of these suite of viruses is co-occurrence by another member within the suite. For the fourth virus, BRSV, year comprised the highest portion of variance explained in occurrence (Figure 3.2, Table B2).

For the bacterial pathogens, host ID comprised the highest portion of variance explained in occurrence of MH while host ID and season comprised the highest portion in variance explained in occurrence of MB (Figure 3.2, Table B2). Interestingly, at the animal-level, there was moderate statistical support suggesting that MH and MB positively co-vary (Figure 3.2, Figure 3.3, Table B3, Table B6). This result suggest that the same animals are likely to be infected with MH repeatedly and, although our model only explained a very small portion of variance in MB occurrence, MB positively associates with MH in these animals.

3.3.4. Characterizing monthly and yearly variation in population-level disease dynamics

We characterized temporal variation in incidence using generalized additive models to explore if the temporally-variable factors identified by our JDSM models corresponded with monthly and yearly variation such that we could describe consistent population-level disease dynamics.

Deviance explained was quite high for each model (MH = 55.00%, MB=65.40%, Pi-3=61.10%, AD-3=59.40%, BRSV=74.80%, BHV = 48.60%), however, some of this deviance explained may be attributed to sample size, which we included as a covariate to account for sampling effort. Figures for the number of new cases and confidence intervals by month are included in Figure B4.

Month had a significant effect on the number of new cases of MH, MB, Pi-3, AD-3 and BRSV (Figure 3.5, Table B7). The number of new cases of Pi-3, AD-3 and MB

peaked during the wet season months (Pi-3: November, AD-3: December, MB: February; Figure 3.5, Figure 3.7) whereas MH peaked at the transition between the wet and dry seasons (May; Figure 3.5, Figure 3.7). The number of new cases of BRSV decreased in October suggesting that the fewest new cases occurred during October (Figure 3.5, Figure 3.7).

Year had a significant effect on the number of new cases of AD-3, BRSV and BHV (Figure 3.6, Table B7). BRSV exhibited one large outbreak during the final year of the project (Figure 3.6, Figure 3.7, Table B7)). The study population also appeared to have two outbreaks of BHV with a larger outbreak occurring within the Nov 2009-Oct 2010 rainfall year and a smaller outbreak occurring within the Nov 2011-Dec 2012 rainfall year (Figure 3.6, Figure 3.7, Table B7). Though AD-3 occurrence exhibited cyclical seasonal dynamics with a consistent peak in the wet season months, our population-level models suggest that fluctuations in incidence were higher towards the end of the project (Figure 3.6, Figure 3.7, Table B7).

3.4 Discussion

We first aimed to evaluate determinants of within-host pathogen occurrence by partitioning variance among the fixed effects (host traits, season) and random effects (sample, animal ID, year) with a JSDM. We next sought to characterize yearly and monthly trends in population disease-dynamics to explore if the pathogen had epidemiological dynamics consistent with what we expected from the JSDM result. We found that a mosaic of factors explained occurrence in the guild of pathogens we tested for, but the factors explaining the largest portion of variation were not consistent. Pathogen co-occurrence explained the largest portion of variation in the viral pathogens: AD-3, Pi-3 and BHV. Host ID explained the largest portion of variation in occurrence of the bacterial pathogens: MH and MB. Additionally, season explained another significant portion of variation in the occurrence of MB. The best explanatory factor of BRSV occurrence was year. We found evidence of seasonal cycling consistent with predictions resulting from our JDSMs for Pi-3, AD-3 and MB. We also found seemingly stochastic outbreaks at the population level for BRSV. However, no set of specified host traits helped clearly elucidate temporal variation in incidence.

We hypothesized that viral co-infection would be the strongest determinant of viral pathogen occurrence for pathogens associated with BRDC in cattle. Consistent with our hypothesis, we found that concomitant infections were more important indicators of occurrence than host traits for AD-3, Pi-3, and BHV. These pathogens commonly co-occur in cattle but physiological risk factors are currently unknown and an active area of research (Taylor et al., 2010). Co-occurrence could be the product of a direct (e.g., tissue damage (DaPalma et al., 2010)) or indirect interaction (e.g., immunomodulation (Cavanaugh et al., 1998)) between these viruses. AD-3, Pi-3 and BHV have been found to co-circulate in cattle during short periods of water and food limitation and/or exposure to environmental pollutants (Earley et al., 2017), thus change in physiological status could drive co-variation patterns and associations could be a result of a correlated decrease in host defenses. However, physiological risk factors associated with cattle shipping are often inconsistent or inconclusive (Taylor et al., 2010). We included coarse proxies of host immune status (age-horn residuals, body condition) and found that host quality only had a small but significant, negative effect on Pi-3. Future work could quantify finer scale immune-competence and evaluate if an immunological mechanism underlies virus co-occurrence in this system (e.g., molecular markers of inflammation correlate with Pi-3 occurrence in buffalo (Glidden et al., 2018)). Alternatively, BRDC most often arises during cattle transport, which causes increased co-mingling of cattle (Taylor et al., 2010). As such, increased contact rates and a general increase in exposure probability could underlie viral co-occurrence. We roughly accounted for temporal and spatial variation in contact (increased condition, herd, pregnancy status) in our model and found that these variables had a significant effect on Pi-3, AD-3 and BHV, however, effects were not consistent across pathogens. Future work could better control for the effect of exposure on pathogen occurrence and co-occurrence by using wildlife proximity collars to explicitly quantify contact networks (Rushmore et al., 2020) and using network metrics as a covariate in the JSDM. Alternatively, in cattle, Pi-3 is often a permissive infection for other viral infections, enabling viruses to circumvent host defenses (Smith et al., 2019), pointing to co-occurrence patterns being the result of pathogen-pathogen facilitation. Indeed, pathogen co-occurrence could be driven by an additive or synergistic relationship between host immune status, host behavior and direct pathogen-pathogen

facilitation or a distinct but unmeasured covariate driving synchronous dynamics of these three pathogens.

We found that the animal ID explained the largest portion of variance in MH incidence, suggesting that MH occurrence is more likely to re-occur in the same animals, over many sampling time steps. Similarly, MB occurrence was best explained by season as well as animal ID, but with less explanatory power than for MH. Probability of MB occurrence was higher in the wet season (characterized by high temperatures and humidity (Zambatis 2003)) and population-level incidence peaked towards the end of the wet season. Consequently, MB occurrence may be better explained by environmental exposure. MB is believed to persist in the environment for long periods of time (McAuliffe et al., 2006) and, in humans, mycoplasma incidence has been shown to increase with temperature and humidity (Onozuka et al., 2009).

Part of the animal ID variation in MH occurrence consists of the moderate, positive covariation with MB that we detected. Our study is not the first to detect co-occurrence of MB and MH. In cattle, lesions caused by MH infection are commonly found to be co-infected by MB (Gagea et al., 2006), and MH proliferation is understood to follow mycoplasma infection/proliferation (Rice et al., 2007). However, the reason(s) for the co-occurrence is less understood. MH and MB are normally found in the respiratory tract (Ayling 2000; Cozens et al., 2019) but pathogenic subtypes proliferate under stressful conditions (Maunsell et al., 2011; Cozens et al., 2019). As probiotics have been used in dairy calves to inhibit the invasion and proliferation of pathogenic MH (Amat et al., 2020), the proportion of variance in bacterial occurrence explained by host ID could be related to individual microbiome composition. Alternatively, static host traits, such as immune phenotype, may contribute to likelihood of infection by these bacterial infections (e.g., genetically based immune phenotype regulates bTB susceptibility in buffalo (Tavalire et al., 2019).

With our JDSM models, the best determinant of BRSV occurrence was year which explained 60% of variance. Our population-level analysis corroborate the findings from the JDSM in that we found one large outbreak at the end of the study. In cattle, BRSV outbreaks correlate with moving animals between farms, thus, outbreaks are most likely facilitated by introduction of BRSV by animals not included in the study

(Sarmiento-Silva et al., 2010). Of course, we are limited in our ability to confirm BRSV as an outbreak pathogen because of the length of the study. A longer time series would have enabled us to examine if outbreaks were sporadic or cyclical and thereby allow us to hone in on mechanistic drivers of outbreaks or identify if outbreaks occur stochastically. Contrary to our hypothesis, BRSV did not significantly co-vary with any other pathogen despite being associated with the BRDC in cattle. We expected co-occurrence because BRSV is well known for damaging host tissue and facilitating proliferation of pathogenic bacteria (Lopez, Thomson & Savan 1976; Rice et al., 2007; Srikumaran, Kelling & Ambagala 2007). Of course, there is a possibility that BRSV does co-occur but with a time-lagged. A more frequent sampling regime may uncover cross-taxonomy associations. Similarly, we observed very low incidence of BVDV despite BVDV also being a common infection with the BRDC in cattle.

The second objective of our study characterized monthly and yearly trends in incidence and examined whether the patterns in occurrence were consistent with population-level patterns. We found evidence for seasonal cycling of Pi-3, AD-3, MH and MB. Seasonally variable host traits had a small but significant effect on the occurrence of Pi-3 and AD-3 and a moderate effect on MB and MH, however, counter to our hypotheses, no seasonally variable host trait (body condition, reproductive status) overwhelmingly matched population-level trends. As described previously, seasonal dynamics of MB matched what we would expect if temporal variation is driven by pathogen viability (i.e., MB can persist in the environment during the wet season). In humans, adenovirus incidence typically peaks during cooler, drier months (Price et al., 2019), however, our observations indicate that adenovirus in buffalo peaks during hotter, wetter months suggesting opposite effects of climate on pathogen viability. However, in both systems, seasonal peaks correspond to periods of increased contact rates (Moryiama et al., 2020; Spaan et al., 2019; Rushmore et al., 2020). Perhaps asynchronous disease seasons of human versus buffalo adenovirus are a results of asynchronous contact patterns. Clearly, a mix of host traits, pathogen characteristics (e.g., viability), co-infection dynamics and variables not measured here interact to influence seasonal trends.

This study did not include juveniles so any population-level fluctuations in immune status through birth pulses of newly susceptible animals are difficult to identify.

If we assume calves are protected via maternal immunity throughout the first 6 months but are newly susceptible the following wet season (Combrink et al., 2020) then we may see a spike in incidence at this time as 1-year-old calves act as super-spreaders for the remainder of the population, explaining peaks in incidence during the wet season. We also did not include any males in this study though they likely affect infection dynamics as well. During the wet season, males re-join the herd to breed (Turner et al., 2005) and could be introducing or re-introducing pathogens.

Overall, for each pathogen, we observed a large portion of unexplained variation in within-host occurrence. Our analysis suggests that there are a number of other processes influencing temporal patterns in disease dynamics. As many of these pathogens cause short lived infection or pathology, detection of variables associated with occurrence may necessitate more frequent sampling intervals. For respiratory infections, host traits may only explain a small portion of variation in occurrence but may explain a large portion of variation in ability to clear a pathogen once infected and disease induced morbidity/mortality. Serology data limits our ability to characterize multiple different infection outcomes (i.e., time to clearance, pathogen intensity), however, future work could use higher resolution data (e.g., quantitative PCR) to weigh the effect of host traits on different outcomes of infection.

In summary, we found that drivers of temporal variation in disease dynamics are multi-factorial and pathogen dependent, even within a group of inter-guild pathogens (directly transmitted micro-parasites that infect the upper respiratory tract). Kruger National Park is surrounded by pastoral land and cross-species disease, specifically disease of cattle, causes significant economic loss (Chaminuka, McCrindle & Udo 2011). Our study indicates new avenues of research for monitoring and managing BRDC, especially at this wildlife-livestock interface.

3.5 Acknowledgements

We would like to thank colleagues at the Veterinary Wildlife Services department at Kruger National Park, the State Veterinary Office in Skukuza, and our field and lab technicians Robert and Johannie Spaan. We would like to additionally thank Robert Spaan for providing the map in supplementary materials 1. We would like to also thank

Eilea Delgadillo for insightful discussion on bovine disease complex epidemiology and pathogenesis as well as Professor Otso Ovaskainen for helpful feedback on our JSDM. This study was supported by a National Science Foundation Ecology of Infectious Diseases grant (EF-0723918/DEB-1102493, EF-0723928 to V. Ezenwa and A. Jolles). CKG was supported by an NSF-GRFP and ARCS Fellowship.

3.6 References

Amat, S., Alexander, T. W., Holman, D. B., Schwinghamer, T., & Timsit, E. (2020). Intranasal Bacterial Therapeutics Reduce Colonization by the Respiratory Pathogen Mannheimia haemolytica in Dairy Calves. *mSystems*, *5*(2), e00629-19. https://doi.org/10.1128/mSystems.00629-19

Ayling R, Baker S, Nicholas R, Peek M, Simon A. Comparison of *in vitro* activity of danofloxacin, florfenicol, oxytetracycline, spectinomycin and tilmicosin against *Mycoplasma mycoides* subspecies *Mycoides* small colony type. Vet. Rec. 2000;146(9):243–245.

Beechler, B., Jolles, A. & Ezenwa, V. (2009) Evaluation of hematologic values in free-ranging African buffalo (Syncerus caffer). *Journal of Wildlife Diseases*, 45, 57-66.

Cassirer, E.F., Plowright, R.K., Manlove, K.R., Cross, P.C., Dobson, A.P., Potter, K.A. & Hudson, P.J. (2013) Spatio-temporal dynamics of pneumonia in bighorn sheep. *Journal of Animal Ecology*, 82, 518-528.

Cattadori, I., Boag, B. & Hudson, P. (2008) Parasite co-infection and interaction as drivers of host heterogeneity. *International Journal for Parasitology*, 38, 371-380.

Cavanaugh V. J., Guidotti L. G., Chisari F. V. (1998). Inhibition of Hepatitis B virus replication during adenovirus and cytomegalovirus infections in transgenic mice. *Journal of Virology*. 72 2630–2637.

Chaminuka, P, McCrindle, C.M.E., Udo, H.J. (2011) Cattle farming at the wildlife/livestock interface: assessment of costs and benefits adjacent to Kruger National Park, South Africa. *Society and Natural Resources*, DOI:10.1080/08941920.2011.580417

Coetzer, J.A.W., Thomson, G.R. & Tustin, R.C. (2006) Infectious Diseases of Livestock - With Special Reference to Southern Africa. Oxford University Press.

Combrink, L., Glidden, C. K., Beechler, B. R., Charleston, B., Koehler, A. V., Sisson, D., Gasser, R. B., Jabbar, A., & Jolles, A. E. (2020). Age of first infection across a range of parasite taxa in a wild mammalian population. *Biology letters*, 16(2), 20190811. https://doi.org/10.1098/rsbl.2019.0811

Colwell, R.R. (1996) Global Climate and Infectious Disease: The Cholera Paradigm*. *Science*, 274, 2025-2031.

Cook, S., Glass, R., LeBaron, C. & Ho, M.-S. (1990) Global seasonality of rotavirus infections. *Bulletin of the World Health Organization*, 68, 171.

Cox, F. (2001) Concomitant infections, parasites and immune responses. *Parasitology*, 122, S23-S38.

Cozens, D., Sutherland, E., Lauder, M., Taylor, G., Berry, C. C., & Davies, R. L. (2019). Pathogenic Mannheimia haemolytica Invades Differentiated Bovine Airway Epithelial Cells. *Infection and immunity*, *87*(6), e00078-19. https://doi.org/10.1128/IAI.00078-19

Dallas, T. A., Laine, A. L., & Ovaskainen, O. (2019). Detecting parasite associations within multi-species host and parasite communities. *Proceedings. Biological Sciences*, 286(1912), 20191109. https://doi.org/10.1098/rspb.2019.1109

DaPalma, T., Doonan, B. P., Trager, N. M., & Kasman, L. M. (2010). A systematic approach to virus-virus interactions. *Virus research*, 149(1), 1–9. https://doi.org/10.1016/j.virusres.2010.01.002

Dowell, S.F., Whitney, C.G., Wright, C., Rose Jr, C.E. & Schuchat, A. (2003) Seasonal patterns of invasive pneumococcal disease. *Emerging Infectious Diseases*, 9, 573-579.

Earley, B., Buckham Sporer, K., & Gupta, S. (2017). Invited review: Relationship between cattle transport, immunity and respiratory disease. *Animal : an international journal of animal bioscience*, 11(3), 486–492. https://doi.org/10.1017/S1751731116001622

Ezenwa, V.O., Etienne, R.S., Luikhart, G., Beja-Pereira, A. & Jolles, A.E. (2010) Hidden consequences of living in a wormy world: nematode-induced immune suppression facilitates invasion in the African buffalo. *The American Naturalist*, 176, 613-324.

Ezenwa, V.O. & Jolles, A.E. (2008) Horns honestly advertise parasite infection in male and female African buffalo. *Animal Behaviour*, 75, 2013-2021.

Ezenwa, V.O. & Jolles, A.E. (2015) Opposite effects of anthelmintic treatment on microbial infection at individual versus population scales. *Science*, 347, 175-177.

Ezenwa, V.O., Jolles, A.E. & O'Brien, M.P. (2009) A reliable body condition scoring technique for estimating condition in African buffalo. *African Journal of Ecology*, 47, 476-481.

Fine, P.E. & Clarkson, J.A. (1982) Measles in England and Wales—I: an analysis of factors underlying seasonal patterns. *International journal of epidemiology*, 11, 5-14.

Forbes KM, Mappes T, Sironen T, Strandin T, Stuart P, Meri S, Vapalahti O, Henttonen H, Huitu O. 2016. Food limitation constrains host immune responses to nematode infections. Biol. Lett. 12, 20160471

Gagea, M. I., Bateman, K. G., Shanahan, R. A., van Dreumel, T., McEwen, B. J., Carman, S., … Caswell, J. L. (2006). Naturally Occurring Mycoplasma Bovis—Associated Pneumonia and Polyarthritis in Feedlot Beef Calves. *Journal of Veterinary Diagnostic Investigation*, *18*(1), 29–40. https://doi.org/10.1177/104063870601800105

Gelman, A. (2008). Scaling regression inputs by dividing by two standard deviations. *Statistics in Medicine* 27, 2865–2873.

Gelman, A. and Su, Y. (2018). arm: Data Analysis Using Regression and Multilevel/Hierarchical Models. R package version 1.10-1. https://CRAN.R-project.org/package=arm

Germann, T.C., Kadau, K., Longini, I.M. & Macken, C.A. (2006) Mitigation strategies for pandemic influenza in the United States. *Proceedings of the National Academy of Sciences*, 103, 5935-5940.

Glidden, C. K., Beechler, B., Buss, P. E., Charleston, B., de Klerk-Lorist, L. M., Maree, F. F., Muller, T., Pérez-Martin, E., Scott, K. A., van Schalkwyk, O. L., & Jolles, A. (2018). Detection of Pathogen Exposure in African Buffalo Using Non-Specific Markers of Inflammation. *Frontiers in Immunology*, 8, 1944. https://doi.org/10.3389/fimmu.2017.01944

Gorsich, E.E., Ezenwa, V.O., Cross, P.C., Bengis, R.G. & Jolles, A.E. (2015) Context-dependent survival, fecundity and predicted population-level consequences of brucellosis in African buffalo. *Journal of Animal Ecology,* 84, 999-1009.

Gorsich, E. E., Etienne, R. S., Medlock, J., Beechler, B. R., Spaan, J. M., Spaan, R. S., . . .
Jolles, A. E. (2018). Opposite outcomes of coinfection at individual and population scales. Proceedings of the National Academy of Sciences, 115(29), 7545-7550. doi:10.1073/pnas.1801095115

Graham, A.L. (2008) Ecological rules governing helminth–microparasite co-infection. *Proceedings of the National Academy of Sciences,* 105, 566-570.

Graham, A.L., Lamb, T.J., Read, A.F. & Allen, J.E. (2005) Malaria-filaria co-infection in mice makes malarial disease more severe unless filarial infection achieves patency. *Journal of Infectious Diseases,* 191, 410-421.

Griffiths, E.C., Pedersen, A.B., Fenton, A. & Petchey, O.L. (2011) The nature and consequences of co-infection in humans. *Journal of Infection,* 63, 200-206.

Griffin D. Economic impact associated with respiratory disease in beef cattle. Vet Clin North Am Food Anim Pract. 1997;13:367–377.

Hall, A.J., Jepson, P.D., Goodman, S.J. & Härkönen, T. (2006) Phocine distemper virus in the North and European Seas–Data and models, nature and nurture. *Biological Conservation,* 131, 221-229.

Henrichs, B., Oosthuizen, M.C., Troskie, M., Gorsich, E., Gondhalekar, C., Beechler, B.R., Ezenwa, V.O. & Jolles, A.E. (2016) Within guild co-infections influence parasite community membership: a longitudinal study in African Buffalo. *Journal of Animal Ecology,* 85, 1025-1034.

Huang, Y. & Rohani, P. (2006) Age-Structured Effects and Disease Interference in Childhood Infections. *Proceedings: Biological Sciences,* 273, 1229-1237.

Hurvich, C. M. and Tsai, C.-L. (1989) Regression and time series model selection in small samples, *Biometrika* 76, 297–307.

Jolles, A.E. (2007) Population biology of African buffalo (Syncerus caffer) at Hluhluwe-iMfolozi Park, South Africa. *African Journal of Ecology,* 45, 398-406.

Jolles, A.E., Beechler, B.R. & Dolan, B.P. (2015) Beyond mice and men: environmental change, immunity and infections in wild ungulates. *Parasite Immunology,* 37, 255-266.

Jolles, A.E., Cooper, D.V. & Levin, S.A. (2005) Hidden effects of chronic tuberulosis in African buffalo. *Ecology,* 86, 2358-2364.

Keeling, M.J. & Rohani, P. (2008) *Modeling infectious diseases in humans and animals*. Princeton University Press.

Kiguchi, R. and Minami, M. (2012) Cyclic Cubic Regression Spline Smoothing and Analysis
of CO2 Data at Showa Station in Antarctica, Proceedings of International Biometric Conference 2012.

Krause, J., James, R., Franks, D., & Croft, D. (2015). Animal Social Networks. Oxford, UK: Oxford University Press.

Lillie, L.E. (1974) The bovine respiratory disease complex. *The Canadian Veterinary Journal,* 15, 233-242.

Lopez, A., Thomson, R. & Savan, M. (1976) The pulmonary clearance of Pasteurella hemolytica in calves infected with bovine parainfluenza-3 virus. *Canadian Journal of Comparative Medicine,* 40, 385.

Lowen, A.C., Mubareka, S., Steel, J. & Palese, P. (2007) Influenza Virus Transmission Is Dependent on Relative Humidity and Temperature. *PLoS Pathogens,* 3, e151.

Maclachlan, N.J. & Dubovi, E.J. (2010) *Fenner's veterinary virology*. Academic press.

McAuliffe, L., Ellis, R. J., Miles, K., Ayling, R. D., & Nicholas, R. A. J. (2006). Biofilm formation by mycoplasma species and its role in environmental persistence and survival. *Microbiology, 152*(4), 913-922. doi:https://doi.org/10.1099/mic.0.28604-0

Mallard, B., Dekkers, J., Ireland, M., Leslie, K., Sharif, S., Vankampen, C.L., Wagter, L. & Wilkie, B. (1998) Alteration in immune responsiveness during the peripartum period and its ramification on dairy cow and calf health. *Journal of dairy science,* 81, 585-595.

Maunsell F, Woolums A, Francoz D, Rosenbusch R, Step D, Wilson D.J, Janzen E. *Mycoplasma bovis* infections in cattle. J. Vet. Int. Med. 2011;25(4):772–783.

Michel, A.L., Cooper, D., Jooste, J., De Klerk, L.-M. & Jolles, A. (2011) Approaches towards optimising the gamma interferon assay for diagnosing Mycobacterium bovis infection in African buffalo (Syncerus caffer). *Preventive Veterinary Medicine*, 98, 142-151.

Moriyama, M., Hugentobler, W. J., & Iwasaki, A. (2020). Seasonality of Respiratory Viral Infections. *Annual review of virology*, 10.1146/annurev-virology-012420-022445.

Nelson, R.J. & Demas, G.E. (1996) Seasonal changes in immune function. *The Quarterly Review of Biology,* 71, 511-548.

Onozuka D, Hashizume M, Hagihara A. (2009) Impact of weather factors on *Mycoplasma pneumoniae* pneumonia *Thorax*, 64,507-511.

Ovaskainen, O., Abrego, N., Halme, P. & Dunson, D. (2016a). Using latent variable models to identify large networks of species-to-species associations at different spatial scales. *Methods in Ecology and Evolution*, 7, 549–555.

Ovaskainen, O., Tikhonov, G., Norberg, A., Guillaume Blanchet, F., Duan, L., Dunson, D., Roslin, T. and Abrego, N. (2017), How to make more out of community data? A conceptual framework and its implementation as models and software. *Ecology Letters*, 20, 561-576. doi:10.1111/ele.12757

Pedersen, A.B. & Fenton, A. (2007) Emphasizing the ecology in parasite community ecology. *Trends in Ecology & Evolution,* 22, 133-139.

Price, R., Graham, C., & Ramalingam, S. (2019). Association between viral seasonality and meteorological factors. *Scientific reports*, 9(1), 929. https://doi.org/10.1038/s41598-018-37481-y

Rice, J., Carrasco-Medina, L., Hodgins, D. & Shewen, P. (2007) Mannheimia haemolytica and bovine respiratory disease. *Animal Health Research Reviews,* 8, 117-128.

Rodwell, T.C., Whyte, I.J. & Boyce, W.M. (2001) Evaluation of population effects of bovine tuberculosis in free-ranging African buffalo (Syncerus caffer). *Journal of Mammalogy*, 82, 231-238.

Rohani, P., Earn, D.J., Finkenstädt, B. & Grenfell, B.T. (1998) Population dynamic interference among childhood diseases. *Proceedings of the Royal Society of London B: Biological Sciences,* 265, 2033-2041.

Rushmore, J., Beechler, B.R., Tavalire, H., Gorsich, E., Devan-Song, A., Glidden, C.K., Charleston, B., Jolles, A. The heterogeneous herd: drivers of close contact variation in African buffalo and implications for pathogen invisibility. *Journal of Animal Ecology:* Accepted, major revisions.

SANPARKS (2010-2011) Kruger National Park Biodiversity Statistics. https://www.sanparks.org/parks/kruger/conservation/scientific/ff/biodiversity_statistics.php.

Sarmiento-Silva, R. E., Nakamura-Lopez, Y., & Vaughan, G. (2012). Epidemiology, molecular epidemiology and evolution of bovine respiratory syncytial virus. *Viruses*, *4*(12), 3452–3467. https://doi.org/10.3390/v4123452

Simon, A.K., Hollander, G.A., McMichael, A. (2015) Evolution of the immune system in humans from infancy to old age *Proceedings of the Royal. Society B.* 282, 20143085.

Schiller, I., Waters, W.R., Vordermeier, H.M., Nonnecke, B., Welsh, M., Keck, N., Whelan, A., Sigafoose, T., Stamm, C. & Palmer, M. (2009) Optimization of a whole-blood gamma interferon assay for detection of Mycobacterium bovis-infected cattle. *Clinical and Vaccine Immunology,* 16, 1196-1202.

Smith, B. P., Van Metre, D. C., & Pustrela, N. (2019). Large Animal Internal Medicine (6th ed.). St. Louis, Missouri: Elsevier.

Spaan, RS, Epps, CW, Ezenwa, VO, Jolles, AE. (2019) Why did the buffalo cross the park? Resource shortages, but not infections, drive dispersal in female African buffalo (Syncerus caffer). *Ecology & Evolution*, 9, 5651– 5663. https://doi.org/10.1002/ece3.5145

Srikumaran, S., Kelling, C.L. & Ambagala, A. (2007) Immune evasion by pathogens of bovine respiratory disease complex. *Animal Health Research Reviews,* 8, 215-229.

Susi, H., Barrès, B., Vale, P.F. & Laine, A.-L. (2015) Co-infection alters population dynamics of infectious disease. *Nature communications,* 6.

Swain, D.L., Patison, K. Heath, B., Bishop-Hurley, G. & Finger A., (2015). Pregnant cattle associations and links to maternal reciprocity. *Applied Animal Behavior Science,* 168, 10-17.

Tavalire, H. F., Hoal, E. G., le Roex, N., van Helden, P. D., Ezenwa, V. O., & Jolles, A. E. (2019). Risk alleles for tuberculosis infection associate with reduced immune reactivity in a wild mammalian host. *Proceedings of the Royal Society B*, 286(1907), 20190914. https://doi.org/10.1098/rspb.2019.0914

Taylor, J. D., Fulton, R. W., Lehenbauer, T. W., Step, D. L., & Confer, A. W. (2010). The epidemiology of bovine respiratory disease: What is the evidence for predisposing factors?. *The Canadian veterinary journal = La revue veterinaire canadienne*, *51*(10), 1095–1102.

Telfer, S., Lambin, X., Birtles, R., Beldomenico, P., Burthe, S., Paterson, S. & Begon, M. (2010) Species interactions in a parasite community drive infection risk in a wildlife population. *Science,* 330, 243-246.

Turner, W.C., Jolles, A.E., & Owen-Smith, N. (2005). Alternating sexual segregation during the mating season by male African buffalo (Syncerus caffer).*Journal of Zoology* 267(03), 291 - 299

Tjur, T. (2009) Coefficients of Determination in Logistic Regression Models—A New Proposal: The Coefficient of Discrimination, The American Statistician, 63:4, 366-372, DOI: 10.1198/tast.2009.08210

Trillmich, F., Guenther, A., Jäckel, M., Czirják, G.Á. (2020) Reproduction affects immune defenses in the guinea pig even under ad libitum food. *PLOS ONE* 15(3), e0230081. https://doi.org/10.1371/journal.pone.0230081

Valarcher, J.-F., Bourhy, H., Lavenu, A., Bourges-Abella, N., Roth, M., Andreoletti, O., Ave, P. & Schelcher, F. (2001) Persistent infection of B lymphocytes by bovine respiratory syncytial virus. *Virology,* 291, 55-67.

Van der Poel, W., Brand, A., Kramps, J. & Van Oirschot, J. (1994) Respiratory syncytial virus infections in human beings and in cattle. *Journal of Infection,* 29, 215-228.

Van Vuuren, M. (1994) Bovine respiratory syncytial virus infection. *Intifectious Diseases of Livestock. Oxford University Press, Cape Town.(Links),* 769-772.

Venter, F. & Gertenbach, W. (1986) A cursory review of the climate and vegetation of the Kruger National Park. *Koedoe,* 29, 139-148..

Wood, S. (2017). Generalized Additive Models. New York: Chapman and Hall/CRC, https://doi.org/10.1201/9781315370279

Wood, S.N. (2011) Fast stable restricted maximum likelihood and marginal likelihood estimation of semiparametric generalized linear models. *Journal of the Royal Statistical Society (B),* 73(1), 3-36.

Wood, P. & Jones, S. (2001) BOVIGAM TM: An in vitro cellular diagnostic test for bovine tuberculosis. *Tuberculosis,* 81, 147-155.

Wright, A.N. & Gompper, M.E. (2005) Altered parasite assemblages in raccoons in response to manipulated resource availability. *Oecologia,* 144, 148-156.

Zambatis, N. (2003) Determinants of grass production and composition in the Kruger National Park. MSc (Agric.) dissertation, University of Natal, Pietermaritzburg.

Table 3.1. Biology of respiratory pathogens included in this study, and annual incidence in African buffalo.

Pathogen (Abbreviation)	Family (subfamily)	Type	Description	Average Annual Incidence ± SD
Mycoplasma bovis (MB)	Myco-plasmataceae	Bacterial, opportunistic	MB commonly causes calf pneumonia, mastitis and arthritis while occasionally causing swelling of various reproductive organs and abortion in cattle. Infected cattle can shed the bacteria for months to years (Nicholas & Ayling 2003).	20.2 ± 2.1%
Mannheimia haemolytica (MH)	Pasteurellaceae	Bacterial, opportunistic	Though MH can act as a commensal and commonly exists in the upper respiratory tract of healthy ruminants, it is also associated with pneumonia and bovine respiratory disease complex in cattle after a hosts' immune defenses have been compromised by stress or another infection (Rice et al., 2007).	11.0 ± 1.8%
Bovine Adenovirus-3 (AD-3)	Adenoviridae (mastadenovirus)	Viral, acute	The pathogenic effects of AD-3 alone remain controversial but when associated with disease, can cause oculonasal discharge, colic, diarrhea, enteritis and fever in cattle (Coetzer, Thomson & Tustin 2006).	13.3 ± 3.8%
Bovine Parainfluenza-3 (Pi-3)	Paramyxoviridae (respirovirus)	Viral, acute	When interacting with other disease-causing factors, clinical signs of Pi-3 include coughing, pyrexia, nasal discharge and inappetence. Cattle develop a strong immune response, but sterile immunity is short-lived (Maclachlan & Dubovi 2010).	12.0 ± 3.2%
Bovine Herpesvirus-1 (BHV)	Herpesviridae (Alphaherpes-virinae)	Viral, chronic (latent)	Also known as Infectious Bovine Rhinotracheitis, BHV affects the respiratory and reproductive tracts of bovids; reactivation of latent infections may play an important role in transmission in cattle (Maclachlan & Dubovi 2010).	11.3 ± 5.2%
Bovine Respiratory Syncytial Virus (BRSV)	Paramyxovirus (pneumovirus)	Viral, acute or chronic (latent)	While most infections are unapparent, some BRSV infected animals present with fever, coughing and upper respiratory discharge. Most severe disease is reported in calves under 6mo. Persistent infections have been suggested based on epidemiological and experimental data in cattle (Van Vuuren 1994; Valarcher et al., 2001). Reinfection is also common; in fact, cows can be infected more than once per year (Van der Poel et al., 1994).	12.1 ± 15.0%
Bovine Viral Diarrhea Virus (BVDV)	Flaviviridae (pestivirus)	Viral, acute or chronic (latent)	In cattle, BVDV can present as clinically inapparent, a mild acute diarrheal disease, a fatal mucosal disease or as an *in utero* infection from which persistent infections can develop (Brownlie et al., 1987).	1.9 ± 0.4%

Table 3.2. Within-host traits and environmental variables included in the JSDM. A description of each host trait included in the X matrix of our JSDM.

Variable	Variable type	Collection information, data transformation, and units
Season	Categorical	Pathogen exposure regimes, pathogen viability, host behavior and host immunocompetence may fluctuate with season thus we included season at sampling to detect seasonality of pathogen occurrence and hypothesize about seasonally variables not explicitly defined within our model. Wet = Nov – Apr; Dry = May – Oct.
Age	Continuous	Approximate age of each animal, in months, based on teeth regressions as per Jolles, Cooper and Levin (2005).
Capture herd	Binomial	This variable refers to the herd in which the buffalo was found during the given capture, Crocodile Bridge or Lower Sabie.
Condition	Categorical	Visualization and palpation of the ribs, spine, hips and the base of the tail was scored on a scale of 1 (very poor) to 5 (excellent); overall body condition score was calculated as the average of these four scores. Condition at the beginning of the interval, i.e. at the previous capture, was used in analyses (Ezenwa, Jolles & O'Brien 2009).
Age-horn residual	Continuous	The regression residuals of age at first capture on horn width (cm) was collected at the previous capture. In female buffalo, the variable is a marker of GI parasite infection with higher residuals indicating lower parasite richness as well as lower coccidia occurrence and intensity (Ezenwa & Jolles 2008).
Pregnancy status	Binomial	Pregnancy status is based on palpation by a veterinarian via rectal palpation (Karen et al., 2011)
Lactation status	Binomial	Lactation status was assessed by manual milking of all four teats (Jolles 2007)
Calf at heel status	Binomial	This variable indicates whether there was a calf at the mother's side during visual surveys when animals were being picked out for darting
bTB convert	Binomial	bTB is typically a chronic, subclinical disease of the lung and upper respiratory tract in African buffalo. bTb interactions with host traits and other pathogens have been well characterized in African buffalo. Due to the chronicity of infection, we included if the animal converted to bTb as a host trait.
Anthelmintic bolus treatment	Binomial	As part of another study (Ezenwa & Jolles 2015), half of the buffalo in each herd were administered a slow-release, oral anti-helminthic treatment (Fenbendazole aka Panacur) at every capture.

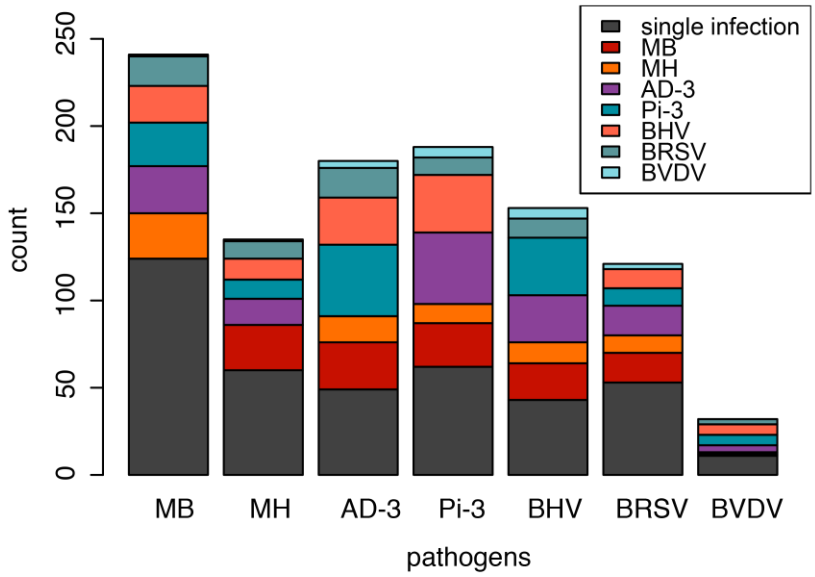

Figure 3.1. Infection by multiple pathogens in the same time period was common. This figure shows the proportion of observations of each infection as a single infection (dark grey) and as a co-infection with other focal pathogens (color corresponds to exact co-infection). For example, we observed 124 samples with only an MB infection (first (grey) portion of the first bar) and 26 samples that had an MB and MH co-infection (second (orange) portion of the first bar). Here we have defined co-infection as an occurrence (initial infection, re-infection or recrudescence) of two or more pathogens between any two sampling events (~6 month period).

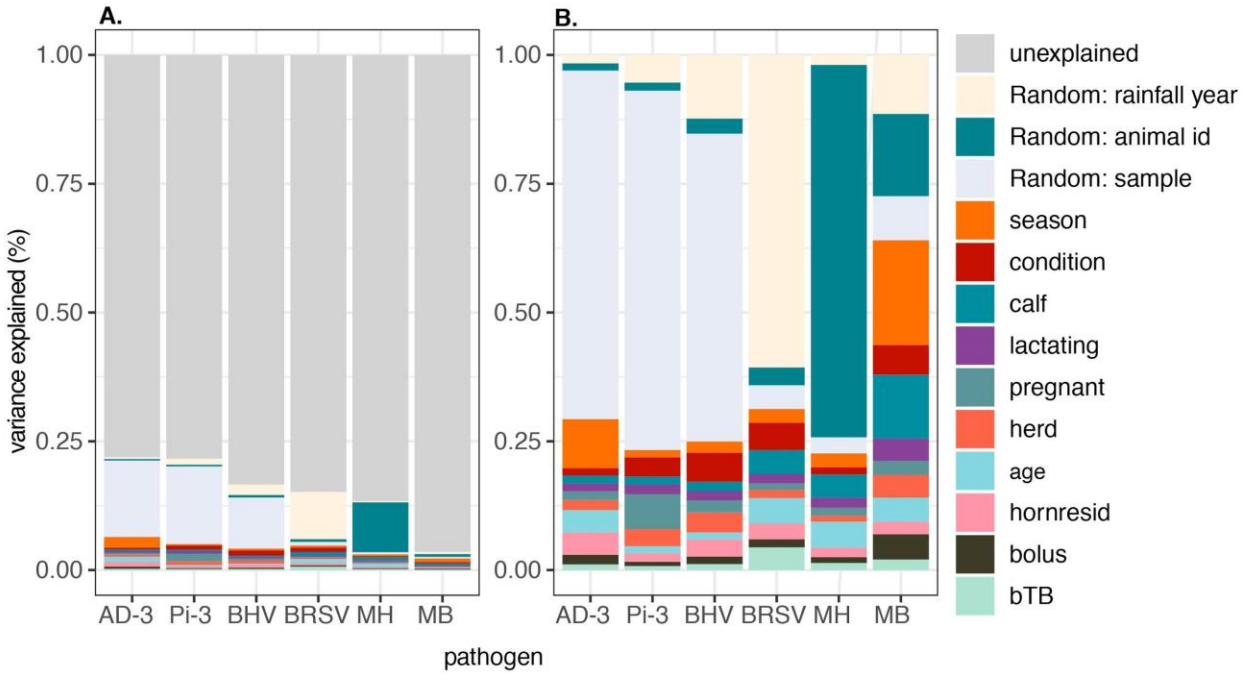

Figure 3.2. Variance in pathogen occurrence explained by specified host traits, season and random effect. The bars are ordered from highest to lowest Tjur's R^2. (A) Bar height was standardized such that, for each pathogen, the terms were scaled to sum to Tjur's R^2. The unexplained variance is equal to 1-Tjur's R^2. (B) Bar height equals Tjur's R^2 for each pathogen. Pathogen associations at the sample and animal-id level explained the largest portion of variance in these models suggesting that pathogen co-occurrence is the best predictor of pathogen occurrence.

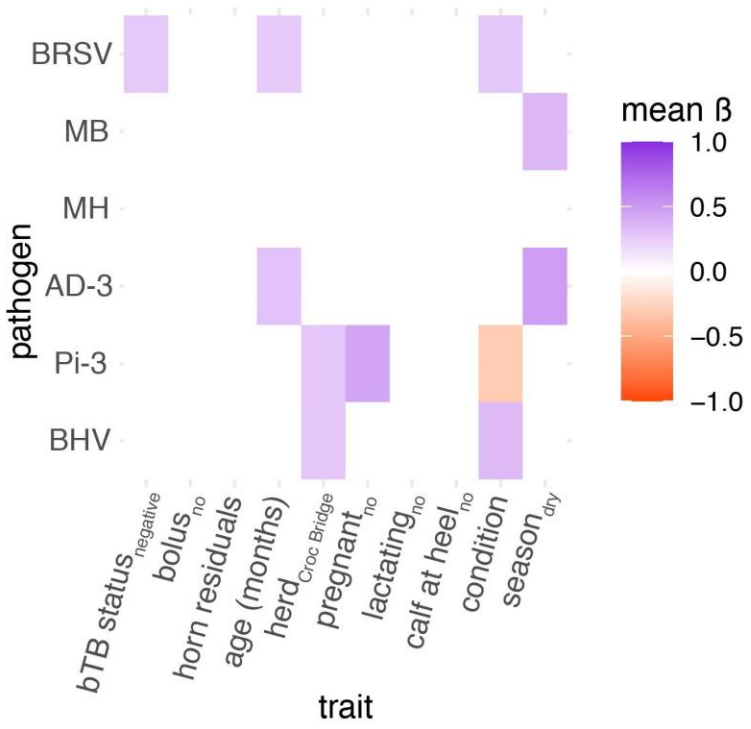

Figure 3.3. Pathogen response to host traits. Significant host traits (support level > 0.95) colored by mean response. For categorical variables, the subscript represents the baseline group. Continuous variables were centered and scaled to two standard deviations from the mean. Color indicates the direction (orange = negative effect or higher for the baseline group, purple = positive effect or higher for non-baseline group) and magnitude of the mean posterior estimate for the effect of each trait on pathogen occurrence. Host traits where support level was > 0.90 are included in supplementary materials figure 3.

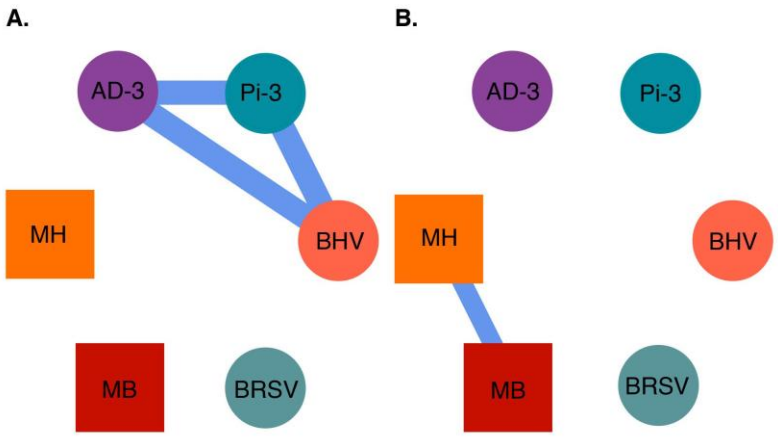

Figure 3. 4. Species co-occurrence: Mean species associations estimated from species-species covariance matrix from (A) the sample-level random effect and (B) animal-level random effect. Circles represent viruses and squares represent bacteria. Purple edges represent positive associations. For the sample-level random effect, the support level was = 0.99 for the associations shown and < 0.90 for all other associations. For the animal-level random effect, the support level was = 0.91 for the associations shown and < 0.90 for all other associations.

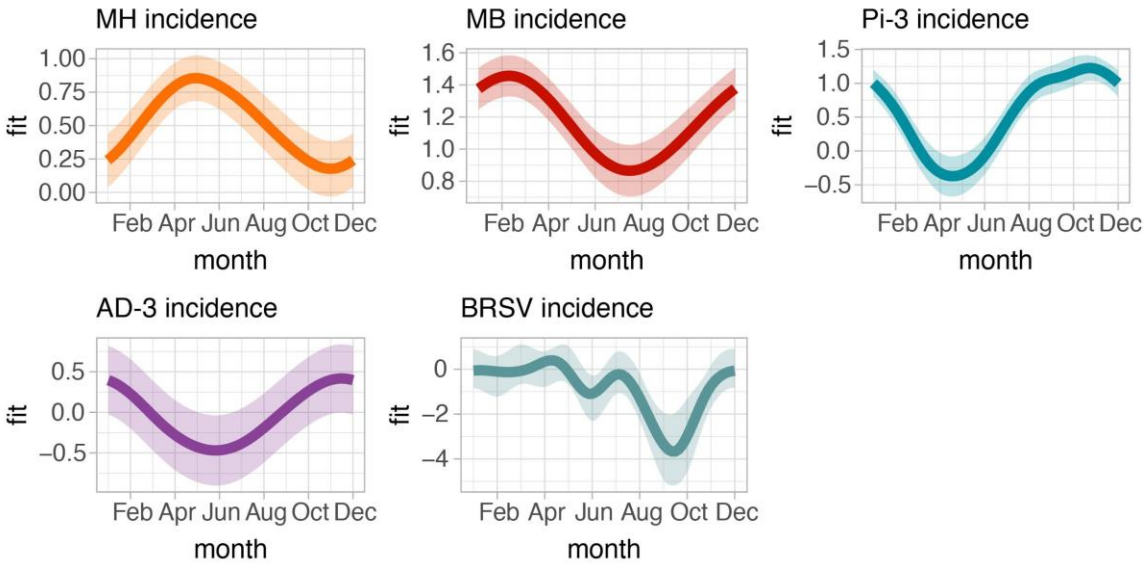

Figure 3.5. GAM predictions for number of new cases per calendar month, after controlling for sample number. Dynamics are depicted for pathogens where the calendar month was significant in our final model.

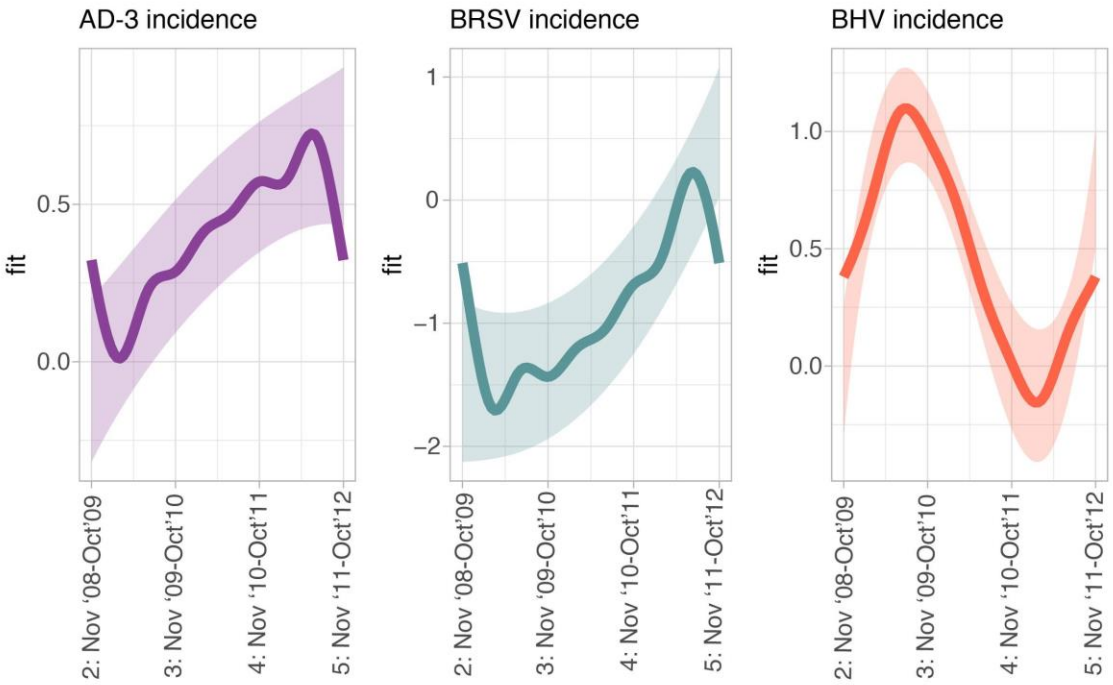

Figure 3.6. GAM predictions for number of new cases per rainfall year, after controlling for sample number. Pathogen dynamics are depicted if the rainfall was significant in our final model. The x-axis marks the rainfall year (year of the study: calendar months it encompassed).

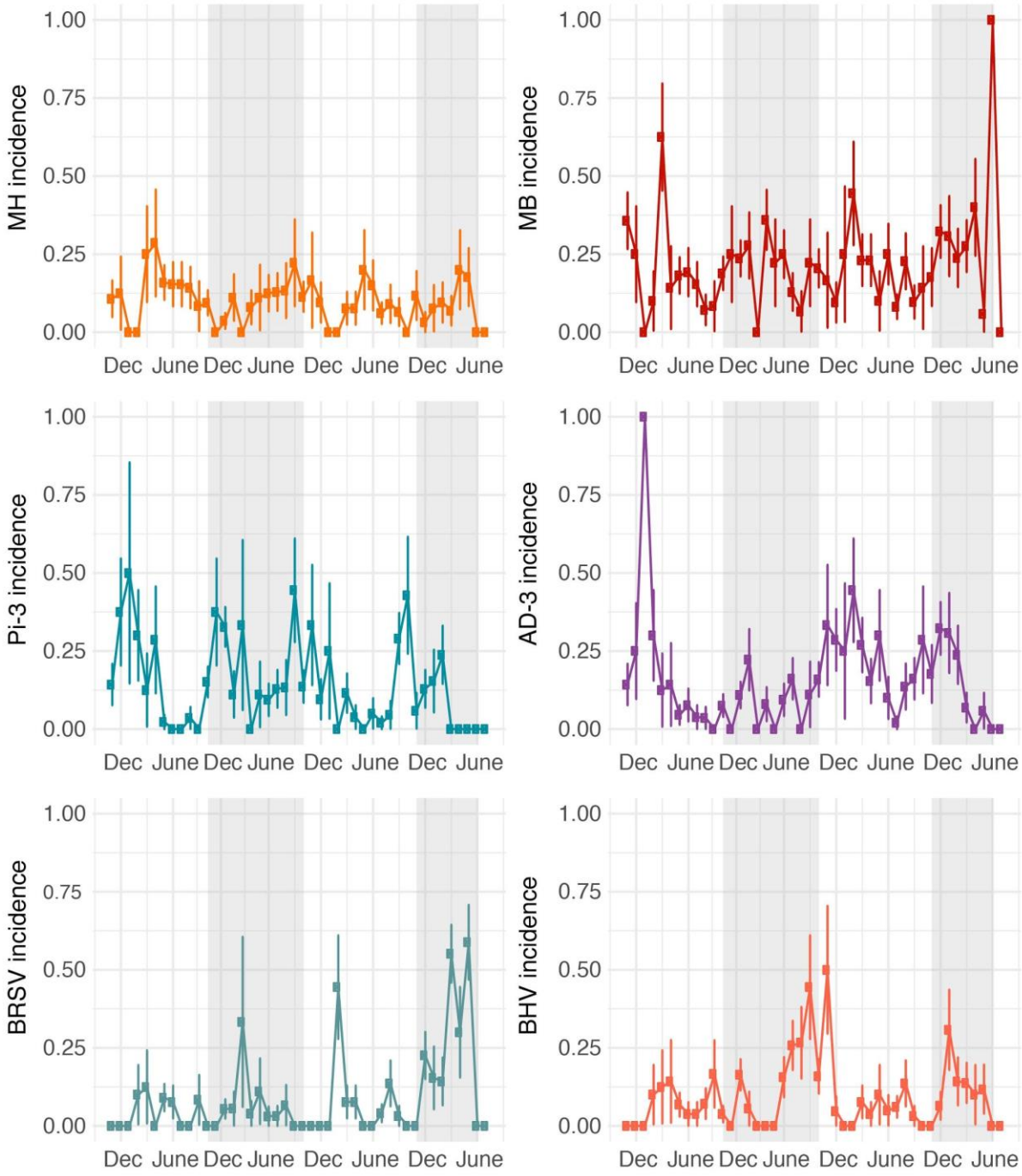

Figure 3.7. Incidence rate per month of the study. Incidence was calculated by summing the number of new cases in a month and dividing by the number of animals sampled. Standard errors were calculated by (√(incidence*(1-incidence)) / number of animals sampled. Rainfall years are shaded by alternating white and grey backgrounds.

ELUCIDATING CRYPTIC DYNAMICS OF *THEILERIA* ASSEMBLAGES IN AFRICAN BUFFALO USING A HIGH-THROUGHPUT SEQUENCING INFORMATIC APPROACH

Caroline K. Glidden, Anson V. Koehler, Ross S. Hall, Muhammad A. Saeed, Mauricio Coppo, Brianna R. Beechler, Bryan Charleston, Robin B. Gasser, Abdul Jabbar, Anna E. Jolles

Ecology and Evolution

111 River Street, Hoboken/New Jersey, United States 07030

Available online: https://doi.org/10.1002/ece3.5758

CHAPTER 4: ELUCIDATING CRYPTIC DYNAMICS OF *THEILERIA* ASSEMBLAGES IN AFRICAN BUFFALO USING A HIGH-THROUGHPUT SEQUENCING INFORMATIC APPROACH

Abstract

Increasing access to next-generation sequencing (NGS) technologies is revolutionizing the life sciences. In disease ecology, NGS-based methods have the potential to provide higher-resolution data on communities of parasites found in individual hosts as well as host populations. Here, we demonstrate how a novel analytical method, utilizing high-throughput sequencing of PCR amplicons, can be used to explore variation in blood-borne parasite (*Theileria*—Apicomplexa: Piroplasmida) assemblages of African buffalo at higher resolutions than has been obtained with conventional molecular tools. Results reveal temporal patterns of synchronized and opposite fluctuations of prevalence and relative abundance of *Theileria* spp. within the host population, suggesting heterogeneous transmission across taxa. Furthermore, we show that the assemblage composition of *Theileria* spp. and their subtypes varies considerably between buffalo, with differences in composition reflected in mean and variance of overall parasitemia, thereby showing the potential to elucidate previously unexplained contrasts in infection outcomes for host individuals. Importantly, our methods are generalizable as they can be utilized to describe blood-borne parasite assemblages and/or communities in any host species. Furthermore, our methodological framework can be adapted to any parasite system given the appropriate genetic marker.The findings of this study demonstrate how a novel NGS-based analytical approach can provide fine-scale, quantitative data, unlocking opportunities for discovery in disease ecology.

4.1 Introduction

The increasing availability of NGS data is revolutionizing many aspects of the life sciences—from novel insights into microbial ecology and microbiomes (Costello et al., 2009) to innovative monitoring tools for biodiversity (Smith, Thomas, Levi, Wang, & Wilmers, 2018; Yoccoz, 2012). In disease ecology, NGS-based analytical methods have the potential to provide higher-resolution data on communities of parasites found in individual hosts and host populations than data obtained using conventional diagnostic approaches (highlighted in Zylberberg, 2019).

Until now, disease ecologists have used standard medical and/ or veterinary diagnostic approaches to detect parasites, including microscopy (Hernandez-Lara, Gonzalez-Garcia, & Santiago-Alarcon, 2017; Jolles, Ezenwa, Etienne, Turner, & Olff, 2008), antibody-based techniques (Beechler et al., 2015; Gorsich et al., 2018), and conventional polymerase chain reaction (PCR) (Telfer et al., 2010). These approaches often suffer, to varying degrees, from three limitations that are relevant for investigating parasites in ecological systems: (A) a lack of breadth, (B) a lack of depth, and/or (C) a lack of precision. (A) With tools that require specific binding agents for each taxon of interest (e.g., PCR- and antibody-based detection), researchers typically only detect the specific parasites or parasite groups for which the diagnostic assay is designed. In particular, in the context of non-model host organisms and emerging infectious diseases, researchers may not detect parasites that are key drivers of community dynamics and/ or novel parasites. Nonspecific methods can ensure broad detection of etiological agents (Glidden et al., 2018); however, (B) identifying important within-host interactions (between parasite and host immune response and/or other parasites) may necessitate identifying infectious agents at low taxonomic levels. For example, infections by *Plasmodium*, the etiological agent of malaria in humans, often consist of multiple genotypes (Arnot, 1998; Smith, Felger, Tanner, & Beck, 1999). *Plasmodium* genotypes can respond differentially to treatments, with particular genotypes resistant to antimalarial medication (Huijben, Sim, Nelson, & Read, 2011). In the absence of treatment, drug-resistant strains are suppressed by their nonresistant counterparts; however, treatment results in a “competitive release” of drug-resistant genotypes

(Huijben et al., 2011), which could result in higher prevalence and abundance of drug-resistant parasites within a host population. (C) Finally, when analyzing the impact of parasite interactions on parasite transmission and host health, presence/absence data (as opposed to abundance or relative abundance) may mask intricate community interactions (Budischack et al., 2018; Lello, Boag, Fenton, Stevenson, & Hudson, 2004). Consequently, conventional diagnostic approaches often fail to capture variation in parasite community structure that is relevant to understanding parasite transmission dynamics and differential infection outcomes for the host.

Promisingly, novel molecular techniques are increasing disease ecologists' capacity to evaluate the structure and dynamics of parasite communities across a range of taxonomic scales. NGS of amplicons (NGSA, hereafter) can magnify the information obtained in one assay (Ogorzaly et al., 2015), as this approach targets one region of DNA and provides millions of sequences with low error rates (Glenn, 2011). Primers designed to target DNA can be conserved across high taxonomic levels, while encompassing enough nucleotide variation to distinguish among species or genotypes, enabling simultaneous detection of a multitude of taxa (Lindahl et al., 2013), and an estimation of the relative abundance of each taxon within a sample (Nelson, Morrison, Benjamino, Grim, & Graf, 2014). NGSA rose to popularity through microbiome research, which uses NGSA to target a short segment of the 16S rRNA gene to describe highly diverse microbial communities (Costello et al., 2009). Recently, NGSA has been used to identify diversity in micro- and macro parasite communities in the rufous mouse lemur (*Microcebus rufus*) (Aivelo & Nordberg, 2018), *Trypanosome* assemblages in the koala (*Phascolarctos cinereus*) (Barbosa et al., 2017), and *Eimeria* assemblages in the brush-tailed rock-wallaby (*Petrogale penicillata*) (Vermeulen, Lott, Eldridge, & Power, 2016). Along with the latest developments in NGSA technologies, new bioinformatic tools (such as SeekDeep; Hathaway et al., 2017) have enabled the detection of variation down to a single nucleotide level in Illumina MiSeq data, thereby allowing for the distinction between or among haplotypes/subtypes (e.g., *Plasmodium* spp.: Hathaway et al., 2017, Boyce et al., 2018; Zhong et al., 2018).

Here, we used NGSA and SeekDeep to obtain qualitative and quantitative sequence data for piroplasm assemblages, at the species clade and subtype levels, in a

herd of African buffalo (Figure 1) caught every 2–3 months for 2 years. Piroplasms are intracellular protists, including the genera *Theileria* and *Babesia*, which infect the red and/or white blood cells of a range of host species (Abdela & Tilahun, 2016; Homer, Aguilar-Delfin, Telford, Krause, & Persing, 2000; Tarav et al., 2017; Yabsley & Shock, 2013). Piroplasms are particularly important parasite species within eastern and southern African ecosystems, as infections can cause substantial mortality in wildlife of conservation concern (Nijhof et al., 2005), as well as mortality and decreased productivity in economically significant livestock (Schoeman, 2009). Although rarely infected with *Babesia* spp. (Henrichs et al., 2016; Mans, Pienaar, Ratabane, Pule, & Latif, 2016), African buffalo have been reported to be simultaneously infected with multiple species of *Theileria*, encompassing a multitude of subtypes (Mans, Pienaar, & Latif, 2015). Infection with multiple *Theileria* spp., as opposed to single-species infections, results in dramatically different pathological disorders in cattle (Woolhouse et al., 2015), indicating that parasite interactions can adversely impact host health.

Disentangling the complex African buffalo—*Theileria* system poses two major challenges that previous studies using conventional approaches were unable to overcome: First, *Theileria* is taxonomically complex and classical taxonomists have difficulty distinguishing between species and haplotypes, requiring genetically distinct, yet closely related organisms, to remain distinguished as "subtypes" (reviewed in Mans et al., 2015). Importantly, subtypes are restricted by host specificity and geographic range, indicating important biological differences (Chaisi, Collins, Potgieter, & Oosthuizen, 2013; Mans, Pienaar, & Latif, 2011; Mans et al., 2016; Pienaar, Potgieter, Latif, Thekisoe, & Mans, 2011). Attempting to differentiate between subtypes using PCR- and antibody-based approaches has been riddled with issues of cross reactivity (Mans et al., 2015). Second, *Theileria* spp. are too common in African buffalo for presence/absence data to be useful in understanding disease dynamics (i.e., animals are almost always infected with all species; Henrichs et al., 2016). Thus, uncovering *Theileria* assemblage dynamics necessitates quantitative data at fine-scale taxonomic resolution, making the African buffalo—*Theileria* system an ideal case study for describing the power of NGSA techniques in disease ecology.

We demonstrate how combining NGSA and novel bioinformatics tools enables a

sound estimation of parasite transmission and persistence dynamics by describing population prevalence (i.e., the number of hosts infected) and population frequency (the relative abundance of each taxon in the host system) of each taxon. We then demonstrate how our methods can be used to evaluate the effect of assemblage dynamics on infection outcome by assessing variation in *Theileria* assemblage among hosts and showing that variation in assemblage structure relates to parasitemia—a proxy for the magnitude of the effect of parasites on host health (e.g., Asghar, Hasselquist, & Bensch, 2011; Sol, Jovani, & Torres, 2003; Stjernman, Raberg, & Nilsson, 2008). Overall, we highlight how novel molecular and bioinformatic techniques can provide the breadth, depth, and precision of data needed to understand parasite community dynamics within host populations and in individual hosts.

4.2 Methods

4.2.1 Study area

African buffalo included in this study were located in a 900-ha enclosure within the Kruger National Park (KNP) a 19,000-km^2 preserve, located in northeastern South Africa (S 24 23′ 52″, E 31 46′ 40″). The enclosure is entirely within KNP and has numerous other wild animals typical of the ecosystem (e.g., giraffes, zebra, warthogs, small mammals, and small predators). However, the enclosure excludes megaherbivores (rhino, hippo, elephant) and large predators (lion, leopard). Study animals graze and breed naturally and find water in seasonal pans and man-made (permanent) water troughs. In extreme dry seasons, supplemental grass and alfalfa hay is supplied.

4.2.2 Sample collection and DNA extraction

A herd of 41–54 individually marked buffalo, of varying sex and age, was maintained throughout this study. Natural births and deaths occurred, leading to a total of 66 individuals sampled for this study and 443 samples. Buffalo were captured every two to three months from February 2014 to October 2015, totaling nine sampling time points. Animals were included in the study if they were captured at least two times. Animal capture and sedation protocols have previously been described by Glidden et al. (2018). During each capture, 2 ml of whole blood was collected via jugular venipuncture directly

into EDTA-coated vacutainers and stored on ice during transport. One milliliter of whole blood was pipetted into sterile microcentrifuge tubes and stored at −80°C until it was used for DNA extractions while the rest of blood was immediately used to measure red blood cell counts using an automated hematology analyzer (Vet ABC, Scil Animal Care Company).

DNA was extracted from 200 µl of EDTA blood using DNeasy Blood and Tissue Kit (Qiagen) following the manufacturer's protocol. DNA extractions were shipped to the University of Melbourne, Australia, and stored at −20°C until further testing.

4.2.3 Next-generation sequencing of PCR amplicons

4.2.3.1 Library preparation and Illumina MiSeq

The V4 hypervariable fragment (~500 bp) of the 18S rRNA gene of *Theileria* was targeted for the NGSA. Briefly, PCR amplicons were generated using the RLBF (5′–GAG GTA GTG ACA AGA AAT AAC AAT–A3′) and RLBR (5′–TCT TCG ATC CCC TAA CTT TC–3′) primers (Gubbels et al., 1999) using the AmpliTaq Gold 360 mastermix (Life Technologies) in a thermal cycler (Veriti-384™; Applied Biosystem). The first PCR was run for the initial denaturation for 2 min at 94°C followed by 30 cycles of 30 s at 94°C, 30 s at 57°C, and 1 min at 72°C and a final extension of 8 min at 72°C. PCR amplicons were purified using magnetic beads and visualized on 2% E-Gel Agarose Gel stained with SYBR Safe DNA Gel Stain (Thermo Fisher). The second PCR was performed to index the amplicons using the TaKaRa Taq DNA Polymerase (Clontech), and it was run for 2 min at 94°C, 15 cycles of 30 s at 94°C, 30 s at 57°C, 1 min at 72°C, and a final extension of 1 min at 72°C. The PCR products were then purified using magnetic beads, quantified by fluorometry (QuantiFlour® dsDNA System), and normalized. The equimolar pool of amplicons was cleaned again using magnetic beads to concentrate the pool and then measured using an Agilent High-Sensitivity D1000 Tape System (Agilent Technologies). The pool was diluted to 5 nM, and the molarity was confirmed again using the Tape System and sequenced on an Illumina MiSeq Reagent Kit v3 (600 cycle) using 2 × 300 base pairs paired-end reads. Positive (*Theileria*

orientalis) and negative (no DNA template) controls were also included during each step of the experiment.

4.2.3.2 Bioinformatic analyses

As this study aimed to describe assemblage dynamics of closely related taxa, the objective of the bioinformatic analysis was to filter and cluster sequences with single base-pair resolution and calculate relative abundance of each unique sequence within a sample.

DADA2 (run in Qiime2 V. 2016.6.0 using the DADA2 plugin: V. 2018.6.0; Callahan et al., 2016) and SeekDeep (V 2.5.1; Hathaway et al., 2017) are two filtering and clustering softwares reported to obtain single base-pair resolution. To decide on the best pipeline to use for the analysis, an in silico mock *Theileria* assemblage analysis was conducted to test reproducibility of each software (Appendix C1). After our mock assemblage analysis, we decided to use SeekDeep for all analyses. Furthermore, 10% of our samples were run in duplicate. We confirmed repeatability up to 1% relative abundance and use this cutoff throughout the rest of our analyses (Appendix C2).

Subsequently, FASTQ files from all samples were processed using a within-sample relative abundance cutoff of 1% and the Illumina MiSeq tag, allowing no mismatches. Within the SeekDeep pipeline, sequences that were marked as likely chimeric were removed. Additionally, we removed any sequences that occurred once within the study as this would imply a unique sequence that occurred in one animal at one time point. Phred quality score of each consensus sequence was assessed in FastQC (V. 0.11.7). As the final PCR amplicon is ~460 bp, sequences were retained in the analysis if bases had an average Phred quality score >30 (1 error per 1,000 bases).

4.3.3.3 Phylogenetic analyses

Bayesian inference (BI) and neighbor joining (NJ) analyses were conducted to identify sequences. First, a nonredundant database of all *Theileria* and *Babesia* subtypes known to infect African buffalo, as well as closely related species, was curated using the existing literature (Mans et al., 2015) and the NCBI database (GenBank). SeekDeep sequences and reference sequences were imported into Mesquite (V 3.51; Maddison &

Maddison, 2018) and aligned using MUSCLE (V 3.8.31; Edgar, 2004). For the BI analysis, the likelihood parameters were based on the Akaike Information Criterion (AIC) test in jModeltest V.2.1.10 (Darriba, Taboada, Doallo, & Posada, 2012; Guindon & Gascuel, 2003). The likelihood parameters used were TrN + I + G (Nst = 6; rates = invariable + gamma). A Bayesian tree was constructed using the Monte Carlo Markov Chain analysis in MrBayes (V.3.1.2). Four simultaneous tree-building chains were used to calculate posterior probabilities for 2,000,000 generations, saving every 100th tree. A consensus tree was constructed based upon the final 75% of trees produced (burnin = 0.25%).

The NJ analyses were conducted in MEGA 7.0 (Kumar, Stecher, & Tamura, 2016), and the nodes were tested for robustness with 10,000 bootstrap replicates. The data format was set to DNA, and gaps were treated as missing data. For the substitution model, substitution type was nucleotide, the method used was the number of differences, substitutions included were transitions and transversions, and rates among sites were uniform. The tree topology was checked for concordance. *Theileria* spp. clades were considered supported if NJ bootstrapping values were >75% and Bayesian posterior probability values were >0.95. Subtype clades were considered supported if NJ bootstrapping values were >75%.

4.3.4 Calculation of parasitemia

Quantitative methodology used to calculate parasitemia of the collective *Theileria* genus (i.e., assemblage abundance), including development of a quantitative PCR, is outlined in Appendix C3.

4.3.5 Describing Theileria composition at the population and individual level

R software (V 3.4.3) was used for all *Theileria* assemblage analyses. To evaluate patterns of *Theileria* assemblages across the host population and generate hypotheses regarding differences in taxon transmission, we calculated prevalence of each taxon over the study period (*Theileria* spp.-positive samples/total number of samples), prevalence of each taxon at each sampling time point (*Theileria* spp. positive samples/total number of samples per sample collecting point), frequency of each taxon over the entire study

(number of individual *Theileria* spp. sequences/total number of *Theileria* sequences), and frequency of each taxon at each sampling time point (number of sequences per *Theileria* spp./total number of *Theileria* sequences per time point).

To evaluate individual patterns of *Theileria* assemblages, we used PERMANOVA to assess whether assemblages were significantly different between individual animals, with assemblages characterized by relative abundance of taxa. PERMANOVA was run for clade and subtype assemblages. We ran PERMONVA using the adonis function in *vegan* (Oksanen et al., 2007), including individual ID and sampling time point as fixed effects. The assemblage dissimilarity matrices were calculated using Bray–Curtis distance measures.

To explore the relationship between *Theileria* assemblages and infection outcome, we visualized variation in assemblage composition (i.e., the presence and relative abundance of each taxon within a sample) in relation to mean (±standard error of mean) parasitemia for each animal. First, we calculated average relative abundance of each taxon, at the clade and subtype level per animal followed by mean (±SE) parasitemia per animal. Subsequently, average (±SE) parasitemia per animal was then plotted from highest to lowest. Stacked bar plots for average assemblages for each animal were plotted using *phyloseq* (McMurdie & Holmes, 2013) and *ggplot2* (Wickham, 2016).

4.3. Results

4.3.1 NGS of PCR amplicons reveals rich parasite assemblages

A total of 440 (of 443) DNA samples were amplified and sequenced. A total of 32,727,499 reads passed quality trimming, with an average of 69,407 ± 1,929 reads per sample. The median number of reads per sample was 60,285 (interquartile 1:48,127; interquartile 3:78,472). Three samples had less than 1,000 reads and were removed from further analyses while 17 unique sequences appeared in only one sample each and were removed from analyses. A total of 29 unique sequences were identified. Our negative control only very weakly amplified (read count = 77), and we did not find any sequences due to contamination. On average, sequences were 455 (SE ± 0.59) nucleotides in length, ranging from 460 to 451 nucleotides. Bayesian inference and NJ phylogenetic methods

produced trees with similar topologies; hence, only a representative NJ tree is presented here (Figure 4.2).

Analyses of 29 unique sequences revealed three main clades (Figure 4.2). The first clade contained four sequences which grouped with previously published sequences of the *T. velifera* clade, with strong statistical support (bootstrap value of NJ = 99%; posterior probability value for BI = 1.0). One of these sequences (MK792966) grouped with *T. velifera* (KU206307), two (MK792967 and MK792974) with *T. velifera* B (GU33376), and one (MK792987) in between *T. velifera* A (GU733375) and *T. velifera*-like sequence (JQ706077) (Figure 2). The second clade contained 11 sequences and grouped within the
T. taurotagi clade (nodal support NJ = 95%; BI = 0.93). Five sequences (MK792969, MK792979, MK792982, MK792989, and MK792991) grouped with *T.* sp. (bougasvlei) (nodal support NJ = 95%; BI = 1.0), whereas the remaining four (MK792971, MK792983, MK792984, and MK792993) and two (MK792981 and MK792988) grouped with
T. parva and *T.* sp. (buffalo), respectively (Figure 4.2). The past literature has obtained similar bootstrap support for *T. parva* and *T.* sp. (buffalo) (Mans et al., 2015: nodal support NJ = 65%; Mans et al., 2011: NJ bootstrap value of 64); however, analysis using alternative markers has differentiated these as unique taxa (Bishop et al., 2015). The third clade contained 14 sequences that grouped within the *T. mutans* clade (nodal support NJ = 100%; BI = 1.0). The *T. mutans* clade included six subtypes: *T. mutans*-like 1 (MK792968, MK792992); *T. mutans*-like 2 (MK792970, MK792980, MK792994, MK792990); *T. mutans*-like 3 (MK792972, MK792973, MK792975); *T. mutans* MSD (MK792977, MK792978, MK792985); *T. mutans* (MK792976); and one in between *T. mutans* and *T. mutans* MSD (MK792986) (Figure 2). Pairwise differences (%), and prevalence and frequencies of 29 sequences are provided in Tables C1 and C2.

4.3.2 Theileria assemblages vary in time and across individuals

4.3.2.1 Population patterns

We evaluated patterns of *Theileria* spp. infection in our study population averaged

over the entire study period and change in infection patterns over time, by assessing the prevalence (number of samples the taxon appeared in/number of samples in study or at time step) and frequency (number of sequences per taxon/number of sequences in study or at time step) of *Theileria* clades and subtypes. Clade-level analysis of *Theileria* spp. prevalence suggested a uniform and time-invariable high prevalence of all three clades (Figure 4.3a, b; Table C2). However, higher taxonomic resolution revealed variation in overall prevalence (Figure 4.3c; Table C2) as well as temporal variation in subtypes in the population (Figure 4.3d). For example, each *Theileria* clade contained 2–3 common subtypes (overall prevalence >0.75) and 1–3 fewer common subtypes (overall prevalence <0.5) (see Table C2). Some subtypes showed little variation in prevalence throughout the study (e.g., *T. velifera* and *T. velifera* B), whereas others exhibited oscillatory patterns (e.g., *T. mutans*, *T. mutans* MSD, and *T.* (sp.) buffalo) (Figure 4.3d). As prevalence is used to estimate transmission of parasites within a system (Hens et al., 2012), our findings suggest there may be variation in transmission between taxa, and within each taxon, over time.

Clade-level analysis of *Theileria* frequency indicates overall and temporal variation in frequency of clades (Figure 4.4a, b; Table C2) and subtypes (Figure 4.4c; Table C2). Notably, subtypes that occur at high prevalence throughout the study period (e.g., *T. mutans*-like 1, *T. mutans*-like 3, *T. velifera,* and *T. velifera* B) also occur at high frequencies; however, the variation in overall frequency between taxa is much more pronounced. As such, including frequency data provides a more informative depiction of population-level parasite dynamics than prevalence alone. Frequency appears to remain somewhat constant for the majority of the subtypes with a few exceptions (Figure 4.4d). Interestingly, *T. mutans*-like 1 and *T. mutans*-like 3 appear to undergo synchronous fluctuations, whereas both *T. mutans*-like 1 and *T. mutans*-like 3 appear to undergo antagonistic fluctuations with *T.* (sp.) bougasvlei (Figure 4.3d).

4.3.2.1 Individual patterns

We found that assemblage composition was significantly different between hosts at the clade (Figure 4.5a; Table 4.1, PERMANOVA, $R^2 = 0.66$, p-value < .001) and subtype level (Figure 4.5b; Table 4.2, PERMANOVA, $R^2 = 0.723$, p-value < .001).

Animals with high parasitemia appeared to have distinctly different assemblages than those with low parasitemia, both at the clade subtype level (Figure 4.5). The variance in parasitemia appeared to increase with mean parasitemia (Figure 4.5c). At the clade level, animals with higher average relative abundance of *T. velifera* had the highest mean and most variable parasitemia (Figure 4.5a, c). Similarly, at the subtype level, animals with a higher relative abundance of *T. velifera* B had the highest mean and the most variable parasitemia

(Figure 4.5b, c). Notably, animals with higher mean parasitemia, and corresponding high parasitemia variance, also had higher average relative abundance of subtype *T. mutans*.

4.4. Discussion

We utilized NGSA to investigate previously cryptic dynamics of *Theileria* assemblages in wild African buffalo at the herd and individual levels over a two-year period.

We found that our methodology increased the breadth of data collected within our system, as we simultaneously identified three species clades, and twelve closely related *Theileria* subtypes, two of which had not previously been reported in our system (see Figure 4.2). We increased the depth of data collected by analyzing data at two taxonomic levels (species group and subtype) and established methodological framework to collect data at broader (genera: all *Theileria* and *Babesia* species) and narrower (genotype) taxonomic groupings (Figures 4.3–4.5). Finally, we increased the precision at which we were able to view assemblage dynamics by obtaining relative abundance data for each taxon (Figures 4.4 & 4.5).

In particular, the increase in depth and precision enabled us to observe patterns not discernible using traditional analytical approaches. When analyzing our data at the clade level, we found uniformly high prevalence across individuals and over time (Figure 4.3a, b). These findings match Henrichs et al. (2016), which found African buffalo to be infected with the same species clades at all points in time and was thus unable to tease apart *Theileria* assemblage dynamics due to the use of invariable, qualitative data at broad taxonomic levels. Subtype analyses revealed a much more dynamic system: subtypes varied in overall prevalence with a handful of subtypes remaining remarkably

constant over time and others exhibiting synchronous and/or antagonist fluctuations in prevalence (Figure 4.3c, d). Variation among taxa and similarities in temporal trends at the clade and subtype level became even more distinct when analyzing the frequency, or relative abundance of each taxon, at the population level (Figure 4.4). Interestingly, examining subtype frequency revealed that only 1–2 subtypes drive dominance of species clades. Furthermore, the high frequency of *T.* sp. (bougasvlei), yet relatively low frequency of the *T. taurotragi* clade, highlights that examining data at coarse taxonomic levels may mask the effects of influential taxa within a system. Overall, variation in population patterns of each taxon suggests heterogeneous transmission within this genus, while synchronous and opposite patterns of abundance may point to significant interactions among *Theileria* subtypes—trends that future research can further investigate.

We found striking associations between mean parasitemia, parasitemia variance, and assemblage composition (Figure 4.5). Our data visualization indicated that animals with higher mean parasitemia have, on average, conspicuously, higher relative abundances of the *T. velifera* species clade and lower relative abundances of the *T. mutans* species clade. Assemblage composition reveals interesting patterns at the subtype level, albeit with additional nuances: trends observed in the *T. velifera* species groups appeared to be primarily driven by dominance of *T. verlifera* B; furthermore, animals with higher mean parasitemia had, on average, lower relative abundances of *T. mutans* species clade but higher relative abundances of *T. mutans* (Figure 4.5b). Parasitemia has been negatively associated with host health outcomes (Asghar et al., 2011; Sol et al., 2003; Stjernman et al., 2008) as such *T. velifera* B and *T. mutans* may be the more pathogenic subtypes within this system. However, hosts may also be tolerant of *Theileria* (i.e., as parasitemia increases, host fitness remains constant; Råberg, Graham, & Read, 2009); in this case, parasitemia would not negatively correlate with host fitness or, perhaps, tolerance varies with assemblage composition. Overall, our methods enable exploring how assemblage composition influences host fitness with initial links to parasitemia offering interesting hypotheses regarding how fine scale in parasite assemblage affects host health outcomes.

Importantly, the diversity of our assemblages is well supported by the existing

literature. We detected almost all *Theileria* subtypes previously detected in southern KNP (Mans et al., 2016). We did not find *T.* sp. (sable), which has previously been reported in African buffalo in KNP (Henrichs et al., 2016). *T.* sp. (sable) may have been previously reported in African buffalo as the *T.* sp. (sable) RLB probe cross hybridizes with *T. velifera* (Mans et al., 2011). Mans et al. (2016) used amplicon sequencing, using the Roche 454 platform, to describe the prevalence of *Theileria* spp. in South Africa, but did not detect

T. sp. (sable) in African buffalo. The absence of *T.* sp. (sable) within our study underlines how NGSA ameliorates specificity and sensitivity issues, such as cross reactivity, that plague alternative diagnostic tools. Notably, we found two species that have not been previously reported. Interestingly, these species, particularly the subtype most closely related to *T. velifera*, were detected in the same animal across multiple time points. We may have detected these species because we used very high read coverage (on average 69,407 ± 1,929 reads per sample).

When adapting our methods to other study systems, we encourage careful consideration of study design. For example, if using markers more variable than the 18S gene (e.g., more low frequency yet biologically important sequences) or addressing questions that necessitate the inclusion of low frequency sequences (e.g., mutation and evolution), we suggest running all samples in triplicate. We found the relative abundances of unique sequences within our samples were highly repeatable at a relative abundance of >1% (Appendix C2). However, during our replication experiment, we found a few low abundance sequences (<1%) that occurred in both replicates. Using duplicates or triplicates of all samples would allow researchers to differentiate between true low abundance sequences and noise, allowing for accurate reporting of genetic diversity within a population.

Overall, we found that using an NGS-based approach allowed us to obtain data powerful enough to further our understanding of assemblage dynamics in the *Theileria*—African buffalo system. Our dataset will enable us to explore a range of questions, including explicitly defining mechanistic links between parasite assemblage and host health as well as assemblage processes that alter pathogen persistence. Notably, the primers used for NGSA are conserved across all species of *Theileria* and *Babesia*,

regardless of host species (Gubbels et al., 1999). Thus, this methodology can be used to study blood-borne parasite assemblages of a broad range of host species, including the tick vector. We believe that, given the appropriate genetic marker, our workflow is readily adaptable to other disease systems. As exemplified by our study, the application of NGSA in disease ecology will exponentially increase our understanding of causes and consequences of variation in parasite assemblages in natural host populations.

4.5 Acknowledgements

We thank Kruger National Park Veterinary Wildlife Services and State Veterinarians for their help with animal capture. We also thank members of the Jolles, Jabbar, and Gasser Laboratories for their contributions to field and laboratory work. We would like to thank Nick Hathaway, the author of SeekDeep, for fast and thoughtful responses in answering questions regarding usage of the SeekDeep pipeline. Finally, we would like to thank two anonymous reviewers for providing constructive feedback on this manuscript.

4.6 References

Abdela, N., & Tilahun, B. (2016). Bovine theileriosis and its control: A review. *Advances in Biological Research*, 10(4), 200– 212.

Aivelo, T., & Norberg, A. (2018). Parasite-microbiota interactions potentially affect intestinal communities in wild mammals. *Journal of Animal Ecology*, 87(2), 438– 447.

Arnot, D. (1998). Meeting at Manson House, London, 11 December 1997: Unstable malaria in the Sudan: The influence of the dry season – Clone multiplicity of *Plasmodium falciparum* infections in individuals exposed to variable levels of disease transmission. *Transactions of the Royal Society of Tropical Medicine and Hygiene*, 92(6), 580– 585.

Asghar, M., Hasselquist, D., & Bensch, S. (2011). Are chronic avian haemosporidian infections costly in wild birds? *Journal of Avian Biology*, 42(6), 530– 537.

Barbosa, A. D., Gofton, A. W., Paparini, A., Codello, A., Greay, T., Gillett, A., … Ryan, U. (2017). Increased genetic diversity and prevalence of co-infection with *Trypanosoma* spp. in koalas (*Phascolarctos cinereus*) and their ticks identified using next-generation sequencing (NGS). *PLoS ONE*, 12(7), e0181279.

Beechler, B. R., Manore, C. A., Reininghaus, B., O'Neal, D., Gorsich, E. E., Ezenwa, V. O., & Jolles, A. E. (2015). Enemies and turncoats: Bovine tuberculosis exposes pathogenic potential of Rift Valley fever virus in a common host, African buffalo (*Syncerus caffer*). *Proceedings of the Royal Society B: Biological Sciences*, 282(1805), 20142942. https://doi.org/10.1098/rspb.2014.2942

Bishop, R. P., Hemmink, J. D., Morrison, W. I., Weir, W., Toye, P. G., Sitt, T., … Odongo, D. O. (2015). The African buffalo parasite *Theileria* sp. (buffalo) can infect and immortalize cattle leukocytes and encodes divergent orthologues of *Theileria parva* antigen genes. *International Journal for Parasitology: Parasites and Wildlife*, 4(3), 333– 342.

Boyce, R. M., Hathaway, N., Fulton, T., Reyes, R., Matte, M., Ntaro, M., … Juliano, J. J. (2018). Reuse of malaria rapid diagnostic tests for amplicon deep sequencing to estimate *Plasmodium falciparum* transmission intensity in western Uganda. *Scientific Reports*, 8(1), 10159.

Budischak, S. A., Wiria, A. E., Hamid, F., Wammes, L. J., Kaisar, M. M. M., van Lieshout, L., … Graham, A. L. (2018). Competing for blood: The ecology of parasite resource competition in human malaria-helminth co-infections. *Ecology Letters*, 21(4), 536– 545.

Callahan, B. J., McMurdie, P. J., Rosen, M. J., Han, A. W., Johnson, A. J., & Holmes, S. P. (2016). DADA2: High-resolution sample inference from Illumina amplicon data. *Nature Methods*, 13(7), 581– 583.

Chaisi, M. E., Collins, N. E., Potgieter, F. T., & Oosthuizen, M. C. (2013). Sequence variation identified in the 18S rRNA gene of *Theileria mutans* and *Theileria velifera* from the African buffalo (*Syncerus caffer*). *Veterinary Parasitology*, 191(1–2), 132– 137.

Costello, E. K., Lauber, C. L., Hamady, M., Fierer, N., Gordon, J. I., & Knight, R. (2009). Bacterial community variation in human body habitats across space and time. *Science*, 326(5960), 1694– 1697. https://doi.org/10.1126/science.1177486

Darriba, D., Taboada, G. L., Doallo, R., & Posada, D. (2012). jModelTest 2: More models, new heuristics and parallel computing. *Nature Methods*, 9(8), 772.
Edgar, R. C. (2004). MUSCLE: Multiple sequence alignment with high accuracy and high throughput. *Nucleic Acids Research*, 32(5), 1792– 1797.
Glenn, T. C. (2011). Field guide to next-generation DNA sequencers. *Molecular Ecology Resources*, 11(5), 759– 769.
Glidden, C. K., Beechler, B., Buss, P. E., Charleston, B., de Klerk-Lorist, L. M., Maree, F. F., … Jolles, A. (2018). Detection of pathogen exposure in African buffalo using non-specific markers of inflammation. *Frontiers in Immunology*, 8, 12.
Gorsich, E. E., Etienne, R. S., Medlock, J., Beechler, B. R., Spaan, J. M., Spaan, R. S., … Jolles, A. E. (2018). Opposite outcomes of coinfection at individual and population scales. *Proceedings of the National Academy of Sciences of the United States of America*, 115(29), 7545– 7550.
Gubbels, J. M., de Vos, A. P., van der Weide, M., Viseras, J., Schouls, L. M., de Vries, E., … Jongejan, F. (1999). Simultaneous detection of bovine *Theileria* and *Babesia* species by reverse line blot hybrdization. *Journal of Clinical Microbiology*, 37(6), 1782– 1789.
Guindon, S., & Gascuel, O. (2003). A simple, fast, and accurate algorithm to estimate large phylogenies by maximum likelihood. *Systematic Biology*, 52(5), 696– 704.
Hathaway, N. J., Parobek, C. M., Juliano, J. J., & Bailey, J. A. (2017). SeekDeep: Single-base resolution de novo clustering for amplicon deep sequencing. *Nucleic Acids Research*, 46(4), e21.
Henrichs, B., Oosthuizen, M. C., Troskie, M., Gorsich, E., Gondhalekar, C., Beechler, B. R., …Jolles, A. E. (2016). Within guild co-infections influence parasite community membership: A longitudinal study in African Buffalo. *Journal of Animal Ecology*, 85(4), 1025– 1034.
Hens, N., Shkedy, Z., Aerts, M., Faes, C., Van Damme, P., & Beutels, P. (2012). *Modeling infectious disease parameters based on serological and social contact data*. New York, NY: Springer-Verlag.
Hernandez-Lara, C., Gonzalez-Garcia, F., & Santiago-Alarcon, D. (2017). Spatial and seasonal variation of avian malaria infections in five different land use types within a Neotropical montane forest matrix. *Landscape and Urban Planning*, 157, 151– 160.
Homer, M. J., Aguilar-Delfin, I., Telford, S. R., Krause, P. J., & Persing, D. H. (2000). Babesiosis. *Clinical Microbiology Reviews*, 13(3), 451– 469.
Huijben, S., Sim, D. G., Nelson, W. A., & Read, A. F. (2011). The fitness of drug-resistant malaria parasites in a rodent model: Multiplicity of infection. *Journal of Evolutionary Biology*, 24(11), 2410– 2422.
Jolles, A. E., Ezenwa, V. O., Etienne, R. S., Turner, W. C., & Olff, H. (2008). Interactions between maroparasites and microparasites drive infection patterns in free-ranging African buffalo. *Ecology*, 89(8), 2239– 2250.
Kumar, S., Stecher, G., & Tamura, K. (2016). MEGA7: Molecular Evolutionary Genetics Analysis Version 7.0 for bigger datasets. *Molecular Biology and Evolution*, 33(7), 1870– 1874.
Lello, J., Boag, B., Fenton, A., Stevenson, I. R., & Hudson, P. J. (2004). Competition and

mutualism among the gut helminths of a mammalian host. *Nature*, 428, 840– 844.
Lindahl, B. D., Nilsson, R. H., Tedersoo, L., Abarenkov, K., Carlsen, T., Kjoller, R., … Kauserud, H. (2013). Fungal community analysis by high-throughput sequencing of amplified markers–a user's guide. *New Phytologist*, 199(1), 288– 299.
Maddison, W. P., & Maddison, D. R. (2018). *Mesquite: A modular system for evolutionary analysis. Version 3.51*. Retrieved from http://www.mesquiteproject.org

Mans, B. J., Pienaar, R., & Latif, A. A. (2015). A review of *Theileria* diagnostics and epidemiology. *International Journal for Parasitology: Parasites and Wildlife*, 4(1), 104– 118.
Mans, B. J., Pienaar, R., Latif, A. A., & Potgieter, F. T. (2011). Diversity in the 18S SSU rRNA V4 hypervariable region of *Theileria* spp. in Cape buffalo (*Syncerus caffer*) and cattle from southern Africa. *Parasitology*, 138(6), 766– 779.
Mans, B., Pienaar, R., Ratabane, J., Pule, B., & Latif, A. A. (2016). Investigating the diversity of the 18S SSU rRNA hyper-variable region of *Theileria* in cattle and Cape buffalo (*Syncerus caffer*) from southern Africa using a next generation sequencing approach. *Ticks and Tick-Borne Diseases*, 7(5), 869– 879.
McMurdie, P. J., & Holmes, S. (2013). phyloseq: An R package for reproducible interactive analysis and graphics of microbiome census data. *PLoS ONE*, 8(4), e61217.
Nelson, M. C., Morrison, H. G., Benjamino, J., Grim, S. L., & Graf, J. (2014). Analysis, optimization and verification of illumina-generated 16S rRNA gene amplicon surveys. *PLoS ONE*, 9(4), e94249.
Nijhof, A. M., Pillay, V., Steyl, J., Prozesky, L., Stoltsz, W. H., Lawrence, J. A., … Jongejan, F. (2005). Molecular characterization of *Theileria* species associated with mortality in four species of African antelopes. *Journal of Clinical Microbiology*, 43(12), 5907– 5911.
Ogorzaly, L., Walczak, C., Galloux, M., Etienne, S., Gassilloud, B., & Cauchie, H. M. (2015). Human adenovirus diversity in water samples using a next-generation amplicon sequencing approach. *Food and Environmental Virology*, 7(2), 112– 121.
Oksanen, J., Kindt, R., Legendre, P., O'Hara, B., Stevens, M. H. H., Oksanen, M. J., & Suggests, M. (2007). *Vegan: Community Ecology Package. R Package v2.0-8*. Vienna, Austria: R Foundation for Statistical Computing.
Pienaar, R., Potgieter, F. T., Latif, A. A., Thekisoe, O. M. M., & Mans, B. J. (2011). Mixed *Theileria* infections in free-ranging buffalo herds: Implications for diagnosing *Theileria parva* infections in Cape buffalo (*Syncerus caffer*). *Parasitology*, 138(07), 884– 895.
Råberg, L., Graham, A. L., & Read, A. F. (2009). Decomposing health: Tolerance and resistance to parasites in animals. *Philosophical Transactions of the Royal Society of London. Series B, Biological Sciences*, 364(1513), 37– 49.
Schoeman, J. P. (2009). Canine babesiosis. *Onderstepoort Journal of Veterinary Research*, 76(1), 59– 66.
Smith, J. A., Thomas, A. C., Levi, T., Wang, Y. W., & Wilmers, C. C. (2018). Human

activity reduces niche partitioning among three widespread mesocarnivores. *Oikos*, 127(6), 890– 901.

Smith, T., Felger, I., Tanner, M., & Beck, H. P. (1999). The epidemiology of multiple *Plasmodium falciparum* infections - 11. Premunition in *Plasmodium falciparum* infection: Insights from the epidemiology of multiple infections. *Transactions of the Royal Society of Tropical Medicine and Hygiene*, 93, S59– S64.

Sol, D., Jovani, R., & Torres, J. (2003). Parasite mediated mortality and host immune response explain age-related differences in blood parasitism in birds. *Oecologia*, 135(4), 542– 547.

Stjernman, M., Raberg, L., & Nilsson, J. A. (2008). Maximum host survival at intermediate parasite infection intensities. *PLoS ONE*, 3(6), e2463.

Tarav, M., Tokunaga, M., Kondo, T., Kato-Mori, Y., Hoshino, B., Dorj, U., & Hagiwara, K. (2017). Problems in the protection of reintroduced Przewalski's horses (*Equus ferus przewalskii*) caused by piroplasmosis. *Journal of Wildlife Diseases*, 53(4), 911– 915.

Telfer, S., Lambin, X., Birtles, R., Beldomenico, P., Burthe, S., Paterson, S., & Begon, M. (2010). Species interactions in a parasite community drive infection risk in a wildlife population. *Science*, 330, 243– 246.

Vermeulen, E. T., Lott, M. J., Eldridge, M. D., & Power, M. L. (2016). Evaluation of next generation sequencing for the analysis of Eimeria communities in wildlife. *Journal of Microbiol Methods*, 124, 1– 9.

Wickham, H. (2016). *ggplot2: Elegant graphics for data analysis*. New York, NY: Springer-Verlag.

Woolhouse, M. E. J., Thumbi, S. M., Jennings, A., Chase-Topping, M., Callaby, R., Kiara, H., … Toye, P. G. (2015). Coinfection determine patterns of mortality in populations exposed to parasite infections. *Scientific Advances*, 1, e1400026.

Yabsley, M. J., & Shock, B. C. (2013). Natural history of Zoonotic Babesia: Role of wildlife reservoirs. *International Journal for Parasitology. Parasites and Wildlife*, 2, 18– 31.

Yoccoz, N. G. (2012). The future of environmental DNA in ecology. *Molecular Ecology*, 21(8), 2031– 2038.

Zhong, D., Lo, E., Wang, X., Yewhalaw, D., Zhou, G., Atieli, H. E., … Yan, G. (2018). Multiplicity and molecular epidemiology of *Plasmodium vivax* and *Plasmodium falciparum* infections in East Africa. *Malaria Journal*, 17, 14.

Zylberberg, M. (2019). Next-generation ecological immunology. *Physiological and Biochemical Zoology*, 92(2), 177– 188.

Table 4.1. PERMANOVA results table for species clade assemblage composition.

	df	**SS**	**MS**	***F* statistic**	R^2	***p***
Time	8	0.687	0.086	4.477	.030	<.001
Animal	65	15.077	0.232	12.092	.662	<.001
Residuals	366	7.021	0.019		.308	
Total	439	22.786			1.000	

Note: p-values based on 999 permutations.
Abbreviations: animal, animal ID; df, degrees of freedom; MS, mean sum of squares; SS, sum of squares; time, sampling time point

Table 4.2. PERMANOVA results table for subtype assemblage composition

	df	**SS**	**MS**	***F* statistic**	R^2	***p***
Time	8	1.374	0.172	5.552	.030	<.001
Animal	65	33.677	0.518	16.746	.726	<.001
Residuals	366	11.323	0.031		.244	
Total	439	46.374			1.000	

Note: p-values based on 999 permutations.
Abbreviations: animal, animal ID; df, degrees of freedom; MS, mean sum of squares; SS, sum of squares; time, sampling time point

Figure 4.1. African buffalo in Kruger National Park, South Africa. Photograph courtesy of Robert Spaan.

Figure 4.2. Phylogenetic relationship among consensus sequences of *Theileria* spp. determined in this study (bold) and the reference sequences for all *Theileria* spp. that infect African buffalo as well as closely related species (regular font, sequences with subtype names). Relationships were inferred from phylogenetic analysis of sequence data for a ~460-bp region of the 18S V4 rRNA gene by neighbor joining and Bayesian inference. Neighbor joining bootstrap values >75% and Bayesian inference posterior probabilities >0.90 are included on tree branches

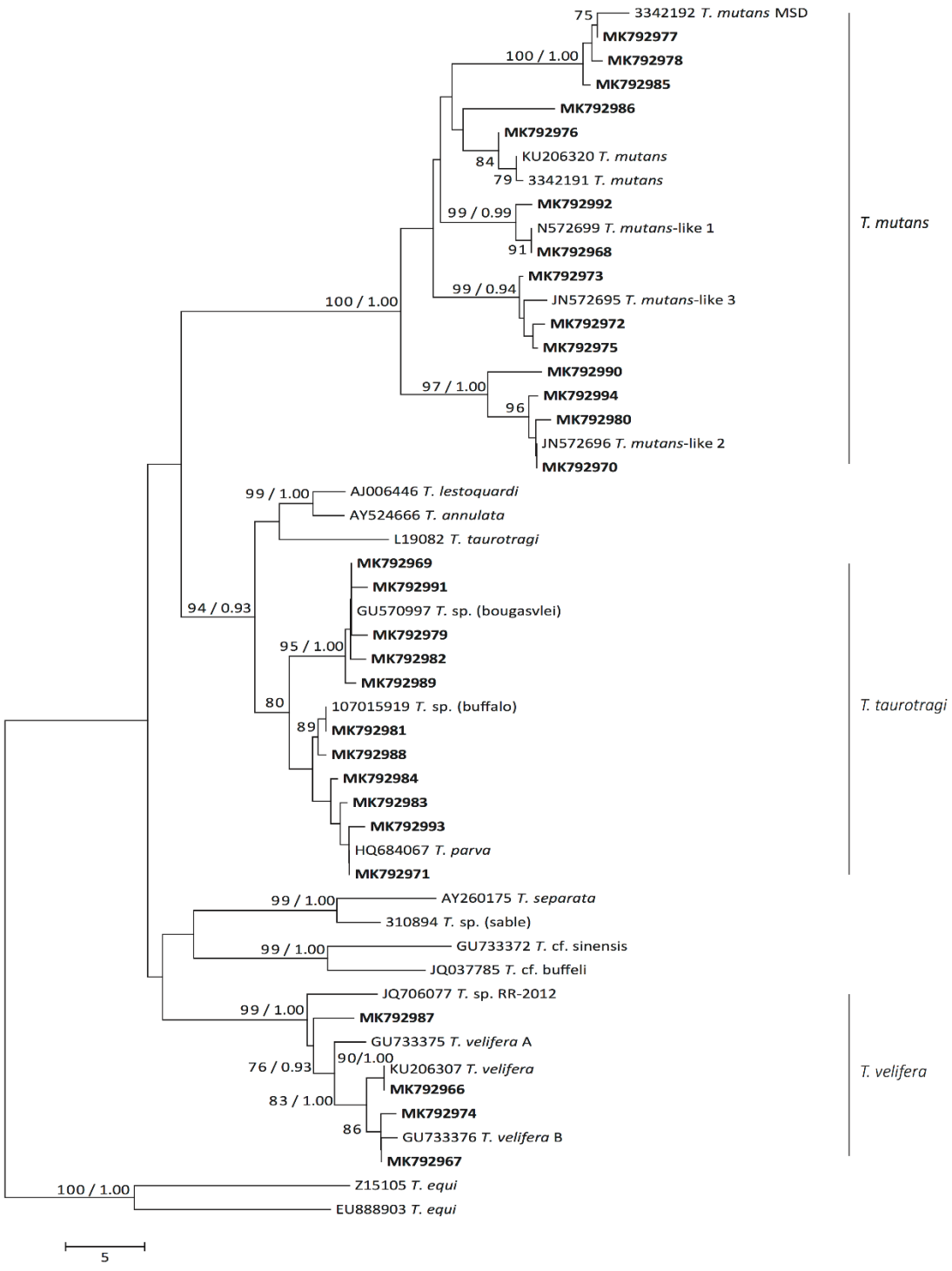
3342192 T. mutans MSD
MK792977
MK792978
MK792985
MK792986
MK792976
KU206320 T. mutans
3342191 T. mutans
MK792992
N572699 T. mutans-like 1
MK792968
MK792973
JN572695 T. mutans-like 3
MK792972
MK792975
MK792990
MK792994
MK792980
JN572696 T. mutans-like 2
MK792970
AJ006446 T. lestoquardi
AY524666 T. annulata
L19082 T. taurotragi
MK792969
MK792991
GU570997 T. sp. (bougasvlei)
MK792979
MK792982
MK792989
107015919 T. sp. (buffalo)
MK792981
MK792988
MK792984
MK792983
MK792993
HQ684067 T. parva
MK792971
AY260175 T. separata
310894 T. sp. (sable)
GU733372 T. cf. sinensis
JQ037785 T. cf. buffeli
JQ706077 T. sp. RR-2012
MK792987
GU733375 T. velifera A
KU206307 T. velifera
MK792966
MK792974
GU733376 T. velifera B
MK792967
Z15105 T. equi
EU888903 T. equi
T. mutans
T. taurotragi
T. velifera
5

Figure 4.2

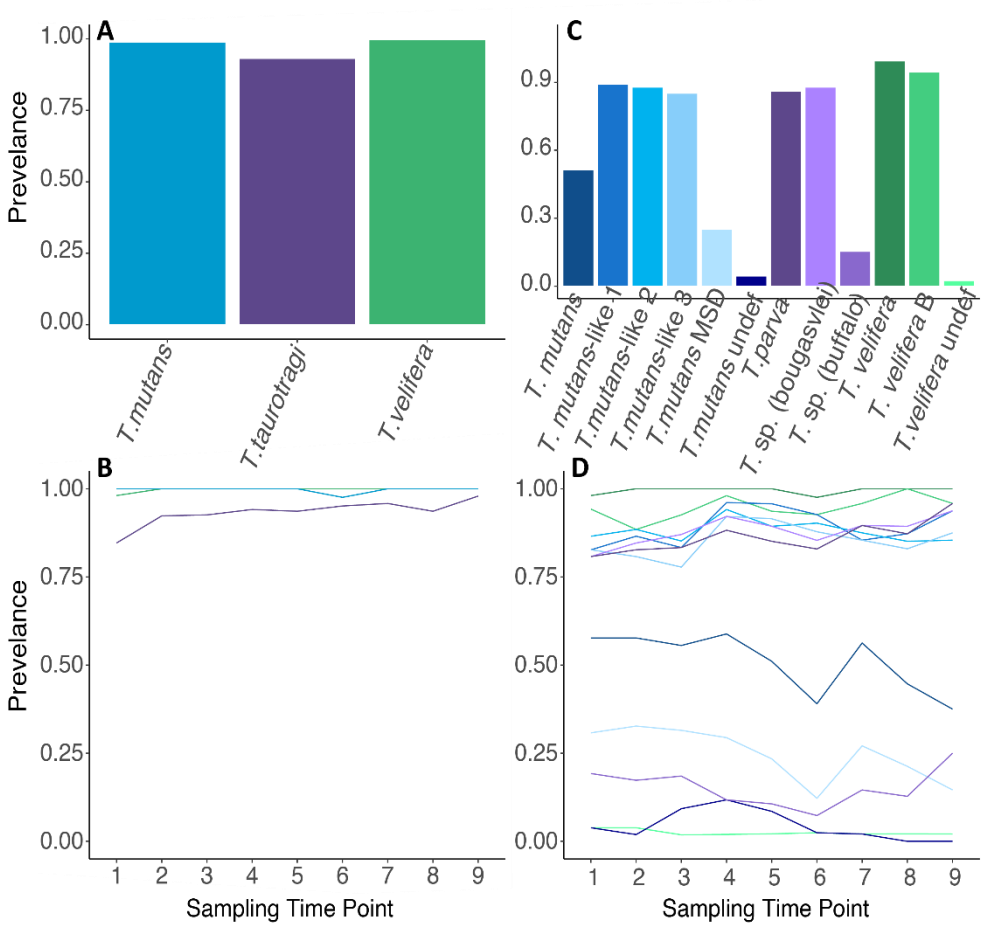

Figure 4.3. Prevalence of *Theileria* species clades and subtypes. The overall prevalence of *Theileria* spp. over the entire study and at each sampling time point for each clade (a, b) and subtype (c, d). Note: Colors for each taxon are identical in bar plots and line graphs.

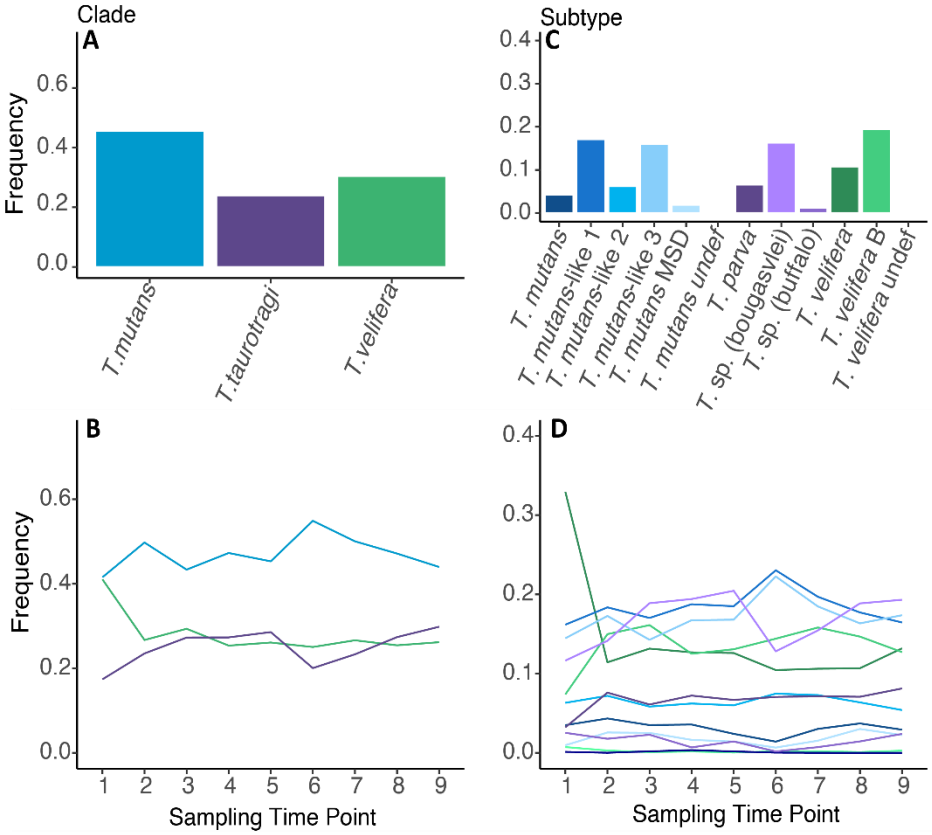

Figure 4.4. Frequencies of *Theileria* species clades and subtypes at a population level. Overall frequencies of *Theileria* spp. over the entire study and at each sampling time point for each clade (a, b, respectively) and subtype (c, d, respectively). Note: Colors for each taxon are identical in bar plots and line graphs

Figure 4.5. Parasitemia and variation in assemblage composition at an individual level. (a) Averaged clade assemblage composition for each animal. (b) Averaged subtype assemblage composition. (c) Percent parasitemia (mean and SE) for each animal. The y-axis extends from 0% to 1% (not 100%). Each figure is ordered from the animal with the lowest mean % parasitemia to the highest % parasitemia.

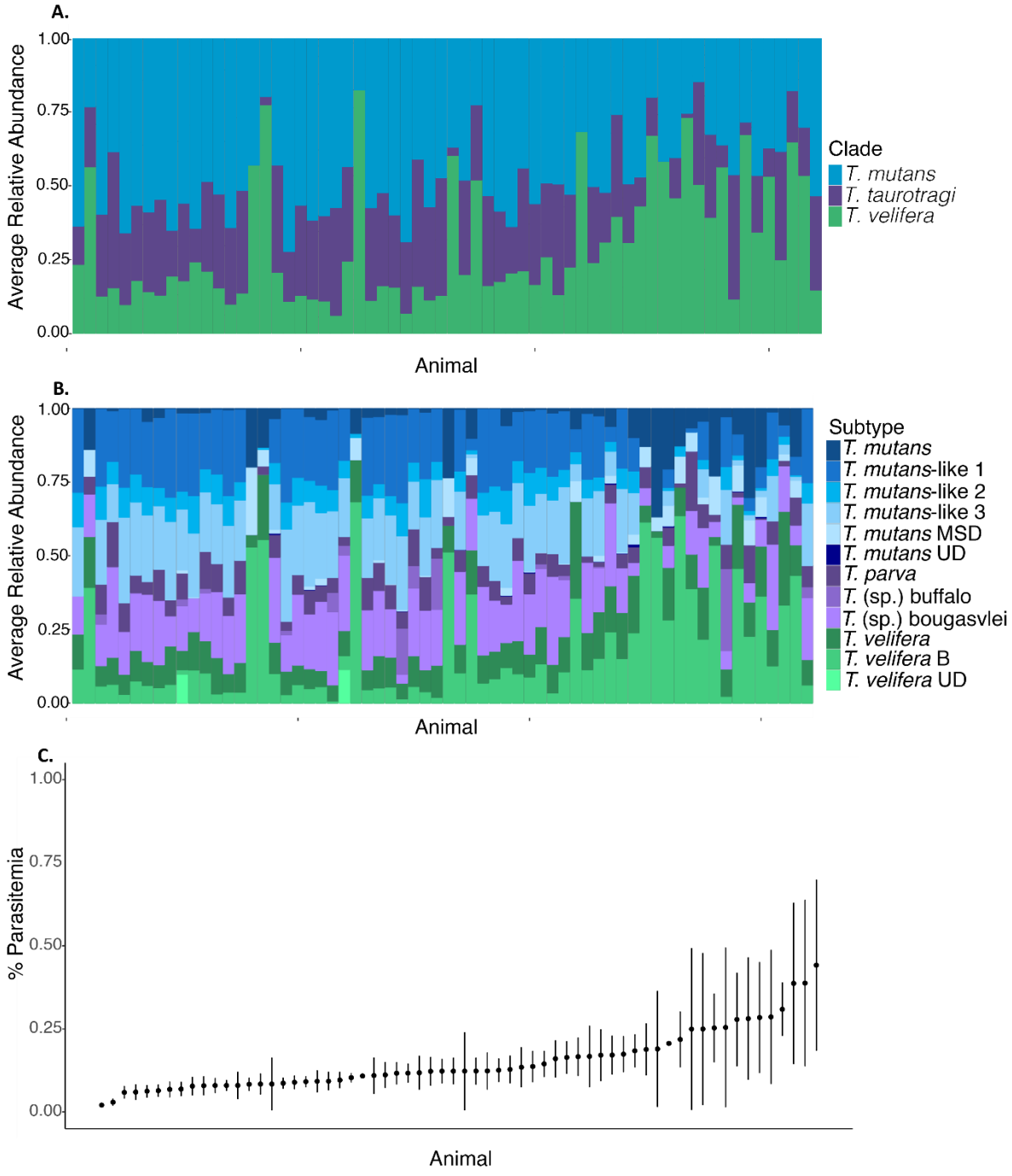
A.
Average Relative Abundance
1.00
0.75
0.50
0.25
0.00
Animal
Clade
T. mutans
T. taurotragi
T. velifera
B.
Average Relative Abundance
1.00
0.75
0.50
0.25
0.00
Animal
Subtype
T. mutans
T. mutans-like 1
T. mutans-like 2
T. mutans-like 3
T. mutans MSD
T. mutans UD
T. parva
T. (sp.) buffalo
T. (sp.) bougasvlei
T. velifera
T. velifera B
T. velifera UD
C.
% Parasitemia
1.00
0.75
0.50
0.25
0.00
Animal

Figure 4.5

CHAPTER 5: MULTIPLE SPATIO-TEMPORAL PROCESSES SHAPE STRUCTURE OF COMPLEX MICROPARASITE ASSEMBLAGES WITHIN AND AMONG HOSTS

Abstract

Understanding the structure and dynamics of complex parasite communities is fundamental to uncovering variation in host susceptibility as well as parasite spread and persistence. Analogous to free-living meta-communities, parasite assemblage structure is governed by an interplay between resource utilization and response, within and among host heterogeneity, and dispersal capacity. Further, death of hosts drives stochastic extinction of parasite populations, with the birth of hosts continually creating new, open habitat patches. The continual opening of new habitats enables patch and/or neutral dynamics to structure parasite communities in absence of differential resources use and response and host heterogeneity. Distribution of parasite assemblages is most likely driven by processes occurring at multiple spatio-temporal scales, however, particularly for micro-parasites, advancing sequencing technology has only just allowed for informative description of temporal and spatial variation in assemblage structure.

Here we investigated the structure and dynamics of a piroplasm assemblage, comprised of twelve strains of *Theileria* parasites, in a herd of African buffalo in Kruger National Park, South Africa. The entire herd was sampled ten times during a period of two years, and included animals of all ages. At each sampling event, hosts were evaluated in terms of high-throughput read counts of all twelve subtypes of *Theileria* and burdens of the two main local tick vectors for *Theilerias,* as well as immunologic and physiologic parameters that might affect *Theileria* infections. We used a life-history analysis to elucidate temporal variation in host and population infection history. For microparasites, life histories are typically described with reference to their host populations, focusing on the infected host as the functional unit, rather than the individual parasite. Microparasite life history variation can thus be conceptualized in terms of host age at first infection, parasite prevalence and within-host abundance throughout the host's life span. We then used multi-variate statistics to determine how host resources and immune response further structure parasite assemblages at varying spatial scales.

We found that subtypes grouped in time and space by their life-history strategy. We found that common *Theileria* parasites group along two life history axes, colonization ability and persistence of infection, with all combinations of these traits represented in our parasite assemblage. Further, we provide evidence that both host traits and vector dynamics contribute to shaping *Theileria* assemblages within and across hosts. Wildlife study systems such as this can serve as model systems to elucidate how parasite assemblages function, how they affect their hosts, and ultimately, how disease control interventions might utilize assemblage dynamics to implement successful and cost-effective practices.

5.1 Introduction

Understanding the structure and dynamics of complex parasite communities within hosts and host populations is fundamental to understanding variable outcomes of infections for individual hosts (Abbate et al., 2018), changing burdens of infection over time in host populations (Budischak et al., 2018), and to predicting effectiveness and side effects of disease control interventions (Ezenwa & Jolles 2015).

Ecological processes that drive parasite distribution within and among hosts, resulting in observed community and meta-community structure, include analogous mechanisms to free-living systems (Johnson, de Roode & Fenton 2015). The distribution of free-living species is governed by their ability to survive and reproduce in a local habitat path (community) as well as their ability to disperse across a region of habitats (meta-community). Neutral models assume species equivalency, whereas niche-based models relax this assumption allowing for differences in species' resource utilization and response (i.e, interspecific interactions) as well as dispersal capacity (Leibold & Chase 2018). In some niche-based systems, local and regional heterogeneity in environmental conditions, and differential use of habitats (i.e, niche), influence species distribution within a community and across a meta-community (Leibold & Chase 2018). Further, demographic stochasticity can cause local extinctions – if local environmental conditions are homogenous, and species exhibit a competitive hierarchy, local extinctions open

habitat for competitively inferior, but dispersal superior, species to colonize before being displaced by competitively superior, dispersal inferior, species (Tillman 1994). In this instance, species co-exist throughout a meta-community using a competition-colonization trade and niche availability changes with temporal variability of local interaction networks (Tillman 1994).

In host-parasite systems, niches emerge through availability of host tissue and/or host nutrients (resources) and regulation by the host immune system (trophic interactions), which can both be influenced by co-infecting parasites (competition-facilitation interactions) (Pedersen & Fenton 2007, Rynkiewicz, Pedersen & Fenton 2015). Thus, niches for parasites can be defined by variation in host immune response and resource utilization, and the resulting parasite-parasite interaction network, on multiple spatio-temporal scales. For example, parasites might use specific host tissue and sort in space within the hosts (Pedersen & Fenton 2007) or might infect specific hosts (e.g., hosts that have different immune phenotypes based upon sex (Krasnov et al., 2005; Metcalf & Graham 2018) or genetics (Williams-Blangero et al., 2012)) and sort among hosts. Niche availability may also vary temporally within hosts, with fluctuations in host resources (e.g., blood cells) or immune responsiveness (Beechler et al., 2017) driving changes to the parasite infra-community (Kendig et al., 2020); and at the population scale, where asynchronous changes in host physiology can alter niche availability among hosts. Additionally, due to birth and death of hosts, habitat patches for parasites are by definition ephemeral, with births driving the continual creation of new, open habitat patches. Although relatively unexplored in host-pathogen systems (but see Harbison et al., 2008, Mordecai et al., 2016), succession dynamics in hosts could thus allow the persistence of competitively inferior, but rapidly dispersing, pathogens, by infecting young animals before being displaced by competitively superior pathogens with slower transmission rates (Tillman 1994).

Dispersal capacity between patches can provide species an advantage which either enables them to colonize new patches (i.e, newborn animals) and occupy environments absent of competitively superior species, or disperse at such high rates between patches that they can persist in unfavorable habitats despite the presence of competitively dominant species, thereby preventing competitive exclusion (Pacala & Roughgarden

1982; Chesson 1985). On the other hand, dispersal capacity can be limited so that species are not present in all habitat patches where they could otherwise maintain positive growth (Cadotte 2006; Condit, Chisolm & Hubbel 2012) – this limitation may slow their ability to colonize new habitat patches or re-colonize existing patches. Alternatively, dispersal capacity can be invariable across species, but sufficient for each species to disperse throughout the meta-community, so that local environment is the only driver of species assemblage (Leibold & Chase 2018). In vector-transmitted disease, dispersal advantages may arise through occupying unique niches within vectors such as infecting vectors that are typically found at higher abundances within the environment or on the intermediate or definitive host, more efficient uptake by the vector, or competitive dominance within the vector. Consequently, vectors might serve as an additional source of niche availability, complementary or contradictory to host-related niche axes (e.g., vector (snail) composition influences parasite community structure in pacific chorus frogs: Mihaljevic et al., 2018).

A majority of work investigating the processes that structure parasite assemblages has focused on the spatial organization of macroparasites (Rigels et al., 2013, Dallas & Presley 2014). Distribution of parasite assemblages is most likely drive by niche occupancy at multiple spatio-temporal scales, however, particularly for micro-parasites, informative temporal and spatial patterns have been challenging to detect. Microparasite communities have been less tractable, in part because microparasite diagnostics, until recently, have tracked prior exposure rather than current infection (i.e., detection of antibodies), or current infection has been characterized merely as present or absent, limiting power to detect variation in community structure and species interactions (Fenton, Viney & Lello 2010). However, new diagnostic tools (e.g., sequencing technologies: chapter 4; Glidden et al., 2019) enable collecting higher resolution data that reveals more variation in parasite distribution. Importantly, we can now unravel temporal variation by classifying microparasites according to their life history strategy as well as examine previously cryptic variation in host resource use and response. Microparasite life histories are aptly classified by focusing on the infected host as the functional unit, rather than the individual parasite (Vicente et al., 2007). Microparasite life history variation can thus be conceptualized in terms of host age at first infection, parasite prevalence and

within-host abundance throughout the host's life span. Thus, characterizing microparasites by their life history strategy enables one to describe parasites' colonization ability and ephemerality within-hosts, as well as speculate on their competitive rank in within-host assemblage. Pairing life-history analyses with typical multivariate community assembly analyses, which align species abundances with habitat characteristics (e.g., resources, predation), allows one to more comprehensively dissect the drivers of parasite assemblages across space and time.

Here we investigated the structure and dynamics of a piroplasm assemblage, comprised of twelve subtypes of *Theileria* microparasites, in a herd of African buffalo in Kruger National Park, South Africa (Glidden et al., 2019). *Theileria* are tick-borne intracellular protists within the phylum Apicomplexa (Norval, Perry & Young 1992). African buffalo are reservoir hosts for three species clades (*T. taurotragi, T. mutans, T.* velifera), which also infect cattle at the wildlife-livestock interface and cause economically significant morbidity and mortality (Mans et al., 2016). In the buffalo host, all *Theileria* have a life stage in which they infect lymphocytes (a type of white blood cell) and red blood cells (Norval, Perry & Young 1992). However, *Theileria* within the *T. taurotragi* species clade (*T. parva, T.* sp. (bougasvlei), *T.* sp. (buffalo)) are primarily transmitted by ticks within the *Rhipicephalus* genus and replicate within white blood cells of the mammalian host, before transfer to red blood cells for uptake by the tick vector; whereas *Theileria* within the *T. mutans* and *T. velifera* clades are transmitted by *Amybolyomma* ticks and primarily replicate within red blood cells of the mammalian host (Norval, Perry & Young 1992). While immune response to *T.mutans* and *T. velifera* is poorly understood, protective immunity against *T. parva* (in the T. taurotragi clade) in cattle is largely mediated by CD8+ cytotoxic T cells (McKeever et al., 1994) and CD4+ cells associated with Type 1 T helper cells (Baldwin et al., 1992) – both of which are typical immune response to intracellular parasites (Murphy 2011). Wild African buffalo tend to be infected by all 3 species clades of *Theileria* at most times (Henrichs et al., 2016), but quantitative diagnostic techniques have revealed striking variation in relative abundance of subtypes within buffalo, and in assemblage structure among hosts (Glidden et al., 2019). These findings raise the question how so many closely related parasite subtypes, with overlapping resource utilization and immune response, can coexist in a

host population, and what processes structure *Theileria* assemblages in individual buffalo hosts.

We assessed *Theileria* life history variation in terms of the initial timing and persistence of infection, as well as the relative abundance of each *Theileria* stubtype throughout the host's life span, providing us with measures of colonization ability, chronicity / ephemerality and relative competitive ability for each strain. Next, we evaluated how the structure of parasite communities within individual buffalo associated with static and temporally variable host traits. Finally, we examined patterns of tick-infestation among the buffalo over time, to understand the role of vector dynamics in driving *Theileria* assemblage dynamics, particularly as they relate to colonization and ephemerality.

5.2 Methods

5.2.1 Study system and sample collection

African buffalo included in this study were located in a 900-hectare enclosure within the Kruger National Park (KNP) a 19,000 km^2 preserve, located in northeastern South Africa (S 24 23' 52", E 31 46' 40") (Figure D1). The enclosure is entirely within the KNP and has numerous other wild animals typical of the ecosystem (e.g., giraffe, zebra, warthogs, small mammals and small predators). However, the enclosure excludes mega-herbivores (rhino, hippo, elephant) and large predators (lion, leopard). Study animals graze and breed naturally and find water in seasonal pans and man-made (permanent) water troughs. In extremely dry conditions, supplemental grass and alfalfa hay was supplied. At any given time, depending on births and deaths, the herd consisted of around 50 buffalo with 66 total animals.

The herd was sampled at two-three month intervals from February 2014 – December 2015 (capture time points = 10). Animal capture and sedation protocols have previously been described by Couch et al. (2017). The study was conducted under South Africa Department of Agriculture, Forestry and Fisheries Section 20 permits Ref 12/11/1, ACUP project number 4478 and 4861, Onderstepoort Veterinary Research Animal Ethics Committee project number 100261-Y5, and the Kruger National Park Animal Care and Use Committee project number JOLAE1157-12.

Body condition was measured during immobilization by visually inspecting and palpating four areas on the buffalo where fat is stored: ribs, spine, hips and base of tail. Each area was scored from 1 (very poor) to 5 (excellent) and an overall body condition score was calculated, as the average of all four areas (Ezwenwa, Jolles & O'Brien 2009). For animals born during the study, their birthdate was recorded and their age was tracked accordingly. Age was assessed from body length and horn length for animals born before the start of the study but < 2 years old, incisor emergence patterns for buffalo aged 2-5 years, and from tooth wear of incisor one for buffalo aged 6 years and older (Jolles 2007). Length (cm) of each buffalo was measured from the base of the skull to the base of the tail; horn length (cm) for animals < 2 years old was measured from the base of the skull to the tip of the horn. Pregnancy was evaluated at each capture time point via rectal palpation (Beechler et al., 2012). To enable estimation of tick abundances, given the constraint of limited immobilization time, a photograph was taken at the base of the inguinal, periaxillary and perianal region (methods of obtaining photographs during immobilization are described in detail in Anderson et al., 2012; methods of measuring abundance from photographs described in 5.2.5 and Sisson et al., 2017). When an animal was initially included in the study (during the first capture period or when the animal was born) an ear clip was taken for genomics analyses.

During each capture, 15 mL of whole blood was collected via jugular venipuncture directly into EDTA-coated and serum-separating vacutainers and stored on ice during transport. One millilitre of whole blood was pipetted into sterile microcentrifuge tubes and stored at -80°C until used for DNA extractions. 10mL of whole blood was centrifuged at 5000g for ten minutes and the serum was pipetted off the cellular layer into a sterile microcentrifuge. Serum was stored at -80°C until serum globulin concentrations (g/dL) were analyzed using Abaxis Vetscan VS2 (Abaxis Inc., Union City, CA, USA) chemistry analyzer on the large animal profile (Abaxis SKU500-023) (detailed methods in Couch et al. (2017)). The remainder of blood was immediately used to measure hematology variables (red blood cell count ($10^6/mm^3$), mean corpuscular volume (μm^3) (representing mean size of a red blood cell); white bloods cell counts($10^6/mm^3$)) using an automated hematology analyzer (Vet ABC, Scil Animal Care Company, USA) as well as make blood slides (protocol described in Broughton et al. (2017)). Once dried, slides

were analyzed, by the same researcher, for the proportion of white blood cell type (neutrophils, lymphocytes, eosinophils, basophils, monocytes). Count of each white blood type was calculated by multiplying the proportion of white blood cells by total white blood cell count.

The KNP experiences pronounced seasonal variation in rainfall and vegetation (MacFadyen et al., 2018), which correlates with changes in buffalo physiology (Ryan et al., 2012) within KNP and vector abundances in similar savannah ecosystems systems (Titcomb *et al.* 2017). Seasonal fluctuations in the environment are well described by an environmental vegetation index (Ryan et al., 2012). We used 16-day composite, 250-m resolution NDVI data from the Moderate Resolution Imaging Spectroradiometer (MODIS). We utilized pre-processed data from January 2014 to December 2015 obtained from MODIS for the North American Carbon Program (MODIS for NACP, https://accweb.gsfc.nasa.gov/; Gao et al., 2008, Tan et al., 2011). We extracted the NDVI data 16-day composite image to the 900-hectare enclosure (Figure D1), located southwest of Satara Rest Camp, Kruger National Park, and generated a median statistic using R [R Core Team (R version 3.6.3)]. R was used for all analyses included in section 5.2.2 – 5.2.5. Rainfall data (mm/capture month) used in the analysis was collected from the weather monitoring station located at the Satara Ranger Station, ~ 1km north of the enclosure (Scientific Services, Kruger National Park MeteorologicalRecords ; http://www.sanparks.org/conservation/scientific_new/savannah_arid/data_resources/weather.php).

5.2.2 Quantifying Theileria assemblages

We used high throughput amplicon sequencing to detect and quantify read counts of *Theileria* subtypes using an 18S rRNA sequence specific to piroplasms (*Theileria* spp. and *Babesia* spp.) (Gubbels et al., 1999). *Theileria* taxon were grouped by subtypes based on Neighbor-Joining and Bayesian Inference analyses using previously published Theileria 18S sequences (chp 4; Glidden et al., 2019). We detected twelve *Theileria* subtypes: *T.mutans* species clade subtypes: *T. mutans, T.mutans* MSD, *T. mutans*-like 1, *T. mutans*-like 2, *T. mutans*-like 3, *T. mutans*-like (undescribed); *T. velifera* species clade subtypes: *T. velifera*, *T. velifera* B, *T. velifera*-like (undescribed); *T. taurotragi* species clade

subtypes: *T. parva*, *T.* (sp) bougasveli, *T.* (sp) buffalo. Detailed methodology is described in Glidden et al. (2019) (chapter 4). In total, we included 488 samples from 66 animals spanning ten capture periods with on average 7.5 time points per animal.

5.2.3 Describing parasite life histories: colonization, ephemerality, extinction and rank through time

We identified unique life histories by considering a newborn animal as a new habitat patch and analyzing change in mean relative abundance and prevalence of each Theileria species by age (months). The relationship between relative abundance of each Theileria subtype and animal age was non-linear, as such we described this relationship using a basis-spline regression (Appendix D1; Duan & Jiang 2020). We fit models with a Dirichlet-multinomial distribution (probability mass function: Eq. 1):

$$\Pr(\boldsymbol{x} \mid \boldsymbol{\alpha}) = \frac{(n!)\Gamma(\sum \alpha_k)}{\Gamma(n+\sum \alpha_k)} \prod_{k=1}^{K} \frac{\Gamma(x_k+\alpha_k)}{(x_k!)\,\Gamma(\alpha_K)} \quad \text{Eq. 1}$$

Where *n* represents the number of read counts in a sample, x_k is the number of read counts for each subtype in a sample and α_k represents the relative abundance (proportion) of that subtype within the sample. Thus, the Dirichlet-multinomial distribution accounts for the compositional nature of our data as well as sampling effort (Appendix D1; Harrison et al., 2019; Duan & Jiang 2020). As we had repeated measures, we weighted each observation by a within-animal dependency (Appendix D1; Duan & Jiang 2020).

After fitting the basis spline regression, we quantified point estimates indicative of different life history strategies (Appendix D1).We first calculated the average host age at first infection (when relative abundance > 0.01; 0.01 is our limit of detection (chapter 4; Glidden et al., 2019)) to identify variation in pathogen colonization ability. Next, we calculated the average relative subtype abundance when the slope of the regression approaches 0 after initial infection (equilibrium); this measure provided us an estimation of subtype rank in climax communities (i.e., competitive rank) as well as subtypes that are cleared from the host (i.e., are transient or go extinct). We calculated average host age at equilibrium to further characterize *Theileria* subtype life histories. We used bootstrapping methods to estimate a 95% confidence interval around these estimates (Appendix D1).

To determine if *Theileria* are cleared from their hosts, thereby quantifying subtype extinction and ephemerality, age-prevalence curves were created by binning animals within 6-month age categories and calculating Eq. 2 for each subtype for each age class:

$$Prevelance = \frac{no.\ animals\ infected}{no.\ animals\ sampled}. \quad \text{Eq. 2}$$

Standard errors for prevalence of each subtype for each age class were calculated by Eq. 3.:

$$Standard\ error = \frac{\sqrt{no.\ animals\ infected - (1 - no.\ animals\ infected)}}{no.\ animals\ sampled}. \quad \text{Eq. 3}$$

Age-prevalence curves were particularly useful in determining parasite clearance and ephemerality in our study as we were tracking the same individuals through time.

2.4 Identifying variation in Theileria assemblages and life history strategies associated with host traits

We examined the effect of host traits on *Theileria* assemblage composition using a combination of multivariate statistics and mixed effects models. Specifically, we examined the effect of fluctuating host traits associated with resource availability and immune responses to *Theileria* parasites (red blood cell count, mean corpuscular volume (MCV; red blood cell size), white blood cell count, white blood cell composition, globulin concentration, body condition, reproductive status), traits that vary unidirectionally (age) and static host traits (sex, genetic background) on distribution of *Theileria.* We also included median NDVI to account for seasonal fluctuations in vector abundances or host physiology not explicitly accounted for in our model. As *Theileria* of buffalo replicate in lymphocytes and red blood cells (Norvak, Perry & Young 1992), which they may further specialize on based upon cell size (Budischak et al., 2018), red blood cell count, MCV, white blood cell count and proportion and abundance of lymphocytes represent parasite resources. Notably, proportion and abundance of each

white blood cell type (lymphocyte, neutrophil, basophil, monocyte, eosinophil) indicates unique immune functions (Murphy 2011). Thus, total white blood cell count, white blood cell composition and counts of each white blood cell type, globulin concentration (which are partially composed of antibodies (Murphy 2011)), body condition (Gilot-Fromont et al., 2012), sex (Krasnov et al., 2005; Metcalf & Graham 2018), and reproductive status (Trillmich et al., 2020) serve as markers of immune response and/or immuno-competence. Genetic background could relate to availability of parasite resources or immune response (Tavalire et al., 2019), depending on the pathways upregulated by the genetic markers that influence parasite distribution.

To initially explore associations between host traits and *Theileria* distribution, we used principle component analysis (PCA) to quantify assemblage composition of samples in *Theileria* ordination space and then used linear mixed models to estimate the effect of host traits (as described in the previous paragraph, with the exception of genetic background) along PCA axes one (PC1), two (PC2) and three (PC3). To account for sampling effort and the compositional nature of our data, *Theileria* read counts were center-log transformed (Gloor et al., 2017) and thus interpreted as abundance relative to the sample mean. For each PCA axis we fit a global linear mixed model with sample PC coordinates as the dependent variable, host traits, and median NDVI as covariates and animal ID and capture number as random intercepts. Our random effects control for the repeated nature of our study design as well as quantify variation in space and time not accounted for by our covariates. We used linear mixed models to explore the effect of host traits on assemblage composition as linear mixed models allow inclusion of continuous and categorical covariates as well as inclusion of random effects. To avoid over-parameterization of this initial analysis, we reduced the dimensionality of white blood cell count and composition by summarizing these variables using a PCA described in Appendix D2. All continuous covariates were transformed to standard deviation from the mean to allow for comparison of effect size across host traits.

When initially visualizing the data we observed that PC1 coordinates follow an exponential decay with age. As such, for PC1, we ran three separate models where age was linear, age was transformed to age + age^2 (quadratic), and age was transformed to $(½)^{age}$ (exponential). We compared these models using AICc (Akaike's Information Criterion

with small-sample correction (Hurvich & Tsai 1989)) and selected the model with the exponential transformation (AICc linear=2465.95, AICc quadratic=2420.82, AICc exponential=2314.32). For each PC, we compared models with and without each random effect using a log likelihood test. After selecting for random effects, we calculated AICc for all combinations of model covariates and selected for the most parsimonious model within two AICc units of the model with the lowest AICc. We further evaluated model fit by calculating marginal and conditional R^2; marginal R^2 represents the portion of variance explained by the fixed effects while conditional R^2 represents the portion of variation explained by the fixed and random effects (Nakagawa & Schielzeth 2012). Model selection tables are included in Tables D1-D3.

We found that variation in host age, hematology and immunology best summarized variation in PC1 (section 5.3.2.1). To better disentangle if particular *Theileria*s were associated with particular hematological or immunological variables, we ran a multi-level partial least square regression. Partial least square regression allows one to evaluate the numerical relationship between multiple continuous response and explanatory variables, even when either set of variables are collinear (Wold, Sjöström & Eriksson 2001). We included abundances of each white blood cell types, globulin concentration, mean corpuscular volume and $(½)^{age}$ as explanatory variables (X matrix - variables that were significant predictors in our PC1 best fit model, all scaled to standard deviations from the mean) and center-log-transformed *Theileria* read counts as response variables (Y matrix). To control for our repeated measure study design, we used a multi-level partial least square regression that decomposes the variance in the X and Y matrix and then applies partial least square regression on the within-subject variation matrix (Liquet et al., 2012). We evaluated model performance by using leave-one-out cross validation to estimate Q^2, R^2, and mean square error of prediction (Lê Cao, González & Déjean 2009).

We found that variation in host ID summarized a large portion of variation in PC2, which was mostly explained by the presence of *T.* sp. (buffalo) (results 5.3.2.2). As such, we ran a genome wide association (GWA) analysis to test for an association between host genetic background and *T.* sp. (buffalo) presence. We included 974 assembled single-nucleotide polymorphisms (SNP) (Appendix D3; Tavalire et al., 2019). To control for genetic substructure in our sample, we performed a PCA using SNP markers in the R

package *adegenet* (Jombart & Ahmed 2011) and included the first three axes of this relatedness PCA as fixed effects in our models (Tavalire et al., 2019). We individually fit each SNP to a mixed effects logistic regression (presence of *T.* sp. (buffalo) as the response), including the fixed effects and random effects that were included in our PC2 best fit model. To account for type 1 errors, we adjusted p-values using a false discovery rate correction (Benjamini & Hochberg 1995; reported here as q-values); we included a SNP in our final model if the q-value was <0.05. We included all SNPs that were significant in these marginal models in a final global model and retained SNPs that did not change in significance level. RAD-tag sequences containing significant SNPs were then mapped to the African buffalo genome (Glanzmann et al., 2016) as in Tavalire et al., (2019). Using the linkage block previously calculated for this population of buffalo, we considered annotated proteins within a 29kb window of each SNP as potential candidates for indicators of host physiological variation (Tavalire et al., 2019). For those RAD-tag sequences that did not map to the genome, we used blastn (Madden 2002) to identify putative candidate proteins, however we could only search for proteins containing each RAD-tag and not within a window around an SNP of unknown location.

We found that variation in host ID also summarized a large portion of variation in PC3; for samples that contained equilibrium assemblages (results 5.3.1; animals > 2 years), sample coordinates along PC3 were primarily dependent upon on the rank of *T.mutans*-like 1-3 versus *T.* sp. (bougasvlei) or *T.parva* (results 5.3.2.3). As such, we ran two GWA analyses identical to the one described in the previous paragraph (one for *T.* sp (bougasvlei), one for *T.* parva). However, for each model, the response variable described whether *T.* sp. (bougasvlei) or *T. parva* ranked higher than *T.mutans*-like 1-3 (binomial: 1=ranked higher, 0=ranked lower).

Linear mixed models and generalized linear mixed models were run using *lme4* (Bates et al., 2015), with p-values calculated via the Satterthwaite's degrees of freedom method in *lmerTest* (Kuznetsova et al., 2017). Selection of random effects was conducted with the package *lmtest* (Zeileis & Hothirn 2002). Selection of fixed effects and evaluation of model fit was conducted using *MuMin* (Barton 2009). For each analysis, influential animals as well as datum were evaluated in the package *influence.ME* (Nieuwenhuis, Grontenhuis, Pelzer 2012): each model was iteratively refit by removing one animal or datum and the

change in significance of each fixed effect was evaluated for each iteration. We detected no influential data. Normality of model residuals and heteroskedasticity were evaluated using normal probability and scale-location plots, respectively. Ordination analyses were conducted in base R, PCA coordinates were extracted using *ggfortify* (Tang, Horikoshi & Li 2016). The multi-level partial least squares regression analysis was conducted in *mixOmics* (Lê Cao, González & Déjean 2009).

5.2.4 Detecting signatures of a competition-colonization trade-off

We hypothesized that dispersal superior, competitively inferior subtypes may specialize on newborn animals because they are absent of dispersal inferior, competitively superior subtypes (i.e., competition-colonization trade-off). We looked for signatures of the competition-colonization trade-off by using a linear regression, modeled in base R, to quantify the relationship between age of first infection (colonization ability) and relative abundance in climax communities (rank, a proxy for competitive ability). We assumed independence of parameter estimates used as data in the model. Normality of model residuals and heteroscedasticity were evaluated using normal probability and scale-location plots, respectively.

5.2.5 Identify potential for niche partitioning within vectors & for vector dynamics to contribute to succession dynamics

Tick pictures were scored as “low”, “medium” or “high” quality. “High” quality pictures were of high enough resolution to determine accurate tick abundances as well as identify tick genus (*Rhipicephalus* or *Amblyomma*), thus, samples in which the photograph quality was “medium” or “low” from any of the three regions were removed from analyses (Sisson et al, 2017). A single observer (DS) then counted and identified, to genus, ticks found on each buffalo at each time point. In total, we had 178 “high” quality samples from 52 animals spanning 9 capture periods. Ticks were counted using the software ImageJ (Schneider, Rasband & Eliceiri 2012). Identically to Anderson et al. (2013), total tick abundance, for each genera, on each buffalo at each capture point, were calculated using Eq.4 :

$$tick\ abundance = (2 \times axillary\ tick\ count) + (2 \times inguinal\ tick\ count) + perianal\ tick\ count. \quad \text{Eq.4}$$

We evaluated the temporal and spatial variation in tick abundance by using a generalized linear mixed model (Negative binomial distribution) to evaluate the relationship between tick abundance and buffalo traits associated with tick abundance (age, condition: Anderson et al., 2013) and environmental conditions related to variability in questing ticks in savannah ecosystems (vegetation cover: Jung Kjær et al. (2019), rainfall: Titcomb et al. (2017)). As animal size also correlates with tick abundance (Harrison et al., 2010; Vor et al., 2010), we originally included body length in our model, however, this was highly correlated (pearson's r = 0.69) with age and thus we removed it from analyses. In preliminary data visualization we observed that both *Amblyomma* and *Rhipicephalus* abundances change non-linearly with age. Thus our global model included age, age^2, condition and median ndvi as fixed effects and animal ID and capture number as random intercepts. We ran individual models for *Amblyomma* and *Rhipicephalus* abundances and compared model output to elucidate variation in *T. taurotragi* vs. *T. velifera* and *T. mutans* species clades dynamics. We compared models with and without each random effect using a log likelihood test. After selecting for our random effects, we calculated AICc for all combinations of model covariates and selected for the most parsimonious model within two AICc units of the model with the lowest AICc. We then calculated marginal and conditional R^2 for the final model. When calculating R^2 the delta method was used for calculating observation level variance as this can be used for the negative binomial distribution (Barton 2009).

We ran generalized linear mixed models using *lme4* (Bates et al., 2015), with p-values calculated via the Satterthwaite's degrees of freedom method in *lmerTest* (Kuznetsova et al., 2017). Model selection and diagnostics tests were run identically to methods outlined in section 5.2.3. Model selection tables are in Tables D4, D5.

5.3. Results

5.3.1 Life history: Subtypes exhibit variation in colonization, ephemerality and rank through time

Individual buffalo typically acquired most subtypes of *Theileria* by the time they were one year old (Figure 5.1, Figure 5.2, Table 5.1). After the host was > 2 years relative abundance of most subtypes remained quite invariable through time (Figure 5.1), suggesting that buffalo over the age of two years tend to harbor relatively stable climax assemblages of *Theileria* parasites (Figure 5.1, Figure 5.2b). However, we found substantial variation in subtype life histories, driven by variable subtype dynamics in young buffalo and differential abundances in climax assemblages (Figure 5.1, Figure 5.2).

T. velifera, *T.velifera* B, *T. mutans*, and *T. mutans* MSD appear to be early colonizers as they were present in most calves at their first sampling time point. Early infection with these subtypes was quite ubiquitous with >75% of animals 0-18 months old infected with these four subtypes. *T. velifera* and *T.velifera* B infected calves at high relative abundances and then persisted at moderate relative abundances in juvenile and adult animals: prevalence across all age groups was 100% for *T. velifera* and >75% for *T. velifera* B. In contrast, *T. mutans*, and *T. mutans* MSD were commonly cleared from the host after initial infection: About ½ of animals cleared *T. mutans* by the time they were 24-30 months old and almost all animals cleared *T. mutans* MSD by the time they reached 18-24 months of age. As such, these subtypes can be divided into two life history groups: Early-persistent (*T. velifera, T.velifera* B) and early-ephemeral (*T. mutans, T.mutans* MSD).

T. mutans-like 1, *T. mutans*-like 2, and *T. mutans*-like 3 appear to be late colonizers, with average age of first infection > 5 months, with *T.mutans*-like 3 not infecting animals until they were, on average 10 months old. From 18-24 months of age, 100% (standard error = 0) of animals were infected with these subtypes indicating that animals harbored persistent infections throughout their lifetime. *T. mutans*-like 3 and *T. mutans*-like 1 had the highest average relative abundance at equilibrium indicating that these two subtypes are commonly the highest ranking within adult animals.

T. sp. (bougasvlei) and *T. parva* exhibit much more variable patterns. The average age of first infection was > 5 months, however, the 95% confidence interval around this estimate is quite large. Likewise, the mean relative abundance of *T.* sp. (bougasvlei) in climax assemblages was very variable (95%CI = 0.02-0.35), and variable prevalence for

these subtypes indicates that some hosts may gain and lose infections throughout their lifetime.

As such these late colonizing subtypes can be divided into two life history groups: late-persistent (*T. mutans*-like 1, *T.mutans*-like 2, *T.mutans*-like-3: *T. mutans*-like 1-3) and late-ephemeral (*T. parv*a, *T.* sp. (bougasvlei)).

Lastly, *T. velifera* undefined, *T. mutans* undefined and *T.* sp. (buffalo) only infected a fraction of the host population and did not exhibit clear within-host infection patterns. These subtypes exhibit no clear life history patterns in buffalo.

Our analyses indicated that, with the exception of the subtypes with no distinct life-history groups, dispersal capacity is high enough that all *Theileria* can reach all habitat patches within a buffalo's first year of life. However, the differences in colonization ability, and ephemerality of late-persistent subtypes, indicate that there is may be some variability in dispersal capacity. Notably, for early colonizers and late-persistent colonizers, age of first infection was noticeably invariable indicating that they were consistent across sample years.

5.3.2 Host traits influence Theileria assemblage composition

We found that our first three PC axes meaningfully polarized differences in life history strategy (Figure 5.3). First, PC1 (50.8% variance explained) split *Theileria* based on their colonization ability: samples with high abundances, relative to the sample mean, of early colonizer subtypes were distributed along the positive pole of PC1 whereas samples with high abundances, relative to the sample mean, of late colonizing subtypes were distributed along the negative pole of PC1. PC2 (13.36% variance explained) split *Theileria* based on their exhibition of clear life histories or no clear life history as PC2 was most obviously explained by differences in presence of *T.* sp. (buffalo). *T. mutans* undefined and *T. mutans* undefined also located along the negative pole of PC2. PC3 (9.57% variance explained) primarily split late-persistent versus late-ephemeral *Theileria*, with samples with higher ranks of *T.* sp. (bougasvlei) and *T. parva* distributed along the negative pole of PC3 and samples with higher ranks of *T. mutans*-like 1-3 distributed along the positive pole. Interestingly, our PCA revealed no clear patterns in differential distribution of early-persistent versus early-ephemeral subtypes within young animals

when both life-history groups were present in juvenile animals (Table D6). Furthermore, our PCA revealed no clear patterns of differential distribution of subtypes within each life history group (Table D6).

5.3.2.1 PC1: Temporally variable host traits drive variation in distribution of early versus late colonizers

For PC1, we found that our best fitting model included $(½)^{age}$, wbc composition, globulin concentration, mean corpuscular volume, pregnancy status, and median NDVI as fixed effects (Table D7) and animal ID as a random intercept. Model comparison did not support the inclusion of capture number (χ2 PC1 = 1.01, p-value=0.31). $(½)^{age}$,wbc composition, globulin concentration and mean corpuscular volume had a significant effect on *Theileria* assemblage PC1. Our fixed effects explained a significant portion of variation in PC1 (marginal R^2 = 0.74, conditional R^2= 0.86) Our partial least squares regression, which was sufficiently explained by the first component (cumulative Q^2 > 0.0975; Table D8), also polarized early versus late colonizers along axis 1, and most strongly polarized early-ephemeral versus late-persistent subtypes. Mean corpuscular volume and globulin concentrations were positively associated with late-colonizers and negatively associated with early-colonizers (Figure 5.4). Our partial least square regression suggests that differences in white blood cell composition across subtypes are driven by monocyte, basophil and eosinophil abundances, with late-colonizers positively associated with eosinophils and early-colonizers positively associated with basophil and monocyte counts (Figure 5.4). The relationship between our age variable ($½^{age}$) and subtypes abundances, relative to the sample mean, is identical to what we report in our succession analysis (Figure 5.4).

5.3.2.2 PC2: Age, genetics and host ID explain presence of *T*. sp. (buffalo)

For PC2, we found that our best fitting model included age, median NDVI and late pregnancy as covariates and animal ID as a random intercept (Figure 5.5, Table D9). Model comparison did not support the inclusion of capture number (χ2 PC2=0.13, p-value=0.93). Only age had a significant effect on PC2 - older animals tended to have

assemblages that included *T.* sp. (buffalo). We found that animal ID explained a large portion of variation in these data (marginal R^2 = 0.07, conditional R^2= 0.58). We found that, throughout the study, only 20 animals were infected with *T.* sp. (buffalo), with 13 of these animals infected for > 50% of the time they were included in the study (Figure 5.5). As such, our random effect describes that *T.* (sp) buffalo was more likely to infect this subset of animals over many sampling points. Consequently, we ran a GWA analysis to identify differences in genetic background that could underpin variation in animal-level variation. We found two genetic markers that had a small but significant effect on odds of *T.* (sp) buffalo infection (Table D10). One genetic marker did not map to the annotated buffalo genome (SNP 488), however, being homozygous (GG) at this marker only increased an animals' odds of infection by ~ 0.5%. SNP 678 mapped to protein coding regions involved in chromatin binding. However, being homozygous (CC) at this marker only increased animals' odds of infection by 2%.

5.3.2.3 PC3: Capture number and host ID drive variation in distribution of late-persistent versus late-ephemeral subtypes

PC3 segregated late-persistent (*T.* mutans-like 1-3) from early-persistent (*T. parva, T.* sp. (bougasvlei)) life histories. Our best fitting model to explain variation in the abundance, relative to the sample mean, of these groups included NDVI as a fixed effect and capture number and animal ID as random intercepts (Figure 5.5, Table D11). However, NDVI did not have a significant effect on PC3. Variation in PC3 explained by the random effects was quite large in comparison to variation explained by the fixed effects (marginal R^2 = 0.005, conditional R^2= 0.59). The variance of animal ID was larger than capture number. We did not find any SNPs that significantly associated with subtype rank.

5.3.3 Succession dynamics influence distribution of late-persistent versus early-ephemeral subtypes: Evidence for a competition-colonization trade-off

There was strong evidence for a colonization-competition trade-off among subtypes within the *T. mutans* and *T. taurotragi* clades: subtypes colonizing hosts at a very young age tended to have relatively low abundance in climax assemblages of *Theileria* parasites

(Figure 5.2, Table D12). However, variation in point estimates for *T. taurotragi* clade suggests that this pattern is driven primarily by subtypes within the *T. mutans* clade. Subtypes within the *T. velifera* clade did not fit this pattern, in that they exhibited high colonization ability and moderate (*T. velifera*) to high (*T. velifera* B) relative abundances at equilibrium (Figure 5.2, Table D12). Thus, the relationship is most clear between early-ephemeral and late-persistent subtypes.

5.3.4 Tick abundances increase and saturate with host age but clear differences exist in abundance of Amyblyomma versus Rhipicephalus abundances throughout time

Tick abundance for both genera was comparable to those reported in free-living African buffalo (Anderson et al., 2013). For both genera of ticks, we found that our best fit model included age, age ^{2} and median NDVI (Figure 5.6, Table D13) and capture number as a random intercept. Our *Amyblyomma* model also included animal ID as a random intercept, however, for *Rhipicephalus,* model comparison did not support the inclusion of animal ID ($\chi 2$ = 0.03, p-value=0.85). For both tick genera, tick abundances significantly increases and saturates with host age, although we found a stronger effect of age on *Amblyomma* abundance (Figure 5.6, Tabld D14). Median NDVI did not have a significant effect on either *Amblyomma* or *Rhipicephalus* abundance. Similarly to Anderson et al., (2013), we observed that *Amblyomma* are much more abundant, particularly on adult animals, than *Rhipicephalus* (Figure 5.6). We found the marginal R^2 for our *Amblyomma* model was quite high (0.70) suggesting that age explains a large portion of variation in our data and the portion of variation explained by the random effects was relatively low (conditional R^2= 0.89) suggesting that *Amblyomma* abundances, after accounting for age and median NDVI, only vary slightly across animal ID and capture number. In contrast, the marginal R^2 for our *Rhipicephalus* was relatively low (0.27) while the proportion of variation explained by capture number was quite high (conditional R^2= 0.68). Our results suggest that *Rhipecephalus* abundances vary temporally, independently of age and NDVI, with *Rhipicephalus* abundance likely to be higher at certain captures than others.

5.4 Discussion

Studying *Theileria* parasites in wild buffalo, we described (for the first time) life history variation in an assemblage of closely related microparasites that commonly co-infect and persist in the same individual hosts and host populations. We found that common *Theileria* parasites group along two life history axes, colonization ability and persistence of infection, with all combinations of these traits represented in our parasite assemblage: efficient colonizers that are quickly displaced by stronger competitors, quick colonizers that persist throughout the host's lifetime maintaining high relative abundance, sluggish colonizers that commonly persist as dominate subtypes throughout the host's lifetime, and slow colonizers that vary in rank and can be temporarily cleared from a host. We also found a subset of relatively rare *Theileria* that follow no clear life-history patterns. While there is, thus, no general trade-off between colonization and persistence across all *Theileria*, we did observe a colonization-persistence trade-off in the largest *Theileria* clade we studied, *T. mutans*. *T. mutans* segregate into early-ephemeral versus late-persistent life history strategies, and these divisions explain a majority of the variation in *T. mutans* subtype distribution among buffalo. Further, we provide evidence that both host traits and vector dynamics contribute to shaping *Theileria* communities within hosts: Across all clades, vector dynamics likely influence differences in colonization and dispersal capacity. The abundance of early vs late colonizing *Theileria* was associated with variation in host resources and immune response, whereas a rare but sometimes locally dominant subtype (*T.* sp. (buffalo)) was primarily influenced by static host traits. In addition, the late-infecting subtypes segregated into persistent versus ephemeral groups according to the host tissue the parasite primarily replicates in as well as the parasites' primary vector species. As such, analyzing our dataset through the lens of life-history variation and spatio-temporal differences in niche availability provided novel insight on the structuring of this diverse vector-borne microparasite assemblage. Interestingly, none of the host or vector data we collected differentiated the distribution of *Theileria* subtypes within the same life history grouping, suggesting functional redundancy within life history groups.

The early-ephemeral and late-persistent subtypes we observed all grouped within the *T. mutans* species clade. The early-ephemeral subtypes were largely extirpated from adult

animals, while the late-persistent subtypes infected 100% of adult animals and *T.mutans*-like 1 & 3 remained at the highest relative abundance within adult animals. Our linear regression indicated a clear, negative relationship between age at first infection and relative abundance in climax assemblages. Taken in concert, these results indicate a competition-colonization trade-off between early-ephemeral and late-persistent subtypes. This trade-off would enable *T. mutans* and *T.mutans* MSD to persist at the population-level despite their clearance from adult animals and explain their variable distribution among age classes. Interestingly, *T. mutans* and *T.mutans* MSD infect cattle and buffalo whereas *T.mutans*-like 1 & 3 have only been reported in buffalo (Mans et al., 2016); these results are consistent with free-living communities where generalist species are superior dispersers, and thus superior colonizers, whereas specialists are dominant local competitors (Fernandez-Fournier & Aviles 2018). The mechanisms underlying variation in colonization ability of *T. mutans* subtypes are unknown. To the best of our knowledge, *T. mutans* subtypes are all transmitted by the tick genus *Amyblyomma* (Mans et al., 2016), which increase and saturate with host age indicating that exposure to *T. mutans* subtypes is constrained by buffalo age. *Amblyomma* ticks found on buffalo in the KNP are typically *A. hebraeum* (Anderson et al., 2013) suggesting that *T. mutans* subtypes share the same tick species. Early-colonizers may infect these ticks at higher prevalence, thereby obtaining a colonization advantage through a dispersal advantage. Early-colonizers may be found at higher prevalence within the tick vector by more effectively reproducing in *A. hebraeum*. Alternatively, Glidden et al., (2019) (chapter 4) noted that animals with higher relative abundances of early-colonizers, including early-ephemeral subtypes, had higher total assemblage abundances (% blood cells infected by all *Theileria*). Thus, ticks that feed on calves have higher exposure rates to *Theileria* than ticks that feed on adult animals, which may lead to a higher prevalence of early-colonizing subtypes in tick populations – however, fewer ticks feed on calves than adult animals, thus, exposure rates for ticks feeding on calves would have to be high enough to overcome the difference in abundance of ticks feeding on juvenile versus adult animals.

Early-colonizing and late-colonizing *Theileria* associated with distinct host traits. The only host resource that associated with abundance, relative to the sample mean, of early-colonizing versus late-colonizing subtypes was red blood cell size (MCV) – MCV

increase with late-colonizing subtypes indicating that early-colonizing subtypes are associated with small red blood cells, typical or microcytic anemia, or late-colonizing subtypes are associated with large red blood cells, typical of regenerative anemia (Neiger, Hadley & Pfeiffer 2002). Thus, early vs. late colonizing subtypes may specialize on different red blood cells sizes, as is hypothesized with the etiological agent of malaria (Budischack et al., 2018). *Theileria* infections are generally associated with loss of red blood cells (Norval, Perry & Young 1992). As regenerative anemia indicates that a host can rapidly replace red blood cells, hosts may be able to better tolerate late-colonizing subtypes. In this case, host health and ability to replace damaged tissue, as opposed to characteristics of individual cells, may be the niche. A natural follow-up to our work is to determine the relationship between the dynamics of the *Theileria* assemblage and host health to better predict and understand the outcomes of disease management interventions. *Theileria* is typically managed, with variable success (Woolhouse et al., 2015), by treating cattle with arachnicide to periodically remove ticks – our analyses indicate that treating cattle for ticks could change the ecological and evolutionary trajectory of *Theileria* assemblages by shifting communities toward dominance by early, efficient colonizers. A shift could be deleterious or protective of the host depending on the health effects of different *Theileria* life history groups.

Our analysis indicated that white blood cells did not serve as differential resources for early versus late colonizing subtypes as proportion of lymphocytes did not have an effect on PC1 in our linear mixed model and subtype center-log-transformed read counts did not associate with lymphocyte abundance in our partial least squares regression analysis. However, we did observe that globulins (a proxy for antibody concentration) and abundances of basophils, eosinophils, and monocytes associated with differences in abundances, relative to the sample, mean of early versus late colonizing *Theileria.* These white blood cells are not involved in the life cycle of *Theileria*, instead they each orchestrate a unique immune responses (Murphy 2011). Consequently, our analyses indicate that immune response mediates variation in *Theileria* distribution. We found that late-colonizing subtypes were associated with higher abundances of globulins. As antibodies can have neutralizing effects on *Theileria* (Musoke et al., 1992), host immune response may be less effective at removing late-colonizing subtypes. Perhaps, late-

colonizing subtypes drive an upregulation in immune response that excludes early-ephemeral subtypes (e.g., apparent competition: Råberg et al., 2006). Interestingly, in our partial least squares analysis, cells associated with upregulation of T helper cell-2 (Th2) immunity (eosinophils) positively correlated with late-colonizing *Theilerias*; whereas effector cells in T helper cell-1 (Th1) immunity (monocytes) and Th2 immunity (basophils) positively correlated with early-colonizing subtypes. Th1 immunity is associated with *Theileria* clearance (Baldwin et al., 1992; McKeever et al., 1994) whereas Th2 immunity has been found to associate with *Theileria* manipulation of the immune response and subsequent within host persistence (Yamada et al., 2009). Furthermore, heavy tick infestation also promotes a Th2 response (Ferreira & Silva 1999). Th2 immunity is historically understood to downregulate Th1 immunity (Fenton, Lamb & Graham 2008) – perhaps immunomodulation by both *Theileria* and vector promotes persistence of some subtypes. Future work could more precisely characterize immune response against versus immune-modulation by each subtype as well as examine how parasite-parasite and vector-host interactions affect the host immune system to promote subtype clearance or persistence.

Three of the *Theileria* subtypes we examined were rare in the buffalo herd, and thus could not be classified in terms of life history traits. Variation in PC2, which was primarily polarized by presence of *T.* sp. (buffalo), was partially explained by age but mostly explained by host ID. As tick abundances generally increased with age, the age effect may be due to an increase in probability of exposure with age. Interestingly, this subtype repeatedly, or persistently, infected a small subset of individuals throughout the study, suggesting that *T.* sp. (buffalo) exploits specific susceptibilities in some hosts. A GWA analysis identified two loci with small but significant effects on the odds of *T.* sp. (buffalo) infection. *T.* sp. (buffalo) transforms leukocytes by causing them to proliferate indefinitely (Bishop et al., 2015) and our analysis indicated that genes associated with chromatin binding proteins, which are important in transcription, had a small effect on *T.* sp. (buffalo) presence. The difference in African buffalo's ability to inhibit or promote *T.* sp. (buffalo) ability to manipulate host resources (i.e, cells to reproduce in) provides an interesting avenue for future molecular research. Advancing molecular methods are allowing researchers to translate high throughput sequencing data to absolute abundances

as well as better account for sequencing biases (McLaren et al., 2019, William, Hughes & Willis 2019). Additional GWA studies could examine the relationship between absolute abundance of *T.* sp. (buffalo) to examine if the same genetic markers account for variability in the absolute abundance of *T.* sp. (buffalo) in peripheral blood, which may be a more meaningful proxy for intra-lymphocyte replication rate. Moreover, gene expression is important for regulation of *Theileria* parasites (Dewangan et al., 2015); future work could examine if animal-level differences in gene expression better describe variation associated with animal ID.

None of the host traits we evaluated explained variation in the distribution of late-ephemeral (*T. parva, T.* sp. (bougasvlei)) versus late-persistent (*T.* mutans-like 1-3) *Theileria* life history groups among buffalo, but host ID and capture number seemed to play a role. Genomic and gene expression differences among hosts might account for the observed effect of host ID (Dewangan et al., 2015); however, a GWA analysis failed to identify any loci associated with the relative abundance of these groups. As briefly described with *T.* sp. (buffalo), late-ephemeral subtypes grouped in the *T. taurotragi* clade, which primarily reproduce within lymphocytes in the host's lymphatic system (Norval, Perry & Young 1992). As such, the fluctuations in abundances of these subtypes, detected by sampling peripheral blood, could be attributed to rate of proliferation occurring within the lymphatic system – this may also explain ephemerality of these subtypes as proliferation in the lymphatic system can occur at a low enough rates that parasitemia is not detected in peripheral blood (Olds, Mason & Scoles 2018). Alternatively, differences in vector dynamics may influence distribution of late-colonizing life-history subtypes within and among hosts. The vector of late-persistent subtypes, *Amblyomma,* is consistently high in adults whereas the vector of late-ephemeral subtypes *Rhipecephalus,* is low and variable over-time. Fluctuating abundances of the vector could influence variable (re) exposure rates thereby influencing temporal variability observed within the host. In support of this, PC3 (rank of late-colonizing subtypes) and *Rhipephalus* abundance were both explained by capture number. Variability in exposure rates could also account for the high variability in colonization rate and relative abundance at equilibrium of late-ephemeral subtypes. However, the effect of exposure on within-host dynamics is confounded by taxonomy dependent

within-host clearance rates. *T. mutans* subtypes, as well as *T. velifera*, can persist in cattle for years without re-infection (Norval, Perry & Young), whereas *T. taurotragi* subtypes may persist for a fraction of that time (Norval, Perry & Young). As such, the effect of vector dynamics on within-host persistence versus ephemerality may only be fully elucidated once subtype specific clearance rates vs. rate of (re) infection are precisely quantified.

None of our analysis provided clear direction for understanding distribution patterns of early-persistent (*T. velifera*, *T. velifera* B) versus early-ephemeral (*T. mutans*, *T. mutans* MSD) life histories. Astonishingly, *T. velifera* subtypes infected all animals early and remained at near-constant relative abundances throughout the life-time of the host: it is unclear how *T. velifera* subtypes excel at colonization and persistence. Perhaps these early-persistent subtypes benefit from facilitative interactions with other subtypes (e.g., Ramiro et al., 2016) – future work analyzing parasite interactions in this system will test this idea (Appendix D4). Maybe *T. velifera* subtypes are such efficient dispersers that constant re-invasion of hosts swamps any effects of competition by other *Theilerias* (Pacala & Roughgarden 2009, Chesson 1985). Even vertical transmission may play a role in the life history strategy of these subtypes (Baek et al., 2003; Mekata et al., 2018), as buffalo calves were consistently infected by the time we first captured them, and all reproductive age animals were infected. How the success of this group of *Theileria* relates to its effects on host health is yet to be explored – based on their ubiquity and distribution across all ages of hosts one would expect that adverse effects on the health should be minimal. Interestingly, work in cattle has shown that *T. velifera* parasites may even confer indirect benefits on host health, in that co-infection with *T. velifera* appears to protect against mortality associated with far more virulent *T. parva* infection (Woolhouse et al., 2015). If *T.velifera* is transmitted vertically then perhaps, a long-term management plan could infect reproductive age females with *T. velifera*, preemptively conferring calf tolerance to *T. parva*. Removal of ticks could then be done with less frequency, or perhaps even eliminated, depending on how important tick induced Th2 immunity is for influencing *Theileria* assemblage structure and how long *T. velifera* persist in the host without re-infection.

While we have documented some of the factors driving the distribution of *Theileria* parasites with different life histories among buffalo, our study does not address variation in the abundance of subtypes sharing the same life history patterns. *Theileria* within each life-history group were also the most taxonomically related (chapter 4; Glidden et al., 2019), which is consistent with patterns one would expect if an assemblage was influenced by niche filtering (Fowler, Lessard & Sanders 2013). Future work could evaluate if this pattern is indeed due to niche filtering and if niche filtering is occurring at the host and/or vector level.

Our research illustrates the value of a pairing life-history analyses with typical community assembly analyses to understand the structure and dynamics of complex parasite assemblages. Evaluating a parasite assemblage through the lens of life history variation revealed an interplay of host-parasite, host-vector and parasite-parasite relationships that underlie the spatio-temporal distribution of parasite taxa in a natural host population. Many questions remain – with the most immediate questions regarding mechanisms enabling functional redundancy of parasite strains with similar life histories, infection dynamics in the tick vectors and the influence of different parasite functional groups on host health. Our analyses illustrate innovative analytical approaches to determine parasite colonization rates and assemblage rank, and evaluate host susceptibility, providing the tools for discovering how dispersal may pair with parasite interactions and host filtering to influence parasite distributions. Wildlife study systems such as this can serve as model systems to elucidate how parasite assemblages function, how they affect their hosts, and ultimately, how disease control interventions might utilize assemblage dynamics to implement successful and cost-effective practices.

5.5 Acknowledgements

We thank Kruger National Park Veterinary Wildlife Services and State Veterinarians for their help with animal capture. We also thank members of the Jolles, Jabbar, and Gasser Laboratories for their contributions to field and laboratory work. We also thank members of the Jolles Lab for feedback on analyses and manuscript drafts.

5.6 References

Abbate, J. L., Ezenwa, V. O., Guégan, J. F., Choisy, M., Nacher, M., & Roche, B. (2018). Disentangling complex parasite interactions: Protection against cerebral malaria by one helminth species is jeopardized by co-infection with another. *PLoS Neglected Tropical Diseases*, *12*(5), 1–13. https://doi.org/10.1371/journal.pntd.0006483

Alzate, A., Janzen, T., Bonte, D., Rosindell, J., & Etienne, R. S. (2019). A simple spatially explicit neutral model explains the range size distribution of reef fishes. *Global Ecology and Biogeography*, *28*(7), 875–890. https://doi.org/10.1111/geb.12899

Anderson, K., Ezenwa, V. O., & Jolles, A. E. (2013). Tick infestation patterns in free ranging African buffalo (Syncercus caffer): Effects of host innate immunity and niche segregation among tick species. *International Journal for Parasitology. Parasites and Wildlife*, *2*, 1–9. https://doi.org/10.1016/j.ijppaw.2012.11.002

Baek, B. K., Soo, K. B., Kim, J. H., Hur, J., Lee, B. O., Jung, J. M., … Kakoma, I. (2003). Verification by polymerase chain reaction of vertical transmission of Theileria sergenti in cows. *Canadian Journal of Veterinary Research = Revue Canadienne de Recherche Veterinaire*, *67*(4), 278–282.

Baldwin, C. L., Iams, K. P., Brown, W. C., & Grab, D. J. (1992). Theileria parva: CD4+ helper and cytotoxic T-cell clones react with a schizont-derived antigen associated with the surface of Theileria parva-infected lymphocytes. *Experimental Parasitology*, *75*(1), 19–30. https://doi.org/10.1016/0014-4894(92)90118-t

Barton, K. (2009). Mu-MIn: Multi-model inference. *R Package Version 0.12.2/R18*, (1). https://doi.org/http://R-Forge.R-project.org/projects/mumin/

Bates, D., Mächler, M., Bolker, B. M., & Walker, S. C. (2015). Fitting linear mixed-effects models using lme4. *Journal of Statistical Software*, *67*(1). https://doi.org/10.18637/jss.v067.i01

Beechler, B. R., Broughton, H., Bell, A., Ezenwa, V. O., & Jolles, A. E. (2012). Innate Immunity in Free-Ranging African Buffalo (Syncerus caffer): Associations with Parasite Infection and White Blood Cell Counts. *Physiological and Biochemical Zoology*, *85*(3), 255–264. https://doi.org/10.1086/665276

Beechler, B. R., Jolles, A. E., Budischak, S. A., Corstjens, P. L. A. M., Ezenwa, V. O., Smith, M., … Steinauer, M. L. (2017). Host immunity, nutrition and coinfection alter longitudinal infection patterns of schistosomes in a free ranging African buffalo population. *PLoS Neglected Tropical Diseases*, *11*(12), 1–24. https://doi.org/10.1371/journal.pntd.0006122

Benjamini, Y., & Hochberg, Y. (1995). Controlling the False Discovery Rate: A Practical and Powerful Approach to Multiple Testing. *Journal of the Royal Statistical Society. Series B (Methodological)*, *57*(1), 289–300.

Bishop, R. P., Hemmink, J. D., Morrison, W. I., Weir, W., Toye, P. G., Sitt, T., … Odongo, D. O. (2015). The African buffalo parasite Theileria. sp. (buffalo) can infect and immortalize cattle leukocytes and encodes divergent orthologues of Theileria parva antigen genes. *International Journal for Parasitology: Parasites and Wildlife*, *4*(3), 333–342. https://doi.org/https://doi.org/10.1016/j.ijppaw.2015.08.006

Broughton, H. M., Govender, D., Shikwambana, P., Chappell, P., & Jolles, A. (2017). Bridging gaps between zoo and wildlife medicine: establishing reference intervals for free-ranging african lions (*panthera leo*). *Journal of Zoo and Wildlife Medicine*, *48*(2), 298–311. https://doi.org/10.1638/2016-0021R.1

Budischak, S. A., Wiria, A. E., Hamid, F., Wammes, L. J., Kaisar, M. M. M., van Lieshout, L., … Graham, A. L. (2018). Competing for blood: the ecology of parasite resource competition in human malaria–helminth co-infections. *Ecology Letters*, *21*(4), 536–545. https://doi.org/10.1111/ele.12919

Cadotte, M., Loreau, A. E. M., & Losos, E. J. B. (2006). Dispersal and Species Diversity: A Meta‐Analysis. *The American Naturalist*, *167*(6), 913–924. https://doi.org/10.1086/504850

Chesson, P. (1985). Coexistence of competitors in spatially and temporally varying environments: A look at the combined effects of different sorts of variability. *Theoretical Population Biology*, *28*(3). https://doi.org/10.1016/0040-5809(85)90030-9

Clay, P. A., Cortez, M. H., Duffy, M. A., & Rudolf, V. H. W. (2019). Priority effects within coinfected hosts can drive unexpected population-scale patterns of parasite prevalence. *Oikos*, *128*(4), 571–583. https://doi.org/10.1111/oik.05937

Condit, R., Chisholm, R. A., & Hubbell, S. P. (2012). Thirty Years of Forest Census at Barro Colorado and the Importance of Immigration in Maintaining Diversity. *PLOS ONE*, *7*(11), e49826.

Dewangan, P., Panigrahi, M., Kumar, A., Saravanan, B. C., Ghosh, S., Asaf, V. N. M., … Bhushan, B. (2015). The mRNA expression of immune-related genes in crossbred and Tharparkar cattle in response to in vitro infection with Theileria annulata. *Molecular Biology Reports*, *42*(8), 1247–1255. https://doi.org/10.1007/s11033-015-3865-y

Duan, C., and Jiang, Y. (2020). Subgroup analysis of longitudinal profiles for compositional count data. Technical report.

Ezenwa, V. O., Jolles, A. E., & Brien, M. P. O. (2009). A reliable body condition scoring technique for estimating condition in African buffalo, 476–481.

Ezenwa, V. O., & Jolles, A. E. (2015). Opposite effects of anthelmintic treatment on microbial infection at individual versus population scales. *Science*, *347*(6218), 175–177. https://doi.org/10.1126/science.1261714

Fenton, A., Lamb, T., & Graham, A. L. (2008). Optimality analysis of Th1/Th2 immune responses during microparasite- macroparasite co-infection, with epidemiological feedbacks. *Parasitology*, *135*(7), 841–853. https://doi.org/10.1017/S0031182008000310

Fenton, A., Viney, M. E., & Lello, J. (2010). Detecting interspecific macroparasite interactions from ecological data: patterns and process. *Ecology Letters*, *13*(5), 606–615. https://doi.org/10.1111/j.1461-0248.2010.01458.x

Fernandez-Fournier, P., & Avilés, L. (2018). Environmental filtering and dispersal as drivers of metacommunity composition: Complex spider webs as habitat patches: Complex. *Ecosphere*, *9*(2). https://doi.org/10.1002/ecs2.2101

Ferreira, B. R., & Silva, J. S. (1999). Successive tick infestations selectively promote a T-helper 2 cytokine profile in mice. *Immunology*, *96*(3), 434–439. https://doi.org/10.1046/j.1365-2567.1999.00683.x

Fowler, D., Lessard, J. P., & Sanders, N. J. (2014). Niche filtering rather than partitioning shapes the structure of temperate forest ant communities. *Journal of Animal Ecology*, *83*(4), 943–952. https://doi.org/10.1111/1365-2656.12188

Gao, F., Morisette, J. T., Wolfe, R. E., Ederer, G., Pedelty, J., Masuoka, E., … Nightingale, J. (2008). An algorithm to produce temporally and spatially continuous MODIS-LAI time series. *IEEE Geoscience and Remote Sensing Letters*, *5*(1), 60–64. https://doi.org/10.1109/LGRS.2007.907971

Gilot-Fromont, E., Jégo, M., Bonenfant, C., Gibert, P., Rannou, B., Klein, F., & Gaillard, J.-M. (2012). Immune Phenotype and Body Condition in Roe Deer: Individuals with High Body Condition Have Different, Not Stronger Immunity. *PLOS ONE*, *7*(9), e45576.

Glanzmann, B., Möller, M., le Roex, N., Tromp, G., Hoal, E. G., & van Helden, P. D. (2016). The complete genome sequence of the African buffalo (Syncerus caffer). *BMC Genomics*, *17*(1), 1001. https://doi.org/10.1186/s12864-016-3364-0

Glidden, C. K., Koehler, A. V., Hall, R. S., Saeed, M. A., Coppo, M., Beechler, B. R., … Jabbar, A. (2020). Elucidating cryptic dynamics of Theileria communities in African buffalo using a high-throughput sequencing informatics approach. *Ecology and Evolution*, *10*(1), 70–80. https://doi.org/10.1002/ece3.5758

Gloor, G. B., Macklaim, J. M., Pawlowsky-Glahn, V., & Egozcue, J. J. (2017). Microbiome Datasets Are Compositional: And This Is Not Optional. *Frontiers in Microbiology*, *8*, 2224. https://doi.org/10.3389/fmicb.2017.02224

Gubbels, J. M., de Vos, A. P., van der Weide, M., Viseras, J., Schouls, L. M., de Vries, E., & Jongejan, F. (1999). Simultaneous detection of bovine Theileria and Babesia species by reverse line blot hybridization. *Journal of Clinical Microbiology*, *37*(6), 1782–1789.

Harbison, C. W., Bush, S. E., Malenke, J. R., Clayton, D. H., Harbison, C. W., Bush, S. E., … Clayton, D. H. (2020). Comparative Transmission Dynamics of Competing Parasite Species Published by : Wiley on behalf of the Ecological Society of America Stable URL : https://www.jstor.org/stable/27650873 REFERENCES Linked references are available on JSTOR for this article : c, *89*(11), 3186–3194.

Harrison, J. G., Calder, W. J., Shastry, V., & Buerkle, C. A. (2020). Dirichlet-multinomial modelling outperforms alternatives for analysis of microbiome and other ecological count data. *Molecular Ecology Resources*, *20*(2), 481–497. https://doi.org/10.1111/1755-0998.13128

Henrichs, B., Oosthuizen, M. C., Troskie, M., Gorsich, E., Gondhalekar, C., Beechler, B. R., … Jolles, A. E. (2016). Within guild co-infections influence parasite community membership: a longitudinal study in African Buffalo. *Journal of Animal Ecology*, *85*(4), 1025–1034. https://doi.org/10.1111/1365-2656.12535

Hurvich, C. M., & Tsai, C.-L. (1989). Regression and time series model selection in small samples. *Biometrika*, *76*(2), 297–307. https://doi.org/10.1093/biomet/76.2.297

Johnson, P. T. J., De Roode, J. C., & Fenton, A. (2015). Why infectious disease research needs community ecology. *Science*, *349*(6252). https://doi.org/10.1126/science.1259504

Jolles, A. E. (2007). Population biology of African buffalo (Syncerus caffer) at Hluhluwe-iMfolozi Park, South Africa. *African Journal of Ecology*, *45*(3), 398–406. https://doi.org/10.1111/j.1365-2028.2006.00726.x

Jombart, T., & Ahmed, I. (2011). adegenet 1.3-1: new tools for the analysis of genome-wide SNP data. *Bioinformatics*, *27*(21), 3070–3071. https://doi.org/10.1093/bioinformatics/btr521

Jung Kjær, L., Soleng, A., Edgar, K. S., Lindstedt, H. E. H., Paulsen, K. M., Andreassen, Å. K., … Bødker, R. (2019). Predicting the spatial abundance of Ixodes ricinus ticks in southern Scandinavia using environmental and climatic data. *Scientific Reports*, *9*(1), 18144. https://doi.org/10.1038/s41598-019-54496-1

Kendig, A. E., Borer, E. T., Boak, E. N., Picard, T. C., & Seabloom, E. W. (2019). Host nutritoin mediates interactions between plant viruses, altering transmission and predicted disease spread. *BioRxiv*, 1–31. https://doi.org/10.1007/springerreference_23955

Krasnov, B. R., Morand, S., Hawlena, H., Khokhlova, I. S., & Shenbrot, G. I. (2005). Sex-biased parasitism, seasonality and sexual size dimorphism in desert rodents. *Oecologia*, *146*(2), 209–217. https://doi.org/10.1007/s00442-005-0189-y

Kuznetsova, A., Brockhoff, P. B., & Christensen, R. H. B. (2017). lmerTest Package: Tests in Linear Mixed Effects Models . *Journal of Statistical Software*, *82*(13). https://doi.org/10.18637/jss.v082.i13

Leibold, M. A., & Chase, J. M. (2018). *Metacommunity ecology*. Princeton, NJ: Princeton University Press.

Liquet, B., Cao, K.-A. L., Hocini, H., & Thiébaut, R. (2012). A novel approach for biomarker selection and the integration of repeated measures experiments from two assays. *BMC Bioinformatics*, *13*(1), 325. https://doi.org/10.1186/1471-2105-13-325

MacFadyen, S., Zambatis, N., Van Teeffelen, A. J. A., & Hui, C. (2018). Long-term rainfall regression surfaces for the Kruger National Park, South Africa: a spatio-temporal review of patterns from 1981 to 2015. *International Journal of Climatology*, *38*(5), 2506–2519. https://doi.org/10.1002/joc.5394

MacHugh, N. D., Connelley, T., Graham, S. P., Pelle, R., Formisano, P., Taracha, E. L., … Morrison, W. I. (2009). CD8+ T-cell responses to Theileria parva are preferentially directed to a single dominant antigen: Implications for parasite strain-specific immunity. *European Journal of Immunology*, *39*(9), 2459–2469. https://doi.org/10.1002/eji.200939227

Mans, B. J., Pienaar, R., Ratabane, J., Pule, B., & Latif, A. A. (2016). Investigating the diversity of the 18S SSU rRNA hyper-variable region of Theileria in cattle and Cape buffalo (Syncerus caffer) from southern Africa using a next generation sequencing approach. *Ticks and Tick-Borne Diseases*, *7*(5), 869–879. https://doi.org/10.1016/j.ttbdis.2016.04.005

McKeever, D. J., Taracha, E. L., Innes, E. L., MacHugh, N. D., Awino, E., Goddeeris, B. M., & Morrison, W. I. (1994). Adoptive transfer of immunity to Theileria parva in the CD8+ fraction of responding efferent lymph. *Proceedings of the National Academy of Sciences*, *91*(5), 1959 LP – 1963. https://doi.org/10.1073/pnas.91.5.1959

McLaren, M. R., Willis, A. D., & Callahan, B. J. (2019). Consistent and correctable bias in metagenomic sequencing experiments. *ELife*, *8*, e46923. https://doi.org/10.7554/eLife.46923

Mekata, H., Minamino, T., Mikurino, Y., Yamamoto, M., Yoshida, A., Nonaka, N., & Horii, Y. (2018). Evaluation of the natural vertical transmission of Theileria

orientalis. *Veterinary Parasitology*, *263*, 1–4. https://doi.org/10.1016/j.vetpar.2018.09.017
Metcalf, C. J. E., & Graham, A. L. (2018). Schedule and magnitude of reproductive investment under immune trade-offs explains sex differences in immunity. *Nature Communications*, *9*(1), 4391. https://doi.org/10.1038/s41467-018-06793-y
Mihaljevic, J. R., Hoye, B. J., & Johnson, P. T. J. (2018). Parasite metacommunities: Evaluating the roles of host community composition and environmental gradients in structuring symbiont communities within amphibians. *Journal of Animal Ecology*, *87*(2), 354–368. https://doi.org/10.1111/1365-2656.12735
Mordecai, E. A., Jaramillo, A. G., Ashford, J. E., Hechinger, R. F., Mordecai, E. A., Jaramillo, A. G., … Lafferty, K. D. (2020). The role of competition — colonization tradeoffs and spatial heterogeneity in promoting trematode coexistence, *Ecology 97*(6), 1484–1496.
Morrison, W. I. (2015). The aetiology, pathogenesis and control of theileriosis in domestic animals. *Revue Scientifique et Technique (International Office of Epizootics)*, *34*(2), 599–611. https://doi.org/10.20506/rst.34.2.2383
Morrison, W. I., Hemmink, J. D., & Toye, P. G. (2020). Theileria parva: a parasite of African buffalo, which has adapted to infect and undergo transmission in cattle. *International Journal for Parasitology*. https://doi.org/10.1016/j.ijpara.2019.12.006
Murphy K (2011). Janeway's Immunobiology. New York, USA: Taylor & Francis Inc.
Nakagawa, S., & Schielzeth, H. (2013). A general and simple method for obtaining R2 from generalized linear mixed-effects models. *Methods in Ecology and Evolution*, *4*(2), 133–142. https://doi.org/10.1111/j.2041-210x.2012.00261.x
Neiger, R., Hadley, J., & Pfeiffer, D. U. (2002). Differentiation of dogs with regenerative and non-regenerative anaemia on the basis of their red cell distribution width and mean corpuscular volume. *The Veterinary Record*, *150*(14), 431–434. https://doi.org/10.1136/vr.150.14.431
Nieuwenhuis, R., te Grotenhuis, M., & Pelzer, B. (2012). Influence.ME: Tools for detecting influential data in mixed effects models. *R Journal*, *4*(2), 38–47. https://doi.org/10.32614/rj-2012-011
Norval, R., Perry, B. D., & Young, A. S. (1992). *The Epidemiology of Theileriosis in Africa*. San Diego, CA: Academic Press Inc.
Olds, C. L., Mason, K. L., & Scoles, G. A. (2018). Rhipicephalus appendiculatus ticks transmit Theileria parva from persistently infected cattle in the absence of detectable parasitemia: implications for East Coast fever epidemiology. *Parasites & Vectors*, *11*(1), 126. https://doi.org/10.1186/s13071-018-2727-6
Pacala, S., & Roughgarden, J. (2009). Resource Partitioning and Interspecific Competition in Two Two-Species Insular Anolis Lizard Communities, *Science 217*(4558), 444–446. https://doi.org/10.1126/science.217.4558.444
Pedersen, A. B., & Fenton, A. (2007). Emphasizing the ecology in parasite community ecology. *Trends in Ecology and Evolution*, *22*(3), 133–139. https://doi.org/10.1016/j.tree.2006.11.005
Pienaar, R., Latif, A. A., Thekisoe, O. M. M., & Mans, B. J. (2014). Geographic distribution of Theileria sp. (buffalo) and Theileria sp. (bougasvlei) in Cape buffalo (Syncerus caffer) in southern Africa: implications for speciation. *Parasitology*, *141*(3), 411–424. https://doi.org/10.1017/S0031182013001728

R Core Team (2020). R: A language and environment for statistical computing. R Foundation for Statistical Computing, Vienna, Austria. URL https://www.R-project.org/.

Raberg, L., de Roode, J. C., Bell, A. S., Stamou, P., Gray, D., & Read, A. F. (2006). The role of immune-mediated apparent competition in genetically diverse malaria infections. *The American Naturalist*, *168*(1), 41–53. https://doi.org/10.1086/505160

Ramiro, R. S., Pollitt, L. C., Mideo, N., & Reece, S. E. (2016). Facilitation through altered resource availability in a mixed-species rodent malaria infection. *Ecology Letters*, *19*(9), 1041–1050. https://doi.org/10.1111/ele.12639

Richgels, K. L. D., Hoverman, J. T., & Johnson, P. T. J. (2013). Evaluating the role of regional and local processes in structuring a larval trematode metacommunity of Helisoma trivolvis. *Ecography*, *36*(7), 854–863. https://doi.org/10.1111/j.1600-0587.2013.07868.x

Rynkiewicz, E. C., Pedersen, A. B., & Fenton, A. (2015). An ecosystem approach to understanding and managing within-host parasite community dynamics. *Trends in Parasitology*, *31*(5), 212–221. https://doi.org/10.1016/j.pt.2015.02.005

Sisson, D.R. (2017). *Health and fitness of* Anaplasma *species infection in African buffalo(* Syncerus caffer*)* (Master of Philosophy thesis, University of Melbourne, Werribee). Retrieved from https://minerva-access.unimelb.edu.au/bitstream/handle/11343/197971/Thesis%20Sisson.pdf?sequence=1&isAllowed=y

Schneider, C. A., Rasband, W. S., & Eliceiri, K. W. (2012). NIH Image to ImageJ: 25 years of image analysis. *Nature Methods*, *9*(7), 671–675. https://doi.org/10.1038/nmeth.2089

Tan, B., Gao, F., Tan, B., Gao, F., Wolfe, R. E., Pedelty, J. A., … Nightingale, J. (2011). An Enhanced TIMESAT Algorithm for Estimating Vegetation Phenology Metrics From MODIS Data. *IEEE Journal of Selected Topics in Applied Earth Observations and Remote Sensing*, *4*(2), 361–371. https://doi.org/10.1109/JSTARS.2010.2075916

Tang, Y., Horikoshi, M., & Li, W. (2016). ggfortify: Unified interface to visualize statistical result of popular R packages. *The R Journal*, *8*.

Tavalire, H. F., Hoal, E. G., le Roex, N., van Helden, P. D., Ezenwa, V. O., & Jolles, A. E. (2019). Risk alleles for tuberculosis infection associate with reduced immune reactivity in a wild mammalian host. *Proceedings of the Royal Society B: Biological Sciences*, *286*(1907), 20190914. https://doi.org/10.1098/rspb.2019.0914

Tilman, D. (1994). Competition and Biodiversity in Spatially Structured Habitats Author (s): David Tilman Stable URL : http://www.jstor.org/stable/1939377 REFERENCES Linked references are available on JSTOR for this article : You may need to log in to JSTOR to access the, *75*(1), 2–16.

Titcomb, G., Allan, B. F., Ainsworth, T., Henson, L., Hedlund, T., Pringle, R. M., … Young, H. S. (2017). Interacting effects of wildlife loss and climate on ticks and tick-borne disease. *Proceedings of the Royal Society B: Biological Sciences*, *284*(1862), 20170475. https://doi.org/10.1098/rspb.2017.0475

Trillmich, F., Guenther, A., Jäckel, M., & Czirják, G. Á. (2020). Reproduction affects immune defenses in the guinea pig even under ad libitum food. *PloS One*, *15*(3), e0230081–e0230081. https://doi.org/10.1371/journal.pone.0230081

Vicente, J., Höfle, U., Fernández-De-Mera, I. G., & Gortazar, C. (2007). The importance of parasite life history and host density in predicting the impact of infections in red deer. *Oecologia*, *152*(4), 655–664. https://doi.org/10.1007/s00442-007-0690-6

Williams-Blangero, S., Criscione, C. D., VandeBerg, J. L., Correa-Oliveira, R., Williams, K. D., Subedi, J., … Blangero, J. (2012). Host genetics and population structure effects on parasitic disease. *Philosophical Transactions of the Royal Society B: Biological Sciences*, *367*(1590), 887–894. https://doi.org/10.1098/rstb.2011.0296

Williamson, B. D., Hughes, J. P., & Willis, A. D. (2019). A multi-view model for relative and absolute microbial abundances. *BioRxiv*, 761486. https://doi.org/10.1101/761486

Wold, S., Sjöström, M., & Eriksson, L. (2001). PLS-regression: a basic tool of chemometrics. *Chemometrics and Intelligent Laboratory Systems*, *58*(2), 109–130. https://doi.org/https://doi.org/10.1016/S0169-7439(01)00155-1

Woolhouse, M. E. J., Thumbi, S. M., Jennings, A., Chase-Topping, M., Callaby, R., Kiara, H., … Toye, P. G. (2015). Co-infections determine patterns of mortality in a population exposed to parasite infection. *Science Advances*, *1*(2), e1400026. https://doi.org/10.1126/sciadv.1400026

Yamada, S., Konnai, S., Imamura, S., Simuunza, M., Chembensofu, M., Chota, A., … Ohashi, K. (2009). Quantitative analysis of cytokine mRNA expression and protozoan DNA load in Theileria parva-infected cattle. *Journal of Veterinary Medical Science*, *71*(1), 49–54. https://doi.org/10.1292/jvms.71.49

Zeileis, A., & Hothorn, T. (2002). Diagnostic Checking in Regression Relationships. *R News*, *2*(3), 7–10.

Table 5.1. Point estimates for *Theileria* life history infection patterns. Age (months) 1st infection, age (months) at equilibrium, relative abundance at the equilibrium. Estimates include mean [95% confidence interval].

species clade	subtype	age 1st infection	age at equilibrium	relative abund at equilibrium
T. velifera	*T. velifera*	0.036[0-0.65]	25.86[19.49-32.22]	0.11[0.07-0.14]
	T. velifera B	0.036[0-0.69]	19.81[9.54-30.07]	0.16[0.10-0.21]
	T. velifera UD	NA	0.036[0-0.13]	0.00[0-0.00]
T. mutans	*T. mutans*-like 1	8.03[6.08-9.97]	20.83[10.17-31.48]	0.20[0.13-0.27]
	T. mutans-like 2	7.91[5.11-10.70]	19.27[9.41-29.12]	0.09[0.05-0.13]
	T. mutans-like 3	10.79[8.48-13.09]	36.17[25.10-47.23]	0.20[0.13-0.29]
	T. mutans MSD	0.92[0-3.21]	16.00[10.97-21.02]	0.01[0-0.02]
	T. mutans	0.036[0-0.64]	21.30[16.20-26.39]	0.02[0-0.05]
	T. mutans U D	NA	0.036[0-0.13]	0.00[0-0.00]
T. taurotragi	*T.* sp. (bougasvlei)	6.13[2.097-10.15]	23.32[2.23-44.40]	0.19[0.02-0.35]
	T. sp. (buffalo)	NA	0.036[0-0.13]	0.00[0-0.00]
	T. parva	5.32[1.27-9.36]	35.44[18.48-52.39]	0.06[0.03-0.10]

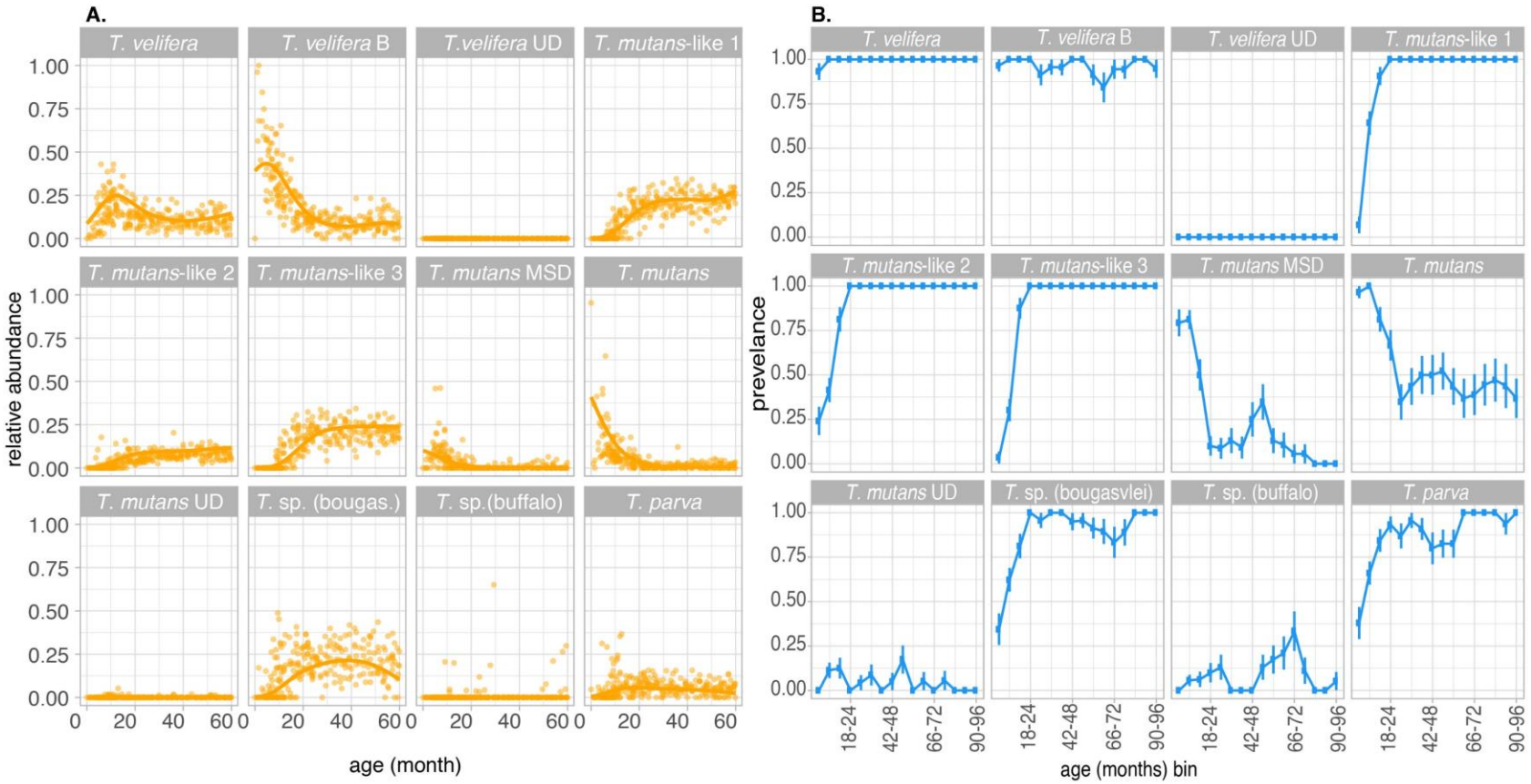

Figure 5.1. Life history variation in *Theileria.* (A) Relative abundance by age: Newborn animals represent new patches allowing us to observe colonization patterns. The points represent data whereas the lines represent estimates for average relative abundance by age fit with a basis-spline regression. Data were weighted by animal ID to account for the repeated measures study design. **(B) Age prevalence curves for each subtype**: Prevalence of each subtype within each age bin (18-24 months = 1.5-2 years, 42-48 months = 3.5-4 years, 66-72=5.5-6 years, 90-96=7.5-8 years). As our study was a repeated sample, longitudinal design subtypes that are highly prevalent in early age bins that are absent or at low prevalence in later age bins indicate that they were cleared from the host as the host age.

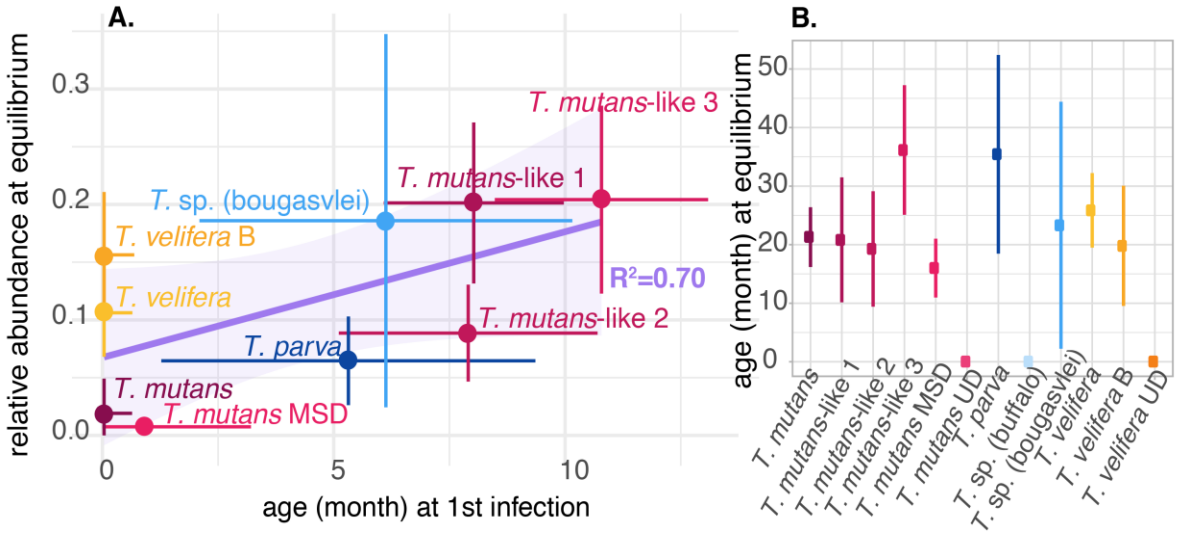

Figure 5.2. Life history analysis point estimates and signatures of a competition-colonization trade-off. (A) Regression line and point estimates (lines indicate 95% CI) indicating a positive correlation between age at first infection and relative abundance at equilibrium. (B) Age at equilibrium indicating that Theileria assemblages reach equilibrium at around 2 years old. *****The regression line is only fit to the *T. taurotragi* (blue) and *T. mutans* (red) species clades as *T. velifera* subtypes do not seem to fit this trade-off (Table D12).

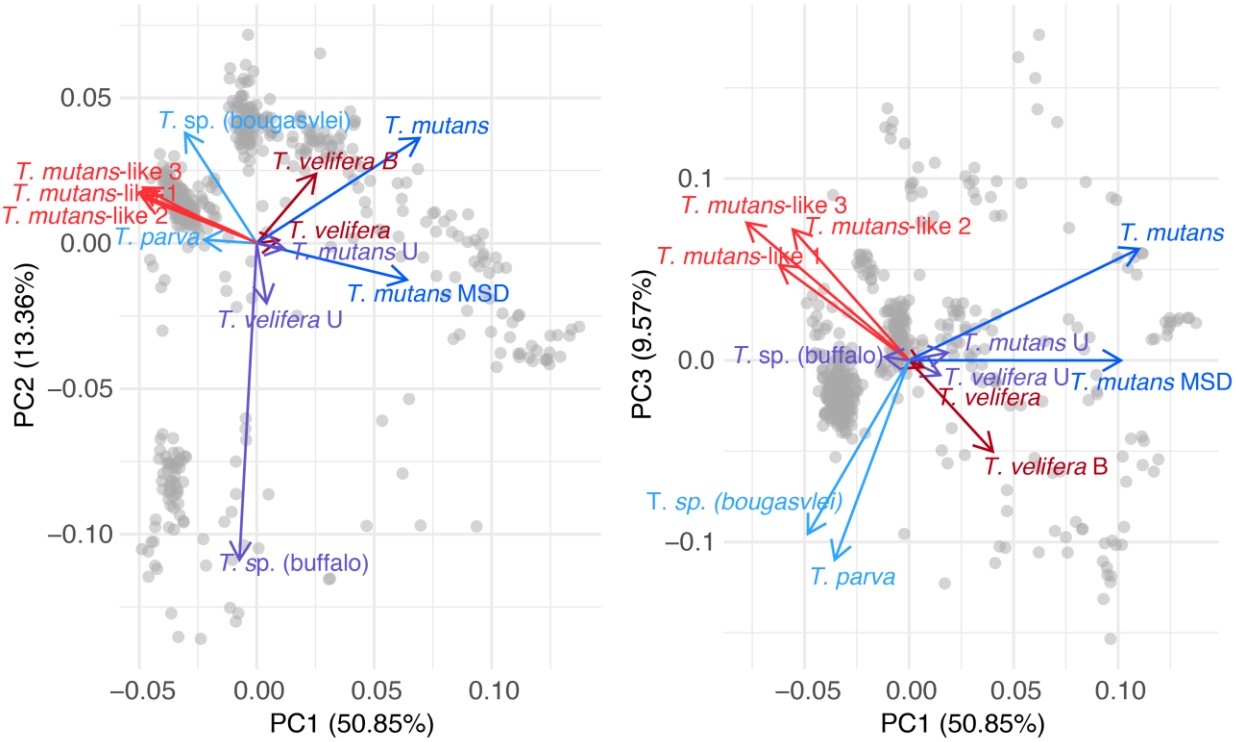

Figure 5.3. PCA describing *Theileria* assemblage composition. Variation along PC1 is best explained by differences in abundances of early colonizing (early-persistent: dark red; early-ephemeral: dark blue) and late colonizing subtypes (late-persistent: light red; late-ephemeral: light glue blue); variation along PC2 is best explained by presence of subtypes with no clear life-history pattern (purple), particularly *T.* sp. (buffalo); variation along PC3 is best explained by differences in rank of late-persistent versus late-ephemeral subtypes. *Theileria* were quantified using amplicon sequencing; read counts for each subtype have been center-log transformed. Points represent samples and axes have been scaled.

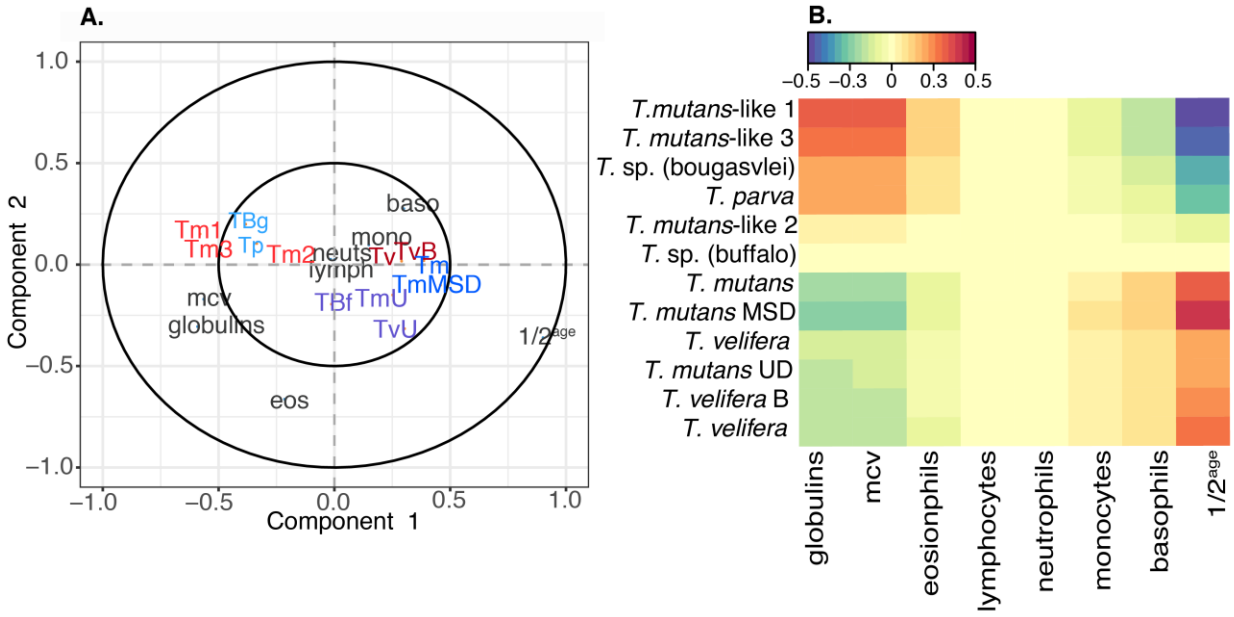

Figure 5.4. Partial least squares regression describing the association between continuous host traits and *Theileria* subtype abundance, relative to the sample mean, along component axis 1. (A) A correlation plot mapping the subtypes and host traits in sample space; the first two components are depicted. Early-ephemeral are show in dark blue, early-persistent in dark red, late-ephemeral in light blue and late-persistent in light red, in clear life history in purple. (B) A heat map describing the correlation between host traits (x axis) and subtypes (y axis) on component axis 1. We used partial least squares to disentangle the relationship between continuous, temporally variables that had a significant effect on *Theileria* PC1.

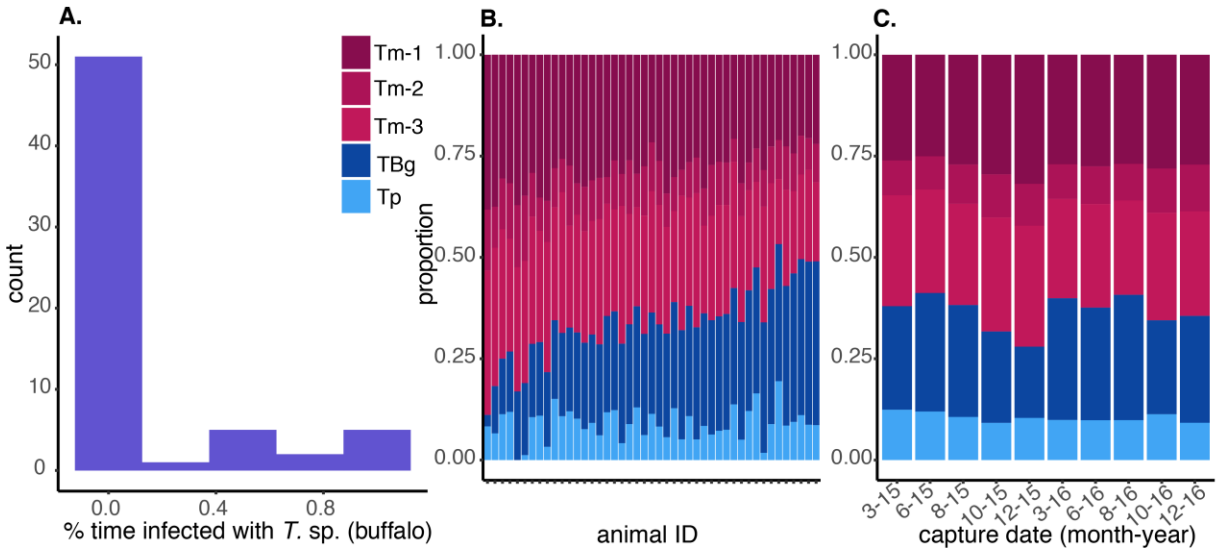

Figure 5.5. Random effects explained the largest amount of variation in PC2 and PC3. (A) A histogram depicting percent time infected with *T.* sp. (buffalo). PC2 polarized based on the presence of *T.* sp. (buffalo), a subtype that displayed no clear life-history traits; animal ID accounted for the largest portion of variation in our linear mixed effects model suggesting a few animals are likely to be infected over many capture periods. (B) A stack bar plot depicting average relative abundance of late-persistent (red, top three bars) versus late-ephemeral (blue, bottom two bars) subtypes for each animal. PC3 polarized based upon the rank of late-persistent versus late-ephemeral subtypes in a sample; our linear mixed model suggests that animal ID accounted for the largest portion of variation in PC3 followed by capture number. (C) Average relative abundance of late-persistent versus late-ephemeral at each capture time point. For (B) and (C) only samples in which the animal was > 2 years old was used; bars were scaled to equal 1. For (B), animals were ordered from the animal with the lowest *T.* sp. (bougasvlei) abundance (TBg) to the highest.

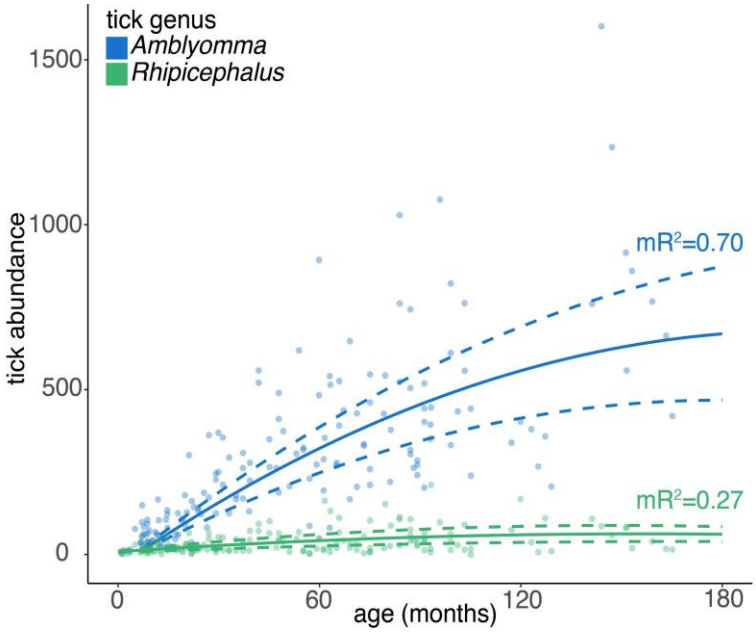

Figure 5.6. Tick abundances and model predictions from generalized mixed models (negative binomial distribution) evaluating the effect of age on tick abundances. In both models, the best fit model included age, age^2, and median NDVI. However, only age and age^2 had a significant effect on tick abundances. The *Amblyomma* model included an animal ID and capture number random effect whereas the *Rhipicephalus* model only included a capture ID random effect. The marginal R^2 represents the proportion of variance explained by the fixed factors alone (Nakagawa & Schilezeth 2013).

CHAPTER 6: GENERAL CONCLUSIONS

The last century has experienced a marked increase in emerging infectious disease (EID, hereafter) (Daszak, Cunningham & Hyatt 2001) – jeopardizing human (Chidiac & Ferry 2016; Bloom & Cadarette 2019), domestic animal (Chomel 2011; Martin et al., 2011), and wildlife health (Thompson, Lymbery & Smith 2010; Loots et al., 2017). EIDs are commonly associated with spillover from one host species into a novel host species (Rhyan & Spraker 2010; Cunningham, Dobson & Hudson 2012; Wood et al., 2012), with many destructive diseases, for both livestock and wildlife, emerging at the wildlife-livestock interface. As global change continues to erode the boundaries between human and wildlife systems (Watson et al., 2018), it will become increasingly more important to understand the key components influencing host susceptibility as well as pathogen/parasite spread and persistence. Disease ecology research has revealed that disease systems are incredibly complex: Host resistance, and consequent parasite/pathogen replication and transmission, is influenced by a multitude of factors including, but not limited to, co-infection patterns (Ezenwa & Jolles 2015; Gorsich et al., 2018) and host immuno-competence (Bakar et al., 2016). Variation within and among hosts leads to, and feedbacks with, population-level disease dynamics (White, Forester & Craft 2018). Studying disease in natural systems enables researchers to observe the outcome of interactions among these sources of variation and predict realistic parasite/pathogen dynamics. Ultimately, this work should enable the development of adaptive disease management.

In this dissertation, I studied within-host and population level dynamics of pathogen and parasite assemblages of African buffalo. Specifically, I studied infectious agents associated with two diseases that increase tension at the human-wildlife-livestock interface in southern African by jeopardizing livestock health: the bovine respiratory disease complex (Taylor et al., 2010) and theileriosis (Norval, Perry & Young 1992). My work illustrates how buffalo can be used to better understand processes influencing host susceptibility and disease persistence within and around Kruger National Park – hopefully extensions of this work will use research findings to evaluate and develop more effective disease management programs. A central pillar of my work was developing and adapting laboratory and analytical tools to better uncover non-linear and cryptic

processes in noisy systems. The skills I developed during my PhD will help me to continue to advance our understanding of disease ecology within complex, multi-scale systems.

In Chapter 2, I developed foundational knowledge in eco-immunology and found that non-specific markers of inflammation can be used to detect pathogen exposure. Specifically, I found that markers that are associated with inflammation but do no cause immuno-pathology (haptoglobin) are the most promising markers as they are systemically present at high concentrations and elevated for long periods of time. Future work should identify other non-specific markers of inflammation that possess similar properties thereby increasing our capacity to detect exposure history without *a priori* knowledge of the pathogen identity. Development of these tools would be valuable across a range of systems, particularly vulnerable wildlife in which we have little knowledge of their patho-biome and/or alternative methods of detecting a history of exposure (e.g., invertebrates that lack adaptive immunity).

In Chapter 3, I learned new statistical tools for describing ecological communities and non-linear trends (joint-species distribution models, general additive model) as well as the advantages and disadvantages of using serology data. I used a variance partitioning methods to compare the importance of pathogen-pathogen associations, environmental variability, and host traits on probability of infection of upper respiratory tract pathogens within the bovine respiratory disease complex. I found that the importance of each factor was inconsistent across pathogens. However, for three out of the five respiratory viruses investigated, the best indicator of infection was co-occurrence by another virus. In contrast, the best indicator of infection for bacterial pathogens was host ID. Importantly, I found that within-host dynamics only partially elucidated seasonal cycling in population-level disease dynamics. I am currently working with another Jolles Lab graduate student to evaluate if inclusion of metrics associated with host contact (e.g., number of contacts within an observation period, duration of contacts) better describes variation in within-host occurrence and temporal variation in incidence for these pathogens. I also plan to work with co-author Courtney Coon to conduct a similar analysis using identical data collected from cattle herds surrounding KNP.

In Chapter 4, I learned new laboratory and bioinformatics tools for describing *Theileria* assemblages at multiple taxonomic scales. This work unveiled previously cryptic spatial and temporal variation in African buffalo-*Theileria* assemblages. Using the data from Chapter 4, I was able to identify possible processes structuring *Theileria* assemblages within and among buffalo in Chapter 5. In Chapter 5, I teamed up with researchers from the Department of Statistics to develop analytical tools for describing non-linear trends in compositional data within a repeated study design. These tools increase the capacity for researchers to accurately (i.e., the structure of the data is properly accounted for) use sequencing data to map non-linear patterns and process in ecological systems. Using this analysis, I was able to identify that *Theileria* vary in their colonization rate and persistence within the host (i.e., life history strategies). Furthermore, I identified that a subset of *Theileria* co-exist within the same host throughout their lifetime, whereas a subset is extirpated from adult animals but co-exists at the population level through a competition-colonization trade-off. Life history patterns, and co-existence among life-history groups, is likely driven by a combination of host physiology, vector dynamics, and parasite-parasite interactions. Better understanding the mechanisms supporting *Theileria* assemblage distribution has immediate implications for disease management at the buffalo-cattle interface.

References

Bakar, A. A., Bower, D. S., Stockwell, M. P., Clulow, S., Clulow, J., & Mahony, M. J. (2016). Susceptibility to disease varies with ontogeny and immunocompetence in a threatened amphibian. *Oecologia*, 181(4), 997–1009. https://doi.org/10.1007/s00442-016-3607-4

Bloom, D. E., & Cadarette, D. (2019). Infectious Disease Threats in the Twenty-First Century: Strengthening the Global Response. *Frontiers in Immunology*, 10, 549. https://doi.org/10.3389/fimmu.2019.00549

Chidiac, C., & Ferry, T. (2016). [Emerging infectious agents]. *Transfusion clinique et biologique : journal de la Societe francaise de transfusion sanguine*, 23(4), 253–262. https://doi.org/10.1016/j.tracli.2016.08.007

Chomel, B. (2011). Tick-borne infections in dogs-an emerging infectious threat. *Veterinary Parasitology*, 179(4), 294–301. https://doi.org/10.1016/j.vetpar.2011.03.040

Cunningham, A. A., Dobson, A. P., & Hudson, P. J. (2012). Disease invasion: impacts on biodiversity and human health. *Philosophical Transactions of the Royal Society of London. Series B, Biological Sciences*, 367(1604), 2804–2806. https://doi.org/10.1098/rstb.2012.0331

Daszak, P., Cunningham, A. A., & Hyatt, A. D. (2001). Anthropogenic environmental change and the emergence of infectious diseases in wildlife. *Acta Tropica*, 78(2), 103–116. https://doi.org/10.1016/s0001-706x(00)00179-0

Ezenwa, V. O., & Jolles, A. E. (2015). Opposite effects of anthelmintic treatment on microbial infection at individual versus population scales. *Science*, 347(6218), 175–177. https://doi.org/10.1126/science.1261714

Gorsich, E. E., Etienne, R. S., Medlock, J., Beechler, B. R., Spaan, J. M., Spaan, R. S., … Jolles, A. E. (2018). Opposite outcomes of coinfection at individual and population scales. *Proceedings of the National Academy of Sciences*, 115(29), 7545 LP – 7550. https://doi.org/10.1073/pnas.1801095115

Loots, A. K., Mitchell, E., Dalton, D. L., Kotze, A., & Venter, E. H. (2017). Advances in canine distemper virus pathogenesis research: a wildlife perspective. *The Journal of General Virology*, 98(3), 311–321. https://doi.org/10.1099/jgv.0.000666

Martin, C., Pastoret, P.-P., Brochier, B., Humblet, M.-F., & Saegerman, C. (2011). A survey of the transmission of infectious diseases/infections between wild and domestic ungulates in Europe. *Veterinary Research*, 42, 70. https://doi.org/10.1186/1297-9716-42-70

Norval, R., Perry, B. D., & Young, A. S. (1992). The Epidemiology of Theileriosis in Africa. San Diego, CA: Academic Press Inc.

Rhyan, J. C., & Spraker, T. R. (2010). Emergence of diseases from wildlife reservoirs. *Veterinary Pathology*, 47(1), 34–39. https://doi.org/10.1177/0300985809354466

Taylor, J. D., Fulton, R. W., Lehenbauer, T. W., Step, D. L., & Confer, A. W. (2010). The epidemiology of bovine respiratory disease: What is the evidence for predisposing factors? *The Canadian Veterinary Journal = La Revue Veterinaire Canadienne*, 51(10), 1095–1102.

Thompson, R. C. A., Lymbery, A. J., & Smith, A. (2010). Parasites, emerging disease

and wildlife conservation. *International Journal for Parasitology*, 40(10), 1163–1170. https://doi.org/10.1016/j.ijpara.2010.04.009

Watson, J. E. M., Venter, O., Lee, J., Jones, K. R., Robinson, J. G., Possingham, H. P., & Allan, J. R. (2018). Protect the last of the wild. *Nature*. https://doi.org/10.1038/d41586-018-07183-6

White, L. A., Forester, J. D., & Craft, M. E. (2018). Covariation between the physiological and behavioral components of pathogen transmission: host heterogeneity determines epidemic outcomes. *Oikos*, 127(4), 538–552. https://doi.org/10.1111/oik.04527

Wood, J. L. N., Leach, M., Waldman, L., Macgregor, H., Fooks, A. R., Jones, K. E., … Cunningham, A. A. (2012). A framework for the study of zoonotic disease emergence and its drivers: spillover of bat pathogens as a case study. *Philosophical Transactions of the Royal Society of London. Series B, Biological Sciences*, 367(1604), 2881–2892. https://doi.org/10.1098/rstb.2012.0228

BIBLIOGRAPHY

Abbate, J. L., Ezenwa, V. O., Guégan, J. F., Choisy, M., Nacher, M., & Roche, B. (2018). Disentangling complex parasite interactions: Protection against cerebral malaria by one helminth species is jeopardized by co-infection with another. *PLoS Neglected Tropical Diseases*, *12*(5), 1–13. https://doi.org/10.1371/journal.pntd.0006483

Abdela, N., & Tilahun, B. (2016). Bovine theileriosis and its control: A review. *Advances in Biological Research*, 10(4), 200– 212.

Adlard RD, Miller TL, Smit NJ. The butterfly effect: parasite diversity, environment, and emerging disease in aquatic wildlife. Trends Parasitol (2015) 31(4):160–6. doi:10.1016/j.pt.2014.11.001

Aivelo, T., & Norberg, A. (2018). Parasite-microbiota interactions potentially affect intestinal communities in wild mammals. *Journal of Animal Ecology*, 87(2), 438–447.

Amat, S., Alexander, T. W., Holman, D. B., Schwinghamer, T., & Timsit, E. (2020). Intranasal Bacterial Therapeutics Reduce Colonization by the Respiratory Pathogen Mannheimia haemolytica in Dairy Calves. *mSystems*, *5*(2), e00629-19. https://doi.org/10.1128/mSystems.00629-19

Anderson, K., Ezenwa, V. O., & Jolles, A. E. (2013). Tick infestation patterns in free ranging African buffalo (Syncercus caffer): Effects of host innate immunity and niche segregation among tick species. *International Journal for Parasitology. Parasites and Wildlife*, *2*, 1–9. https://doi.org/10.1016/j.ijppaw.2012.11.002

Anthony SJ, Epstein JH, Murray KA, Navarrete-Macias I, Zambrana-Torrelio CM, Solovyov A, et al. A strategy to estimate unknown viral diversity in mammals. mBio (2013) 4(5):e000598. doi:10.1128/mBio.00598-13

Arafat, N., Eladl, A. H., Marghani, B. H., Saif, M. A., & El-Shafei, R. A. (2018). Enhanced infection of avian influenza virus H9N2 with infectious laryngeotracheitis vaccination in chickens. *Veterinary Microbiology*, *219*, 8–16. https://doi.org/10.1016/j.vetmic.2018.04.009

Arnot, D. (1998). Meeting at Manson House, London, 11 December 1997: Unstable malaria in the Sudan: The influence of the dry season – Clone multiplicity of *Plasmodium falciparum* infections in individuals exposed to variable levels of disease transmission. *Transactions of the Royal Society of Tropical Medicine and Hygiene*, 92(6), 580– 585.

Asghar, M., Hasselquist, D., & Bensch, S. (2011). Are chronic avian haemosporidian infections costly in wild birds? *Journal of Avian Biology*, 42(6), 530– 537.

Ayling R, Baker S, Nicholas R, Peek M, Simon A. Comparison of *in vitro* activity of danofloxacin, florfenicol, oxytetracycline, spectinomycin and tilmicosin against *Mycoplasma mycoides* subspecies *Mycoides* small colony type. Vet. Rec. 2000;146(9):243–245.

Baek, B. K., Soo, K. B., Kim, J. H., Hur, J., Lee, B. O., Jung, J. M., … Kakoma, I. (2003). Verification by polymerase chain reaction of vertical transmission of Theileria sergenti in cows. *Canadian Journal of Veterinary Research = Revue Canadienne de Recherche Veterinaire*, *67*(4), 278–282.

Bailey AL, Lauck M, Ghai RR, Nelson CW, Heimbruch K, Hughes AL, et al. Arteriviruses, pegiviruses, and lentiviruses are common among wild African monkeys. J Virol (2016) 90(15):6724–37. doi:10.1128/JVI.00573-16

Baldwin, C. L., Iams, K. P., Brown, W. C., & Grab, D. J. (1992). Theileria parva: CD4+ helper and cytotoxic T-cell clones react with a schizont-derived antigen associated with the surface of Theileria parva-infected lymphocytes. *Experimental Parasitology*, *75*(1), 19–30. https://doi.org/10.1016/0014-4894(92)90118-t

Bakar, A. A., Bower, D. S., Stockwell, M. P., Clulow, S., Clulow, J., & Mahony, M. J. (2016). Susceptibility to disease varies with ontogeny and immunocompetence in a threatened amphibian. *Oecologia*, 181(4), 997–1009. https://doi.org/10.1007/s00442-016-3607-4

Barbosa, A. D., Gofton, A. W., Paparini, A., Codello, A., Greay, T., Gillett, A., … Ryan, U. (2017). Increased genetic diversity and prevalence of co-infection with *Trypanosoma* spp. in koalas (*Phascolarctos cinereus*) and their ticks identified using next-generation sequencing (NGS). *PLoS ONE*, 12(7), e0181279.

Barton, K. (2009). Mu-MIn: Multi-model inference. *R Package Version 0.12.2/R18*, (1). https://doi.org/http://R-Forge.R-project.org/projects/mumin/

Bates D, Maechler M, Bolker B, Walker S. Fitting linear mixed-effects models using lme4. J Stat Softw (2015) 67(1):1–48. doi:10.18637/jss.v067.i01

Beechler, B., Jolles, A. & Ezenwa, V. (2009) Evaluation of hematologic values in free-ranging African buffalo (Syncerus caffer). *Journal of Wildlife Diseases,* 45, 57-66.

Beechler, B. R., Broughton, H., Bell, A., Ezenwa, V. O., & Jolles, A. E. (2012). Innate Immunity in Free-Ranging African Buffalo (Syncerus caffer): Associations with Parasite Infection and White Blood Cell Counts. *Physiological and Biochemical Zoology*, *85*(3), 255–264. https://doi.org/10.1086/665276

Beechler, B. R., Manore, C. A., Reininghaus, B., O'Neal, D., Gorsich, E. E., Ezenwa, V. O., & Jolles, A. E. (2015). Enemies and turncoats: Bovine tuberculosis exposes pathogenic potential of Rift Valley fever virus in a common host, African buffalo (*Syncerus caffer*). *Proceedings of the Royal Society B: Biological Sciences*, 282(1805), 20142942. https://doi.org/10.1098/rspb.2014.2942

Beechler BR, Jolles AE, Budischak SA, Corstjens P, Ezenwa VO, Smith M, et al. Host immunity, nutrition and coinfection alter longitudinal infection patterns of schistosomes in a free ranging African buffalo population. PLoS Negl Trop Dis (2017) 11(12):e0006122. doi:10.1371/journal.pntd.0006122

Benjamini Y, Yekutieli D. The control of the false discovery rate in multiple testingunder dependency. Ann Statist (2001) 29(4):665–1188.

Bishop, R. P., Hemmink, J. D., Morrison, W. I., Weir, W., Toye, P. G., Sitt, T., … Odongo, D. O. (2015). The African buffalo parasite *Theileria* sp. (buffalo) can infect and immortalize cattle leukocytes and encodes divergent orthologues of *Theileria parva* antigen genes. *International Journal for Parasitology: Parasites and Wildlife*, 4(3), 333– 342.

Blackwell M. The fungi: 1,2,3…5.1 million species? Am J Bot (2011) 98(3):426–38. doi:10.3732/ajb.1000298

Bloom, D. E., & Cadarette, D. (2019). Infectious Disease Threats in the Twenty-First Century: Strengthening the Global Response. *Frontiers in Immunology*, 10, 549. https://doi.org/10.3389/fimmu.2019.00549

Boyce, R. M., Hathaway, N., Fulton, T., Reyes, R., Matte, M., Ntaro, M., … Juliano, J. J.

(2018). Reuse of malaria rapid diagnostic tests for amplicon deep sequencing to estimate *Plasmodium falciparum* transmission intensity in western Uganda. *Scientific Reports*, 8(1), 10159.

Brierley L, Vonhof MJ, Olival KJ, Daszak P, Jones KE. Quantifying global drivers of zoonotic bat viruses: a process-based perspective. Am Nat (2016) 187(2):E53–64. doi:10.1086/684391

Broughton, H. M., Govender, D., Shikwambana, P., Chappell, P., & Jolles, A. (2017). Bridging gaps between zoo and wildlife medicine: establishing reference intervals for free-ranging african lions (*panthera leo*). *Journal of Zoo and Wildlife Medicine*, *48*(2), 298–311. https://doi.org/10.1638/2016-0021R.1

Budischak, S. A., Wiria, A. E., Hamid, F., Wammes, L. J., Kaisar, M. M. M., van Lieshout, L., … Graham, A. L. (2018). Competing for blood: The ecology of parasite resource competition in human malaria-helminth co-infections. *Ecology Letters*, 21(4), 536– 545.

Cadotte, M., Loreau, A. E. M., & Losos, E. J. B. (2006). Dispersal and Species Diversity: A Meta‐Analysis. *The American Naturalist*, *167*(6), 913–924. https://doi.org/10.1086/504850

Callahan, B. J., McMurdie, P. J., Rosen, M. J., Han, A. W., Johnson, A. J., & Holmes, S. P. (2016). DADA2: High-resolution sample inference from Illumina amplicon data. *Nature Methods*, 13(7), 581– 583.

Cassirer, E.F., Plowright, R.K., Manlove, K.R., Cross, P.C., Dobson, A.P., Potter, K.A. & Hudson, P.J. (2013) Spatio-temporal dynamics of pneumonia in bighorn sheep. *Journal of Animal Ecology,* 82, 518-528.

Cattadori, I., Boag, B. & Hudson, P. (2008) Parasite co-infection and interaction as drivers of host heterogeneity. *International Journal for Parasitology,* 38, 371-380.

Cavanaugh V. J., Guidotti L. G., Chisari F. V. (1998). Inhibition of Hepatitis B virus replication during adenovirus and cytomegalovirus infections in transgenic mice. *Journal of Virology*. 72 2630–2637.

Ceciliani F, Ceron JJ, Eckersall PD, Sauerwein H. Acute phase proteins in ruminants. J Proteomics (2012) 75(14):4207–31. doi:10.1016/j.jprot.2012.04.004

Chaisi, M. E., Collins, N. E., Potgieter, F. T., & Oosthuizen, M. C. (2013). Sequence variation identified in the 18S rRNA gene of *Theileria mutans* and *Theileria velifera* from the African buffalo (*Syncerus caffer*). *Veterinary Parasitology*, 191(1–2), 132– 137.

Chaminuka, P, McCrindle, C.M.E., Udo, H.J. (2011) Cattle farming at the wildlife/livestock interface: assessment of costs and benefits adjacent to Kruger National Park, South Africa. *Society and Natural Resources,* DOI:10.1080/08941920.2011.580417

Chesson, P. (1985). Coexistence of competitors in spatially and temporally varying environments: A look at the combined effects of different sorts of variability. *Theoretical Population Biology*, *28*(3). https://doi.org/10.1016/0040-5809(85)90030-9

Chidiac, C., & Ferry, T. (2016). [Emerging infectious agents]. *Transfusion clinique et biologique : journal de la Societe francaise de transfusion sanguine*, 23(4), 253–262. https://doi.org/10.1016/j.tracli.2016.08.007

Chomel, B. (2011). Tick-borne infections in dogs-an emerging infectious threat. *Veterinary Parasitology*, 179(4), 294–301. https://doi.org/10.1016/j.vetpar.2011.03.040

Coetzer, J.A.W., Thomson, G.R. & Tustin, R.C. (2006) Infectious Diseases of Livestock - With Special Reference to Southern Africa. Oxford University Press.

Clay, P. A., Cortez, M. H., Duffy, M. A., & Rudolf, V. H. W. (2019). Priority effects within coinfected hosts can drive unexpected population-scale patterns of parasite prevalence. *Oikos*, *128*(4), 571–583. https://doi.org/10.1111/oik.05937

Colwell DD, Dantas-Torres F, Otranto D. Vector-borne parasitic zoonoses: emerging scenarios and new perspectives. Vet Parasitol (2013) 182(1):14–21. doi:10.1016/j.vetpar.2011.07.012

Combrink, L., Glidden, C. K., Beechler, B. R., Charleston, B., Koehler, A. V., Sisson, D., Gasser, R. B., Jabbar, A., & Jolles, A. E. (2020). Age of first infection across a range of parasite taxa in a wild mammalian population. *Biology letters*, 16(2), 20190811. https://doi.org/10.1098/rsbl.2019.0811

Condit, R., Chisholm, R. A., & Hubbell, S. P. (2012). Thirty Years of Forest Census at Barro Colorado and the Importance of Immigration in Maintaining Diversity. *PLOS ONE*, *7*(11), e49826.

Cook, S., Glass, R., LeBaron, C. & Ho, M.-S. (1990) Global seasonality of rotavirus infections. *Bulletin of the World Health Organization,* 68, 171.

Costello, E. K., Lauber, C. L., Hamady, M., Fierer, N., Gordon, J. I., & Knight, R. (2009). Bacterial community variation in human body habitats across space and time. *Science*, 326(5960), 1694– 1697. https://doi.org/10.1126/science.1177486

Cox, F. (2001) Concomitant infections, parasites and immune responses. *Parasitology,* 122, S23-S38.

Couch CE, Movius MA, Jolles AE, Gorman ME, Rigas JD, Beechler BR. Serum biochemistry panels in African buffalo: defining reference intervals and assessing variability across season, age, sex. PLoS One (2017) 12(5):e0176830. doi:10.1371/journal.pone.0176830

Cozens, D., Sutherland, E., Lauder, M., Taylor, G., Berry, C. C., & Davies, R. L. (2019). Pathogenic Mannheimia haemolytica Invades Differentiated Bovine Airway Epithelial Cells. *Infection and immunity*, *87*(6), e00078-19. https://doi.org/10.1128/IAI.00078-19

Craft, M. E. (2015). Infectious disease transmission and contact networks in wildlife and livestock. *Philosophical Transactions of the Royal Society of London. Series B, Biological Sciences*, *370*(1669). https://doi.org/10.1098/rstb.2014.0107

Cray C, Hammond E, Haefele H. Acute phase protein and protein electrophoresis values for captive Grant's zebra (*Equus burchelli*). J Zoo Wildl Med (2013) 44(4):1107–10. doi:10.1638/2013-0033R.1

Cray C, Zaias J, Altman NH. Acute phase response in animals: a review. Comp Med (2009) 59(6):517–26.

Cunningham, A. A., Dobson, A. P., & Hudson, P. J. (2012). Disease invasion: impacts on biodiversity and human health. *Philosophical Transactions of the Royal Society of London. Series B, Biological Sciences*, 367(1604), 2804–2806. https://doi.org/10.1098/rstb.2012.0331

Dallas, T. A., Laine, A. L., & Ovaskainen, O. (2019). Detecting parasite associations

within multi-species host and parasite communities. *Proceedings. Biological Sciences*, 286(1912), 20191109. https://doi.org/10.1098/rspb.2019.1109

DaPalma, T., Doonan, B. P., Trager, N. M., & Kasman, L. M. (2010). A systematic approach to virus-virus interactions. *Virus research*, 149(1), 1–9. https://doi.org/10.1016/j.virusres.2010.01.002

Darriba, D., Taboada, G. L., Doallo, R., & Posada, D. (2012). jModelTest 2: More models, new heuristics and parallel computing. *Nature Methods*, 9(8), 772.

Daszak P, Berger L, Cunningham AA, Hyatt AD, Green DE, Speare R. Emerging infectious diseases and amphibian population declines. Emerg Infect Dis (1999) 5(6):735–48. doi:10.3201/eid0506.990601

Daszak, P., Cunningham, A. A., & Hyatt, A. D. (2001). Anthropogenic environmental change and the emergence of infectious diseases in wildlife. *Acta Tropica*, 78(2), 103–116. https://doi.org/10.1016/s0001-706x(00)00179-0

Dewangan, P., Panigrahi, M., Kumar, A., Saravanan, B. C., Ghosh, S., Asaf, V. N. M., … Bhushan, B. (2015). The mRNA expression of immune-related genes in crossbred and Tharparkar cattle in response to in vitro infection with Theileria annulata. *Molecular Biology Reports*, *42*(8), 1247–1255. https://doi.org/10.1007/s11033-015-3865-y

Dowell, S.F., Whitney, C.G., Wright, C., Rose Jr, C.E. & Schuchat, A. (2003) Seasonal patterns of invasive pneumococcal disease. *Emerging Infectious Diseases*, 9, 573-579.

Duan, C., and Jiang, Y. (2020). Subgroup analysis of longitudinal profiles for compositional count data. Technical report.

Dugovich BS, Peel MJ, Palmer AL, Zielke RA, Sikora AE, Beechler BR, et al. Detection of bacterial-reactive natural IgM antibodies in desert bighorn sheep populations. PLoS One (2017) 12(6):e0180415. doi:10.1371/journal. pone.0180415

Earley, B., Buckham Sporer, K., & Gupta, S. (2017). Invited review: Relationship between cattle transport, immunity and respiratory disease. *Animal : an international journal of animal bioscience*, 11(3), 486–492. https://doi.org/10.1017/S1751731116001622

Edgar, R. C. (2004). MUSCLE: Multiple sequence alignment with high accuracy and high throughput. *Nucleic Acids Research*, 32(5), 1792– 1797.

Ezenwa, V.O. & Jolles, A.E. (2008) Horns honestly advertise parasite infection in male and female African buffalo. *Animal Behaviour*, 75, 2013-2021.

Ezenwa, V.O., Jolles, A.E. & O'Brien, M.P. (2009) A reliable body condition scoring technique for estimating condition in African buffalo. *African Journal of Ecology*, 47, 476-481.

Ezenwa, V.O., Etienne, R.S., Luikhart, G., Beja-Pereira, A. & Jolles, A.E. (2010) Hidden consequences of living in a wormy world: nematode-induced immune suppression facilitates invasion in the African buffalo. *The American Naturalist*, 176, 613-324.

Ezenwa, V.O. & Jolles, A.E. (2015) Opposite effects of anthelmintic treatment on microbial infection at individual versus population scales. *Science*, 347, 175-177.

Ezenwa, V. O., Jolles, A. E., Beechler, B. R., Budischak, S. A., & Gorsich, E. E. (2019). The causes and consequences of parasite interactions: Afrivan buffalo as a case study. In C. U. Press (Ed.), *Wildlife Disease Ecology*. New York.

Fenton, A., Lamb, T., & Graham, A. L. (2008). Optimality analysis of Th1/Th2 immune responses during microparasite- macroparasite co-infection, with epidemiological feedbacks. *Parasitology*, *135*(7), 841–853. https://doi.org/10.1017/S0031182008000310

Fenton, A., Viney, M. E., & Lello, J. (2010). Detecting interspecific macroparasite interactions from ecological data: patterns and process. *Ecology Letters*, *13*(5), 606–615. https://doi.org/10.1111/j.1461-0248.2010.01458.x

Fernandez-Fournier, P., & Avilés, L. (2018). Environmental filtering and dispersal as drivers of metacommunity composition: Complex spider webs as habitat patches: Complex. *Ecosphere*, *9*(2). https://doi.org/10.1002/ecs2.2101

Ferreira, B. R., & Silva, J. S. (1999). Successive tick infestations selectively promote a T-helper 2 cytokine profile in mice. *Immunology*, *96*(3), 434–439. https://doi.org/10.1046/j.1365-2567.1999.00683.x

Fine, P.E. & Clarkson, J.A. (1982) Measles in England and Wales—I: an analysis of factors underlying seasonal patterns. *International journal of epidemiology*, 11, 5-14.

Forbes KM, Mappes T, Sironen T, Strandin T, Stuart P, Meri S, Vapalahti O, Henttonen H, Huitu O. 2016. Food limitation constrains host immune responses to nematode infections. Biol. Lett. 12, 20160471

Fowler, D., Lessard, J. P., & Sanders, N. J. (2014). Niche filtering rather than partitioning shapes the structure of temperate forest ant communities. *Journal of Animal Ecology*, *83*(4), 943–952. https://doi.org/10.1111/1365-2656.12188

Gagea, M. I., Bateman, K. G., Shanahan, R. A., van Dreumel, T., McEwen, B. J., Carman, S., … Caswell, J. L. (2006). Naturally Occurring Mycoplasma Bovis—Associated Pneumonia and Polyarthritis in Feedlot Beef Calves. *Journal of Veterinary Diagnostic Investigation*, *18*(1), 29–40. https://doi.org/10.1177/104063870601800105

Gao, F., Morisette, J. T., Wolfe, R. E., Ederer, G., Pedelty, J., Masuoka, E., … Nightingale, J. (2008). An algorithm to produce temporally and spatially continuous MODIS-LAI time series. *IEEE Geoscience and Remote Sensing Letters*, *5*(1), 60–64. https://doi.org/10.1109/LGRS.2007.907971

Gelman, A. (2008). Scaling regression inputs by dividing by two standard deviations. *Statistics in Medicine* 27, 2865–2873.

Gelman, A. and Su, Y. (2018). arm: Data Analysis Using Regression and Multilevel/Hierarchical Models. R package version 1.10-1. https://CRAN.R-project.org/package=arm

Genton C, Cristescu R, Gatti S, Levréro F, Bigot E, Caillaud D, et al. Recovery potential of a western lowland gorilla population following a major Ebola out- break: results from a ten year study. PLoS One (2012) 7(5):e37106. doi:10.1371/journal.pone.0037106

Germann, T.C., Kadau, K., Longini, I.M. & Macken, C.A. (2006) Mitigation strategies for pandemic influenza in the United States. *Proceedings of the National Academy of Sciences,* 103, 5935-5940.

Gilot-Fromont, E., Jégo, M., Bonenfant, C., Gibert, P., Rannou, B., Klein, F., & Gaillard, J.-M. (2012). Immune Phenotype and Body Condition in Roe Deer: Individuals with

High Body Condition Have Different, Not Stronger Immunity. *PLOS ONE, 7*(9), e45576.

Glanzmann, B., Möller, M., le Roex, N., Tromp, G., Hoal, E. G., & van Helden, P. D. (2016). The complete genome sequence of the African buffalo (Syncerus caffer). *BMC Genomics*, *17*(1), 1001. https://doi.org/10.1186/s12864-016-3364-0

Glenn, T. C. (2011). Field guide to next-generation DNA sequencers. *Molecular Ecology Resources*, 11(5), 759– 769.

Glidden, C. K., Beechler, B., Buss, P. E., Charleston, B., de Klerk-Lorist, L. M., Maree, F. F., … Jolles, A. (2018). Detection of pathogen exposure in African buffalo using non-specific markers of inflammation. *Frontiers in Immunology*, 8, 12.

Glidden, C. K., Koehler, A. V., Hall, R. S., Saeed, M. A., Coppo, M., Beechler, B. R., … Jabbar, A. (2019). Elucidating cryptic dynamics of Theileria communities in African buffalo using a high-throughput sequencing informatics approach. *Ecology and Evolution*, *10*(1), 70–80. https://doi.org/10.1002/ece3.5758

Gloor, G. B., Macklaim, J. M., Pawlowsky-Glahn, V., & Egozcue, J. J. (2017). Microbiome Datasets Are Compositional: And This Is Not Optional. *Frontiers in Microbiology*, *8*, 2224. https://doi.org/10.3389/fmicb.2017.02224

Godson DL, Campos M, Attah-Poku SK, Redmond MJ, Corediro DM, Manjeet SS, et al. Serum haptoglobin as an indicator of the acute phase response in bovine respiratory disease. Vet Immunol Immunopathol (1996) 51(3–4):277–92. doi:10.1016/0165-2427(95)05520-7

Graham, A.L. (2008) Ecological rules governing helminth–microparasite co-infection. *Proceedings of the National Academy of Sciences*, 105, 566-570.

Graham, A.L., Lamb, T.J., Read, A.F. & Allen, J.E. (2005) Malaria-filaria co-infection in mice makes malarial disease more severe unless filarial infection achieves patency. *Journal of Infectious Diseases,* 191, 410-421.

Gorsich, E. E., Bengis, R. G., Ezenwa, V. O., & Jolles, A. E. (2014). Evalution of the sensitivity and specificity of an enzyme-linked immunosorbent assay for diagnosing brucellosis in African buffalo (Syncerus caffer). *Journal of Wildlife Diseases*, *51*(1), 9–18. https://doi.org/10.7589/2013-12-334

Gorsich, E. E., Etienne, R. S., Medlock, J., Beechler, B. R., Spaan, J. M., Spaan, R. S., … Jolles, A. E. (2018). Opposite outcomes of coinfection at individual and population scales. *Proceedings of the National Academy of Sciences of the United States of America*, 115(29), 7545– 7550.

Gorsich, E.E., Ezenwa, V.O., Cross, P.C., Bengis, R.G. & Jolles, A.E. (2015) Context-dependent survival, fecundity and predicted population-level consequences of brucellosis in African buffalo. *Journal of Animal Ecology*, 84, 999-1009.

Graham AL, Allen JE, Read AF. Evolutionary causes and consequences of immunopathology. Annu Rev Ecol Evol Syst (2005) 36(1):373–97. doi:10.1146/annurev.ecolsys.36.102003.152622

Griffiths, E.C., Pedersen, A.B., Fenton, A. & Petchey, O.L. (2011) The nature and consequences of co-infection in humans. *Journal of Infection*, 63, 200-206.

Griffin D. Economic impact associated with respiratory disease in beef cattle. Vet Clin North Am Food Anim Pract. 1997;13:367–377.

Gubbels, J. M., de Vos, A. P., van der Weide, M., Viseras, J., Schouls, L. M., de Vries,

E., … Jongejan, F. (1999). Simultaneous detection of bovine *Theileria* and *Babesia* species by reverse line blot hybrdization. *Journal of Clinical Microbiology*, 37(6), 1782– 1789.

Guerrant RL, Walker DH, Weller PF. Tropical Infectious Diseases. Edinburgh: Elsevier (2011).

Guindon, S., & Gascuel, O. (2003). A simple, fast, and accurate algorithm to estimate large phylogenies by maximum likelihood. *Systematic Biology*, 52(5), 696– 704.

Hall, A.J., Jepson, P.D., Goodman, S.J. & Härkönen, T. (2006) Phocine distemper virus in the North and European Seas–Data and models, nature and nurture. *Biological Conservation*, 131, 221-229.

Harbison, C. W., Bush, S. E., Malenke, J. R., Clayton, D. H., Harbison, C. W., Bush, S. E., … Clayton, D. H. (2020). Comparative Transmission Dynamics of Competing Parasite Species Published by : Wiley on behalf of the Ecological Society of America Stable URL : https://www.jstor.org/stable/27650873 REFERENCES Linked references are available on JSTOR for this article : c, *89*(11), 3186–3194.

Harrison, J. G., Calder, W. J., Shastry, V., & Buerkle, C. A. (2020). Dirichlet-multinomial modelling outperforms alternatives for analysis of microbiome and other ecological count data. *Molecular Ecology Resources*, *20*(2), 481–497. https://doi.org/10.1111/1755-0998.13128

Hassell, J. M., Begon, M., Ward, M. J., & Fevre, E. M. (2017). Urbanization and Disease Emergence: Dynamics at the Wildlife-Livestock-Human Interface. *Trends in Ecology & Evolution*, *32*(1), 55–67. https://doi.org/10.1016/j.tree.2016.09.012

Hathaway, N. J., Parobek, C. M., Juliano, J. J., & Bailey, J. A. (2017). SeekDeep: Single-base resolution de novo clustering for amplicon deep sequencing. *Nucleic Acids Research*, 46(4), e21.

Heard MJ, Smith KF, Ripp KJ, Berger M, Chen J, Dittmeier J, et al. The threat of disease increases as species move toward extinction. Conserv Biol (2013) 27(6):1378–88. doi:10.1111/cobi.12143

Hegemann A, Pardal S, Matson KD. Indices of immune function used by ecologists are mostly unaffected by repeated freeze-thaw cycles and methodological deviations. Front Zool (2017) 14:43. doi:10.1186/s12983-017-0226-9

Henrichs, B., Oosthuizen, M. C., Troskie, M., Gorsich, E., Gondhalekar, C., Beechler, B. R., …Jolles, A. E. (2016). Within guild co-infections influence parasite community membership: A longitudinal study in African Buffalo. *Journal of Animal Ecology*, 85(4), 1025– 1034.

Hens, N., Shkedy, Z., Aerts, M., Faes, C., Van Damme, P., & Beutels, P. (2012). *Modeling infectious disease parameters based on serological and social contact data*. New York, NY: Springer-Verlag.

Hernandez-Lara, C., Gonzalez-Garcia, F., & Santiago-Alarcon, D. (2017). Spatial and seasonal variation of avian malaria infections in five different land use types within a Neotropical montane forest matrix. *Landscape and Urban Planning*, 157, 151– 160.

Homer, M. J., Aguilar-Delfin, I., Telford, S. R., Krause, P. J., & Persing, D. H. (2000). Babesiosis. *Clinical Microbiology Reviews*, 13(3), 451– 469.

Höfner MC, Fosbery MW, Eckersall PD. Haptoglobin response of cattle infected with foot-and-mouth disease virus. Res Vet Sci (1994) 57(1):125–8. doi:10.1016/0034-

5288(94)90093-0
Huijben, S., Sim, D. G., Nelson, W. A., & Read, A. F. (2011). The fitness of drug-resistant malaria parasites in a rodent model: Multiplicity of infection. *Journal of Evolutionary Biology*, 24(11), 2410– 2422.
Huang, Y. & Rohani, P. (2006) Age-Structured Effects and Disease Interference in Childhood Infections. *Proceedings: Biological Sciences,* 273, 1229-1237.
Hudson, P. J., Dobson, A. P., & Newborn, D. (1998). Prevention of Population Cycles by Parasite Removal. *Science, 282*(5397), 2256 LP – 2258. https://doi.org/10.1126/science.282.5397.2256
Hurvich, C. M. and Tsai, C.-L. (1989) Regression and time series model selection in small samples, *Biometrika* 76, 297–307.
Ingersoll TE, Sewall BJ, Amelon SK. Effects of white-nose syndrome on regional population patterns of 3 hibernating bat species. Conserv Biol (2016) 30(5):1048–59. doi:10.1111/cobi.12690
Johnson, P. T. J., de Roode, J. C., & Fenton, A. (2015). Why infectious disease research needs community ecology. *Science (New York, N.Y.), 349*(6252), 1259504. https://doi.org/10.1126/science.1259504
Jones KE, Patel NG, Levy MA, Storeygard A, Balk D, Gittleman JL, et al. Global trends in emerging infectious disease. Nature (2008) 451:990–3. doi:10.1038/ nature06536
Jolles, A.E., Cooper, D.V. & Levin, S.A. (2005) Hidden effects of chronic tuberulosis in African buffalo. *Ecology,* 86, 2358-2364.
Jolles, A.E. (2007) Population biology of African buffalo (Syncerus caffer) at Hluhluwe-iMfolozi Park, South Africa. *African Journal of Ecology,* 45, 398-406.
Jolles, A. E., Ezenwa, V. O., Etienne, R. S., Turner, W. C., & Olff, H. (2008). Interactions between maroparasites and microparasites drive infection patterns in free-ranging African buffalo. *Ecology*, 89(8), 2239– 2250.
Jolles, A.E., Beechler, B.R. & Dolan, B.P. (2015) Beyond mice and men: environmental change, immunity and infections in wild ungulates. *Parasite Immunology,* 37, 255-266.
Jombart, T., & Ahmed, I. (2011). adegenet 1.3-1: new tools for the analysis of genome-wide SNP data. *Bioinformatics, 27*(21), 3070–3071. https://doi.org/10.1093/bioinformatics/btr521
Jung Kjær, L., Soleng, A., Edgar, K. S., Lindstedt, H. E. H., Paulsen, K. M., Andreassen, Å. K., … Bødker, R. (2019). Predicting the spatial abundance of Ixodes ricinus ticks in southern Scandinavia using environmental and climatic data. *Scientific Reports, 9*(1), 18144. https://doi.org/10.1038/s41598-019-54496-1
Keeling, M.J. & Rohani, P. (2008) *Modeling infectious diseases in humans and animals*. Princeton University Press.
Kendig, A. E., Borer, E. T., Boak, E. N., Picard, T. C., & Seabloom, E. W. (2019). Host nutritoin mediates interactions between plant viruses, altering transmission and predicted disease spread. *BioRxiv*, 1–31. https://doi.org/10.1007/springerreference_23955
Kelser EA. Meet dengue's cousin, Zika. Microbes Infect (2016) 18(3):163–6. doi:10.1016/jmicinf.2015.12.003
Kiguchi, R. and Minami, M. (2012) Cyclic Cubic Regression Spline Smoothing and

Analysis of CO2 Data at Showa Station in Antarctica, Proceedings of International Biometric Conference 2012.

Krasnov, B. R., Morand, S., Hawlena, H., Khokhlova, I. S., & Shenbrot, G. I. (2005). Sex-biased parasitism, seasonality and sexual size dimorphism in desert rodents. *Oecologia*, *146*(2), 209–217. https://doi.org/10.1007/s00442-005-0189-y

Krause, J., James, R., Franks, D., & Croft, D. (2015). Animal Social Networks. Oxford, UK: Oxford University Press.

Krogh AK, Lundsgaard JF, Bakker J, Langermans JA, Verreck FA, Kjelgaard-Hansen M, et al. Acute-phase responses in healthy and diseased rhesus macaques (*Macaca mulatta*). J Zoo Wildl Med (2014) 45(2):306–14. doi:10.1638/2013-0153R.1

Kumar, S., Stecher, G., & Tamura, K. (2016). MEGA7: Molecular Evolutionary Genetics Analysis Version 7.0 for bigger datasets. *Molecular Biology and Evolution*, 33(7), 1870– 1874.

Kuznetsova A, Brockhoff P, Christensen RHB. lmerTest: Tests in Linear Mixed Effects Models. R Package Version 2.0-33 (2016). Available from: https://CRAN.R project.org/package=lmerTest.

Leibold, M. A., & Chase, J. M. (2018). *Metacommunity ecology*. Princeton, NJ: Princeton University Press.

Lello, J., Boag, B., Fenton, A., Stevenson, I. R., & Hudson, P. J. (2004). Competition and mutualism among the gut helminths of a mammalian host. *Nature*, 428, 840– 844.

Lindahl, B. D., Nilsson, R. H., Tedersoo, L., Abarenkov, K., Carlsen, T., Kjoller, R., … Kauserud, H. (2013). Fungal community analysis by high-throughput sequencing of amplified markers–a user's guide. *New Phytologist*, 199(1), 288– 299.

Lillie, L.E. (1974) The bovine respiratory disease complex. *The Canadian Veterinary Journal*, 15, 233-242.

Liquet, B., Cao, K.-A. L., Hocini, H., & Thiébaut, R. (2012). A novel approach for biomarker selection and the integration of repeated measures experiments from two assays. *BMC Bioinformatics*, *13*(1), 325. https://doi.org/10.1186/1471-2105-13-325

Loots, A. K., Mitchell, E., Dalton, D. L., Kotze, A., & Venter, E. H. (2017). Advances in canine distemper virus pathogenesis research: a wildlife perspective. *The Journal of General Virology*, 98(3), 311–321. https://doi.org/10.1099/jgv.0.000666

Lopez, A., Thomson, R. & Savan, M. (1976) The pulmonary clearance of Pasteurella hemolytica in calves infected with bovine parainfluenza-3 virus. *Canadian Journal of Comparative Medicine*, 40, 385.

Lowen, A.C., Mubareka, S., Steel, J. & Palese, P. (2007) Influenza Virus Transmission Is Dependent on Relative Humidity and Temperature. *PLoS Pathogens*, 3, e151.

MacFadyen, S., Zambatis, N., Van Teeffelen, A. J. A., & Hui, C. (2018). Long-term rainfall regression surfaces for the Kruger National Park, South Africa: a spatio-temporal review of patterns from 1981 to 2015. *International Journal of Climatology*, *38*(5), 2506–2519. https://doi.org/10.1002/joc.5394

MacHugh, N. D., Connelley, T., Graham, S. P., Pelle, R., Formisano, P., Taracha, E. L., … Morrison, W. I. (2009). CD8+ T-cell responses to Theileria parva are preferentially directed to a single dominant antigen: Implications for parasite strain-specific immunity. *European Journal of Immunology*, *39*(9), 2459–2469. https://doi.org/10.1002/eji.200939227

Maclachlan, N.J. & Dubovi, E.J. (2010) *Fenner's veterinary virology*. Academic press.

Macpherson CN. The epidemiology and public health importance of toxocariasis: a zoonosis
of global importance. Int J Parasitol (2013) 43(12–13): 999–1008. doi:10.1016/j.ijpara.2013.07.004

Maddison, W. P., & Maddison, D. R. (2018). *Mesquite: A modular system for evolutionary analysis. Version 3.51*. Retrieved from http://www.mesquiteproject.org

Mallard, B., Dekkers, J., Ireland, M., Leslie, K., Sharif, S., Vankampen, C.L., Wagter, L. & Wilkie, B. (1998) Alteration in immune responsiveness during the peripartum period and its ramification on dairy cow and calf health. *Journal of dairy science*, 81, 585-595.

Martin, C., Pastoret, P.-P., Brochier, B., Humblet, M.-F., & Saegerman, C. (2011). A survey of the transmission of infectious diseases/infections between wild and domestic ungulates in Europe. *Veterinary Research*, 42, 70. https://doi.org/10.1186/1297-9716-42-70

Mans, B. J., Pienaar, R., Latif, A. A., & Potgieter, F. T. (2011). Diversity in the 18S SSU rRNA V4 hypervariable region of *Theileria* spp. in Cape buffalo (*Syncerus caffer*) and cattle from southern Africa. *Parasitology*, 138(6), 766– 779.

Mans, B. J., Pienaar, R., & Latif, A. A. (2015). A review of *Theileria* diagnostics and epidemiology. *International Journal for Parasitology: Parasites and Wildlife*, 4(1), 104– 118.

Mans, B., Pienaar, R., Ratabane, J., Pule, B., & Latif, A. A. (2016). Investigating the diversity of the 18S SSU rRNA hyper-variable region of *Theileria* in cattle and Cape buffalo (*Syncerus caffer*) from southern Africa using a next generation sequencing approach. *Ticks and Tick-Borne Diseases*, 7(5), 869– 879.

Marree F, de Klerk-Lorist LM, Gubbins S, Zhang F, Seago J, Pérez-Martin E, et al. Differential persistence of foot-and-mouth disease virus in African buffalo is related to virus virulence. J Virol (2016) 90(10):5132–40. doi:10.1128/ JVI.00166-16

Maunsell F, Woolums A, Francoz D, Rosenbusch R, Step D, Wilson D.J, Janzen E. *Mycoplasma bovis* infections in cattle. J. Vet. Int. Med. 2011;25(4):772–783.

Maynard J, van Hooidonk R, Harvell CD, Eakin CM, Liu G, Willis BL, et al. Improving marine disease surveillance through sea temperature monitoring, outlooks and projections. Phil Trans R Soc (2016) 371:20150208. doi:10.1098/rstb.2015.0208

McAuliffe, L., Ellis, R. J., Miles, K., Ayling, R. D., & Nicholas, R. A. J. (2006). Biofilm formation by mycoplasma species and its role in environmental persistence and survival. *Microbiology, 152*(4), 913-922. doi:https://doi.org/10.1099/mic.0.28604-0

McKeever, D. J., Taracha, E. L., Innes, E. L., MacHugh, N. D., Awino, E., Goddeeris, B. M., & Morrison, W. I. (1994). Adoptive transfer of immunity to Theileria parva in the CD8+ fraction of responding efferent lymph. *Proceedings of the National Academy of Sciences*, *91*(5), 1959 LP – 1963. https://doi.org/10.1073/pnas.91.5.1959

McKenzie A. The Capture and Care Manual: Capture, Care, and Accommodation, and Transportation of Wild African Animals. Lynwood Ridge, South Africa: South African Veterinary Foundation (1993).

McMurdie, P. J., & Holmes, S. (2013). phyloseq: An R package for reproducible

interactive analysis and graphics of microbiome census data. *PLoS ONE*, 8(4), e61217.

McLaren, M. R., Willis, A. D., & Callahan, B. J. (2019). Consistent and correctable bias in metagenomic sequencing experiments. *ELife*, *8*, e46923. https://doi.org/10.7554/eLife.46923

McNulty C. African Buffalo as Reservoir Hosts for Infectious Respiratory Pathogens in Kruger National Park. MS Thesis, University of Wisconsin- Madison College of Veterinary Medicine, South Africa (2015).

Mekata, H., Minamino, T., Mikurino, Y., Yamamoto, M., Yoshida, A., Nonaka, N., & Horii, Y. (2018). Evaluation of the natural vertical transmission of Theileria orientalis. *Veterinary Parasitology*, *263*, 1–4. https://doi.org/10.1016/j.vetpar.2018.09.017

Menge BA, Cerny-Chipman EB, Johnson A, Sullivan J, Gravem A, Chen F. Insights into differential population impacts, recovery, predation rate and temperature effects from long-term research. PLoS One (2016) 11(5): e0153994. doi:10.1371/journal.pone.0153994

Metcalf, C. J. E., & Graham, A. L. (2018). Schedule and magnitude of reproductive investment under immune trade-offs explains sex differences in immunity. *Nature Communications*, *9*(1), 4391. https://doi.org/10.1038/s41467-018-06793-y

Metzker M. Sequencing technologies – the next generation. Nat Rev Genet (2010) 11(1):31–46. doi:10.1038/nrg2626

Meyer Steiger DB, Ritchie SA, Laurance SGW. Mosquito communities and disease risk influenced by land use change and seasonality in the Australian tropics. Parasit Vectors (2016) 9:387. doi:10.1186/s13071-016-1675-2

Mihaljevic, J. R., Hoye, B. J., & Johnson, P. T. J. (2018). Parasite metacommunities: Evaluating the roles of host community composition and environmental gradients in structuring symbiont communities within amphibians. *Journal of Animal Ecology*, *87*(2), 354–368. https://doi.org/10.1111/1365-2656.12735

Michel, A.L., Cooper, D., Jooste, J., De Klerk, L.-M. & Jolles, A. (2011) Approaches towards optimising the gamma interferon assay for diagnosing Mycobacterium bovis infection in African buffalo (Syncerus caffer). *Preventive Veterinary Medicine*, 98, 142-151.

Michel, A. L., & Bengis, R. G. (2012). The African buffalo: a villain for inter-species spread of infectious diseases in southern Africa. *The Onderstepoort Journal of Veterinary Research*, *79*(2), 453. https://doi.org/10.4102/ojvr.v79i2.453

Mogensen TH. Pathogen recognition and inflammatory signaling in innate immune defenses. Clin Microbiol Rev (2009) 22(2):240–73. doi:10.1128/ CMR.00046-08

Mordecai, E. A., Jaramillo, A. G., Ashford, J. E., Hechinger, R. F., Mordecai, E. A., Jaramillo, A. G., … Lafferty, K. D. (2020). The role of competition — colonization tradeoffs and spatial heterogeneity in promoting trematode coexistence, *Ecology 97*(6), 1484–1496.

Moriyama, M., Hugentobler, W. J., & Iwasaki, A. (2020). Seasonality of Respiratory Viral Infections. *Annual review of virology*, 10.1146/annurev-virology-012420-022445.

Morrison, W. I. (2015). The aetiology, pathogenesis and control of theileriosis in domestic animals. *Revue Scientifique et Technique (International Office of Epizootics), 34*(2), 599–611. https://doi.org/10.20506/rst.34.2.2383

Morrison, W. I., Hemmink, J. D., & Toye, P. G. (2020). Theileria parva: a parasite of African buffalo, which has adapted to infect and undergo transmission in cattle. *International Journal for Parasitology*. https://doi.org/10.1016/j.ijpara.2019.12.006

Murphy K. Janeway's Immunobiology. New York, USA: Taylor & Francis Inc. (2011).

Nakagawa, S., & Schielzeth, H. (2013). A general and simple method for obtaining R2 from generalized linear mixed-effects models. *Methods in Ecology and Evolution*, *4*(2), 133–142. https://doi.org/10.1111/j.2041-210x.2012.00261.x

Neiger, R., Hadley, J., & Pfeiffer, D. U. (2002). Differentiation of dogs with regenerative and non-regenerative anaemia on the basis of their red cell distribution width and mean corpuscular volume. *The Veterinary Record*, *150*(14), 431–434. https://doi.org/10.1136/vr.150.14.431

Nelson, R.J. & Demas, G.E. (1996) Seasonal changes in immune function. *The Quarterly Review of Biology*, 71, 511-548.

Nelson, M. C., Morrison, H. G., Benjamino, J., Grim, S. L., & Graf, J. (2014). Analysis, optimization and verification of illumina-generated 16S rRNA gene amplicon surveys. *PLoS ONE*, 9(4), e94249.

Nieuwenhuis, R., te Grotenhuis, M., & Pelzer, B. (2012). Influence.ME: Tools for detecting influential data in mixed effects models. *R Journal*, *4*(2), 38–47. https://doi.org/10.32614/rj-2012-011

Nijhof, A. M., Pillay, V., Steyl, J., Prozesky, L., Stoltsz, W. H., Lawrence, J. A., … Jongejan, F. (2005). Molecular characterization of *Theileria* species associated with mortality in four species of African antelopes. *Journal of Clinical Microbiology*, 43(12), 5907– 5911.

Norval, R., Perry, B. D., & Young, A. S. (1992). *The Epidemiology of Theileriosis in Africa.* San Diego, CA: Academic Press Inc.

Ogorzaly, L., Walczak, C., Galloux, M., Etienne, S., Gassilloud, B., & Cauchie, H. M. (2015). Human adenovirus diversity in water samples using a next-generation amplicon sequencing approach. *Food and Environmental Virology*, 7(2), 112–121.

Oksanen, J., Kindt, R., Legendre, P., O'Hara, B., Stevens, M. H. H., Oksanen, M. J., & Suggests, M. (2007). *Vegan: Community Ecology Package. R Package v2.0-8*. Vienna, Austria: R Foundation for Statistical Computing.

Olds, C. L., Mason, K. L., & Scoles, G. A. (2018). Rhipicephalus appendiculatus ticks transmit Theileria parva from persistently infected cattle in the absence of detectable parasitemia: implications for East Coast fever epidemiology. *Parasites & Vectors*, *11*(1), 126. https://doi.org/10.1186/s13071-018-2727-6

Onozuka D, Hashizume M, Hagihara A. (2009) Impact of weather factors on *Mycoplasma pneumoniae* pneumonia *Thorax,* 64,507-511.

Openshaw JJ, Hegde S, Sazzad HM, Khan SU, Hossain MJ, Epstein JH, et al. Increased morbidity and mortality in domestic animals eating dropped and bitten fruit in Bangladeshi villages: implications for zoonotic disease transmission. Ecohealth (2016) 13(1):39–48. doi:10.1007/s10393-015-1080-x

Ovaskainen, O., Abrego, N., Halme, P. & Dunson, D. (2016a). Using latent variable models to identify large networks of species-to-species associations at different spatial scales. *Methods in Ecology and Evolution*, 7, 549–555.

Ovaskainen, O., Tikhonov, G., Norberg, A., Guillaume Blanchet, F., Duan, L., Dunson, D., Roslin, T. and Abrego, N. (2017), How to make more out of community data? A conceptual framework and its implementation as models and software. *Ecology Letters*, 20, 561-576. doi:10.1111/ele.12757

Owen-Smith N & Mills, M.G.L. (2008) Shifting prey selection generates constrasting herbivore dynamics within a large-mammal predatory-prey web. *Ecology*, *89*, 1120-1133.

Pacala, S., & Roughgarden, J. (2009). Resource Partitioning and Interspecific Competition in Two Two-Species Insular Anolis Lizard Communities, *Science*, *217*(4558), 444–446. https://doi.org/10.1126/science.217.4558.444

Pedersen, A.B. & Fenton, A. (2007) Emphasizing the ecology in parasite community ecology. *Trends in Ecology & Evolution*, 22, 133-139.

Pérez JM, Meneguz PG, Dematteis A, Rossi L, Serrano E. Parasites and conservation biology: the 'ibex-ecosystem'. Biodivers Conserv (2006) 15:2033–47. doi:10.1007/s10531-005-0773-9

Petti CA. Detection and identification of microorganisms by gene amplification and sequencing. Clin Infect Dis (2007) 44(8):1108–14. doi:10.1086/512818

Pienaar, R., Potgieter, F. T., Latif, A. A., Thekisoe, O. M. M., & Mans, B. J. (2011). Mixed *Theileria* infections in free-ranging buffalo herds: Implications for diagnosing *Theileria parva* infections in Cape buffalo (*Syncerus caffer*). *Parasitology*, 138(07), 884– 895.

Pienaar, R., Latif, A. A., Thekisoe, O. M. M., & Mans, B. J. (2014). Geographic distribution of Theileria sp. (buffalo) and Theileria sp. (bougasvlei) in Cape buffalo (Syncerus caffer) in southern Africa: implications for speciation. *Parasitology*, *141*(3), 411–424. https://doi.org/10.1017/S0031182013001728

Polley L. Navigating parasite webs and parasite flow: emerging and re- emerging parasitic zoonoses of wildlife origin. Int J Parasitol (2005) 35 (11–12):1279–94. doi:10.1016/j.ijpara.2005.07.003

Preston DL, Mishler JA, Townsend AR, Johnson PTJ. Disease ecology meets ecosystem science. Ecosystems (2016) 19:737–48. doi:10.1007/ s10021-016-9965-2

Price SJ, Garner TWJ, Cunningham AA, Langton TES, Nichol RA. Reconstructing the emergence of a lethal infectious disease of wildlife sup- ports a key role for spread through translocations by humans. Proc Biol Sci (2016) 283:20160952. doi:10.1098/rspb.2016.0952

Price, R., Graham, C., & Ramalingam, S. (2019). Association between viral seasonality and meteorological factors. *Scientific reports*, 9(1), 929. https://doi.org/10.1038/s41598-018-37481-y

Prins, H. H. (1996). *Ecology and behavior of the African buffalo: Social inequality and decision making*. London, UK: Chapman & Hall.

R Core Team (2015). R: A Language and Environment for Statistical Computing. Vienna, Australia: R Foundation for Statistical Computing.

R Core Team (2020). R: A language and environment for statistical computing. R

Foundation for Statistical Computing, Vienna, Austria. URL https://www.R-project.org/.

Raberg, L., de Roode, J. C., Bell, A. S., Stamou, P., Gray, D., & Read, A. F. (2006). The role of immune-mediated apparent competition in genetically diverse malaria infections. *The American Naturalist*, *168*(1), 41–53. https://doi.org/10.1086/505160

Råberg, L., Graham, A. L., & Read, A. F. (2009). Decomposing health: Tolerance and resistance to parasites in animals. *Philosophical Transactions of the Royal Society of London. Series B, Biological Sciences*, 364(1513), 37– 49.

Ramiro, R. S., Pollitt, L. C., Mideo, N., & Reece, S. E. (2016). Facilitation through altered resource availability in a mixed-species rodent malaria infection. *Ecology Letters*, *19*(9), 1041–1050. https://doi.org/10.1111/ele.12639

Rhyan, J. C., & Spraker, T. R. (2010). Emergence of diseases from wildlife reservoirs. *Veterinary Pathology*, 47(1), 34–39. https://doi.org/10.1177/0300985809354466

Richgels, K. L. D., Hoverman, J. T., & Johnson, P. T. J. (2013). Evaluating the role of regional and local processes in structuring a larval trematode metacommunity of Helisoma trivolvis. *Ecography*, *36*(7), 854–863. https://doi.org/10.1111/j.1600-0587.2013.07868.x

Rice, J., Carrasco-Medina, L., Hodgins, D. & Shewen, P. (2007) Mannheimia haemolytica and bovine respiratory disease. *Animal Health Research Reviews*, 8, 117-128.

Rodicio MR, Mendoza MC. Identification of bacteria through 16S rRNA sequencing: principles, methods, and applications in clinical microbiology. Enferm Infecc Microbiol Clin (2004) 22(4):238–45. doi:10.1157/13059055

Rodrigues MC, Cooke RF, Marques RS, Cappellozza BI, Arispe SA, Keisler DH, et al. Effects of vaccination against respiratory pathogens on feed intake, metabolic, and inflammatory responses in beef heifers. J Anim Sci (2015) 93(9):4443–52. doi:10.2527/jas.2015-9277

Rodwell, T.C., Whyte, I.J. & Boyce, W.M. (2001) Evaluation of population effects of bovine tuberculosis in free-ranging African buffalo (Syncerus caffer). *Journal of Mammalogy*, 82, 231-238.

Roeder, P., Mariner, J., & Kock, R. (2013). Rinderpest: the veterinary perspective on eradication. *Philosophical Transactions of the Royal Society of London. Series B, Biological Sciences*, *368*(1623), 20120139. https://doi.org/10.1098/rstb.2012.0139

Rohani, P., Earn, D.J., Finkenstädt, B. & Grenfell, B.T. (1998) Population dynamic interference among childhood diseases. *Proceedings of the Royal Society of London B: Biological Sciences*, 265, 2033-2041.

Rowley AF. The evolution of inflammatory mediators. Mediators Inflamm (1996) 5(1):3–13. doi:10.1155/S0962935196000014

Rushmore, J., Beechler, B.R., Tavalire, H., Gorsich, E., Devan-Song, A., Glidden, C.K., Charleston, B., Jolles, A. The heterogeneous herd: drivers of close contact variation in African buffalo and implications for pathogen invisibility. *Journal of Animal Ecology:* Accepted, in revision.

Rynkiewicz, E. C., Pedersen, A. B., & Fenton, A. (2015). An ecosystem approach to understanding and managing within-host parasite community dynamics. *Trends in Parasitology*, *31*(5), 212–221. https://doi.org/10.1016/j.pt.2015.02.005

SANPARKS (2010-2011) Kruger National Park Biodiversity Statistics. https://www.sanparks.org/parks/kruger/conservation/scientific/ff/biodiversity_statistics.php.

Sander SJ, Joyner PH, Cray C, Rostein DS, Aitken-Palmer C. Acute phase proteins as a marker of respiratory inflammation in Prezewalski's horse (*Equus ferus prezwalski*). J Zoo Wildl Med (2016) 47(2):654–8. doi:10.1638/2015- 0059.1

Sarmiento-Silva, R. E., Nakamura-Lopez, Y., & Vaughan, G. (2012). Epidemiology, molecular epidemiology and evolution of bovine respiratory syncytial virus. *Viruses*, *4*(12), 3452– 3467. https://doi.org/10.3390/v4123452

Schiller, I., Waters, W.R., Vordermeier, H.M., Nonnecke, B., Welsh, M., Keck, N., Whelan, A., Sigafoose, T., Stamm, C. & Palmer, M. (2009) Optimization of a whole-blood gamma interferon assay for detection of Mycobacterium bovis-infected cattle. *Clinical and Vaccine Immunology,* 16, 1196-1202.

Schoeman, J. P. (2009). Canine babesiosis. *Onderstepoort Journal of Veterinary Research*, 76(1), 59– 66.

Schneider, C. A., Rasband, W. S., & Eliceiri, K. W. (2012). NIH Image to ImageJ: 25 years of image analysis. *Nature Methods*, *9*(7), 671–675. https://doi.org/10.1038/nmeth.2089

Sears BF, Rohr JR, Allen JE, Martin LB. The economy of inflammation: when is less more? Trends Parasitol (2011) 27(9):382–7. doi:10.1016/j.pt.2011. 05.004

Simon, A.K., Hollander, G.A., McMichael, A. (2015) Evolution of the immune system in humans from infancy to old age *Proceedings of the Royal. Society B.* 282, 20143085.

Shears P, O'Dempsey TJD. Ebola virus disease in Africa: epidemiology and nosocomial transmission. J Hosp Infect (2015) 90(1):1–9. doi:10.1016/j. jhin.2015.01.002

Sikhweni, N.P. & Hassan, R. (2013). Opportunities and challenges facing small-scale cattle farmers living adjacent to Kruger National Park , Limpopo Province NP Sikhweni and R Hassan Corresponding Author : NP Sikhweni. *Journal of Emerging Trends in Economics and Management Sciences*, *5*(1), 38–43.]

Sisson, D.R. (2017). *Health and fitness of* Anaplasma *species infection in African buffalo(* Syncerus caffer*)* (Master of Philosophy thesis, University of Melbourne, Werribee). Retrieved from https://minerva-access.unimelb.edu.au/bitstream/handle/11343/197971/Thesis%20Sisson.pdf?sequence=1&isAllowed=y

Smith, B. P., Van Metre, D. C., & Pustrela, N. (2019). Large Animal Internal Medicine (6th ed.). St. Louis, Missouri: Elsevier.

Smith, J. A., Thomas, A. C., Levi, T., Wang, Y. W., & Wilmers, C. C. (2018). Human activity reduces niche partitioning among three widespread mesocarnivores. *Oikos*, 127(6), 890– 901.

Smith KF, Sax DF, Lafferty KD. Evidence for the role of infectious disease in species extinction and endangerment. Conserv Biol (2006) 20(5):1349–57. doi:10.1111/j.1523-1739.2006.00524.x

Smith, T., Felger, I., Tanner, M., & Beck, H. P. (1999). The epidemiology of multiple *Plasmodium falciparum* infections - 11. Premunition in *Plasmodium falciparum* infection: Insights from the epidemiology of multiple infections. *Transactions of the Royal Society of Tropical Medicine and Hygiene*, 93, S59– S64.

Smitka P, Tóthová C, Curlík J, Lazar P, Bíres J, Posiváková T. Serum concen- tration of haptoglobin in European mouflon (Ovis musimon L.) from a game reserve. Acta Vet Brno (2015) 84:25–8. doi:10.2754/avb201584010025

Sol, D., Jovani, R., & Torres, J. (2003). Parasite mediated mortality and host immune response explain age-related differences in blood parasitism in birds. *Oecologia*, 135(4), 542– 547.

Spaan, RS, Epps, CW, Ezenwa, VO, Jolles, AE. (2019) Why did the buffalo cross the park? Resource shortages, but not infections, drive dispersal in female African buffalo (Syncerus caffer). *Ecology & Evolution*, 9, 5651– 5663. https://doi.org/10.1002/ece3.5145

Srikumaran, S., Kelling, C.L. & Ambagala, A. (2007) Immune evasion by pathogens of bovine respiratory disease complex. *Animal Health Research Reviews*, 8, 215-229.

Stenfeldt C, Heegaard PMH, Stockman A, Tjomehoj K, Belsham GJ. Analysis of the acute phase responses of serum amyloid A, haptoglobin and type 1 interferon in cattle experimentally infected with foot-and-mouth disease virus serotype O. Vet Res (2011) 42:66. doi:10.1186/1297-9716-42-66

Stjernman, M., Raberg, L., & Nilsson, J. A. (2008). Maximum host survival at intermediate parasite infection intensities. *PLoS ONE*, 3(6), e2463.

Susi, H., Barrès, B., Vale, P.F. & Laine, A.-L. (2015) Co-infection alters population dynamics of infectious disease. *Nature communications*, 6.

Swain, D.L., Patison, K. Heath, B., Bishop-Hurley, G. & Finger A., (2015). Pregnant cattle associations and links to maternal reciprocity. *Applied Animal Behavior Science,* 168, 10-17.

Takeda K, Kaisho T, Akira S. Toll-like receptors. Annu Rev Immunol (2003) 21:335–76. doi:10.1146/annurev.immunol.21.120601.141126

Tan, B., Gao, F., Tan, B., Gao, F., Wolfe, R. E., Pedelty, J. A., … Nightingale, J. (2011). An Enhanced TIMESAT Algorithm for Estimating Vegetation Phenology Metrics From MODIS Data. *IEEE Journal of Selected Topics in Applied Earth Observations and Remote Sensing*, *4*(2), 361–371. https://doi.org/10.1109/JSTARS.2010.2075916

Tang, Y., Horikoshi, M., & Li, W. (2016). ggfortify: Unified interface to visualize statistical result of popular R packages. *The R Journal*, *8*.

Tarav, M., Tokunaga, M., Kondo, T., Kato-Mori, Y., Hoshino, B., Dorj, U., & Hagiwara, K. (2017). Problems in the protection of reintroduced Przewalski's horses (*Equus ferus przewalskii*) caused by piroplasmosis. *Journal of Wildlife Diseases*, 53(4), 911– 915.

Tavalire, H. F., Hoal, E. G., le Roex, N., van Helden, P. D., Ezenwa, V. O., & Jolles, A. E. (2019). Risk alleles for tuberculosis infection associate with reduced immune reactivity in a wild mammalian host. *Proceedings of the Royal Society B*, 286(1907), 20190914. https://doi.org/10.1098/rspb.2019.0914

Taylor, J. D., Fulton, R. W., Lehenbauer, T. W., Step, D. L., & Confer, A. W. (2010). The epidemiology of bovine respiratory disease: What is the evidence for predisposing factors? *The Canadian veterinary journal = La revue veterinaire canadienne*, *51*(10), 1095–1102.

Telfer, S., Lambin, X., Birtles, R., Beldomenico, P., Burthe, S., Paterson, S. & Begon, M.

(2010) Species interactions in a parasite community drive infection risk in a wildlife population. *Science*, 330, 243-246.

Tilman, D. (1994). Competition and Biodiversity in Spatially Structured Habitats Author (s): David Tilman Stable URL : http://www.jstor.org/stable/1939377 REFERENCES Linked references are available on JSTOR for this article : You may need to log in to JSTOR to access the, *75*(1), 2–16.

Titcomb, G., Allan, B. F., Ainsworth, T., Henson, L., Hedlund, T., Pringle, R. M., … Young, H. S. (2017). Interacting effects of wildlife loss and climate on ticks and tick-borne disease. *Proceedings of the Royal Society B: Biological Sciences*, *284*(1862), 20170475. https://doi.org/10.1098/rspb.2017.0475

Trillmich, F., Guenther, A., Jäckel, M., & Czirják, G. Á. (2020). Reproduction affects immune defenses in the guinea pig even under ad libitum food. *PloS One*, *15*(3), e0230081–e0230081. https://doi.org/10.1371/journal.pone.0230081

Thompson, R. C. A., Lymbery, A. J., & Smith, A. (2010). Parasites, emerging disease and wildlife conservation. *International Journal for Parasitology*, 40(10), 1163–1170. https://doi.org/10.1016/j.ijpara.2010.04.009

Tjur, T. (2009) Coefficients of Determination in Logistic Regression Models—A New Proposal: The Coefficient of Discrimination, The American Statistician, 63:4, 366-372, DOI: 10.1198/tast.2009.08210

Trillmich, F., Guenther, A., Jäckel, M., Czirják, G.Á. (2020) Reproduction affects immune defenses in the guinea pig even under ad libitum food. *PLOS ONE* 15(3), e0230081. https://doi.org/10.1371/journal.pone.0230081

Turner, W.C., Jolles, A.E., & Owen-Smith, N. (2005). Alternating sexual segregation during the mating season by male African buffalo (Syncerus caffer).*Journal of Zoology* 267(03), 291 - 299

Valarcher, J.-F., Bourhy, H., Lavenu, A., Bourges-Abella, N., Roth, M., Andreoletti, O., Ave, P. & Schelcher, F. (2001) Persistent infection of B lymphocytes by bovine respiratory syncytial virus. *Virology,* 291, 55-67.

Vandegrift KJ, Wale N, Epstein JH. An ecological and conservation perspective on advances in the applied virology of zoonoses. Viruses (2011) 3(4):379–97. doi:10.3390/v3040379

Van der Poel, W., Brand, A., Kramps, J. & Van Oirschot, J. (1994) Respiratory syncytial virus infections in human beings and in cattle. *Journal of Infection,* 29, 215-228.

Van Vuuren, M. (1994) Bovine respiratory syncytial virus infection. *Intifectious Diseases of Livestock. Oxford University Press, Cape Town.(Links),* 769-772.

Venter, F. & Gertenbach, W. (1986) A cursory review of the climate and vegetation of the Kruger National Park. *Koedoe,* 29, 139-148.

Vermeulen, E. T., Lott, M. J., Eldridge, M. D., & Power, M. L. (2016). Evaluation of next generation sequencing for the analysis of Eimeria communities in wildlife. *Journal of Microbiol Methods*, 124, 1– 9.

Vicente, J., Höfle, U., Fernández-De-Mera, I. G., & Gortazar, C. (2007). The importance of parasite life history and host density in predicting the impact of infections in red deer. *Oecologia*, *152*(4), 655–664. https://doi.org/10.1007/s00442-007-0690-6

Vosloo W, Thomson GR. Natural habitats in which foot-and-mouth disease viruses are maintained. In: Sobrino F, Domingo E, editors. Foot-and-Mouth Disease Virus: Current Research and Emerging Trends. Madrid, Spain: CSIC- UAM (2017). p.

179–210.
Vurro M, Bonciani B, Vannacci G. Emerging infectious diseases of crop plants in developing countries: impact on agriculture and socio-economic consequences. Food Sec (2010) 2:113. doi:10.1007/s12571-01-00627
Watson, J. E. M., Venter, O., Lee, J., Jones, K. R., Robinson, J. G., Possingham, H. P., & Allan, J. R. (2018). Protect the last of the wild. *Nature*. https://doi.org/10.1038/d41586-018-07183-6
White, L. A., Forester, J. D., & Craft, M. E. (2018). Covariation between the physiological and behavioral components of pathogen transmission: host heterogeneity determines epidemic outcomes. *Oikos*, 127(4), 538–552. https://doi.org/10.1111/oik.04527
Wickham, H. (2016). *ggplot2: Elegant graphics for data analysis*. New York, NY: Springer-Verlag.
Wiethoelter, A. K., Beltrán-Alcrudo, D., Kock, R., & Mor, S. M. (2015). Global trends in infectious diseases at the wildlife–livestock interface. *Proceedings of the National Academy of Sciences*, *112*(31), 9662 LP – 9667. https://doi.org/10.1073/pnas.1422741112
Williams-Blangero, S., Criscione, C. D., VandeBerg, J. L., Correa-Oliveira, R., Williams, K. D., Subedi, J., … Blangero, J. (2012). Host genetics and population structure effects on parasitic disease. *Philosophical Transactions of the Royal Society B: Biological Sciences*, *367*(1590), 887–894. https://doi.org/10.1098/rstb.2011.0296
Williamson, B. D., Hughes, J. P., & Willis, A. D. (2019). A multi-view model for relative and absolute microbial abundances. *BioRxiv*, 761486. https://doi.org/10.1101/761486
Wold, S., Sjöström, M., & Eriksson, L. (2001). PLS-regression: a basic tool of chemometrics. *Chemometrics and Intelligent Laboratory Systems*, *58*(2), 109–130. https://doi.org/https://doi.org/10.1016/S0169-7439(01)00155-1
Wood, P. & Jones, S. (2001) BOVIGAM TM: An in vitro cellular diagnostic test for bovine tuberculosis. *Tuberculosis*, 81, 147-155.
Wood, S.N. (2011) Fast stable restricted maximum likelihood and marginal likelihood estimation of semiparametric generalized linear models. *Journal of the Royal Statistical Society (B)*, 73(1), 3-36.
Wood, J. L. N., Leach, M., Waldman, L., Macgregor, H., Fooks, A. R., Jones, K. E., … Cunningham, A. A. (2012). A framework for the study of zoonotic disease emergence and its drivers: spillover of bat pathogens as a case study. *Philosophical Transactions of the Royal Society of London. Series B, Biological Sciences*, 367(1604), 2881–2892. https://doi.org/10.1098/rstb.2012.0228
Wood, S. (2017). Generalized Additive Models. New York: Chapman and Hall/CRC, https://doi.org/10.1201/9781315370279
Woolhouse, M. E. J., Thumbi, S. M., Jennings, A., Chase-Topping, M., Callaby, R., Kiara, H., … Toye, P. G. (2015). Coinfection determine patterns of mortality in populations exposed to parasite infections. *Scientific Advances*, 1, e1400026.
Woolhouse M, Scott F, Hudson Z, Howey R, Chase-Topping M. Disease invasion impacts on biodiversity and human health. Philos T R Soc B (2012) 367(1604):2804–6. doi:10.1098/rstb.2012.0331

Wright, A.N. & Gompper, M.E. (2005) Altered parasite assemblages in raccoons in response to manipulated resource availability. *Oecologia*, 144, 148-156.

Xavier R, Turck N, Hainard A, Tiberti N, Lisacek F, Sanchez J, et al. pROC: an open-source package for R and S+ to analyze and compare ROC curves. BMC Bioinformatics (2011) 12:77. doi:10.1186/1471-2105-12-77

Yabsley, M. J., & Shock, B. C. (2013). Natural history of Zoonotic Babesia: Role of wildlife reservoirs. *International Journal for Parasitology. Parasites and Wildlife*, 2, 18– 31.

Yamada, S., Konnai, S., Imamura, S., Simuunza, M., Chembensofu, M., Chota, A., … Ohashi, K. (2009). Quantitative analysis of cytokine mRNA expression and protozoan DNA load in Theileria parva-infected cattle. *Journal of Veterinary Medical Science*, *71*(1), 49–54. https://doi.org/10.1292/jvms.71.49

Yoccoz, N. G. (2012). The future of environmental DNA in ecology. *Molecular Ecology*, 21(8), 2031– 2038.

Zambatis, N. (2003) Determinants of grass production and composition in the Kruger National Park. MSc (Agric.) dissertation, University of Natal, Pietermaritzburg.

Zeileis, A., & Hothorn, T. (2002). Diagnostic Checking in Regression Relationships. *R News*, *2*(3), 7–10.

Zhong, D., Lo, E., Wang, X., Yewhalaw, D., Zhou, G., Atieli, H. E., … Yan, G. (2018). Multiplicity and molecular epidemiology of *Plasmodium vivax* and *Plasmodium falciparum* infections in East Africa. *Malaria Journal*, 17, 14.

Zylberberg, M. (2019). Next-generation ecological immunology. *Physiological and Biochemical Zoology*, 92(2), 177– 188.

APPENDICES

APPENDIX A – CHAPTER 2 SUPPLEMENTARY FIGURES

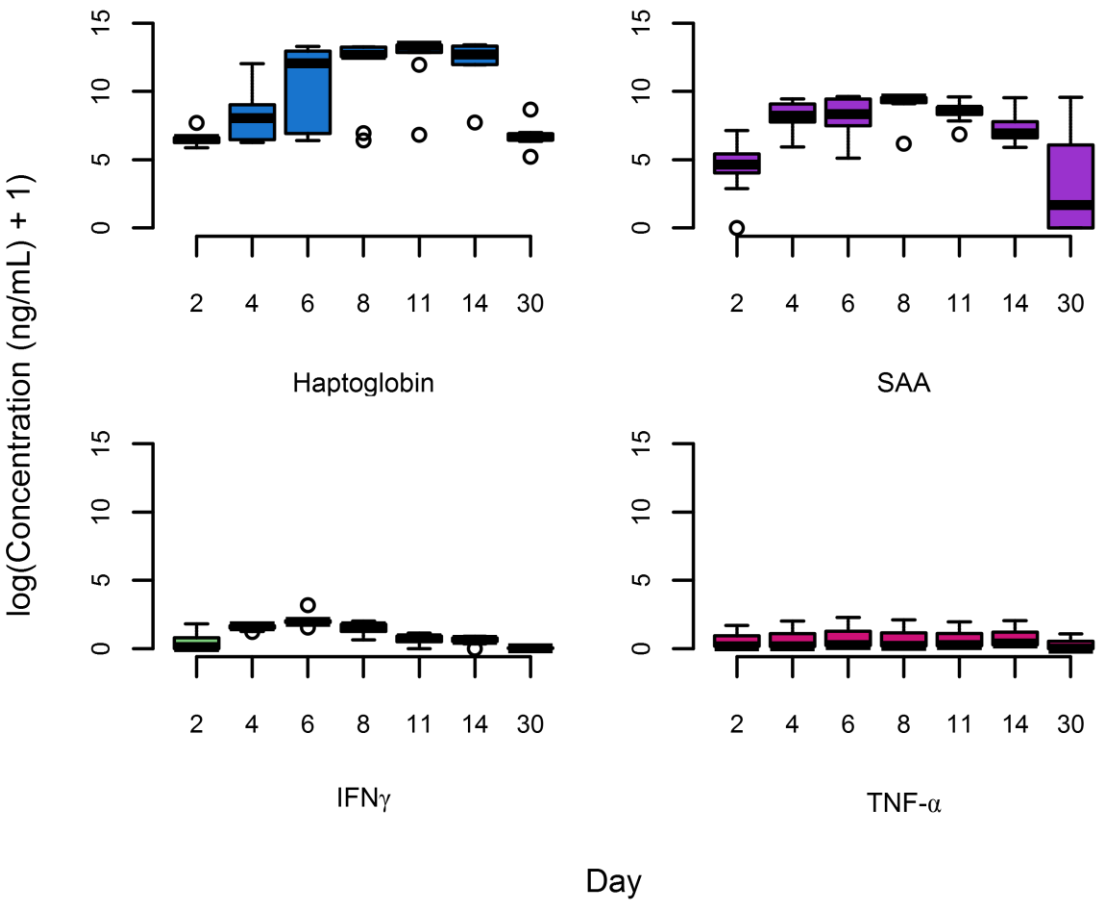

Figure A1. Box plots depicting NSMI concentrations for each day of the FMDV experiment. Animals were excluded from the figure if they did not mount an NSMI response (concentrations did not exceed 2-fold the baseline) or the concentrations peaked on day 30. Concentrations were log transformed to reduce the range of all NSMI axes. The horizontal bands represent the 25%, 50% and 75% quartiles whereas the vertical lines represent 1.5 times the interquartile range above the upper quartiles and below the lower quartile, and dots represent outliers.

APPENDIX B – CHAPTER 3 SUPPLEMENTARY TABLES AND FIGURES

Table B1. Mean estimate (β) for each host trait and season; estimates where the support was > 0.95 are bolded and highlighted in **dark grey** and where the support was >0.90 are highlighted in light grey.

	BHV	Pi-3	AD-3	MH	MB	BRSV
intercept	-1.799	-1.997	-1.729	-1.536	-1.145	-1.581
bTB status[1]	0.086	0.019	0.095	0.107	0.017	**0.267**
bolus[2]	0.117	0.024	-0.174	-0.015	0.134	-0.105
horn residuals	0.218	0.108	0.282	-0.140	-0.022	-0.195
age (months)	0.011	-0.105	**0.301**	-0.316	-0.109	**0.262**
herd[3]	**0.273**	**0.279**	0.161	0.020	-0.128	-0.090
pregnant[4]	0.191	**0.438**	0.147	-0.118	0.066	0.038
lactating[5]	-0.047	-0.147	-0.036	-0.168	-0.052	0.006
calf at heel[6]	-0.004	0.057	-0.031	0.370	0.295	0.289
condition	**0.334**	**-0.301**	0.098	0.066	0.150	**0.281**
season[7]	-0.177	0.113	**0.483**	-0.219	**0.348**	0.164

[1]baseline = negative; [2]baseline=no bolus;[3]baseline = crocodile bridge; [4]baseline=not pregnant;[5]baseline=not lactating; [6]baseline=calf at heel; [7]baseline = dry season

Table B2. Sample-level species-species residual associations. Covariance matrix (Ω) for pathogens (sample level random effect); covariance has been converted to correlation to scale from -1 to +1. Estimates where the support was > 0.95 are bolded and highlighted in **dark grey**. Support was < 0.90 for all other pathogens.

	BHV	**Pi-3**	**AD-3**	**MH**	**MB**	**BRSV**
BHV	1.000	**0.996**	**0.996**	0.297	0.210	-0.374
Pi-3	**0.996**	1.000	**0.997**	0.298	0.211	-0.375
AD-3	**0.996**	**0.997**	1.000	0.298	0.210	-0.374
MH	0.297	0.298	0.298	1.000	0.090	-0.082
MB	0.210	0.211	0.210	0.090	1.000	-0.100
BRSV	-0.374	-0.375	-0.374	-0.082	-0.100	1.000

Table B3. Animal ID-level species-species residual associations. Covariance matrix (Ω) for pathogens (Animal ID-random effect); covariances have been converted to correlation to scale from -1 to +1. Estimates where the support was > 0.90 are highlighted in light grey. Support was < 0.90 for all other pathogens.

	BHV	**Pi-3**	**AD-3**	**MH**	**MB**	**BRSV**
BHV	1.000	-0.097	0.140	0.455	0.377	0.067
Pi-3	-0.097	1.000	-0.087	-0.316	-0.243	-0.065
AD-3	0.140	-0.087	1.000	0.253	0.202	0.018
MH	0.455	-0.316	0.253	1.000	0.782	0.170
MB	0.377	-0.243	0.202	0.782	1.000	0.128
BRSV	0.067	-0.065	0.018	0.170	0.128	1.000

Table B4. Rainfall year-level species-species residual associations. Covariance matrix (Ω) for pathogens (rainfall year random effect); covariances have been converted to correlation to scale from -1 to +1. There was no statistical support for species-species associations at the rainfall year-level.

	BHV	**Pi-3**	**AD-3**	**MH**	**MB**	**BRSV**
BHV	1.00	0.30	-0.33	0.24	0.59	0.25
Pi-3	0.30	1.00	-0.09	0.02	0.15	-0.48
AD-3	-0.33	-0.09	1.00	-0.12	-0.29	-0.17
MH	0.24	0.02	-0.12	1.00	0.22	0.20
MB	0.59	0.15	-0.29	0.22	1.00	0.32
BRSV	0.25	-0.48	-0.17	0.20	0.32	1.00

Table B5. Estimates of model fit. We evaluated model explanatory power using area under the receiving operator characteristic (AUC), root-mean-squared-error (RMSE) and Tjur's R^2. AUC quantifies the ability of a model to rank occurrences correctly, RMSE measures the squared difference between estimated occurrence and true species occurrence and Tjur's R^2 measures the difference in predicted probabilities of occurrence and probabilities of absence. The table is ordered from lowest to highest Tjur's R^2.

	RMSE	AUC	TjurR2
AD-3	0.279	0.964	0.219
Pi-3	0.255	0.972	0.216
BHV	0.258	0.943	0.166
BRSV	0.268	0.813	0.152
MH	0.266	0.935	0.134
MB	0.389	0.660	0.035

Table B6. Variance partitioning for each pathogen. Note that values displayed in the table are the proportion of variance explained by each covariate and random effect of the total variance explained by the model, as opposed to the proportion of variance in the data explained by each covariate or random effect. As such, these values sum to 1 but our models did not account for all variation in the data.

	BHV	Pi-3	AD-3	MH	MB	BRSV
bTB status	0.012	0.008	0.011	0.014	0.021	0.044
bolus	0.015	0.008	0.019	0.011	0.049	0.015
horn residuals	0.033	0.016	0.043	0.018	0.024	0.031
age (months)	0.014	0.014	0.044	0.051	0.047	0.049
herd	0.039	0.034	0.020	0.012	0.044	0.016
pregnant	0.024	0.068	0.017	0.015	0.028	0.013
lactating	0.018	0.019	0.015	0.019	0.043	0.018
calf at heel	0.018	0.016	0.015	0.045	0.124	0.047
condition	0.056	0.037	0.014	0.013	0.057	0.052
season	0.022	0.015	0.095	0.028	0.204	0.027
Random: sample	0.598	0.698	0.677	0.031	0.086	0.046
Random: Animal ID	0.029	0.016	0.014	0.723	0.160	0.034
Random: Rainfall year	0.123	0.053	0.016	0.019	0.114	0.607

Table B7. GAM model output for number of new cases by calendar month and rainfall year. For each pathogen, a global model was fit for the number of cases per month ~ s(calendar month) + s(rainfall year) + sample number. We selected the final model by choosing the model with the lowest AICc.

	MH, deviance explained = 56.90%			
parametric terms	Estimate	SE	z-value	p-value
(Intercept)	-0.18	0.23	-0.82	0.44
sample.number	0.04	0.01	5.00	**<0.001**
nonparametric terms		edf	chi squared	p-value
s(month)		1.75	6.95	**0.009**
	MB, deviance explained = 65.40%			
parametric terms	Estimate	SE	z-value	p-value
(Intercept)	0.37	0.16	2.39	0.02
sample.number	0.04	0.00	8.41	**<0.001**
nonparametric terms		edf	chi squared	p-value
s(month)		1.92	8.47	**0.005**
	Pi-3, deviance explained = 60.40%			
parametric terms	Estimate	SE	z-value	p-value
(Intercept)	-0.30	0.20	-1.28	0.20
sample.number	0.04	0.01	6.51	**<0.001**
nonparametric terms		edf	chi squared	p-value
s(month)		3.34	26.27	**<0.001**

Table B7 continued.

	AD-3, deviance explained = 59.40%			
parametric terms	Estimate	SE	z-value	p-value
(Intercept)	0.17	0.19	0.88	0.38
sample.number	0.03	0.01	5.11	**<0.001**
nonparametric terms		edf	chi squared	p-value
s(month)		2.00	14.28	**<0.001**
s(year)		1.46	5.56	**0.03**

	BRSV, deviance explained = 74.80%			
parametric terms	Estimate	SE	z-value	p-value
(Intercept)	-1.45	0.43	-3.37	**<0.001**
sample.number	0.06	0.01	4.39	**<0.001**
nonparametric terms		edf	chi squared	p-value
s(month)		7.96	20.69	**<0.006**
s(year)		1.88	40.68	**<0.001**

	BHV, deviance explained = 48.60%			
parametric terms	Estimate	SE	z-value	p-value
intercept	-0.36	0.23	-1.55	0.12
sample number	0.04	0.01	5.47	**<0.001**
nonparametric terms		edf	chi squared	p-value
s(year)		2.94	17.54	**<0.001**

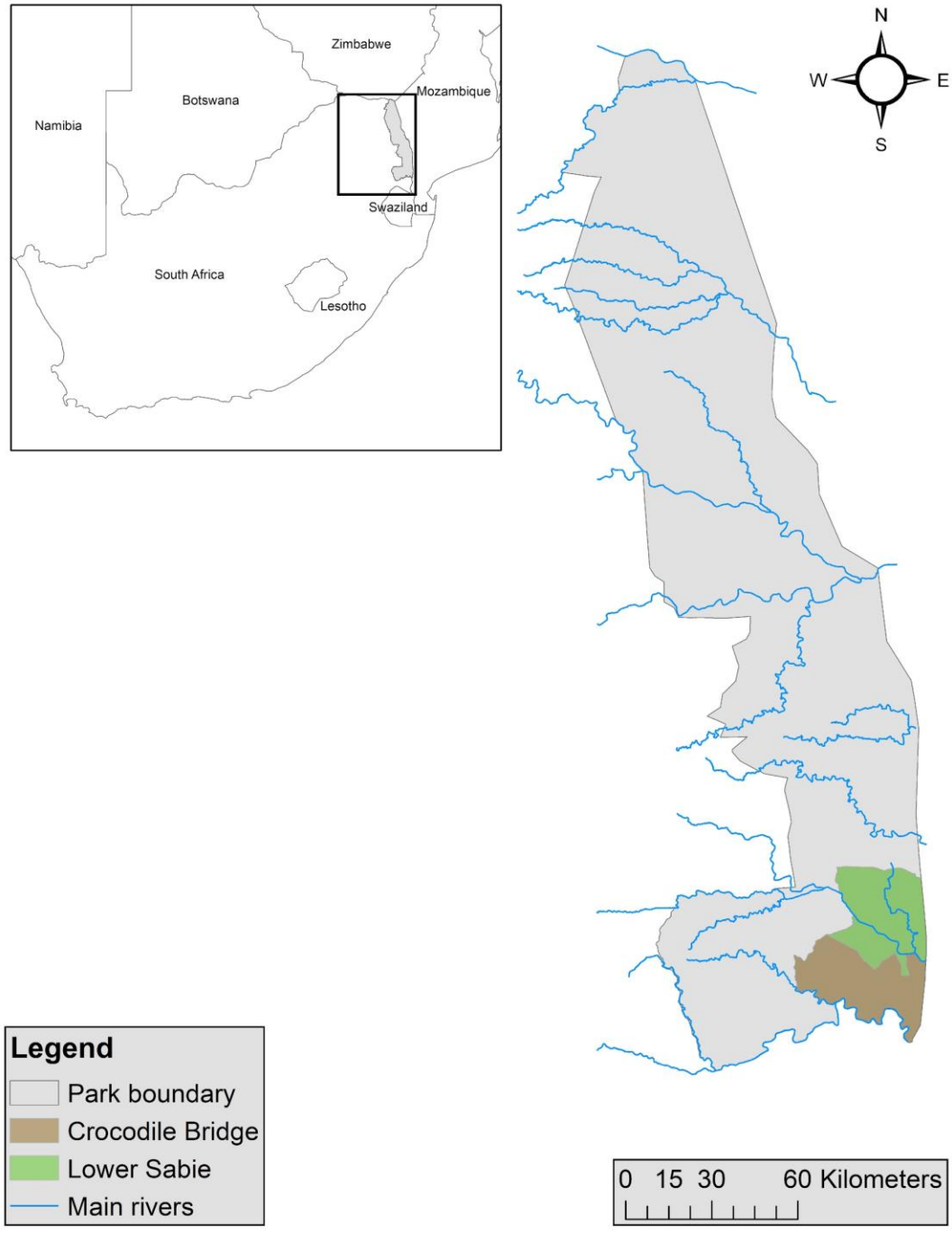

Figure B1. Map of Lower Sabie & Crocodile Bridge herd locations. Map courtesy of Rob S. Spaan.

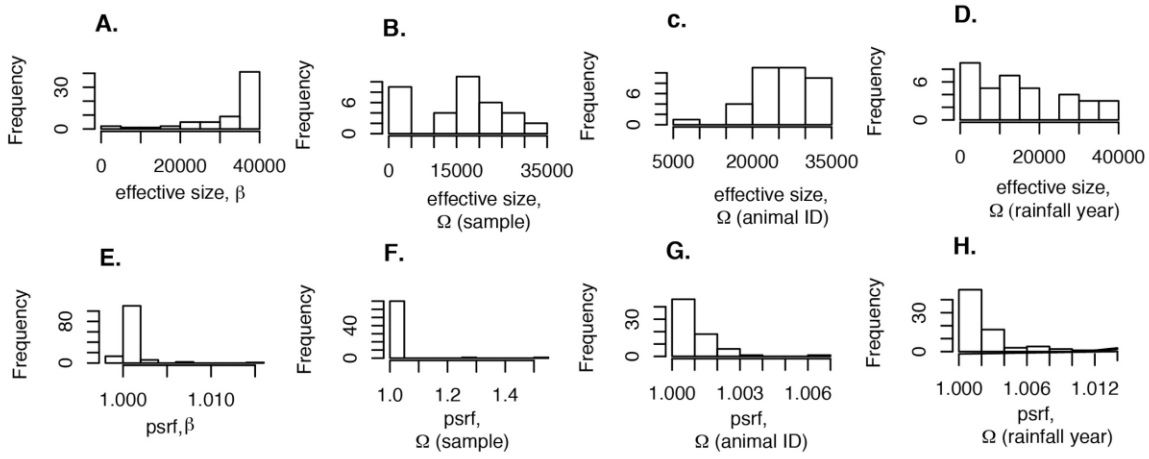

Figure B2. Histograms of effective size and Gelman-Rubin diagnostic (potential scale reduction factor). A-D) Effective sample size; E-H) Gelman-Rubin diagnostic, potential scale reduction factor.

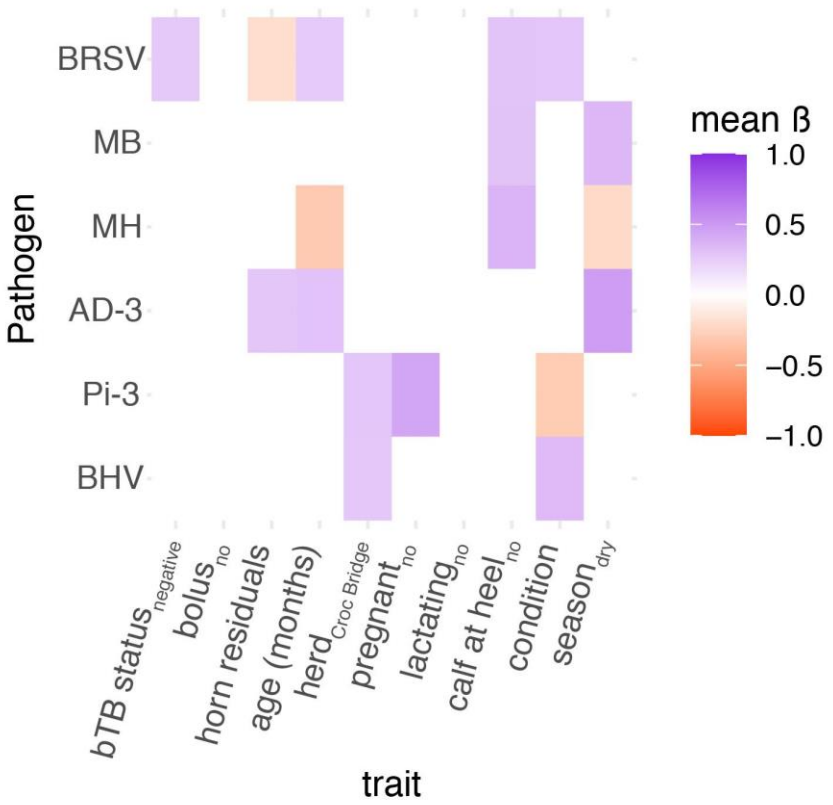

Figure B3. Pathogen response to host trait covariates. Host traits with posterior probability > 0.90, colored by mean response. For categorical variables, the subscript represents the baseline group. Continuous variables were centered and scaled to two standard deviations from the mean. Color indicates the direction (orange = negative effect or higher for the baseline group, purple = positive effect or higher for non-baseline group) and magnitude of the mean posterior estimate for the effect of each trait on pathogen occurrence.

APPENDIX C – CHAPTER 4 SUPPLEMENTARY TEXT, TABLES AND FIGURES

Appendix C1. *In silico* mock community analysis.

First, using GenBank, a library of 63 previously published 18S *Theileria* sequences was compiled. An in-house Python script, looping an ART (V 3.19.15; Haung et al., 2012) script, was used to randomly select and generate FASTQ files from two *Theileria* species and three haplotypes per species 25 times. Illumina MiSeq forward and reverse read error profiles were averaged across 300 samples to obtain an error profile for each simulated FASTQ file. Each simulation iteration produced one major haplotype (high relative abundance) per species and two minor haplotypes (low relative abundance) per *Theileria* species. The collective mock community consisted of 25 simulated samples, with major haplotypes sampled at 35%, 47%, 48.5%, 49.25% and 49.625% relative abundances and minor haplotypes sampled at 10%, 5%, 2%, 1%, 0.5%, 0.25% and 0.125% relative abundances.

SeekDeep (Hathaway, Parobek, Juliano, & Bailey, 2017) and DADA2 (Callahan et al., 2016) were run using default settings for Illumina MiSeq paired-end reads. For SeekDeep, FASTQ files from all samples were processed using a within-sample relative abundance cutoff of 0% and the Illumina MiSeq tag, allowing no mismatches. Within the SeekDeep pipeline, sequences that were marked as likely chimeric were removed. For DADA2, FASTQ files were processes using the denoise-paired command, trimming sequences at 20 base pairs. No additional parameters were included in the command. Relative abundance matrixes produced by each software were exported into R software (version 3.4.3) and compared to known relative abundances using the Mantel test (Bray-Curtis distance measures) in *vegan* (Oksanen et al., 2007). For both software packages, Mantel correlation coefficient was > 0.99. Subsequently, the number of false haplotypes produced by each software was evaluated. Here, we define false haplotypes as sequences that were produced by the software which were not included in our mock community.

When evaluating haplotypes that occurred at > 0.1% relative abundance within a sample, SeekDeep produced no false haplotypes whereas DADA2 produced two false haplotypes; hence, SeekDeep was used for all further analyses.

References

Callahan, B. J., McMurdie, P. J., Rosen, M. J., Han, A. W., Johnson, A. J., & Holmes, S. P. (2016). DADA2: High-resolution sample inference from Illumina amplicon data.
Nature Methods, 13(7), 581– 583.

Hathaway, N. J., Parobek, C. M., Juliano, J. J., & Bailey, J. A. (2017). SeekDeep: Single-base resolution de novo clustering for amplicon deep sequencing. *Nucleic Acids Research*, 46(4), e21

Huang, W., Li, L., Myers, J. R., & Marth, G. T. (2012). ART: a next-generation sequencing read simulator. *Bioinformatics (Oxford, England)*, *28*(4), 593–594. https://doi.org/10.1093/bioinformatics/btr708

Oksanen, J., Kindt, R., Legendre, P., O'Hara, B., Stevens, M. H. H., Oksanen, M. J., & Suggests, M. (2007). *Vegan: Community Ecology Package. R Package v2.0-8*. Vienna, Austria: R Foundation for Statistical Computing.

Appendix C1, Table 1. Layout of *in silico* mock community: Relative abundance of each sequence included in each simulated sample. Species 1 and species 2 varied between each sample.

Sample	Relative abundance species 1.A (%)	Relative abundance species 1.B (%)	Relative abundance species 1.C (%)	Relative abundance species 2.A (%)	Relative abundance species 2.B (%)	Relative abundance species 2.C (%)
1	35	10	5	35	10	5
2	35	10	5	35	10	5
3	35	10	5	35	10	5
4	35	10	5	35	10	5
5	35	10	5	35	10	5
6	47	2	1	47	2	1
7	47	2	1	47	2	1
8	47	2	1	47	2	1
9	47	2	1	47	2	1
10	47	2	1	47	2	1
11	48.5	1	0.5	48.5	1	0.5
12	48.5	1	0.5	48.5	1	0.5
13	48.5	1	0.5	48.5	1	0.5
14	48.5	1	0.5	48.5	1	0.5
15	48.5	1	0.5	48.5	1	0.5
16	49.25	0.5	0.25	49.25	0.5	0.25
17	49.25	0.5	0.25	49.25	0.5	0.25
18	49.25	0.5	0.25	49.25	0.5	0.25
19	49.25	0.5	0.25	49.25	0.5	0.25
20	49.25	0.5	0.25	49.25	0.5	0.25
21	49.625	0.25	0.125	49.625	0.25	0.125
22	49.625	0.25	0.125	49.625	0.25	0.125
23	49.625	0.25	0.125	49.625	0.25	0.125
24	49.625	0.25	0.125	49.625	0.25	0.125
25	49.625	0.25	0.125	49.625	0.25	0.125

Appendix C2. Duplication study

Prior to running FASTQ files from all samples through the bioinformatics pipeline, 10% of samples were run in duplicates in separate library assembly reactions and de-multiplexed, filtered and clustered on SeekDeep (Hathaway et al., 2017) using the Illumina MiSeq tag and a within-sample relative abundance cutoff of 0.1%. Pairwise differences were assessed using the paired Wilcoxon signed-rank test in the software R (version 3.4.3). After increasing the relative abundance cutoff to 1%, there were no significant differences in the distribution of relative abundances within duplicate pairs ($P > 0.05$). To further confirm the repeatability of duplicates, an ordination was plotted after applying the within-sample 1% relative abundance cutoff using the *vegan* (Appendix C2, Figure 1; non-metric multi-dimensional scaling, Bray-Curtis distance measures, stress = 0.07) (Oksanen et al., 2007).

References

Hathaway, N. J., Parobek, C. M., Juliano, J. J., & Bailey, J. A. (2017). SeekDeep: Single-base resolution de novo clustering for amplicon deep sequencing. *Nucleic Acids Research*, 46(4), e21

Oksanen, J., Kindt, R., Legendre, P., O'Hara, B., Stevens, M. H. H., Oksanen, M. J., & Suggests, M. (2007). *Vegan: Community Ecology Package. R Package v2.0-8*. Vienna, Austria: R Foundation for Statistical Computing.

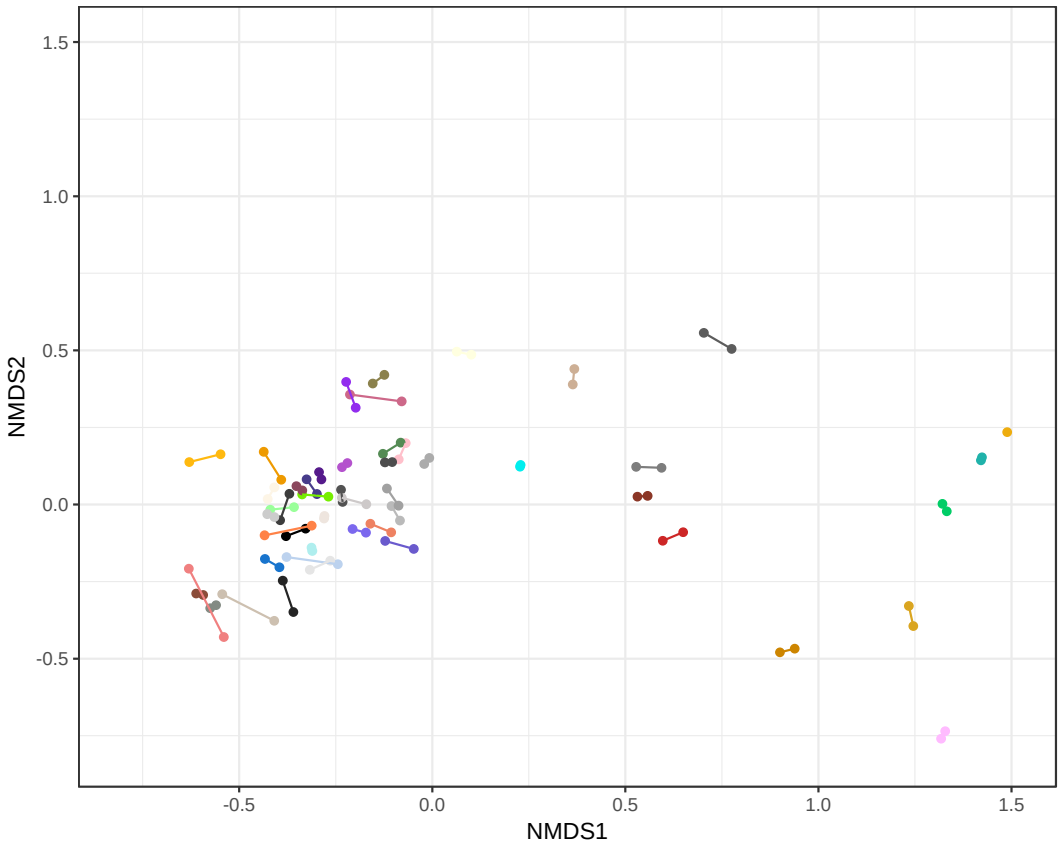

Appendix C1, Figure 1. A non-metric multidimensional scaling (NDMS) plot for the ordination of distance between duplicates PCR of amplicons sequenced using next-generation sequencing. Each duplicate is a unique color and connected with a line. Duplicates are closer to each other in ordination space than other duplicates, particularly along the first axis. Additionally, for each pair of duplicates, a Wilcoxon sum signed-rank test was conducted to ensure duplicate relative abundances came from the same distribution ($P > 0.05$).

Appendix C3. Calculation of % parasitemia

(i) Plasmid construction

To prepare a template for the standard curve, a 178 bp region of the V4 hypervariable 18S ribosomal RNA fragment of *Theileria orientalis* was amplified using the forward (5'–GAC TTT GGT TCT ATT TTG TTG GA–3') and the reverse RLBR (5'–TCT TCG ATC CCC TAA CTT TC–3') oligonucleotide primers. The forward primer is the reverse complement of the reverse primer originally described by Sibeko et al. (2008) whereas the reverse primer was designed by Gubbels et al. (1999). The reagents and PCR conditions were optimised in a series of experiments; the final PCR was conducted in a 25 µL volume containing 10 mM Tris-HCl (pH 8.4), 50 mM KCl (Promega, Madison, WI, USA), 3.5 mM $MgCl_2$, deoxynucleotide triphosphates (dNTPs; 200 µM each), primers (50 pmol each) and 1 U Go*Taq* polymerase (Promega) using the following protocol: 5 min at 95°C, followed by 35 cycles of 30 s at 95°C, 20 s at 60°C and 1 min at 72°C, followed by a final extension of 5 min at 72°C. PCR products were run on 3% (w/v) agarose gel-purified using the QIAquick Gel Extraction kit (Qiagen) and cloned into the pGEM®-T Easy Vector System (Promega) as per manufacturer's instructions. Plasmid DNA was purified from transformed cells (JM109 competent cells, Promega) using Wizard® Plus SV Minipreps (Promega), quantified by spectrophotometer (Nanodrop 3000?) at 260 nm wavelength, and then subjected to bi-directional, automated Sanger sequencing using the same primers used in PCR. The quality of the sequences was assessed using the program Geneious Pro 2.0.10 (Kearse et al., 2012) and the specificity was confirmed with previously published 18S sequences of *T. orientalis*.

Molecular conversion calculations, based on size and base composition of the DNA fragment, were used to estimate the DNA copy number in each plasmid solution. A 10-fold serial dilution in molecular grade water ($1x10^8$ copy number per reaction – $1x10^1$ copy number per reaction) was created for use as the standard curve.

(ii) qPCR validation

Reagents and conditions of the qPCR were optimised in a series of experiments. The final qPCR was conducted in 20 µL volume containing 10 µL of Dye Based Master Mix (Promega, Australia), 1 µL of each primer (10 pmol), 4 µL ddH_20 and 4 µL of

DNA template using the following conditions: 5 min at 95 °C, followed by 40 cycles of 30 s at 95 °C, 30 s at 58 °C, 20 s at 72 °C, followed by a final extension of 5 min at 72 °C. Amplicon melt analysis was performed using temperature ramps of 0.3 °C between 70 and 99 °C. Each plasmid DNA dilution was run in triplicate and samples were run in duplicates. All reactions were prepared using the QIAgility (Qiagen) automated PCR setup system. qPCR reactions were run using a Rotor-gene Q (Qiagen) thermocycler. A positive (*T. orientalis*) and no-template controls were included in each assay. The specificity of the assay was based on the analyses of the conventional and normalised high resolution melt (HRM) curves of amplicons derived from the positive control samples, and *Theileria* was assigned in test samples based on mean HRM temperature. Selected qPCR products were cloned using methods as above and sequenced.

The analytical sensitivity was determined using a 10-fold serial dilution of plasmids whereas the analytical specificity was assessed using DNAs of *T. orientalis, T. velifera, T. mutans, Babesia bovis, B. bigemina, Anaplasma marginale, A. centrale, A. platys and Ehrlichia canis*. Assay repeatability was confirmed by running each standard curve in triplicate across three separate qPCR reactions over two days. Inter-assay variability was determined by comparing amplification efficiency (efficiency = $-1 + 10^{(-1/\text{slope})}$, the slope is of the log-linear relationship between DNA copy number and the cycle threshold (C_T) values) and correlation coefficient (R^2) across plates. Additionally, for each plate, the mean C_T value was calculated for each dilution. The coefficient of variation (CV: standard deviation/mean) of mean C_T value per standard curve dilution was calculated across plates. Intra-assay variability was assessed by calculating the CV of C_T values for each dilution within each plate.

(iii) qPCR validation results

The identity of individual products was confirmed by sequencing, and no product was amplified when the DNA template was used from *A. marginale, A. centrale, A. platys* or *E. canis*. When comparing across plates, for *T. orientalis*, mean amplification efficiency was 0.93±0.02, mean R^2 was 0.987±0.005 and mean CV was 8.81±0.49 (range 5.47-16.13). Intra-assay CV values for *T. orientalis* ranged from 0.0017-0.0218 with a mean of 0.0112 (SE±0.0003).

(iv) Calculation of parasitaemia

We calculated % parasitaemia (parasitaemia, hereafter) from the qPCR result by following a method previously described by Pienaar et al. (2011). Volume of whole blood used in the qPCR assay was calculated by multiplying the proportion of DNA extract used in the assay by volume of whole blood used in the DNA extraction. Subsequently, the number of red blood cells in each reaction was then calculated by multiplying volume (number of microliters) of whole blood used in each reaction by the number of red blood cells per microliter. As the 18S gene of *Theileria* is believed to have two copies per genome (Gardner et al., 2005; Pain et al., 2005; Hayashida et al., 2012), copy number per sample (calculated from mean of duplicates) was divided by two to obtain the number of parasites per reaction. Parasites in each qPCR reaction per sample was divided by red blood cells per reaction and multiplied by 100 to obtain % parasitemia (i.e. parasitemia).

(v) Parasitaemia summary statistics

Following the establishment of qPCR assay, a total of 440 (out of 443) samples were successfully amplified, and the cloning and sequencing of selected qPCR amplicons confirmed their identity as *Theileria* spp. Parasitaemia ranged from 0.001% - 1.151%; mean parasitemia was 0.126% (SE ± 0.008).

References

Gardner, M. J., Bishop, R., Shah, T., de Villiers, E. P., Carlton, J. M., Hall, N., Ren, Q., Paulsen, I. T., Pain, A., Berriman, M., Wilson, R. J., Sato, S., Ralph, S. A., Mann, D. J., Xiong, Z., Shallom, S. J., Weidman, J., Jiang, L., Lynn, J., Weaver, B., … Nene, V. (2005). Genome sequence of Theileria parva, a bovine pathogen that transforms lymphocytes. Science (New York, N.Y.), 309(5731), 134–137. https://doi.org/10.1126/science.1110439

Gubbels, J. M., de Vos, A. P., van der Weide, M., Viseras, J., Schouls, L. M., de Vries, E., … Jongejan, F. (1999). Simultaneous detection of bovine *Theileria* and *Babesia* species by reverse line blot hybrdization. *Journal of Clinical Microbiology*, 37(6), 1782– 1789.

Hayashida, K., Hara, Y., Abe, T., Yamasaki, C., Toyoda, A., Kosuge, T., Suzuki, Y., Sato, Y., Kawashima, S., Katayama, T., Wakaguri, H., Inoue, N., Homma, K., Tada-Umezaki, M., Yagi, Y., Fujii, Y., Habara, T., Kanehisa, M., Watanabe, H., Ito, K., … Sugimoto, C. (2012). Comparative genome analysis of three eukaryotic parasites with differing abilities to transform leukocytes reveals key mediators of Theileria-induced leukocyte transformation. mBio, 3(5), e00204–e212. https://doi.org/10.1128/mBio.00204-12

Kearse, M., Moir, R., Wilson, A., Stones-Havas, S., Cheung, M., Sturrock, S., Buxton, S., Cooper, A., Markowitz, S., Duran, C., Thierer, T., Ashton, B., Meintjes, P., & Drummond, A. (2012). Geneious Basic: an integrated and extendable desktop software platform for the organization and analysis of sequence data. Bioinformatics (Oxford, England), 28(12), 1647–1649. https://doi.org/10.1093/bioinformatics/bts199

Pain, A., Renauld, H., Berriman, M., Murphy, L., Yeats, C. A., Weir, W., Kerhornou, A., Aslett, M., Bishop, R., Bouchier, C., Cochet, M., Coulson, R. M., Cronin, A., de Villiers, E. P., Fraser, A., Fosker, N., Gardner, M., Goble, A., Griffiths-Jones, S., Harris, D. E., … Hall, N. (2005). Genome of the host-cell transforming parasite Theileria annulata compared with T. parva. Science (New York, N.Y.), 309(5731), 131–133. https://doi.org/10.1126/science.1110418

Pienaar, R., Potgieter, F. T., Latif, A. A., Thekisoe, O. M. M., & Mans, B. J. (2011). Mixed *Theileria* infections in free-ranging buffalo herds: Implications for diagnosing *Theileria parva* infections in Cape buffalo (*Syncerus caffer*). *Parasitology*, 138(07), 884– 895.

Sibeko, K. P., Oosthuizen, M. C., Collins, N. E., Geysen, D., Rambritch, N. E., Latif, A. A., Groeneveld, H. T., Potgieter, F. T., & Coetzer, J. A. (2008). Development and evaluation of a real-time polymerase chain reaction test for the detection of Theileria parva infections in Cape buffalo (Syncerus caffer) and cattle. Veterinary parasitology, 155(1-2), 37–48. https://doi.org/10.1016/j.vetpar.2008.03.033

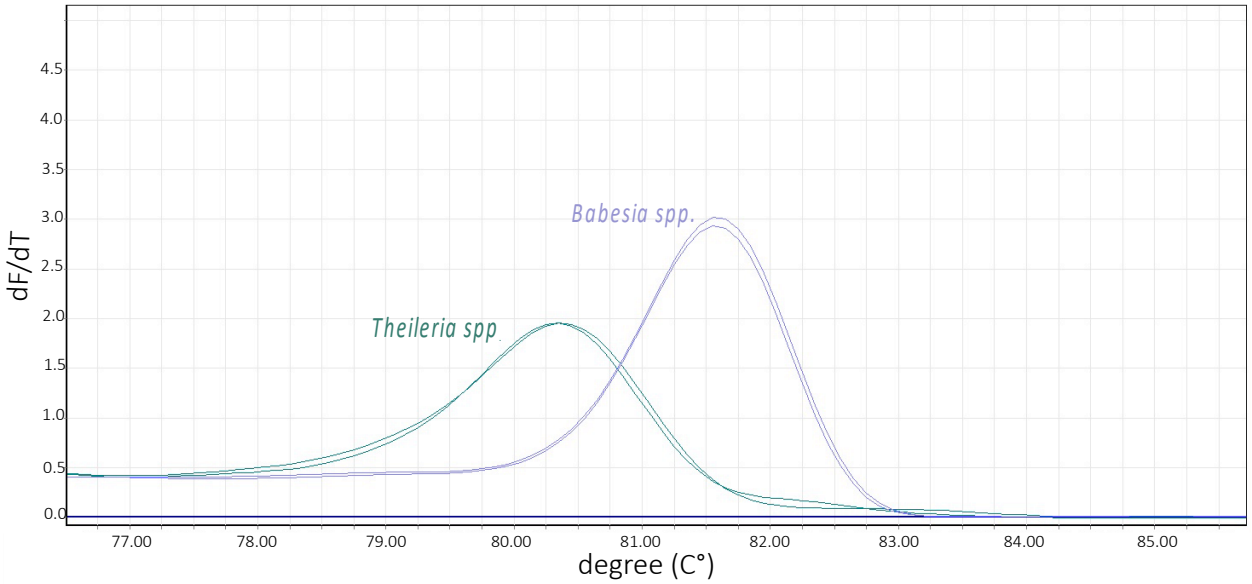

Appendix C3, Figure 1. qPCR melt curves for *Theileria* spp. and *Babesia* spp. positive controls

Table C1. Pairwise distances (number of base pairs) between each unique sequence; sequences are grouped by taxa.

	1	2	3	4	5	6	7	8	9	10	11	12	13	14	15	16	17	18	19	20	21	22	23	24	25	26	27	28	29
1.MK792977		1	2	15	18	18	23	21	22	18	20	19	22	21	51	52	52	50	52	54	54	53	53	54	54	56	53	56	57
2.MK792978	1		1	16	19	19	24	22	23	19	19	18	23	20	51	52	52	50	52	54	54	53	53	54	54	57	54	57	58
3.MK792985	2	1		15	18	18	23	21	22	18	20	19	24	21	50	51	51	49	51	53	53	52	52	53	53	56	53	56	57
4.MK792976	15	16	15		10	10	14	12	13	12	16	17	19	16	43	44	44	42	44	43	43	40	40	41	41	49	45	49	50
5.MK792968	18	19	18	10		2	12	11	11	15	20	21	25	20	47	48	46	46	48	49	49	46	46	47	47	49	45	49	50
6.MK792992	18	19	18	10	2		13	11	12	17	20	21	25	20	47	48	46	46	48	49	49	46	46	47	47	47	43	47	48
7.MK792972	23	24	23	14	12	13		2	1	13	17	18	21	17	48	48	47	47	49	48	48	47	47	48	48	54	50	54	55
8.MK792973	21	22	21	12	11	11	2		1	12	15	16	19	15	46	46	45	45	47	47	47	46	46	47	47	53	49	53	54
9.MK792975	22	23	22	13	11	12	1	1		12	16	17	20	16	47	47	46	46	48	48	48	47	47	48	48	54	50	54	55
10.MK792986	18	19	18	12	15	17	13	12	12		18	19	20	18	49	50	50	48	50	50	50	49	49	50	50	57	54	57	58
11.MK792970	20	19	20	16	20	20	17	15	16	18		1	8	1	47	48	48	46	48	47	47	46	46	47	47	52	50	53	54
12.MK792980	19	18	19	17	21	21	18	16	17	19	1		9	2	48	49	49	47	49	48	48	47	47	48	48	53	51	54	55
13.MK792990	22	23	24	19	25	25	21	19	20	20	8	9		9	46	47	47	45	47	46	46	45	45	46	46	55	53	56	57
14.MK792994	21	20	21	16	20	20	17	15	16	18	1	2	9		47	48	48	46	48	47	47	46	46	47	47	52	50	53	54
15.MK792969	51	51	50	43	47	47	48	46	47	49	47	48	46	47		1	1	1	1	9	9	11	10	10	12	44	40	44	45
16.MK792979	52	52	51	44	48	48	48	46	47	50	48	49	47	48	1		2	2	2	10	10	12	11	11	13	45	41	45	46

17.MK792982	52	52	51	44	46	46	47	45	46	50	48	49	47	48	1	2		2	2	10	10	12	11	11	13	44	40	44	45
18.MK792989	50	50	49	42	46	46	47	45	46	48	46	47	45	46	1	2	2		2	10	10	12	11	11	13	45	41	45	46
19.MK792991	52	52	51	44	48	48	49	47	48	50	48	49	47	48	1	2	2	2		10	10	12	11	11	13	45	41	45	46
20.MK792981	54	54	53	43	49	49	48	47	48	50	47	48	46	47	9	10	10	10	10		1	3	4	2	4	41	36	40	41
21.MK792988	54	54	53	43	49	49	48	47	48	50	47	48	46	47	9	10	10	10	10	1		3	4	2	4	41	36	40	41
22.MK792971	53	53	52	40	46	46	47	46	47	49	46	47	45	46	11	12	12	12	12	3	3		1	1	1	38	33	37	38
23.MK792983	53	53	52	40	46	46	47	46	47	49	46	47	45	46	10	11	11	11	11	4	4	1		2	2	38	33	37	38
24.MK792984	54	54	53	41	47	47	48	47	48	50	47	48	46	47	10	11	11	11	11	2	2	1	2		2	39	34	38	39
25.MK792993	54	54	53	41	47	47	48	47	48	50	47	48	46	47	12	13	13	13	13	4	4	1	2	2		38	33	37	38
26.MK792966	56	57	56	49	49	47	54	53	54	57	52	53	55	52	44	45	44	45	45	41	41	38	38	39	38		10	2	3
27.MK792987	53	54	53	45	45	43	50	49	50	54	50	51	53	50	40	41	40	41	41	36	36	33	33	34	33	10		8	8
28.MK792967	56	57	56	49	49	47	54	53	54	57	53	54	56	53	44	45	44	45	45	40	40	37	37	38	37	2	8		1
29.MK792974	57	58	57	50	50	48	55	54	55	58	54	55	57	54	45	46	45	46	46	41	41	38	38	39	38	3	8	1	

Table C2. Table of prevalence and frequency for each clade, subtype and unique (consensus) sequence

	Parasite				Parasite subtype					Consensus sequences				
clade	No. sample	Prevalence	No. reads	Frequency	subtype	No. samples	Prevalence	No. reads	Frequency	sequence	No. samples	Prevalence	No. reads	Frequency
T. mutans	435	0.989	14881605	0.455	T. mutans	226	0.514	1365312	0.042	MK792976	226	0.514	1365312	0.042
					T. mutans MSD	111	0.252	617170	0.019	MK792977	108	0.245	337939	0.01
										MK792978	87	0.198	228888	0.007
										MK792985	30	0.068	50343	0.002
					T. mutans-like 1	392	0.891	5600756	0.171	MK792992	4	0.009	4441	0
										MK792968	393	0.893	5596315	0.171
					T. mutans-like 2	387	0.880	2034428	0.062	MK792970	388	0.882	1941601	0.059
										MK792980	70	0.159	78515	0.002
										MK792990	7	0.016	8476	0
										MK792994	2	0.005	5836	0
					T. mutans-like 3	375	0.852	5236552	0.16	MK792972	374	0.850	2381203	0.073
										MK792973	371	0.843	2012109	0.061
										MK792975	262	0.595	843240	0.026
					T. mutans-like undefined	20	0.045	27387	0.001	MK792986	20	0.045	27387	0.001
T. taurotragi	410	0.932	7870959	0.24	T. parva	379	0.861	2146789	0.066	MK792971	379	0.861	1991976	0.061
										MK792983	61	0.139	92841	0.003
										MK792984	41	0.093	58853	0.002
										MK792993	4	0.009	3119	0
					T. sp. bougasvlei	387	0.880	5320496	0.163	MK792969	388	0.882	5062700	0.155
										MK792979	72	0.164	120269	0.004

										MK792982	63	0.143	113107	0.003
										MK792989	8	0.018	16811	0.001
										MK792991	7	0.016	7609	0
					T. sp. buffalo	68	0.155	403674	0.012	MK792981	69	0.157	371345	0.011
										MK792988	12	0.027	32329	0.001
T. velifera	439	0.998	9974935	0.305	T. velifera	438	0.995	3541422	0.108	MK792966	439	0.998	3541422	0.108
					T. velifera B	416	0.945	6367970	0.195	MK792967	401	0.911	3311741	0.101
										MK792974	300	0.682	3056229	0.093
					T. velifera-like undefined	11	0.025	65543	0.002	MK792987	11	0.025	65543	0.002

APPENDIX D – CHAPTER 5 SUPPLEMENTARY TEXT, TABLES AND FIGURES

Appendix D1. Description of basis-spline approach to modeling non-linear compositional data with repeated measures

The statistical modeling in this paper includes three components as follows. First, we use Dirichlet-multinomial distribution to model the abundance of parasite subtypes to account for the compositional and discrete nature of the count data (Holmes et al. 2012; Chen and Li 2013; Tang and Chen 2018). The Dirichlet-multinomial distribution is able to include the extra variation of the abundance data, which is called over-dispersion, that cannot be captured by the multinomial distribution. Second, we link the logarithm of each parameter in the Dirichlet-multinomial distribution to the longitudinal covariate, the age of the animal at the capture time, through a smooth function of the covariate. This model represents the longitudinal trajectory of the abundance of each parasite subtype by an individual smooth function. Third, we use B-spline functions to approximate the above-mentioned smooth functions for the longitudinal trajectories (Zhu and Qu 2018; Duan and Jiang 2020). A B-spline function is a linear combination of known basis functions that are piecewise polynomial functions (De Boor 1978), in which the coefficients of the basis functions are regarded as the unknown parameters in our statistical model.

Traditionally, one can use the maximum likelihood principle to obtain the estimated values of the unknown parameters, the coefficients of the B-spline basis functions. If the observed data are assumed to be independent, then the log-likelihood function is simply the sum of the log-likelihood functions of each data point. However, since the parasite abundance is measured at different capture time on the same animal, there exist potential correlations between these longitudinal measurements. Unfortunately, it is statistically challenging to specify the full joint distribution of these correlated observations. Therefore, instead of incorporating these correlations into a statistical model, we propose to use the weighted log-likelihood function of our statistical model to approximate the joint log-likelihood function. In particular, the optimal weights depend on how strongly an observation is correlated with the rest of the observations and can be numerically

identified with the approach in Ostrovnaya and Nicolae (2012). Finally, we compute the estimated values of the unknown parameters in our model by maximizing the B-spline objective function, the sum of the weighted log-likelihood function and a penalty function on the B-spline coefficients that controls the smoothness of the B-spline functions (Zhu and Qu 2018; Duan and Jiang 2020).

After we obtain the B-spline coefficients and thus the fitted longitudinal curves of relative abundances, we can determine a number of point estimates indicative of different life history strategies for each subtype of parasites, including the age of first infection, the maximum relative abundance, the age at the maximum relative abundance, the relative abundance that becomes stable (equilibrium), and the age when the relative abundance becomes stable (equilibrium). In particular, the age of first infection is defined to be the age at which the relative abundance exceeds 0.01 for the first time. The age when the relative abundance becomes stable is theoretically defined to be when the slope of the fitted longitudinal curve becomes zero. However, the slope of the fitted curve can never be exactly zero numerically. Thus, we set a small positive constant (is set to be 0.004 in our analysis) and find all time points where the slope of the fitted curve is smaller than. For each time point where the slope of the fitted curve is smaller than, we also check the slope of the fitted curve at its following time points (is set to be 2000 in our analysis). The time point that has the largest number of time points with slope smaller than within its following time points is defined to be the age when the relative abundance becomes stable.

In addition, to evaluate the goodness of fit, we use a likelihood ratio test to compare the fitted model with the saturated model. The saturated model denotes the model that "perfectly" fits the data; in this case, the saturated model is reduced to the observation-specific multinomial distribution whose parameters, i.e., the multinomial probabilities, are estimated by the relative abundances of the parasite subtypes at each observation (at each capture time for each animal). If our model fits the data nearly as well as the saturated model, the likelihood ratio test statistic, defined to be twice the difference of the log-likelihoods between the fitted model and the saturated model, follows asymptotically a chi-squared distribution with degree of freedoms equal to the difference of the numbers

of parameters between these two models. A goodness of fit p-value is obtained by comparing the observed value of the test statistic with its reference distribution. The larger the p-value is, the better our model fits the data.

References

Holmes, I., Harris, K., and Quince, C. (2012). Dirichlet multinomial mixtures: Generative models for microbial metagenomics. PLoS One 7, e30126.

Chen, J., and Li, H. (2013). Variable selection for sparse Dirichlet-multinomial 1693 regression with an application to microbiome data analysis. Ann. App. Stat. 7, 418–442.

Tang, Z.-Z., and Chen, G. (2018). Zero-inflated generalized Dirichlet multinomial 2019 regression model for microbiome compositional data analysis. Biostatistics, 20, 698–713.

Zhu, X., and Qu, A. (2018). Cluster analysis of longitudinal profiles with subgroups. Electronic Journal of Statistics, 12, 171–193.

De Boor, C. (1978). A practical guide to splines. Vol. 27. Springer-Verlag, New York.

Ostrovnaya, I., and Nicolae, D. L. (2012). Estimating the proportion of true null hypotheses under dependence. Statistica Sinica, 22, 1689–1716.

Duan, C., and Jiang, Y. (2020). Subgroup analysis of longitudinal profiles for compositional count data. Technical report.

Appendix D2. Principle component analysis describing white blood cell abundance and composition.

In our initial model linear mixed model describing the effect of host traits on *Theileria* distributions, we reduced dimensionality of white blood cell (wbc) variables, to avoid problems with overfitting, by using principle component analysis (PCA) to plot samples in white blood cell space and quantify white blood cell abundance and composition by extracting coordinates along PCA axis one and two. We used the first two PCA axes as this explained > 50% of variation in wbc composition (Figure 1). The first principle component described wbc abundance, with samples with higher wbc abundances located along the negative pole (Figure 1). The second principle component described wbc composition (Figure 1). We conducted all analyses in R (v 3.6.3). We conducted the PCA in base R, extracted PCA coordinates using *ggfortify* (Tang, Horikoshi & Li 2016).

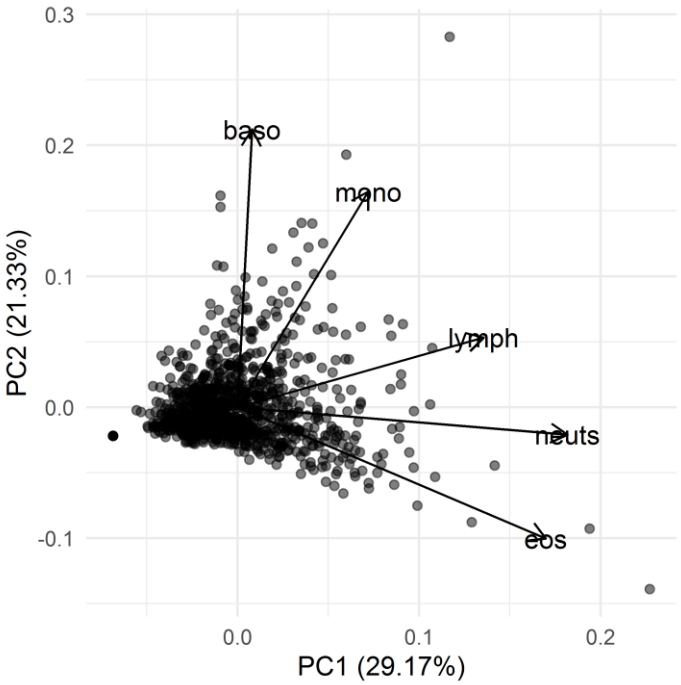

Appendix D2, figure 1. Principle component analysis of white blood cell composition.

References

R Core Team (2020). R: A language and environment for statistical computing. R Foundation for
Statistical Computing, Vienna, Austria. URL https://www.R-project.org/.

Tang, Y., Horikoshi,M., Wenxuan, L. (2016) ggfortify: Unified Interface to Visualize Sta tistical Result of Popular R Packages. *The R Journal* 8.2 : 478-489.

Appendix D3. SNP assembly (from *Tavalire* et al., 2019)

SNP genotyping and filtering

We extracted 100-200ng/ml genomic DNA from dried ear tissue samples (DNeasy blood & tissue kit, Qiagen) and prepared individual libraries for sequencing using type IIB restriction associated DNA (2bRAD) methods, detailed in Wang et al. (2012). Briefly, this method uses a type IIB restriction endonuclease (Alf1; Thermo Scientific #ER1801) to extract thousands of36bp reads from across the genome. After quality filtering, we used SHRiMP (Rumble et al. 2009) to map each individual to the de novo assembly of AlfI sites, and we filtered the resultingmatches for statistically weak or ambiguous alignments following parameters described by the software authors. We determined genotypes at each AlfI site with > 5x coverage, then filtered out monomorphic loci. We allowed for 10% missing data at any given locus and one polymorphism per tag. Animals that were genotyped at 33% or fewer (< 11800) loci were removed from the dataset. The analysis pipeline outlined above was developed by Eli Meyer (available at https://github.com/Eli-Meyer). Markers were discarded if they violated Hardy Weinberg Equilibrium ($p < 0.0001$) or had a minor allele frequency less than 10%. Ultimately, filtering yielded samples genotyped at 2505 SNPs. 2505 SNPs we used to create the relatedness matrix whereas 974 SNPs were used for the GWAS study.

References

Wang, S., Meyer, E., McKay, J. K., & Matz, M. V. (2012). 2b-RAD: a simple and flexible method for genome-wide genotyping. *Nature methods*, *9*(8), 808–810. https://doi.org/10.1038/nmeth.2023

Appendix D4. Characterizing a *Theileria* interaction network.
Caroline Glidden & Canan Karakoç

METHODS: Quantifying a Theileria subtype interaction network

To test for signatures of *Theileria* interactions, we used empirical dynamic modelling tools as described below. We included all center-log-transformed read counts of all subtypes detected except for *T. mutans*-like (undescribed) and *T. velifera*-like (undescribed) as infection by these subtypes is rare in this population (Figure 1, Glidden et al., 2019). We tested for causal interactions between pairs of subtypes using convergent cross mapping (CCM), which detects information transfer from one variable to another using nonparametric state space reconstruction (Takens 1981; Sugihara et al., 2012; Clark et al., 2015). Since stable estimates from CCM typically require a time series of at least 30 sequential observations, we pooled time series across captured animals to fill in the state space manifold (Hsieh et al., 2008, Clark et al., 2015). For the initial network, we pooled all animals. We initially assumed this was possible, since we have similar trajectories of subtypes across animals (Figure 1). However, after observing distinct life histories for each subtypes, which indicates that trajectories change based on animal age class, we created to additional networks using observations from animals < 2 years (subadults, age before equilibrium, chapter 5) and > 2 years old (adults, age after equilibrium, chapter 5).

Embedding dimension (E, time-lags used for state space reconstruction) was chosen using simplex projection which tests the ability of variables to predict their own dynamics through "leave-one-out cross-validation". We chose E as the smallest dimension that is within 1% of the best predictive value across the dimensions tested, and maximum E is limited to square root of the time series length (Sugihara & May 1990; Sugihara et al., 2012; Clark et al., 2015; Ye et al., 2015). For the network using all animal and adult animals, as our time series for each buffalo for was ≤10, we chose a maximum embedding dimension of four (~√10, Cheng & Tong 1992). For the network using subadult animals, as our time series for each buffalo for was ≤8, we chose a maximum embedding dimension of three (~√8, Cheng & Tong 1992).

We used mean absolute error (MAE) to test predictive ability. In order to detect interactions with the time lagged effects, we applied CCM with varying prediction lags (-

1 to 0). Significance of results were determined using nonparametric bootstrapping by sampling from the observations with replacement and recalculating statistics for 10,000 iterations. In cases where CCM identified significant causal interactions, we computed a series of Jacobian-like matrices to determine the direction and strength of species interactions in each time-step using S-mapping, which is a locally weighted multivariate linear regression method in state-space (Deyle et al., 2016). Variables for S-mapping were selected based on the number of E of each target variable. If the number of E was larger than the number of variables causing the target variable, predictor variables were complemented with the time-lagged observations of the target variables. Nonlinearity parameter (θ) for S-mapping was defined based on univariate predictive ability (Sugihara & May 1990). For the network with all animals and adult animals, due to allowing an embedding dimension of 4, we removed animals with less than four time steps from our analysis ($N_{\text{all animals}} = 481$, $N_{\text{adult animals}} = 335$). For the network with subadult animals, due to allowing an embedding dimension of 3, we removed animals with less than four time steps from our analysis ($N_{\text{subadults}} = 136$). We performed empirical dynamical modeling using the R package *rEDM* (Ye et al., 2019) and *EDMhelper* (Karakoç & Clark 2020) in R (version 3.6.1). We visualized out networks using *igraph* (Csardi & Nepusz).

Results & Discussion: Networks are heterogeneous between age classes

Our empirical dynamical modeling analysis included 90 pairwise associations between *Theileria* subtypes. When analyzing the interaction network using all animals, of those 90 subtype-subtype pairs, we detected nine significant interactions, with five mean (of the smap-coefficient, across samples) interactions positive and four mean interactions negative (Table 1, Figure 2). When analyzing the interaction network using only subadult animals, we detected 22 significant interactions, with 6 interactions positive, on average, and 14 interactions negative, on average (Table 3, Figure 3A). In contrast, when analyzing the interaction network using only adult animals, we detected 6 significant interactions, with 2 mean interactions positive and four mean interactions negative (Table 2, Figure 3B). Notably, the subtypes interacting and direction of interactions changed across age classes. Interactions occurred across taxonomic groups in subadults but were primarily limited to the *T. mutans* clade in adults. Our initial interaction network

indicates our interaction networks in young animals are characterized by many, strong interactions and interaction networks in adult animals, when relative abundances of each subtype reach an equilibrium-like state, are characterized by few, weak interactions. Consistent with our competition-colonization trade-off indicated in this manuscript, late-persistent subtypes (*T. mutans*-like 1-3) cause a decrease in abundance, relative to the sample mean, in early-ephemeral subtypes (*T. mutans*, *T. mutans* MSD) (Figure 3, Table 2, Table 3). However, in young animals, early-ephemeral subtypes interact with many other subtypes indicating that their final clearance from the host is quite complex and perhaps the result of additive or higher-order interactions. Future work could use higher sample sizes for each age-class (50 animals, ~10 animals per sample: Clark et al., 2015) to more definitively describe these networks. With more data, we may also be able to use emperical dynamical modeling to evaluate how *Theileria* center-log-transformed read counts and network properties (mean interaction strength, pairwise interaction strength) relate to assemblage stability (e.g., Ushio et al., 2018) and animal health, thereby, evaluating if the assemblage dynamics we observed in this paper are indeed conducive to host health and survival.

Diagnostic plots for each network are presented in Figure 4 (all animals), Figure 5 (subadult animals), and Figure 6 (adult animals).

References

Cheng, B., & Tong, H. (1992). On Consistent Nonparametric Order Determination and Chaos. *Journal of the Royal Statistical Society. Series B (Methodological)*, *54*(2), 427–449.

Clark, A. T., Ye, H., Isbell, F., Deyle, E. R., Cowles, J., Tilman, G. D., & Sugihara, G. (2015). Spatial convergent cross mapping to detect causal relationships from short time series. *Ecology*, *96*(5), 1174–1181. https://doi.org/10.1890/14-1479.1

Deyle, E. R., May, R. M., Munch, S. B., & Sugihara, G. (2016). Tracking and forecasting ecosystem interactions in real time. *Proceedings of the Royal Society B: Biological Sciences*, *283*(1822), 20152258. https://doi.org/10.1098/rspb.2015.2258

Glidden, C. K., Koehler, A. V., Hall, R. S., Saeed, M. A., Coppo, M., Beechler, B. R., … Jabbar, A. (2019). Elucidating cryptic dynamics of Theileria communities in African buffalo using a high-throughput sequencing informatics approach. *Ecology and Evolution*, *10*(1), 70–80. https://doi.org/10.1002/ece3.5758

Hsieh, C., Anderson, C., & Sugihara, G. (2008). Extending nonlinear analysis to short ecological time series. *The American Naturalist*, *171*(1), 71–80. https://doi.org/10.1086/524202

Karakoç, C. & Clark, A.T.. (2020, February 24). EDMhelper: A collection of tools for the EDM routines (Version v1.0). Zenodo.

Sugihara, G., & May, R. M. (1990). Nonlinear forecasting as a way of distinguishing chaos from measurement error in time series. *Nature*, *344*(6268), 734–741. https://doi.org/10.1038/344734a0

Sugihara, G., May, R., Ye, H., Hsieh, C., Deyle, E., Fogarty, M., & Munch, S. (2012). Detecting Causality in Complex Ecosystems. *Science*, *338*(6106), 496 LP – 500. https://doi.org/10.1126/science.1227079

Takens F. (1981) Detecting strange attractors in turbulence. In: Rand D., Young LS. (eds) Dynamical Systems and Turbulence, Warwick 1980. Lecture Notes in Mathematics, vol 898. Springer, Berlin, Heidelberg

Ushio, M., Hsieh, C.-H., Masuda, R., Deyle, E. R., Ye, H., Chang, C.-W., … Kondoh, M. (2018). Fluctuating interaction network and time-varying stability of a natural fish community. *Nature*, *554*(7692), 360–363. https://doi.org/10.1038/nature25504

Ye, H., Beamish, R. J., Glaser, S. M., Grant, S. C. H., Hsieh, C., Richards, L. J., … Sugihara, G. (2015). Equation-free mechanistic ecosystem forecasting using empirical dynamic modeling. *Proceedings of the National Academy of Sciences*, *112*(13), E1569 LP-E1576. https://doi.org/10.1073/pnas.1417063112

Ye, H., Clark,A., Deyle, E., Munch,S., Cai,J.,Cowles,J., et al. (2018).rEDM: Applications of Empirical Dynamic Modeling from Time Series. R package version 0.7.1.

Appendix D4, Table 1. Mean interaction pairwise strength (average smap-coefficient) throughout the study for the interaction network with all animals. Interactions highlighted in dark grey were significant (p value <0.05) while interactions highlighted in light grey are marginally significant (p value < 0.1 & > 0.05). Row causes (→) column.

row → column	Tm	Tm1	Tm2	Tm3	TmMSD	Tp	TBf	TBg	Tv	TvB
T. mutans	0.00	-0.06	-0.10	-0.08	0.05	-0.15	-0.03	-0.04	0.00	-0.06
T. mutans-like 1	-0.45	0.00	0.32	0.32	-0.40	0.10	-0.07	0.04	-0.04	-0.12
T. mutans-like 2	-0.38	0.09	0.00	0.36	-0.21	0.18	-0.02	0.08	-0.05	-0.04
T. mutans-like 3	-0.28	0.01	0.31	0.00	-0.02	0.16	0.06	0.04	-0.05	-0.12
T. mutans MSD	0.27	0.00	-0.12	-0.18	0.00	-0.17	-0.04	-0.08	0.01	-0.32
T. parva	-0.23	0.04	0.00	0.01	-0.27	0.00	-0.05	0.20	-0.04	0.00
T. sp. (buffalo)	-0.15	-0.04	-0.04	-0.07	0.05	-0.04	0.00	-0.06	-0.02	-0.10
T. sp. (bougasvlei)	-0.24	0.01	0.01	-0.05	-0.26	0.25	-0.23	0.00	-0.03	0.18
T. velifera	-0.04	0.02	-0.33	-0.23	-0.17	-0.07	-0.19	0.10	0.00	-0.35
T. velifera B	0.02	-0.07	-0.13	-0.12	-0.03	0.00	-0.15	0.03	0.11	0.00

Appendix D4, Table 2. Mean interaction pairwise strength (average smap-coefficient) throughout the study for the interaction network with only subadult animals (< 2 years). Interactions highlighted in dark grey were significant (p value <0.05) while interactions highlighted in light grey are marginally significant (p value < 0.1 & > 0.05). Row causes (→) column.

row → column	Tm	Tm1	Tm2	Tm3	TmMSD	Tp	TBf	TBg	Tv	TvB
T. mutans	0.00	-0.21	-0.99	-0.21	1.67	-0.24	-0.01	-0.21	0.13	0.04
T. mutans-like 1	-0.34	0.00	0.52	0.42	-1.51	0.06	-0.02	0.00	-0.07	-0.10
T. mutans-like 2	-0.17	-0.01	0.00	0.26	-0.34	-0.08	-0.07	-0.08	-0.09	-0.06
T. mutans-like 3	-0.21	0.20	0.65	0.00	-0.73	0.09	-0.03	0.02	-0.04	-0.10
T. mutans MSD	0.07	-0.18	-0.81	-0.19	0.00	-0.18	-0.07	-0.18	0.03	0.03
T. parva	-0.12	0.10	-1.08	-0.03	0.53	0.00	0.01	0.28	-0.02	-0.04
T. sp. (buffalo)	-0.11	-0.20	-1.26	-0.41	0.93	0.02	0.00	-0.03	0.18	0.04
T. sp. (bougasvlei)	-0.39	0.02	-0.50	0.03	-0.84	0.34	0.06	0.00	-0.07	-0.06
T. velifera	0.10	-0.49	-0.91	-0.28	1.28	0.005	0.27	-0.43	0.00	-0.28
T. velifera B	0.56	-0.56	-1.02	-0.59	1.66	-0.08	0.12	-0.23	0.50	0.00

Appendix D4, Table 3. Mean interaction pairwise strength (average smap-coefficient) throughout the study for the interaction network with only adult animals (> 2 years). Interactions highlighted in dark grey were significant (p value <0.05) while interactions highlighted in light grey are marginally significant (p value < 0.1 & > 0.05). Row causes (→) column.

row → column	Tm	Tm1	Tm2	Tm3	TmMSD	Tp	TBf	TBg	Tv	TvB
T. mutans	0.00	-0.04	-0.04	-0.06	0.04	-0.22	-0.31	-0.03	-0.05	-0.11
T. mutans-like 1	-0.37	0.00	-0.09	0.99	-0.29	0.06	-0.73	-0.10	0.45	-0.26
T. mutans-like 2	-1.22	-0.03	0.00	0.18	-0.25	0.16	-0.73	-0.04	0.43	-0.07
T. mutans-like 3	-0.78	0.53	0.42	0.00	-0.19	0.16	-0.26	-0.14	0.19	-0.23
T. mutans MSD	0.24	-0.10	-0.07	0.04	0.00	-0.27	-0.22	-0.13	-0.09	-0.45
T. parva	-0.33	0.02	0.01	0.14	-0.21	0.00	0.01	0.09	-0.02	-0.04
T. sp. (buffalo)	-0.18	-0.02	-0.03	0.00	0.01	-0.15	0.00	-0.10	-0.04	-0.18
T. sp. (bougasvlei)	-0.22	-0.03	-0.03	0.08	-0.18	0.30	-0.77	0.00	0.04	0.19
T. velifera	-1.17	0.39	0.43	0.32	-0.23	-0.190	-0.95	0.15	0.00	0.60
T. velifera B	-0.19	-0.03	-0.04	0.06	-0.06	-0.05	-0.53	0.03	0.05	0.00

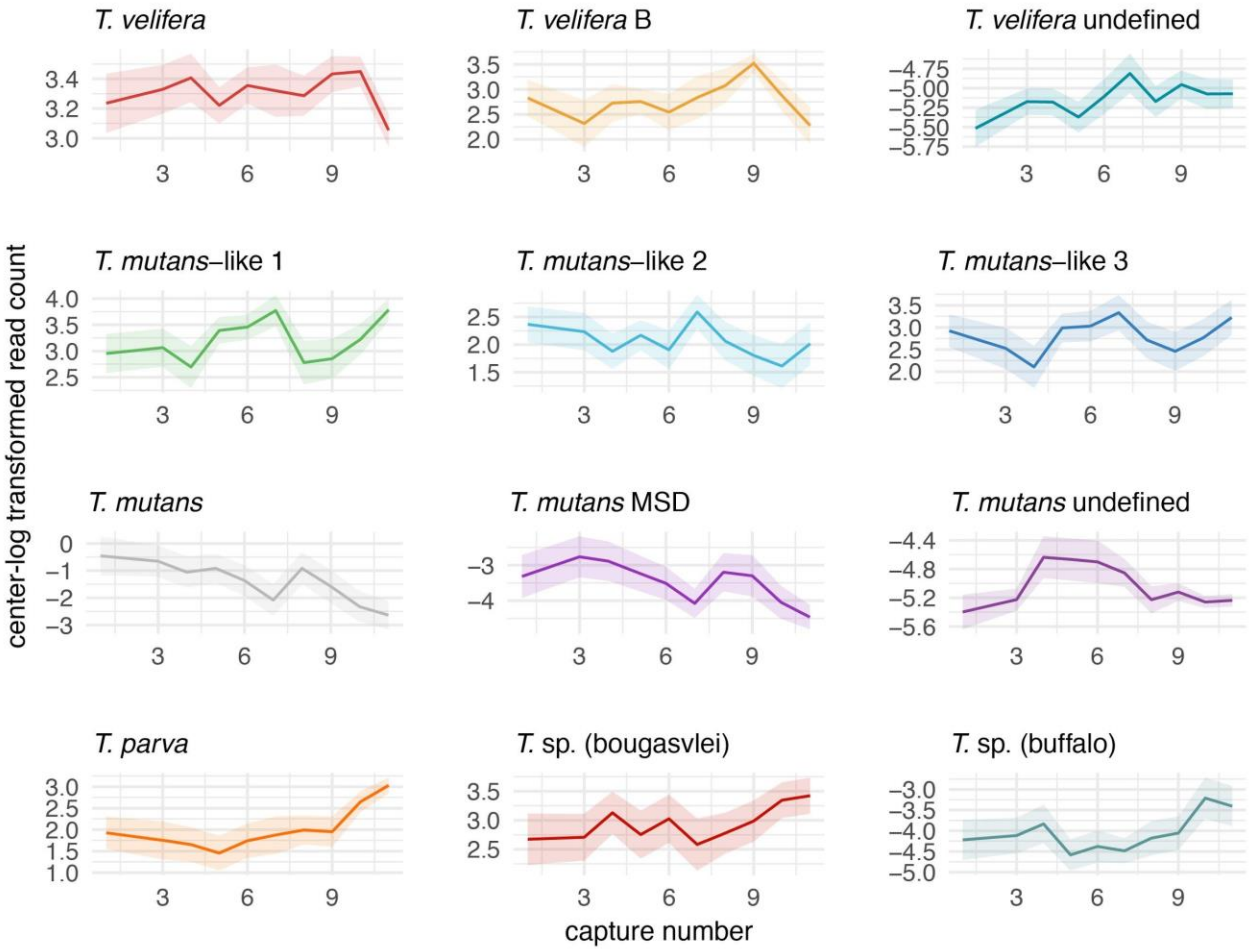

Appendix D4, Figure 1. Center-log transformed read counts by study capture number, averaged over the population for each capture. Shaded regions indicate standard error. Abundance, relative to the sample mean, of each subtype changes non-linearly over time.

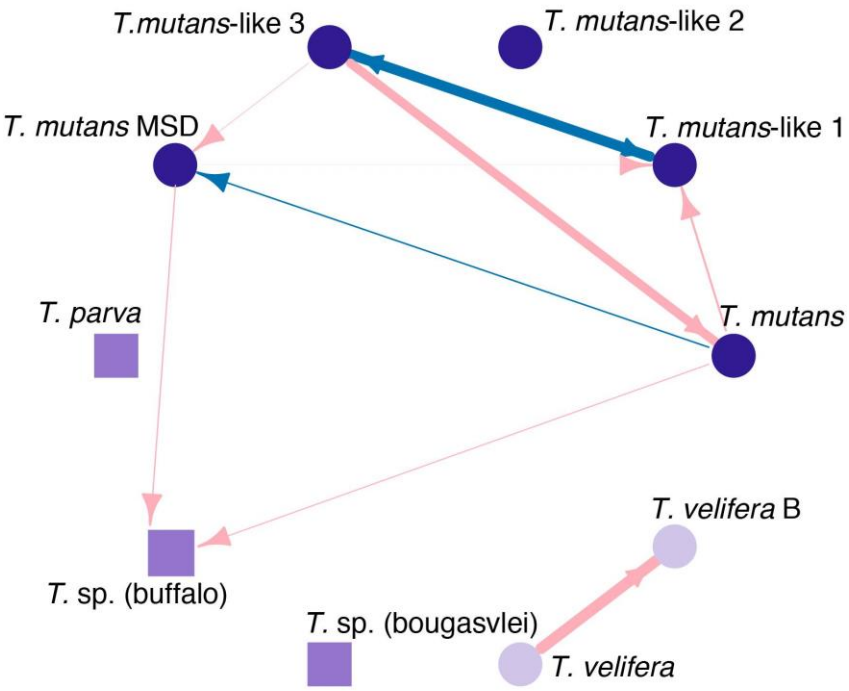

Appendix D4, Figure 2. *Theileria* interaction network when all animals are pooled. Significant interactions between *Theileria* subtypes, indicated by the empirical dynamic modeling analysis. Arrows indicate the direction of the interaction ($subtype_A \rightarrow subtype_B$ = $subtype_A$ causes $subtype_B$). Red arrows (light) indicate a negative interaction whereas blue arrows (dark) indicate a positive interaction. Arrows are weighted by average interaction strength (s-map coefficient averaged over all animals and all captures). Nodes represent each subtype (labeled) and hue indicates subtypes in the same species clade. Square nodes indicate subtypes that mainly replicate within white blood cells whereas circle nodes indicate subtypes that replicate within red blood cells. Interactions are typically limited to taxonomic groups.

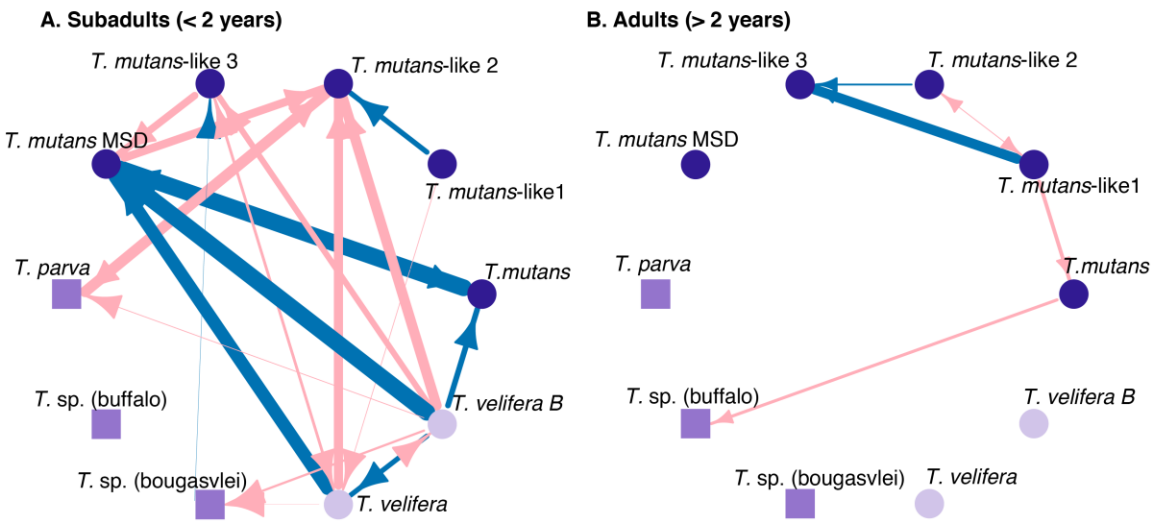

Appendix D4, Figure 3. *Theileria* interaction network for (A) animals < 2 years old and (B) animals > 2 years old. The interaction network for animals < 2 years old (before assemblage reaches an equilibrium-like point) is characterized by many interactions across taxonomic groups whereas the interaction network for animals > 2 years old is characterized by a few interactions primarily within the *T. mutans* species clade. Significant interactions between *Theileria* subtypes, indicated by the empirical dynamic modeling analysis. Arrows indicate the direction of the interaction ($subtype_A \rightarrow subtype_B$ = $subtype_A$ causes $subtype_B$). Red arrows (light) indicate a negative interaction whereas blue arrows (dark) indicate a positive interaction. Arrows are weighted by average interaction strength (s-map coefficient averaged over all animals and all captures). Nodes represent each subtype (labeled) and hue indicates subtypes in the same species clade. Square nodes indicate subtypes that mainly replicate within white blood cells whereas circle nodes indicate subtypes that replicate within red blood cells. Interactions are typically limited to taxonomic groups

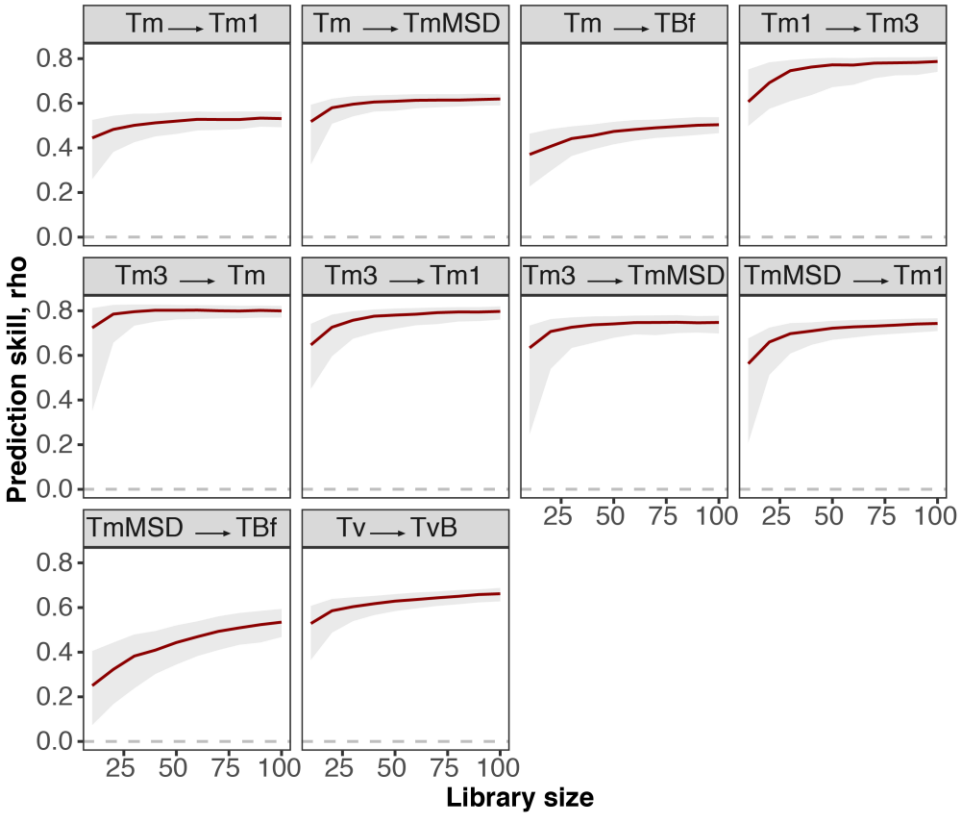

Appendix D4, Figure 4. Library size by prediction skill (rho) for significant interactions from the network including all animals. For a system to be a non-linear dynamical system, and thus be able to be modeled by empirical dynamical modeling, prediction skill should first increase, then saturate with library size.

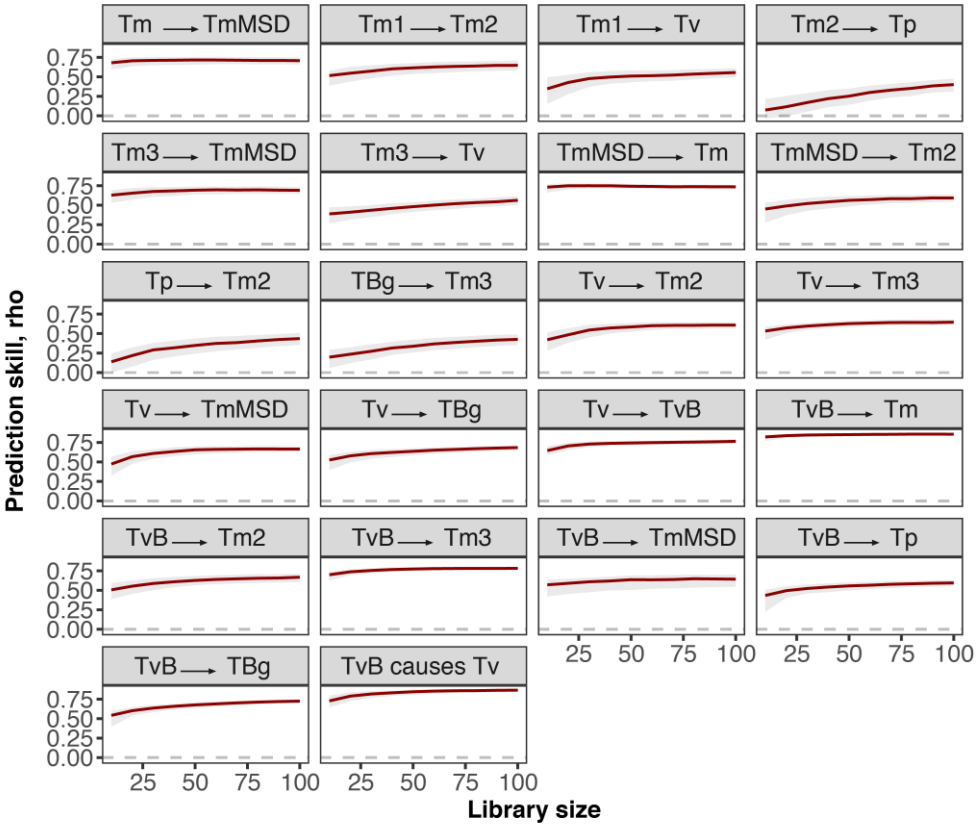

Appendix D4, Figure 5. Library size by prediction skill (rho) for significant interactions from the network including only subadult animals (<2 years old). For a system to be a non-linear dynamical system, and thus be able to be modeled by empirical dynamical modeling, prediction skill should first increase, then saturate with library size.

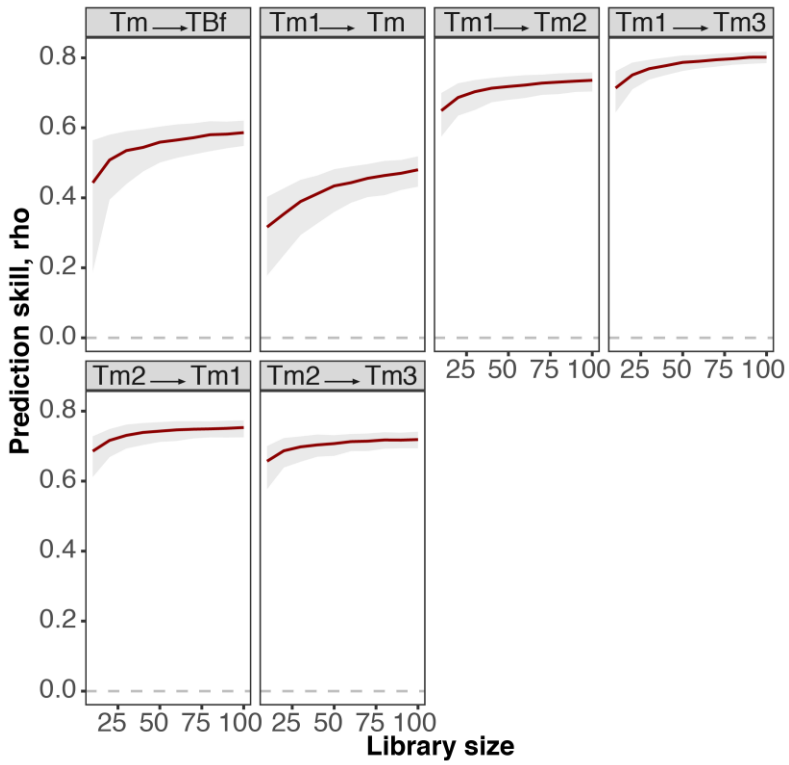

Appendix D4, Figure 6. Library size by prediction skill (rho) for significant interactions from the network including only adult animals (>2 years old). For a system to be a non-linear dynamical system, and thus be able to be modeled by empirical dynamical modeling, prediction skill should first increase, then saturate with library size.

Table D1. Model selection tables for linear mixed models describing variation in PC1. Only the first eight models with the lowest AICc are presented. The global model included condition + white blood cell abundance (wbc PC1) + white blood cell composition (wbc PC2) + globulins + pregnancy status + mean corpuscular volume + NDVI + $1/2^{age}$ + red blood cell count + sex + (1|animal ID). Only combinations of fixed effects are displayed as the random effect remained the same for all models. The final model reported in the manuscript is reported in bold.

	AICc	delta
wbc composition + globulins + pregnancy status + mcv + NDVI + $1/2^{age}$	**2307.60**	**0.00**
wbc composition + globulins + pregnancy status + mcv + NDVI +$1/2^{age}$ + sex	2308.53	0.93
wbc composition + globulins + mcv + NDVI + $1/2^{age}$	2308.68	1.07
condition + wbc abundance + wbc composition + globulins + preganancy status + mcv + NDVI + $1/2^{age}$	2308.94	1.34
wbc abundance + wbc composition + globulins + pregnancy status + mcv + NDVI + $1/2^{age}$	2309.00	1.40
condition + wbc composition + globulins + pregnancy status + mcv + NDVI + $1/2^{age}$	2309.35	1.74
condition + wbc abundance + wbc composition + globulins + mcv + NDVI + $1/2^{age}$	2309.47	1.87
wbc composition + globulins + mcv + NDVI + $1/2^{age}$	2309.56	1.96

Table D2. Model selection tables for linear mixed models describing variation in PC2. Only the first eight models with the lowest AICc are presented. The global model included condition + white blood cell abundance (wbc PC1) + white blood cell composition (wbc PC2) + globulins + pregnancy status + mean corpuscular volume + NDVI + $1/2^{age}$ + red blood cell count + sex + (1|animal ID). Only combinations of fixed effects are displayed as the random effect remained the same for all models. The final model reported in the manuscript is reported in bold.

	AICc	delta
age + condition + pregnancy status + NDVI	**2180.27**	**0.00**
age + NDVI	2180.27	0.00
age + condition + NDVI	2180.39	0.12
age + NDVI + sex	2180.50	0.23
age + pregnancy status + NDVI + sex	2180.57	0.31
age + condition + NDVI + sex	2180.74	0.48
condition + NDVI	2180.91	0.64
age + condition + pregnancy status + NDVI	2180.96	0.70

Table D3. Model selection tables for linear mixed models describing variation in PC3. Only the first eight models with the lowest AICc are presented. The global model included condition + white blood cell abundance (wbc PC1) + white blood cell composition (wbc PC2) + globulins + pregnancy status + mean corpuscular volume + NDVI + $1/2^{age}$ + red blood cell count + sex + (1|capture number) + (1|animal ID). Only combinations of fixed effects are displayed as the random effect remained the same for all models. The final model reported in the manuscript is reported in bold.

	AICc	delta
NDVI	**2102.80**	**0.00**
NDVI + pregnancy status	2103.75	0.95
NDVI + sex	2103.92	1.12
NDVI + condition	2104.57	1.76
NDVI + rbc	2104.77	1.97
NDVI + pregnancy status + sex	2104.88	2.07
intercept only	2105.10	2.30
NDVI + pregnancy status + condition	2105.38	2.58

Table D4. Model selection tables for generalized linear mixed models (negative binomial distribution) describing variation in *Rhipicephalus* abundance. Only the first eight models with the lowest AICc are presented. The global model included age + age^2 + condition + NDVI + rainfall + (1| capture number). Only combinations of fixed effects are displayed as the random effect remained the same for all models. The final model reported in the manuscript is reported in bold.

	AICc	delta
age + age^2	1528.70	0.00
age + age^2 + rainfall	1530.37	1.67
age + age^2 + NDVI	**1530.46**	**1.76**
age + age^2 + condition	1530.79	2.10
age + age^2 + NDVI + rainfall	1532.38	3.69
age + age^2 + condition + rainfall	1532.50	3.80
age + age^2 + condition + NDVI	1532.62	3.92
age + age^2 + condition + NDVI + rainfall	1534.56	5.86

Table D5. Model selection tables for generalized linear mixed models (negative binomial distribution) describing variation in *Amblyomma* abundance. Only the first eight models with the lowest AICc are presented. The global model included age + age^2 + condition + NDVI + rainfall + (1|animal ID) + (1| capture number). Only combinations of fixed effects are displayed as the random effect remained the same for all models. The final model reported in the manuscript is reported in bold.

	AICc	delta
age + age^2 + rainfall	2165.38	0.00
age + age^2	2166.36	0.98
age + age^2 + NDVI	**2167.17**	**1.79**
age + age^2 + NDVI + rainfall	2167.21	1.83
age + age^2 + condition + rainfall	2167.57	2.19
age + age^2 + condition	2168.52	3.14
age + age^2 + condition + NDVI	2169.15	3.77
age + age^2 + condition + NDVI + rainfall	2169.34	3.96

Table D6. Coordinates and variance explained (% variance) for the first 8 PCA axes.

	PC1	PC2	PC3	PC4	PC5	PC6	PC7	PC8
% variance	50.85	13.36	9.57	8.07	4.76	4.35	2.75	2.34
coordinate								
T. velifera	0.07	0.01	-0.04	0.14	-0.04	0.14	-0.10	-0.02
T. velifera B	0.20	0.19	-0.25	0.51	-0.29	0.56	0.18	-0.01
T. velifera UD	0.03	-0.16	-0.02	0.00	0.00	-0.15	-0.67	-0.05
T. mutans-like 1	-0.31	0.13	0.26	-0.01	0.09	-0.03	0.23	-0.48
T. mutans-like 2	-0.27	0.08	0.35	0.13	0.08	0.04	-0.06	0.79
T. mutans-like 3	-0.38	0.13	0.37	0.00	0.09	0.04	0.15	-0.24
T. mutans MSD	0.50	-0.10	0.00	0.28	0.52	-0.43	0.33	0.04
T. mutans	0.54	0.28	0.30	-0.60	-0.29	0.06	0.05	0.04
T. mutans UD	0.09	-0.01	0.02	0.15	0.10	0.02	-0.50	-0.26
T. sp. (bougasvlei)	-0.24	0.30	-0.47	-0.01	-0.42	-0.59	0.09	0.07
T. sp. (buffalo)	-0.06	-0.85	0.01	-0.12	-0.33	0.02	0.24	0.02
T. parva	-0.17	0.01	-0.54	-0.48	0.49	0.33	0.05	0.09

Table D7. Linear mixed model evaluating the effect of host traits on *Theileria* assemblage composition along pca axis 1. (A) Describes PCA axis 1 coordinates and (B) describes model output. Continuous variables (white blood cell composition (wbc pca axis 2 coordinates), globulin concentration (g/dL), mean corpuscular volume (μm^3), $1/2^{age\ (years)}$, and median ndvi) were transformed to standard deviation from the mean to compare effect size).

A.

PC1 subtype	coordinate
T. mutans-like 3	-2.35
T. mutans-like 1	-1.88
T. mutans-like 2	-1.66
T. sp. (bougasvlei)	-1.49
T. parva	-1.09
T. sp. (buffalo)	-0.30
T. velifera UD	0.28
T. velifera	0.47
T. mutans UD	0.55
T. velifera B	1.19
T. mutans MSD	3.03
T. mutans	3.26

B.

	***Theileria* composition P1**			
Predictors	*β*	*std. Error*	*Statistic*	*p*
(Intercept)	-0.16	0.33	-0.47	0.636
wbc composition	0.36	0.13	2.89	**0.004**
globulin	-0.52	0.19	-2.72	**0.006**
pregnancy status	0.95	0.64	1.49	0.136
mean corpuscular volume	-0.71	0.23	-3.16	**0.002**
median ndvi	-0.20	0.13	-1.52	0.128
$1/2^{age}$	5.15	0.31	16.86	**<0.001**
Random Effects				
σ^2	6.25			
$\tau_{00\ animal\text{-}ID}$	5.53			
$N_{\ amo,a;s}$	60			
Observations	465			
Marginal R^2 / Conditional R^2	0.744 / 0.864			

Table D8. Model fit for the partial least squares regression.

cumulative Q^2						
	component 1	0.12				
	component 2	0.01				
	component 3	0.00				
	component 4	0.00				
	component 5	0.00				
MSEP		comp 1	comp 2	comp 3	comp 4	comp 5
T. velifera		0.97	0.98	0.99	0.99	1.00
T. velifera B		0.92	0.93	0.94	0.94	0.95
T. velifera UD		0.92	0.84	0.84	0.83	0.82
T. mutans-like 1		0.68	0.66	0.66	0.66	0.66
T.mutans-like 2		1.01	1.01	1.01	1.01	1.02
T. mutans-like 3		0.74	0.73	0.73	0.73	0.74
T. mutans MSD		0.80	0.80	0.80	0.81	0.81
T. mutans		0.86	0.86	0.86	0.86	0.86
T. mutans UD		0.95	0.93	0.91	0.91	0.91
T. sp. (bougasvlei)		0.86	0.83	0.84	0.84	0.83
T. sp. (buffalo)		1.01	0.99	0.99	0.98	0.98
T. parva		0.90	0.90	0.90	0.91	0.91
R^2						
		comp 1	comp 2	comp 3	comp 4	comp 5
T. velifera		0.03	0.02	0.02	0.02	0.02
T. velifera B		0.07	0.07	0.06	0.06	0.05
T. velifera UD		0.08	0.16	0.16	0.17	0.18
T. mutans-like 1		0.32	0.34	0.34	0.34	0.34
T.mutans-like 2		0.00	0.00	0.00	0.00	0.00
T. mutans-like 3		0.26	0.27	0.27	0.27	0.26
T. mutans MSD		0.19	0.20	0.19	0.19	0.19
T. mutans		0.14	0.13	0.14	0.14	0.14
T. mutans UD		0.05	0.07	0.09	0.09	0.09
T. sp. (bougasvlei)		0.13	0.16	0.16	0.16	0.17
T. sp. (buffalo)		0.07	0.02	0.02	0.02	0.02
T. parva		0.10	0.10	0.10	0.10	0.09

Table D9. Linear mixed model evaluating the effect of host traits on Theileria assemblage composition along pca axis 2. (A) Describes PCA axis 2 coordinates and (B) describes model output. Age (years) and median ndvi were transformed to standard deviations from the mean.

A.

PC2 subtype	coordinate
T. sp. (buffalo)	-2.62
T. velifera UD	-0.25
T. mutans MSD	-0.24
T. mutans UD	-0.08
T. velifera	-0.02
T. parva	0.06
T. mutans-like 2	0.19
T. mutans-like 3	0.35
T. mutans-like 1	0.35
T. velifera B	0.38
T. mutans	0.90
T. sp. (bougasvlei)	0.97

B.

	***Theileria* composition PC2**			
Predictors	*β*	*std. Error*	*Statistic*	*p*
(Intercept)	-0.16	0.32	-0.48	0.391
age	-0.87	0.30	-2.86	**0.004**
median ndvi	0.11	0.10	1.07	0.283
pregnancy status	0.64	0.54	1.19	0.233
Random Effects				
σ^2	4.61			
$\tau_{00\ animal\text{-}ID}$	5.71			
$N_{\ animals}$	60			
Observations	471			
Marginal R^2 / Conditional R^2	0.065 / 0.583			

Table D10. Mixed effects logistic regression estimating the effect of SNPs on *T.* sp. (buffalo) presence. Covariates were included if they were included in the best fit model for *Theileria* composition PCA axis 2 (table 3). As opposed to the analysis presented in table 3, age (years) and median NDVI were not scaled to standard deviations from the mean to ease interpretation of log odds.

	***T.* (sp) buffalo presence**			
Predictors	*Odds ratios*	*std. Error*	*Statistic*	*p*
(Intercept)	0.15	0.96	-1.99	**0.046**
snp488 [minor]	0.005	1.42	-3.78	**<0.001**
snp678 [minor]	0.0156	1.10	-3.78	**<0.001**
age	1.396	0.09	3.90	**<0.001**
median NDVI	1.062	2.09	0.03	0.977
pregnancy status	0.541	1.13	-0.54	0.588
Axis1	1.066	0.04	1.76	0.078
Axis2	1.176	0.05	3.39	**0.001**
Axis3	1.488	0.10	4.17	**<0.001**
Random Effects				
σ^2	3.29			
$\tau_{00\ \text{Numeric.Animal.ID}}$	1.08			
$N_{\text{Numeric.Animal.ID}}$	52			
Observations	410			
Marginal R^2 / Conditional R^2	0.703 / 0.777			

Table D11. Linear mixed model evaluating the effect of host traits on *Theileria* assemblage composition along pca axis 3. (A) Describes PC 3 coordinates and (B) describes model output. Median ndvi was transformed to standard deviation from the mean.

PC3 subtype	coordinate
T. parva	-0.54
T. sp. (bougasvlei)	-0.47
T. velifera B	-0.25
T. velifera	-0.04
T. mutans MSD	0.00
T. sp. (buffalo)	0.01
T. velifera UD	0.02
T. mutans UD	0.02
T. mutans-like 1	0.26
T. mutans	0.30
T. mutans-like 2	0.35
T. mutans-like 3	0.37

	***Theileria* composition PC3**			
Predictors	*β*	*std. Error*	*Statistic*	*p*
(Intercept)	-0.20	0.33	-0.59	0.555
median ndvi	0.21	0.15	1.40	0.162
Random Effects				
σ^2	3.83			
$\tau_{00\ animal\text{-}ID}$	5.23			
$\tau_{00\ capture\text{-}\#}$	0.14			
$N_{captures}$	10			
$N_{animals}$	60			
Observations	465			
Marginal R^2 / Conditional R^2	0.005 / 0.586			

Table D12. Linear model describing the correlation between average age at first infection and average relative abundance in climax communities for each subtype (Figure 5.2). A linear model was fit with (A) and without (B) subtypes within the *T. velifera* subtype clade. Linear regressions were fit in base R (v 3.6.3). Average age of first infection and average relative abundance of climax communities were derived using the methods listed in section 2.3 and supplementary materials 2.

A. All subtypes

Predictors	*Estimates*	*CI*	*p*
(Intercept)	0.07	-0.01 – 0.15	0.070
age 1st infection	0.01	-0.00 – 0.02	0.107
Observations	9		
R^2 / R^2 adjusted	0.329 / 0.233		

B. No *T. velifera* subtypes

Predictors	*Estimates*	*CI*	*p*
(Intercept)	0.01	-0.08 – 0.10	0.829
age 1st infection	0.02	0.00 – 0.03	**0.020**
Observations	7		
R^2 / R^2 adjusted	0.695 / 0.635		

Table D13. Generalized linear mixed model (negative binomial distribution) evaluating the effect of age and median NDVI on *Rhipicephalus* tick abundance.

Predictors	*Coeffecient*	*SE*	*Statistic*	*p*
(Intercept)	2.01	1.02	1.97	**0.049**
age	0.26	0.03	7.89	**<0.001**
age^2	-0.01	0.00	-5.87	**<0.001**
median NDVI	2.03	3.24	0.63	0.532
Random Effects				
σ^2	0.28			
$\tau_{00\ capture}$	0.36			
$N_{\ capture}$	9			
Observations	178			
Marginal R^2 / Conditional R^2	0.268 / 0.682			

Table D14. The effect of age and median NDVI on *Amyblyomma* tick abundance. Generalized linear mixed model (negative binomial distribution).

Predictors	*Coeffecient*	*SE*	*Statistic*	*p*
(Intercept)	3.32	0.47	7.13	**<0.001**
age	0.43	0.04	11.05	**<0.001**
age^2	-0.02	0.00	-7.76	**<0.001**
median NDVI	1.87	1.44	1.30	0.195
Random Effects				
σ^2	0.11			
$\tau_{00\ animal\ ID}$	0.12			
$\tau_{00\ capture}$	0.07			
$N_{\ capture}$	9			
$N_{\ animal\ ID}$	52			
Observations	178			
Marginal R^2 / Conditional R^2	0.695 / 0.886			

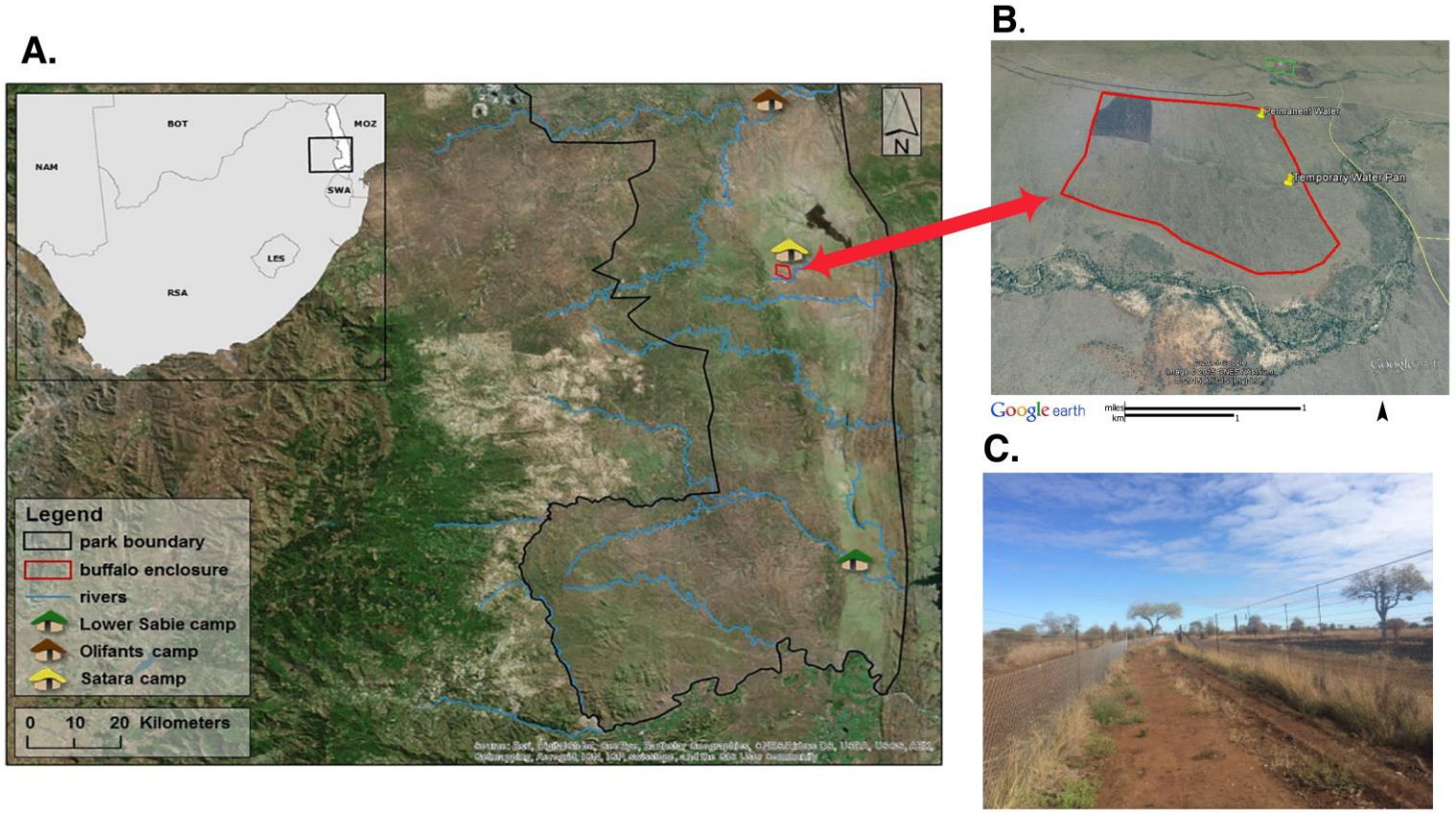

Figure D1. (A) A map of southern Africa inlaid in a map of the south of Kruger National Park; (B) The boma within Kruger National Park (the red outline on (A) indicates the location and size of the boma relative to the park; (C) A photo of the perimeter of the boma.